UNIVERSITY OF LONDON

IMPERIAL COLLEGE OF SCIENCE AND TECHNOLOGY

DEPARTMENT OF ELECTRICAL ENGINEERING

THE DEVELOPMENT OF A HYBRID SIMULATOR FOR POWER SYSTEM CONTROL INVESTIGATIONS.

BY

CHRISTOPHER BRUCE GILES

B.Sc.(Eng), A.C.G.I.

Thesis submitted for the degree of
Doctor of Philosophy in the
Faculty of Engineering.

London, August 1976

"Each venture
Is a new beginning, a raid on the inarticulate
With shabby equipment always deteriorating."

T.S. Eliot
"East Coker"

ABSTRACT

With the increasing use of digital computers in the control of electric power systems a need arises for a means of testing and evaluating different control algorithms before implementing them in the real system. An electronic simulator has been built in the Power Systems Laboratory at Imperial College which is suitable for this purpose.

This simulator consists of two main sections: the actual representation of the power system, and a digital computer to which this representation is interfaced. The dynamic equations of the generating plant are solved using analog circuitry and the network is represented by a scaled model, the whole system being similar to a conventional network analyser.

This thesis is concerned mainly with the analog section of the simulator. A generator unit has been designed on a modular basis, and includes simulations of the synchronous machine, its voltage regulator, and of a steam or hydro turbine. The synchronous machine model is based on an electronic 2 axis representation which gives good results under both steady-state and transient conditions.

Electronically controllable current sinks have been designed and analysed, acting as system loads in which both the real and reactive components of current may be controlled. Interconnections have been specially designed for the network elements and for interfacing the simulator with the computer.

Finally, the whole system has been used in experiments designed to investigate its suitability for diverse purposes. A digital boiler model operating in conjunction with the analog turbine simulation was tested, and the whole model has been used as a test bed for implementing a simple load-frequency control scheme. The analog section has also been used alone to investigate the measurement of system parameters using correlation methods. The success achieved in all of these experiments demonstrates the feasibility of using a simulator of the type described.

Acknowledgements.

This work was carried out under the supervision of Dr. M.J. Short, Ph.D., B.Sc., D.I.C., C.Eng., M.I.E.E., whom I would like to thank for his constant guidance and encouragement.

I would like to thank my colleagues in the Power Systems Laboratory for their advice and assistance, in particular Drs. Sheldrake and Edelstein, and Messrs. Bolton, Horne and Mogridge.

I wish to express my gratitude to the Science Research Council, which provided me with a Research Studentship and which is also funding the whole Simulator project.

Finally, I would like to record my deep gratitude to my wife Daphne, whose patience and encouragement were the most important contribution to the success of this work.

CONTENTS

CHAPTER 1 INTRODUCTION

1.1 Why Real-Time Control?

The fact that electrical energy cannot be directly stored in any appreciable quantity plays an important part in the control of an electric power system. There must, therefore, be an exact match at all times between the mechanical power generated and that consumed by the various loads attached to the system. The control problem is increased by the large number and varied nature of these consumers, whose behaviour exhibits random characteristics, and by the fact that the power is generated by many separate plants.

The shortfall between generation and consumption must be constantly monitored in order to adjust the level of generation to meet the load. The generation deficit manifests itself initially as a change of system frequency, since the machine shafts slow down, and this is detected by the speed governors. The governor constitutes the primary form of generation control, since it is a fast acting device which alters the steam or water flow in such a way as to change the power output of the prime mover to maintain near-constant speed. A governor is characterized both by its dynamic performance and also by its static gain which gives the familiar "droop" characteristic.

In order to change the pattern of generation, or to alter the system frequency, the governor set-point must be changed by actuating the speeder gear. The problem of maintaining frequency and of deciding on the loading levels of different sets is one which is usually solved at a central control centre in a power system, since there are many factors which must be taken into account before a decision can be made. The control problem is further complicated by the interconnection of many smaller systems into one large system using comparatively weak tie lines. This interconnection is performed so that in the event of a fault, mutual assistance can be given, thus lowering the total spinning reserve requirement. Economic advantages can also be obtained if there is a varied plant mix over the constituent sub-systems, such as one area being predominantly hydro, while another might consist of base-load thermal plant. Finally, the effects of random loading can be more easily compensated in a highly interconnected system. The whole interconnection concept is not without its difficulties, however, as it requires good frequency control over the whole system, together with control of tie line flows, in order to avoid possible tie line tripping and consequent system islanding.

Since system interconnection on a large scale became a reality during the 1930's, analog equipment has been employed for the regulation of tie line power flows, and has proved quite adequate for the purpose. However, over the past 15 years many changes have occurred, owing to the increasing size and centralization of power systems. Conventional analog controllers and metering systems are no longer able to conveniently cope with the size of systems, and the advent of the digital computer has allowed a revolution in the concepts of system control and monitoring to occur.

The objectives of an electricity supply system may be listed as:

- the provision of a reliable supply
- the operation of the system in an economic way.

These two requirements naturally conflict, especially if economies are to be made where they can be most effective, namely at the planning stage. The benefits which can be reaped from economic operation, while tangible, are harder to gain, since once a system has been constructed, there is not a great deal of operational flexibility left, especially during periods of peak loading.

It is worth noting some of the factors which must be taken into account in just the day-to-day operation of a power system, for the advantages of installing a computer to assist with these different tasks become apparent immediately:

(i) Protection of generating plant and transmission system

(ii) Run-up and shutdown of generating plant

(iii) Generator scheduling according to plant availability and economic considerations

(iv) Control of frequency and synchronous time

(v) Maintenance of adequate spinning reserve

(vi) Planning of unit commitment on the basis of load forecasting and scheduled maintenance

(vii) Control of interconnection flows

(viii) Ensuring both transient and dynamic stability of the system

(ix) Voltage control

(x) Monitoring of the system configuration

(xi) Formulation of load shedding strategies

(xii) Minimization of reactive power flow by compensation and voltage control

(xiii) Security assessment and line outage studies

(xiv) Scheduling and accounting interconnection flows

(xv) Fault calculations

Although this is a long list, it is by no means complete, and it serves to show the complexity of the whole system operation problem. Indeed, one of the major problems is not the control of the system per se, but merely knowing what the state of the system is at any particular moment.

The first major application of on-line computers in power systems was in the realms of data gathering and display[1,2]. The number of measurements which are made on a system is so large that some kind of digital display system has become necessary merely to present the information to the operator. As soon as a computer is used for driving such displays, there are many other functions which it can usefully perform, such as initial validation of the raw data measurements and the construction of a validated data base. Such a validation process can take a large number of different forms, some of which are mutually compatible. The problem is basically to determine the state of the system from measurements of line flows, nodal injections and circuit breaker status indications. The simplest methods are logical checks on the data, such as ensuring that there is no power flow in a line whose breakers are supposed to be open. or by ensuring that the sum of all the measured flows into a node is nearly zero.At the other extreme, in a system where there are redundant measurements it is possible to use a full state-estimation algorithm[3], where the vector of differences between the measured and estimated values is minimized. Although such algorithms are claimed to be able to detect bad data, the best system is probably a combination of these two methods, where gross errors could be detected by logical checks, the bad values discarded, and a state estimator then used on the remaining data.

Once the computer is used for this data acquisition and display function, it is a natural progression to use it for more of the functions listed above, especially as the computer has access to the data base which contains all the required information about the system state, and may also contain details of plant availability, load forecasts and interconnection schedules. The availability of all this information puts the computer in an unrivaled position to control the system in a reliable and secure manner.

The main areas in which a digital computer can assist in the control of the whole system are load-frequency control[4], on-line security assessment[5] and economic dispatch[6,7]. All these subjects have received great attention over the past 10 years, and many algorithms have been developed. However, the evaluation of the merits of alternative schemes is very difficult, as the results presented are usually obtained from off-line studies, using reliable data, and while this may demonstrate that a method works, it does not show how sensitive it might be to data errors, or how long it will take to execute in a real-time system. These problems can only be answered by testing the algorithms either on a real system, or by using a simulation of the system.

1.2 The Need for a Power System Simulator.

For many years in the design of conventional control systems, a simulation of the system which is to be controlled has been used to evaluate and tune the performance of the controller. Such a simulation is most conveniently performed using an analog computer, a device which is capable of fast parallel integration, and is suitable for the modelling of a dynamic system. Using analog equipment also gives the user a much better feel for the problem than can be achieved when the differential equations are solved numerically. For investigations of power systems problems, the order of the dynamic systems involved is so large that only very small systems can be studied on conventional analog computers. It therefore seems that a purpose built analog model, interfaced to a digital computer, would be useful for studying power system control problems. The construction of such a model, and an examination of its capabilities has been the main aim of this project.

There are other aspects of power systems studies in which such a model might be of use, namely in the fields of operator training and student teaching. Training simulators for complex equipment find widespread use, since despite their often high capital cost, they can offer advantages over training based on a "hands-on" approach with the real equipment. First, it might be cheaper to operate the simulator than the real plant, a good example being the aircraft simulators now in widespread use. With the ever-increasing cost of aviation fuel, it has become much cheaper to purchase and operate a simulator than to use a real aircraft for the training of pilots. Secondly, it is possible to give a much wider range of experience to the trainee through the use of a simulator, for unstable operating conditions can be set up without risk and the operator can then try and restore the system to the normal operating state. This is a point which is particularly valid in the case of a power system operator, for the chance of an operator gaining experience of operating a system which is in danger of breaking up, is very slim through his everyday experience. However, with a simulator such events can be set up with impunity, and the operator trained to respond in the most effective way to the particular contingency.

The teaching of power systems at an elementary level is considerably simplified if demonstrations of the dependence of power flow on angular differences, and of reactive power flow on voltage magnitude differences can be performed. The use of a simulator, which would demonstrate not only the static behaviour of a power system, but also the dynamic charactistics would be a great advantage, since the effects of governor droop and voltage regulator performance can easily be seen.

The objectives of the project, therefore, may be summarised as producing a total power system simulator, consisting of an analog simulation of the plant equations, which is interfaced to a digital computer. This simulator should be suitable not only for control studies, but should also fulfil a training and teaching role. The educational use of the system demands that comprehensive instrumentation and facilities for manual control are included, so that the analog section of the equipment may be used independently of the digital computer.

A subsidiary part of the project was the preparation of a feasibility study by Dr. S. Miniesey and the present writer[8]. This report was further edited by Dr. M.J. Short before being passed to a commercial organization. This report examined the possibility of commercial production of a power system simulator, based on the experience gained in this project, for educational purposes. The proposal was warmly received by the company concerned, but any further action has been delayed until details of the funding of the production prototype have been resolved.

1.3 Organization of the Thesis.

This thesis describes the work carried out by the writer on the construction of the analog hardware, and on the use of the whole simulator for various tasks, in order to demonstrate its complete operation and capabilities.

Chapter 2 deals with the actual structure of the whole simulator, and discusses which items of plant need to be represented. The actual hardware of a generator unit is described in chapters 3 and 4, of which the latter deals at length with the simulation of the synchronous machine, while the former is concerned with the rest ~~of the~~ of the generator unit. Chapters 5 and 6 deal respectively with the load units and the network representation. Also included in chapter 6 are details of the various signal interconnections between the various units.

Chapter 7 deals with a novel method of system representation, in which a high-frequency network signal is employed, instead of the 50 Hz which is used in the conventional model. Chapter 8 describes briefly the computer system, the interfacing arrangements and the basic software which is provided for users of the model.

The penultimate chapter, chapter 9, describes some work which has been carried out using the simulator, and this demonstrates the potential of the whole system. Finally, the conclusions summarize the whole development work which has been carried out, in particular the original contributions of the present writer, and discusses in which directions further work might most profitably be pursued.

2.1 Introduction.

The simulation of electric power systems is a subject which has been of great interest for the past 50 years, but although the actual problems have been well defined for many years, it is the computational aspects which have placed limitations on the ability to solve many problems. The first stage in any simulation is to define the problem, and to examine the plant under consideration.[9] For an electric power system, the main items of plant may be listed as:

(i) The prime mover and governing mechanism
(ii) The boiler plant
(iii) The synchronous machine
(iv) The voltage regulating system
(v) The transmission network
(vi) The protection
(vii) The system loads
(viii) The data acquisition system
(ix) The control systems

For any particular simulation, only certain of these items need to be included, and the selection of which items are to be included is dependent on their dominant time constants. There are five main areas of interest, and these may be defined as:

(i) Travelling wave phenomena - such as lightning and switching overvoltages
(ii) Subsynchronous resonance phenomena
(iii) Transient and dynamic stability
(iv) Plant response to controls
(v) Total system response

The first two of these areas are concerned principally with electrical phenomena associated with the transmission system, and consequently fall outside the scope of the present work. The requirements of plant representation for the last three kinds of problem are all fairly similar, and the basic problem is illustrated in Fig. 2.1. Following some change in the system, such as

(a) A change in network topology

(b) A change of load

(c) A change in the pattern of generation

the problem is to solve for the behaviour of each group of plant, as in Fig. 2.1, and for the real and reactive power flows in the network. For a large system, this is evidently a very considerable problem, and there are three main ways in which it can be simplified, either

(a) By dynamic system reduction - the omission of insignificant time constants

or (b) By the use of dynamic equivalents[10] - grouping together plant which is at some distance from the point of interest in the network, and which under dynamic conditions tends to behave in an aggregated fashion. The plant thus aggregated is replaced by a fictitious equivalent.

or (c) By the use of very simple models - such as ignoring all voltage effects in a total system model, and only considering the active power balance between generation and load[11,12,13].

The total problem which is posed, therefore, is the solution of a large number of differential equations, both linear and non-linear, which describe the behaviour of the plant, and a large set of non-linear simultaneous equations which describe the real and reactive power flows in the network.

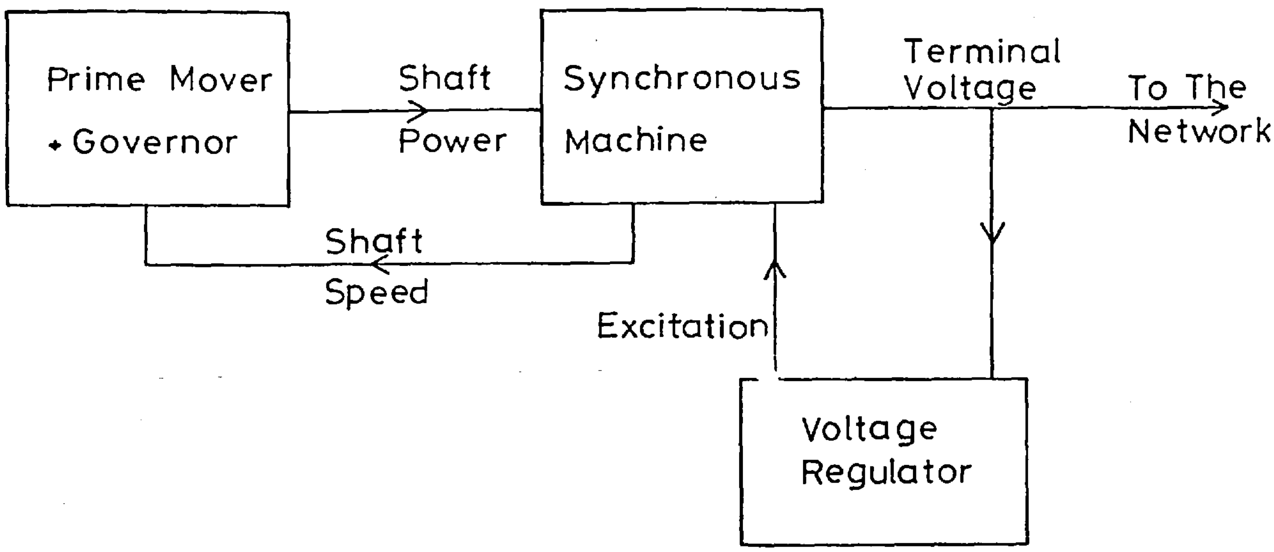

Fig. 2.1 One Group of Generating Plant.

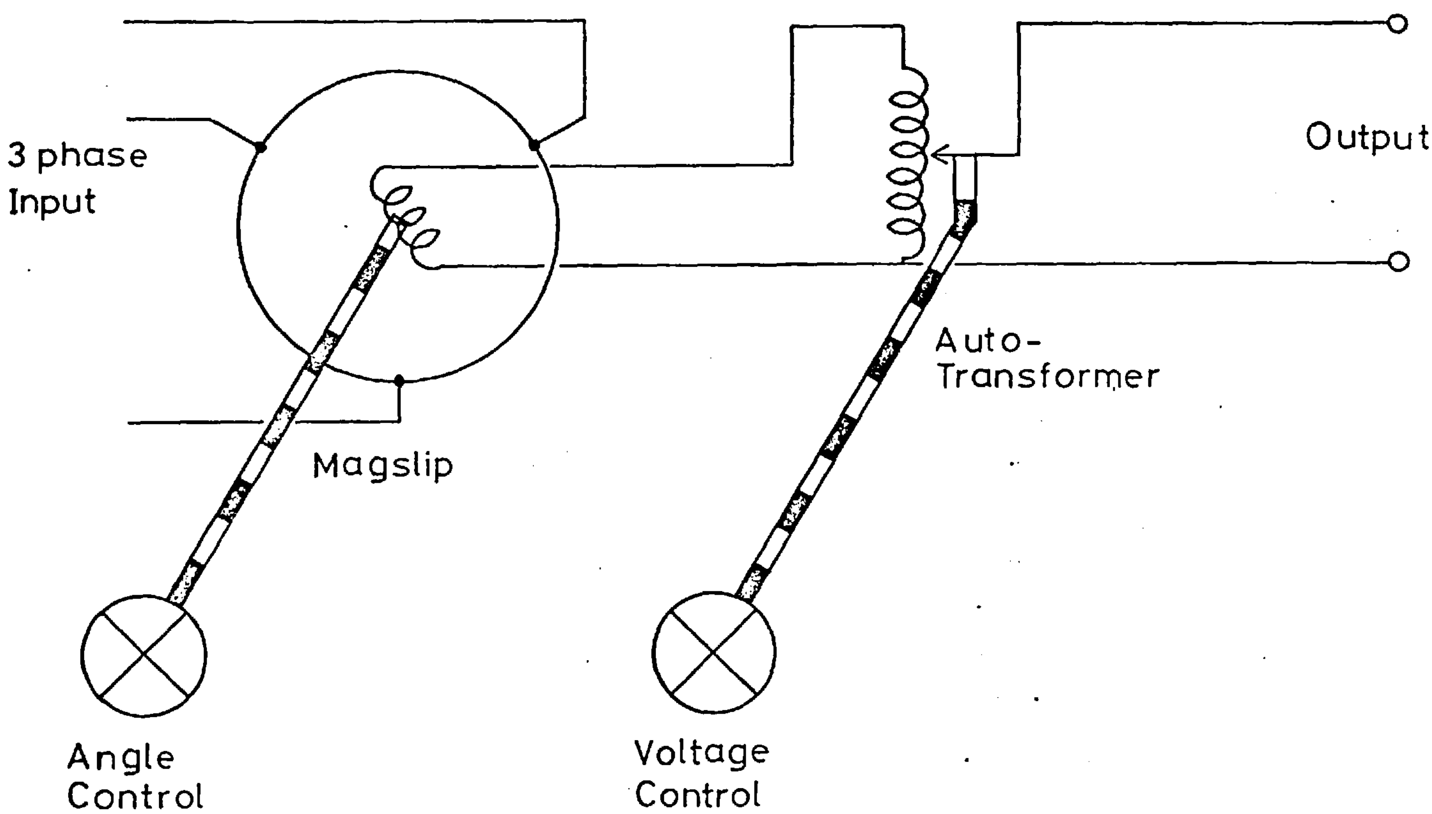

Fig. 2.2 A Generator Unit in a Network Analyser.

2.2 Methods of Solution.

Prior to 1929, calculations made on power systems were all performed by hand, and it was only possible to try and solve the simplest of problems. The first AC network analyser permitted solution not only of the load flow problem, but also step by step solution of transient stability problems, albeit in a very cumbersome way. Continuous solution of differential equations became a reality with the construction by Bush[14] of the first mechanical differential analyser. This used Kelvin's wheel-and-disk integrators with torque amplifiers, and was employed by Lyon[15] to solve single machine - infinite bus problems.

During the 1930's and 1940's, the scarcity of differential analysers led to much work being done on AC network analysers, and also by hand, with no major advances in solution methods being achieved until after the Second World War. The great developments in electronic technology which occured during this war enabled all-electronic analog computation equipment to be constructed. Simulators for fault and critical clearing time studies were constructed by Boast,[16] and Kaneff,[17] and Adamson[18]. Two of the major problems were the measurement of electrical power and the integration of the equation of motion, and electromechanical solutions, using dynamometers and velodynes, were frequently adopted.

In 1957, Adamson[19] produced an electronic 2 axis model of a synchronous machine which was suitable for short-circuit studies, and this was a great advance in the accurate representation of the machine. The next major step foward was the inclusion by Miles[20] and Aldred[21] of governor and voltage regulator action. A large power system model was constructed in 1966 for the Central Electricity Research Laboratories and is described by Bain[22]. This included 40 generators and over 100 transmission lines. Recent work on analog modelling of power systems has been concentrated on high speed transient analysers, working at over 100 times real time[23].

The digital computer has provided a means of solving by numerical methods any problem which can be formulated in mathematical terms, and it has found many applications in the power system field. For the study of power system dynamics, many large-scale transient stability programs have been produced, and solution methods are well established. More recently, the digital differential analyser, an all-digital analog computer, has been applied to a simple problem,[24] but the great cost of the machine seems to preclude its widespread use. However, with the advent of cheap microprocessors, it is possible that a fast and inexpensive digital solution to the problem might be found.

For a fast solution of the network equations, an AC network analyser cannot be bettered, for as soon as the voltages are applied to the network and the initial transients have died away, a steady state solution is present. This suggests that it is worthwhile to consider using a direct representation of the network in a power system model. Fig. 2.2 shows a typical generator unit from a network analyser, comprising a magslip and an auto-transformer. The phase of the generator is determined by the shaft position of the magslip, and the amplitude of the terminal voltage is adjusted using the auto-transformer. During the early 1960's work was done using an existing 50 Hz network analyser, the two shafts being driven by servo motors[25]. These servos were controlled by analog equipment which simulated the dynamics of the governing and voltage regulating plant, and thus a dynamic simulation could be performed.

Although this equipment functioned satisfactorily, the whole system was very large, the servo motors and their amplifiers require high voltages and currents, and as with any mechanical system, problems occur with the moving parts. Replacement of the mechanical parts with electronic circuitry offers many advantages, and this was the starting point of the whole project.

During the late 1960's part of the CERL model, mentioned above, was given to Imperial College, and in 1969 work was started on it by Sheldrake[26,27]. The original equipment used motor-resolvers for changing the shaft position, and initially Sheldrake continued to use these parts. However, after many mechanical problems, an electronic alternative was sought, and this is shown in Fig. 2.3. The heart of the new system is a voltage-controlled oscillator. This produces a sinusoidal output, in the range 45 - 55 Hz, whose frequency is proportional to a d.c. control signal. There are several ways in which such a system can be implemented, and the two main methods will be outlined in Chapter 3.

The advantage of using a voltage-controlled oscillator is that the frequency is variable over a wide range, and a model of a power system can work at different frequencies, rather than only being able to study relative angular swings between machines. However, in a multi-machine system the stability of the oscillators, and their accuracies, must be excellent, since an error in frequency is integrated to give an error in phase angle.

The structure of a whole generator unit[28,29,30] for the model is shown in Fig. 2.4, and the basic items of plant identified. The voltage regulator and the turbine/governor system are represented using standard analog circuitry, since well-established transfer function models exist which are easily implemented. The representation of the synchronous machine is more complex, and this is discussed in greater detail in Chapter 4. The electrical and mechanical power signals, derived respectively from the machine and turbine analogs, are fed into the equation of motion integrator, which drives the voltage-controlled oscillator. The sinusoidal oscillator output is fed to the machine analog, whose other input is the excitation signal derived from the voltage regulator. The simulation of the boiler is a more difficult problem, since it involves

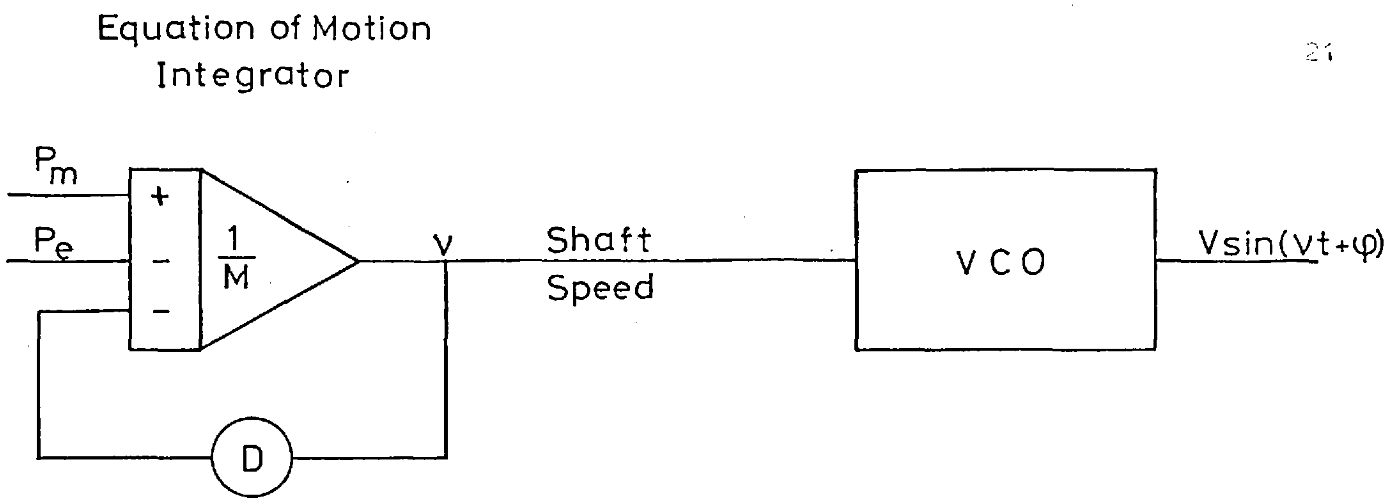

Fig. 2.3 Voltage Controlled Oscillator in a Generator Unit.

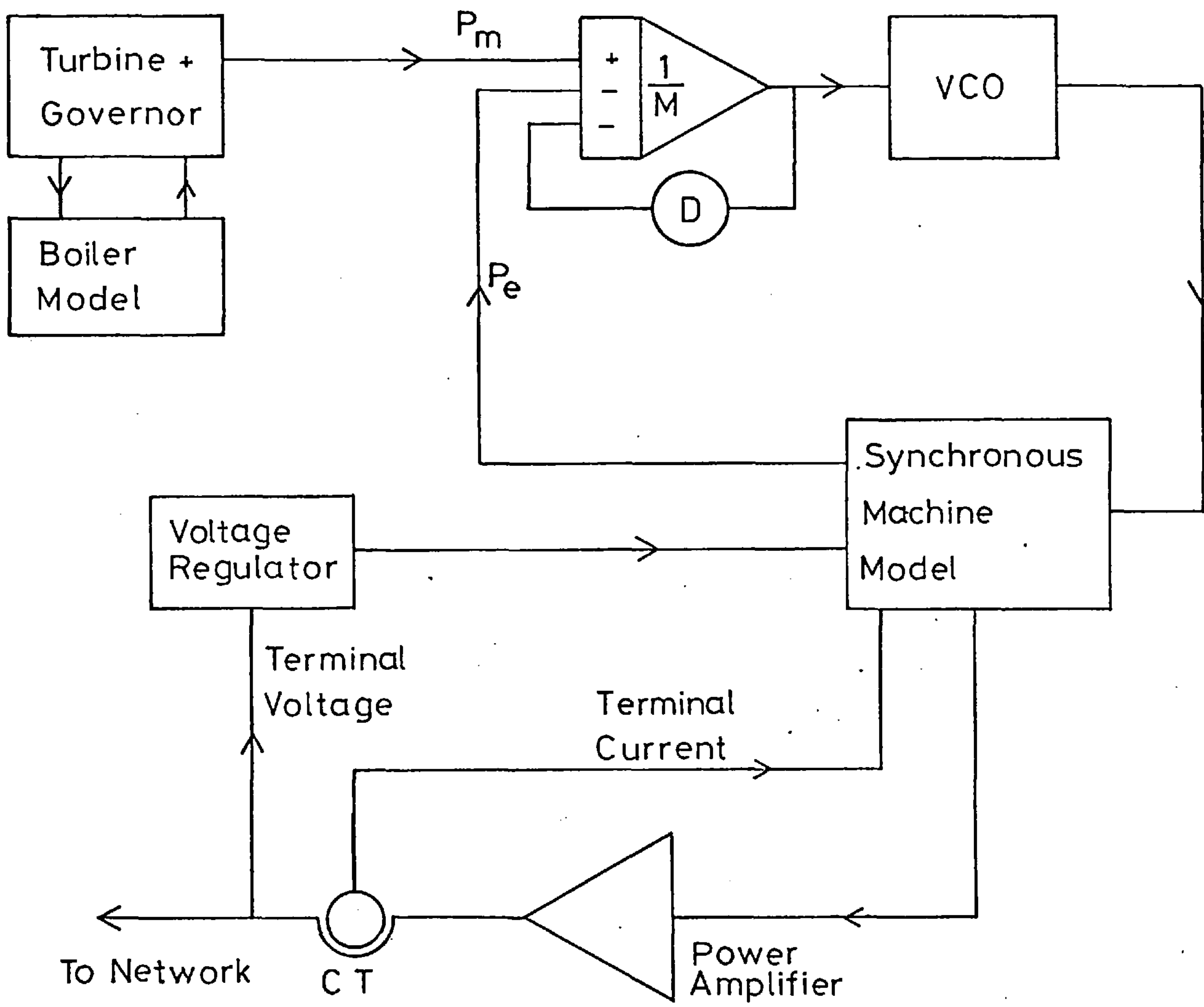

Fig. 2.4 Total Generator Unit Structure.

both long time constants, for the boiler storage effects, and also pure delays, which occur in the fuel feed system. It was therefore decided to simulate the boiler digitally. The sheer size of the dynamic system for a complete power system precludes the use of an analog computer, and demands that special purpose analog circuitry is constructed.

Loads on a power system have six main characteristics[31-35], which are of importance in a dynamic simulation, and these are:

(i) Voltage dependence
(ii) Frequency dependence
(iii) Long-term trends
(iv) Random fluctuations
(v) Block charges
(vi) Dynamic characteristics

Since the inertia of the aggregate load at any given point on a power system is small, the dynamic charactistics are ignored. All the other characteristics could be simulated using analog components, but it was decided that it is simpler to perform these tasks digitally, and to have controllable sinks of real and reactive power attached to the system. The computer then controls the load at a given point acording to the voltage and frequency, the load trend and its random features. This gives a good deal of flexibility coupled with comparatively simple hardware.

The transmission lines are represented by nominal pi lumped models, and facilities are provided for switching the lines, generators and loads. Since all connections are made with a patching system, any configuration within the capacity of the model may be set up. The whole model comprises:

(i) 6 generator units
(ii) 5 load units
(iii) 10 transmission lines
(iv) 16 network switches

Provision is made for measuring both real and reactive power flows at both ends of the lines, and for indicating to the computer the status of each network switch.

No representation is included of the system protection, as this lies outside the scope of this model. However, it is possible to simulate such devices as low-frequency relays using the digital computer. Since the model uses a direct representation of the system network, it is quite feasible to construct electronic circuitry to simulate any type of protective relay, if this is necessary for any particular study.

The per-unit values which have been chosen are the same as those used in the original CERL model, which were:

1 p.u. voltage = 20 V rms

1 p.u. current = 30 mA rms

1 p.u. impedance = 667 Ohms

This gives a per-unit inductance of 2.12 H, and a per-unit capacitance of 4.77μF. In retrospect, the use of a lower voltage would be a great advantage, and the consequent reduction in base impedance would allow the use of smaller inductors to represent the transmission lines.

In a system which is designed to evaluate different kinds of control algorithm, it is essential to include simulation of the problems associated with data acquisition and with the actual control of the plant. The typical stages in the "data gathering to control" process are:

(i) Transducer delays

(ii) Telemetry system delays

(iii) Initial processing of the data

(iv) Construction of a validated data base

(v) Execution of the algorithm

(vi) Telemetry system delays

(vii) Control actuator operation delays

All of these must be borne in mind when devising control strategies, since in a large system the whole chain might take tens of seconds to operate. The delays associated with the transducers and the control actuators are easily included in the analog hardware of a generator unit, whereas all the other processes must be simulated in the computer. The initial processing of the data might consist of parity checking and digital filtering, in the case of a digital telemetry system, and these are performed in the system model. The construction of a validated data base might take the form of either a complete state estimation routine, or it might only be a system of logical checks, such as ascertaining that there is no current flowing through an open circuit breaker.

The advantages of testing algorithms in a real-time system is that they have to deal with real data, and severe constraints are placed on their execution time and their length, since they must run in a control type of computer, rather than as a job in a specialized batch processing computer which is designed for scientific computation. Additionally, redundancy requirements can be assessed, and any fail-safe features checked.

The control requirements for one generator unit are shown in Fig. 2.5, and it can be seen that there is a bidirectional transfer of analog data, and digital status indications are provided to indicate whether a particular unit is under manual or computer control. The computer must therefore be fitted with analog to digital and digital to analog converters, together with a digital input/output unit.

2.3 Conclusion.

The structure of the whole simulator has been explained, and the the methods of simulation which are used fulfil the objectives which were set in the first chapter. The requirements of an accurate simulation can be met, provided that sufficient care is taken in the electronic design, and the adoption of analog simulation and a direct representation of the

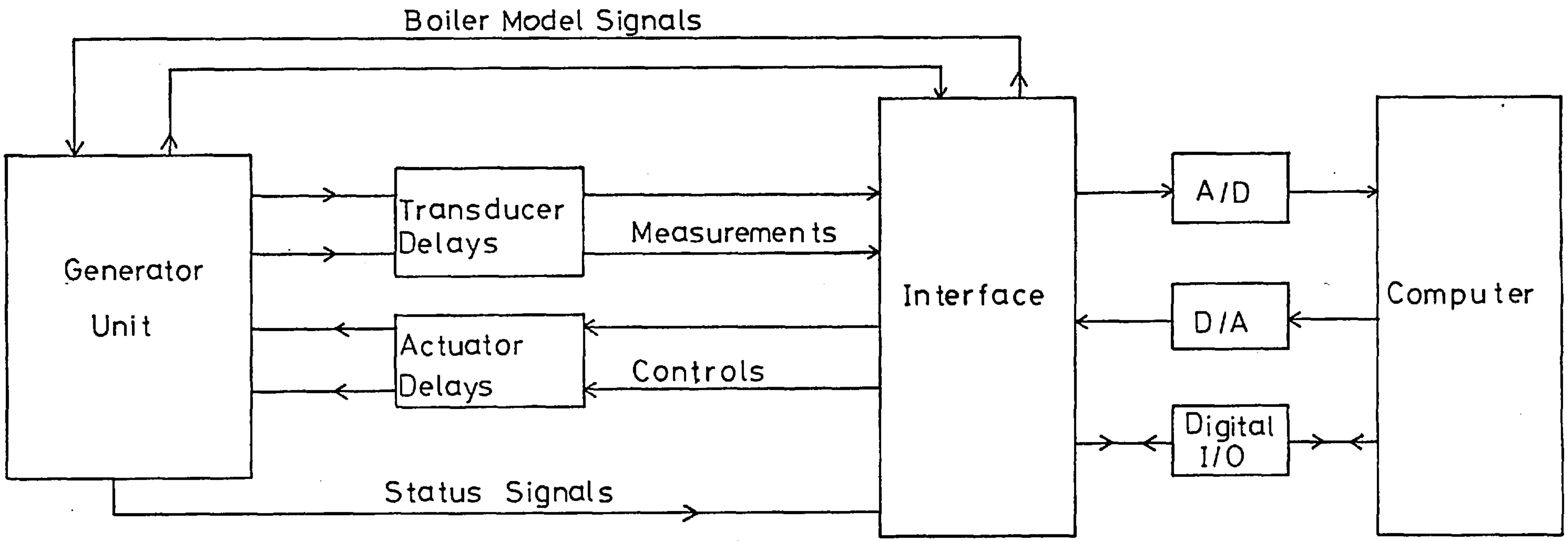

Fig. 2.5 Connection of one Generator Unit to the Computer.

network facilitate understanding of the operation of an electric power system. This is particularly suitable for meeting the training and teaching objectives, since the changes in phase angle, voltage magnitude and power flow can instantly be seen.

CHAPTER 3 THE GENERATOR UNIT

3.1 Introduction.

In the previous chapter it was explained that the sections of the generating plant to be simulated using analog equipment are the synchronous machine, its voltage regulator, and the governor and turbine. Despite the varied nature of power system plant, it is apparent that certain sections of the analog equipment are common to all simulations, and so it was realized that if a generator unit were to be built on a modular basis, it would be a simple matter to assess different models and different types of plant. The generator unit has been broken down into four sections, each of which represents a section of the actual plant. These are:

(i) The main chassis unit - comprising all the circuits common to any simulation

(ii) The synchronous machine analog

(iii) The automatic voltage regulator

(iv) The turbine and governor model

The modular system utilises a 24 way bus, to which each of the above sections is connected. This bus carries power supplies and all the necessary interconnecting signals between the sections. Provision is also made for the bus to be connected to external equipment, such as an analog computer, which can be used to test simulations easily without having to build special prototype equipment. Each section will be described in turn,its circuit will be explained, and calibration details will be given.

3.2 The Main Chassis Unit.

The following circuits are included in the main chassis unit, as they are common to all the proposed simulations:

(i) The power amplifier

(ii) The voltage-controlled oscillator

(iii) The supply regulators

(iv) Terminal current measuring circuit

(v) Terminal voltage measuring circuit

(vi) Reactive power measuring circuit

(vii) Rotor angle meter

Each of these circuits will now be described, and calibration details given where necessary.

3.2.1 The Power Amplifier.

The amplifier is required to provide the alternating voltage which drives the network, and this places certain rather unusual requirements on the amplifier. It must have good regulation, a low output impedance and must also be capable of operating with a load of any power factor. There were financial constraints on the design, and these necessitated the use of the output transformer and power supply form the original CERL model. Depending on the type of representation usedfor the synchronous machine, the amplifier must also be able to provide up to 80 V rms at the terminals, at full load current. The circuit diagram is shown in Fig. 3.1. The design is based on one by Sheldrake and Giles, with subsequent modification by Tan[36].

The output stage consists of a transformer-coupled push-pull transistor pair, Tr 3 and Tr 4, and these in turn are biassed and driven by a pair of emitter followers, Tr 1 and Tr 2. The complementary drive to these transistors comes from OA 3 and OA 4, with the first of these combining the input signal and the feedback derived from the output, while OA 4 provides a phase reversal to give the balanced drive. The amplifier proper is preceeded by a 2 pole low-pass filter, OA 1, and a phase correction circuit, OA 2. This is included to remove any distortion which might be present in the 50 Hz waveform, and is arranged to have two coincident poles, with a cut-off frequency of 80 Hz. The actual power amplifier has a flat frequency response from 25 Hz to 1 kHz, with a phase

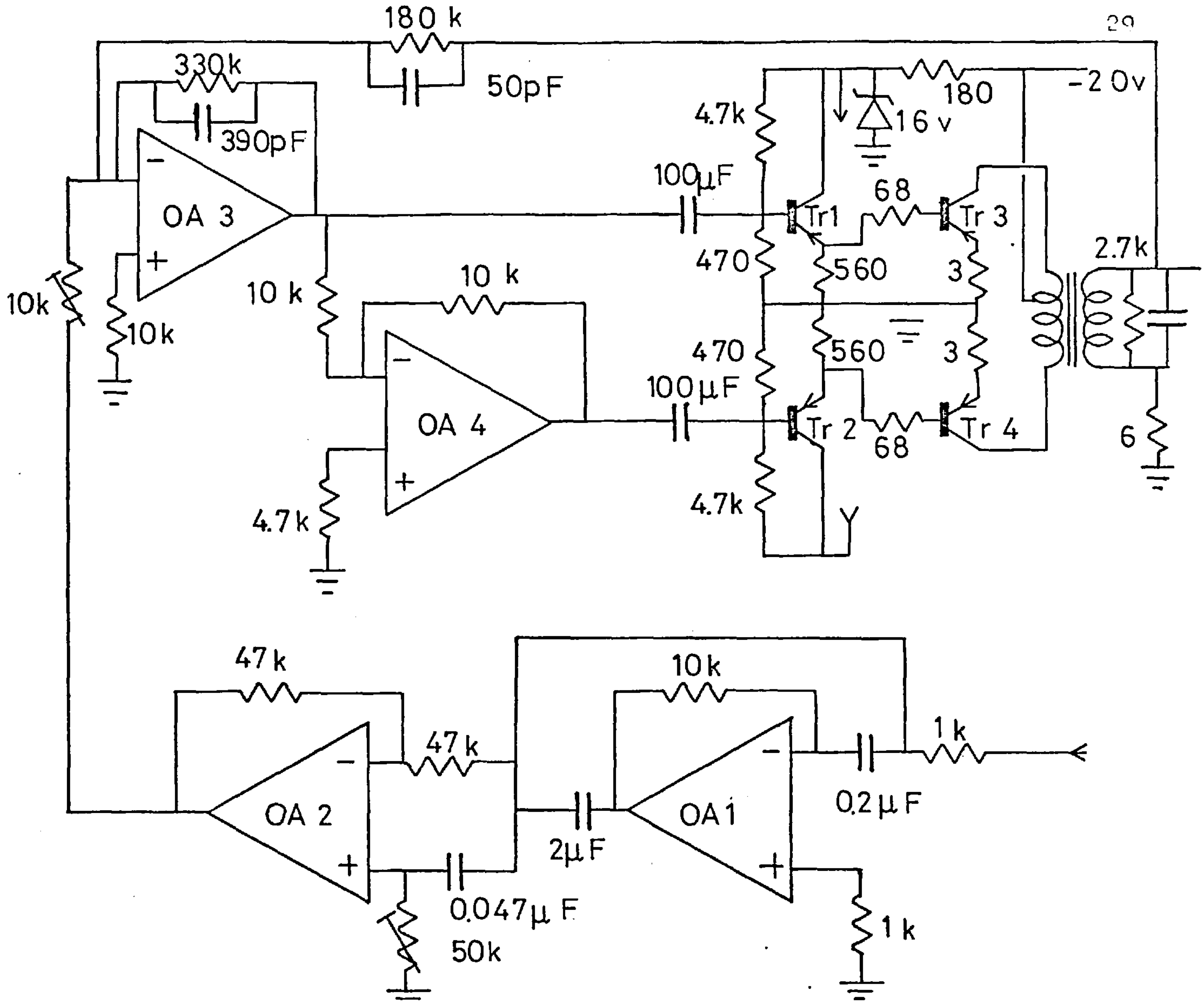

Fig. 3.1 The Power Amplifier and Filter.

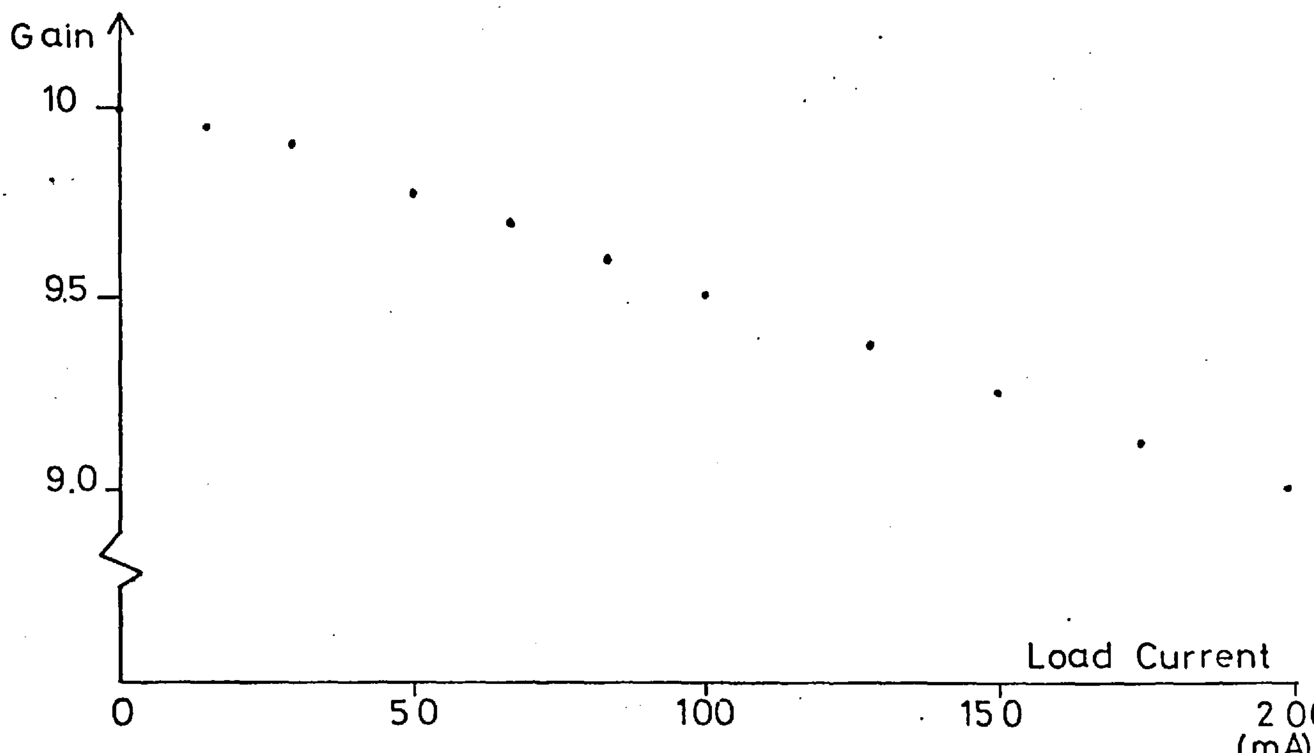

Fig. 3.2 Amplifier Regulation Test.

error of less than 2 degrees. The overall gain of this section is adjusted to be 10, and Fig. 3.2 shows the regulation for different load currents at unity power factor, and it can be seen that the regulation for 1 p.u. current is better than 2%. The gain is also constant for output voltages up to 75 V rms, and the maximum voltage attainable is 83 V rms.

3.2.2 The Voltage Controlled Oscillator.

The voltage-controlled oscillator (vco) is the most important part of the simulator, for the ultimate accuracy of the whole simulation depends on it. There are two main approaches to the problem, one of which depends upon varying the feedback gain of a second order system. This is shown in Fig. 3.3. The frequency is given by K, where K is the loop gain, and thus if a voltage-controlled attenuator is inserted in the loop, such that $K \propto V^2$, where V is the controlling voltage, then the frequency will be proportional to this controlling voltage. The magnitude of the oscillation, however, is determined by the integrator initial conditions, in the case of ideal integrators, but in practice a limit cycle oscillation will occur, giving a non-sinusoidal output. This approach was adopted by Ehsan,[38] who managed to produce a working circuit, but it required careful adjustment, and was considered unsuitable for general use.

The other technique does not produce a sine wave directly, but rather a triangular wave. The principle is shown in Fig. 3.4. A capacitor is charged from a voltage-controlled current source, VCCS 1, with a current I, and it can be discharged by connecting a second current source, VCCS 2, across it. This second source is connected by a comparator when the capacitor voltage reaches a certain value, and is then disconnected when the voltage is reduced to zero. The rate of change of voltage is proportional to the current, and hence the frequency is proportional to the controlling voltage, provided the switching thresholds remain constant.

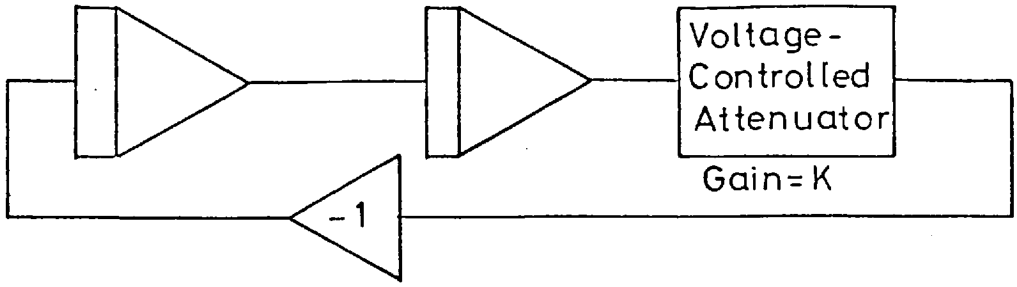

Fig. 3.3 Analog Computer Type VCO.

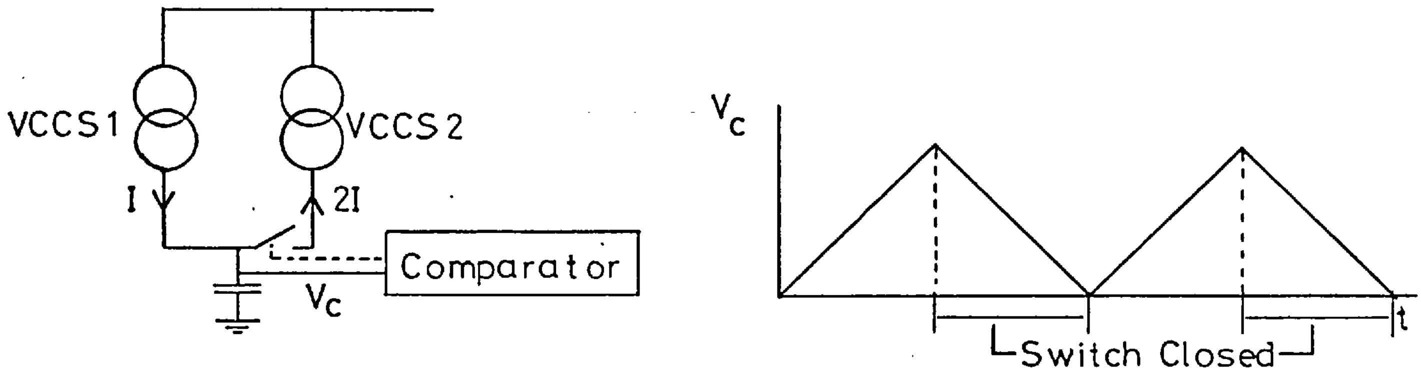

Fig. 3.4 I.C. Type VCO.

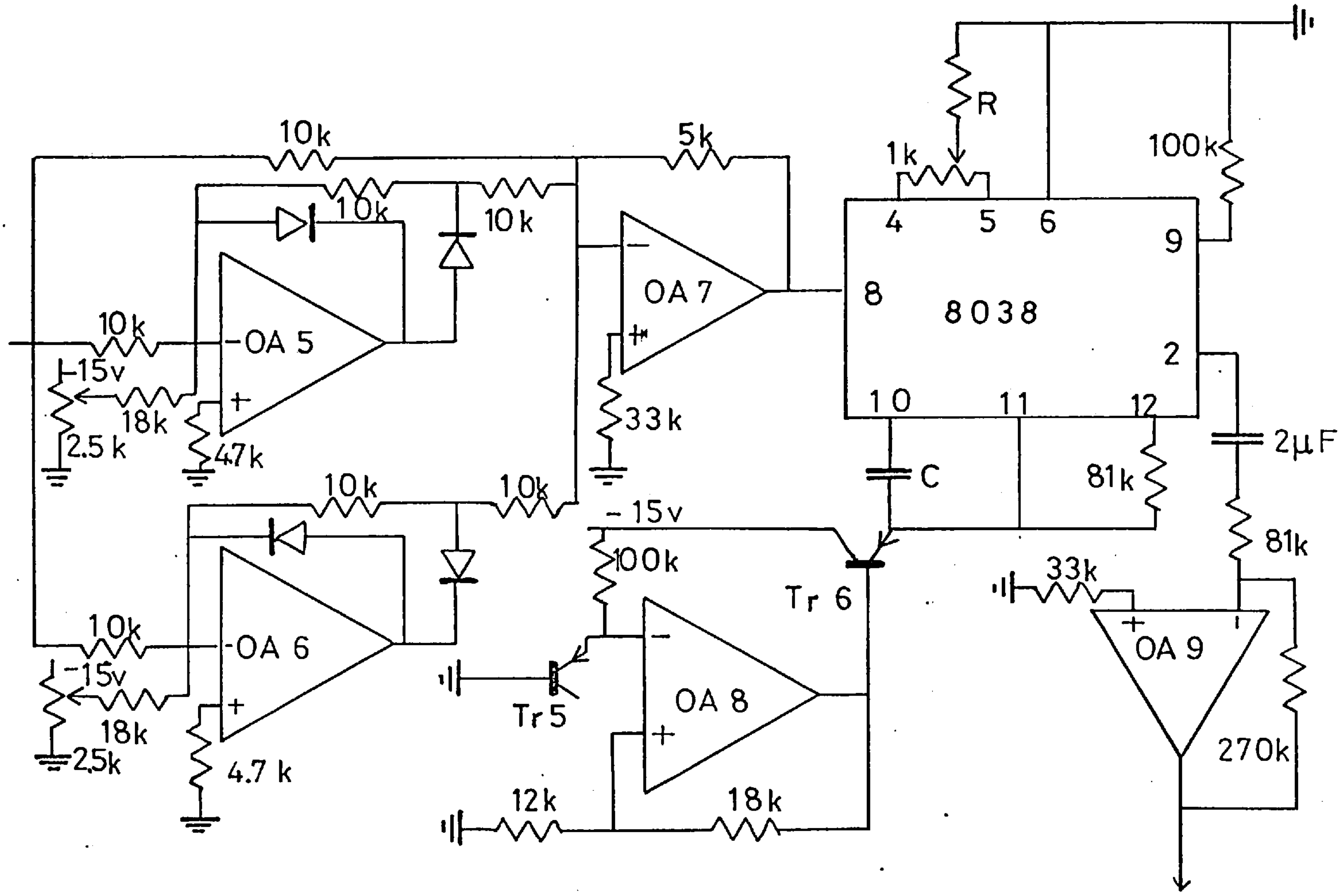

Fig. 3.5 VCO Circuit Diagram.

The triangular wave can be fed into a diode function generator, to give a good approximation to a sine wave. An oscillator based on this technique is manufactured in integrated circuit form by Intersil[39], and one of these devices was tested in the circuit shown in Fig. 3.5. The frequency of oscillation is given by

$$f = \frac{3 \quad V_{68}}{2\ R\ C\ V_{6\ 11}}$$ where V_{68} is the voltage between

pins 6 and 8, and $V_{6\ 11}$ is the power supply voltage. The first of these is the controlling voltage, and the switching thresholds are determined by the supply voltage. Thus the frequency is very dependent on the power supply voltage, and for this purpose a precision voltage regulator was built. This comprises OA 8, Tr 5 and Tr 6. The reference element, Tr 5, is a reversed-biased base-emitter junction of a planar transistor, which has a sharper cut-off and is thermally more stable than a zener diode. OA 8 acts as a comparator, and drives Tr 6 which is the series regulating transistor. The voltage is adjusted to be exactly -12 V, and this has been found to be accurately maintained in use. The controlling voltage is passed through a limiting circuit, consisting of OA 5, OA 6 and OA 7, and this prevents the oscillator from operating at abnormally low or high frequencies. The limits are set to give a frequency range of 45 - 55 Hz. The actual frequency of oscillation is adjusted by changing the RC combination associated with the oscillator, and is set to give 50 Hz for an input of +5 V, with a sensitivity of 0.1V/Hz. The output of the oscillator is capacitively coupled to an amplifier, OA 9, whose gain is adjusted to give a sinusoidal output of 10 V p-p. A calibration curve showing the frequency of the output against the control voltage is given in Fig. 3.6.

3.2.3 <u>The Voltage Regulators</u>.

Two voltage regulators are included in the main chassis, for supplying those circuits which require a stable voltage, and also for use as manual reference control signals. One positive and one negative regulator were built, using a circuit similar to that employed in the voltage-

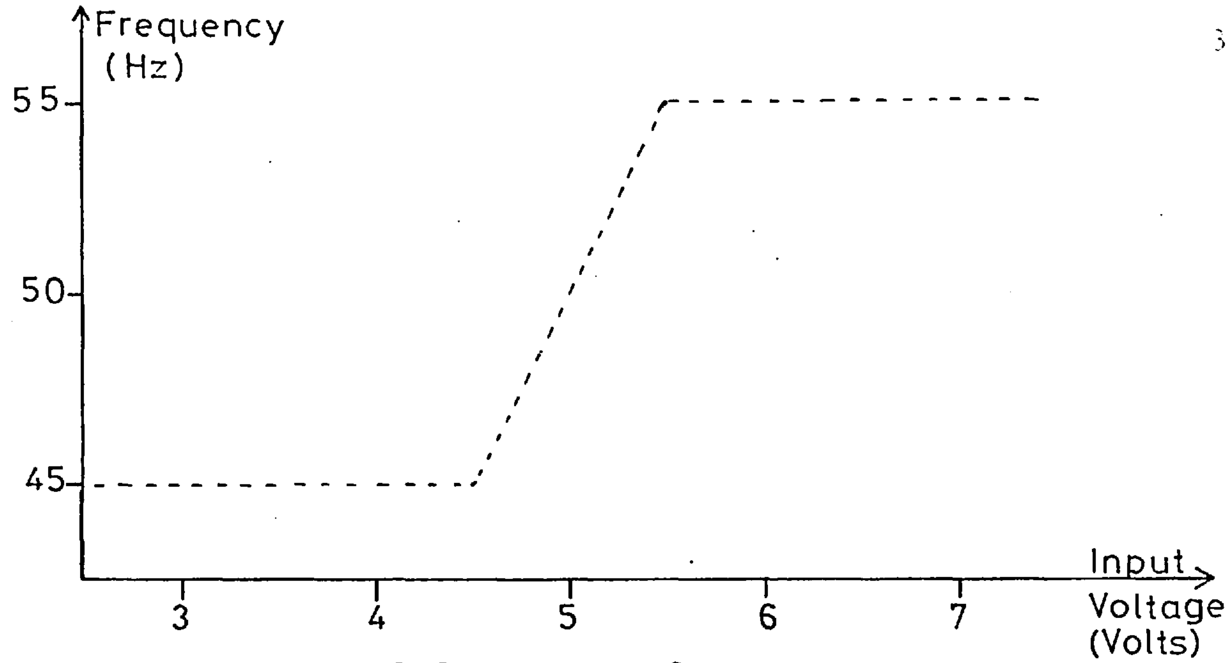

Fig. 3.6 VCO Calibration Curve.

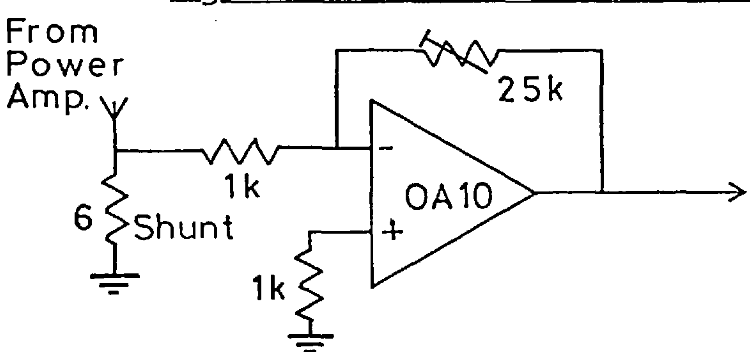

Fig. 3.7 Current Signal Amplifier.

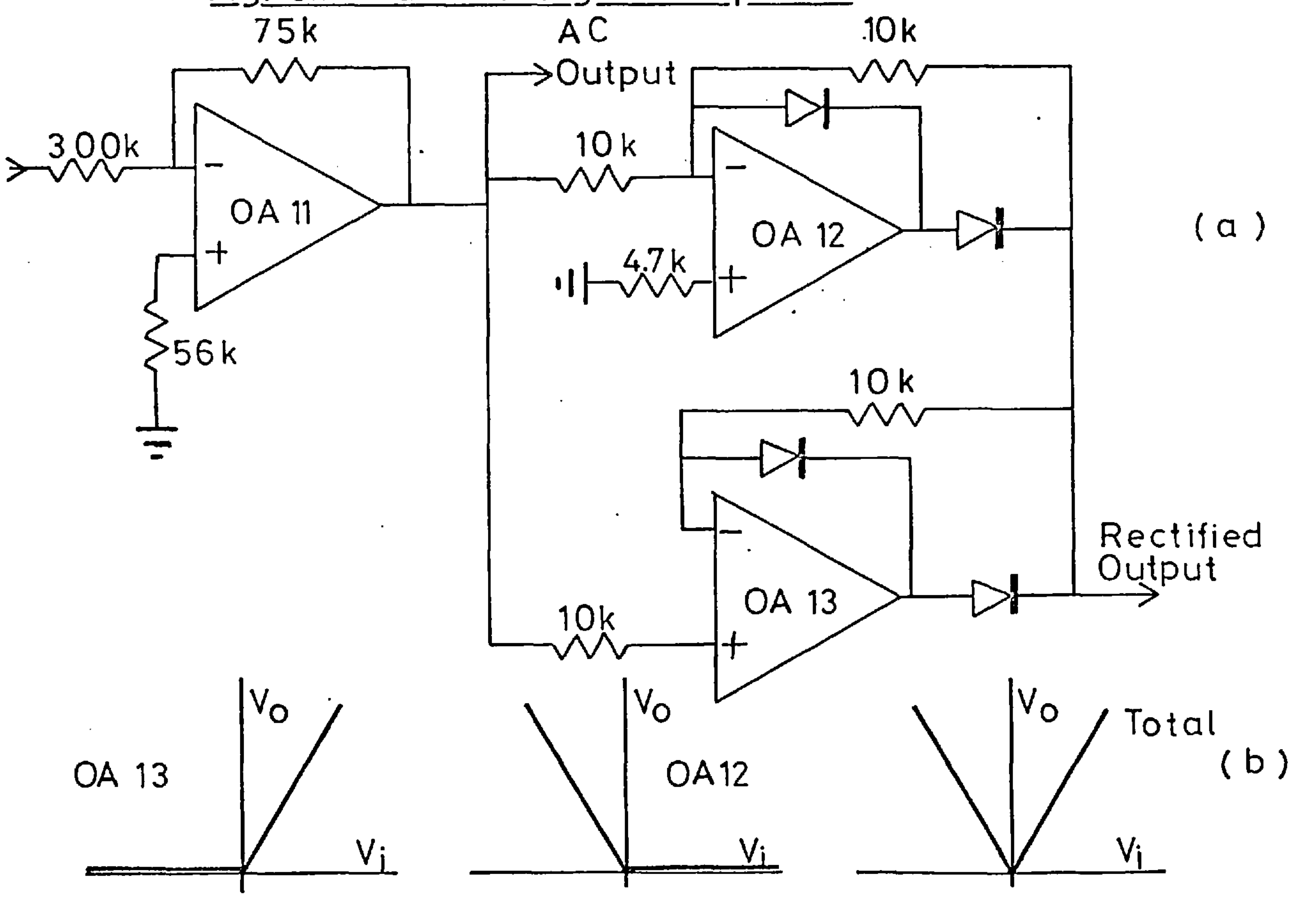

Fig. 3.8 (a) + (b) Voltage Measuring Circuit + Transfer Function.

controlled oscillator. The outputs were adjusted to $\pm$ 12 volts, and the regulation for a load current of 150 mA was found to be better than $\frac{1}{2}$%.

3.2.4 Current and Voltage Measurement.

The terminal current of a generator unit is measured by a resistive shunt which is included in the secondary of the amplifier output transformer. The circuit is shown in Fig. 3.7. The gain of the amplifier is adjusted such that 1 p.u. current gives 8 V p-p at the output. The circuit to measure the terminal voltage is shown in Fig. 3.8, and it consists of two stages. The first, OA 11, is a buffer stage with a gain of -0.25, and its output is used to drive the VAr meter and the rotor angle meter. The next stage, OA 12 and OA 13, is a "perfect" rectifier circuit, which produces a full-wave rectified version of the terminal voltage. Each of these two amplifiers acts as a perfect half-wave rectifier on alternate half-cycles, and the output is the sum of the two amplifier outputs, as shown in Fig. 3.8(b). This connection gives complete compensation for the diode voltage drops, and consequently is very linear.

3.2.5 Reactive Power Measurement.

While there are different methods of measuring the real power produced by a generator unit, depending on the machine representation employed, the most satisfactory method of measuring reactive power is from the product of the voltage and current at the terminals. If the voltage signal is shifted in phase by 90 degrees, and multiplied with the current, the average value of the product is the reactive power. Thus

$$\frac{1}{T}\int_0^T V\sin(\omega t+90).I\sin(\omega t+\phi) = \frac{VI}{2}\sin\phi$$

$$= \text{Reactive power}$$

The circuit employed is shown in Fig. 3.9. The current and voltage are derived from the measurement circuits already described, and the

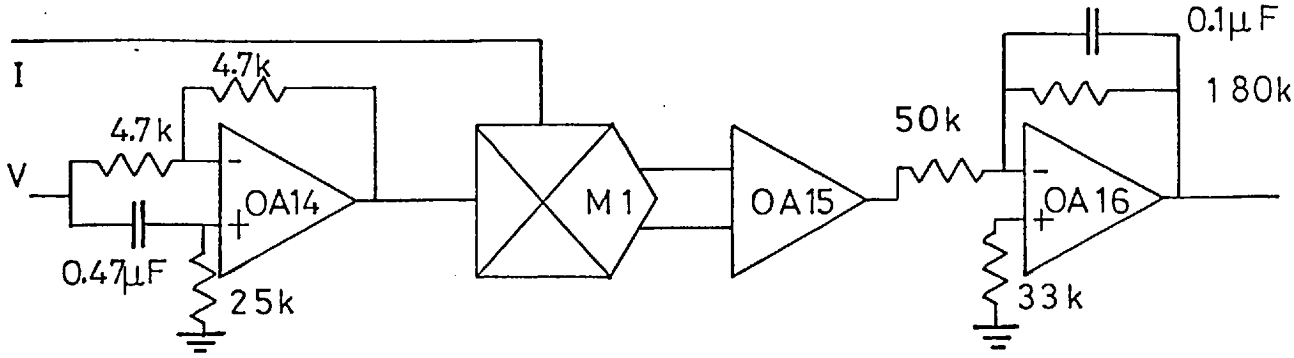

Fig. 3.9 Var Meter.

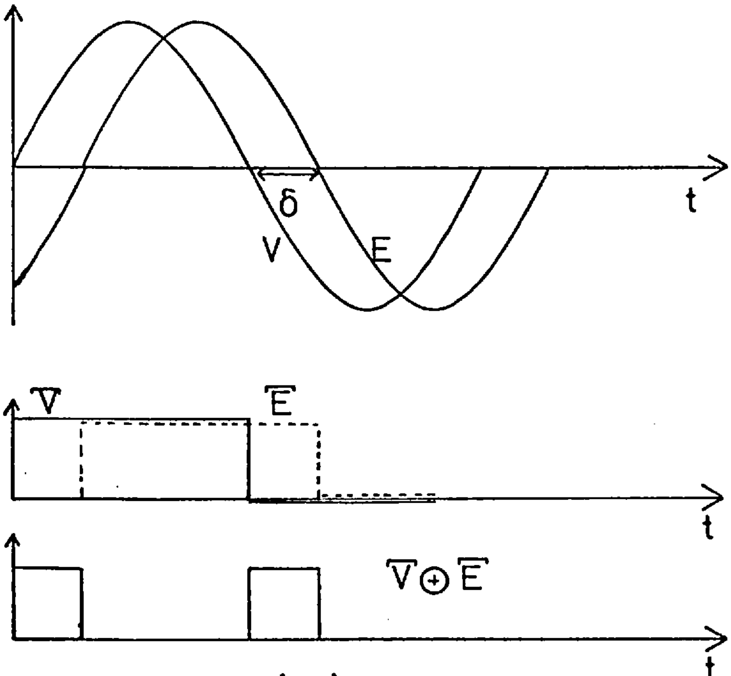

(a)

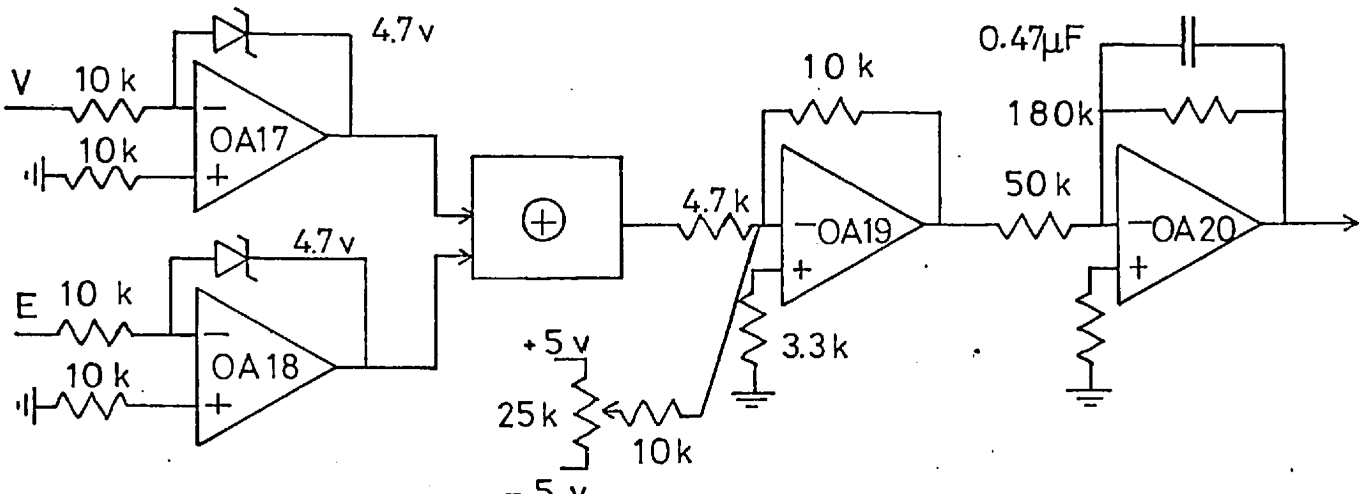

(b)

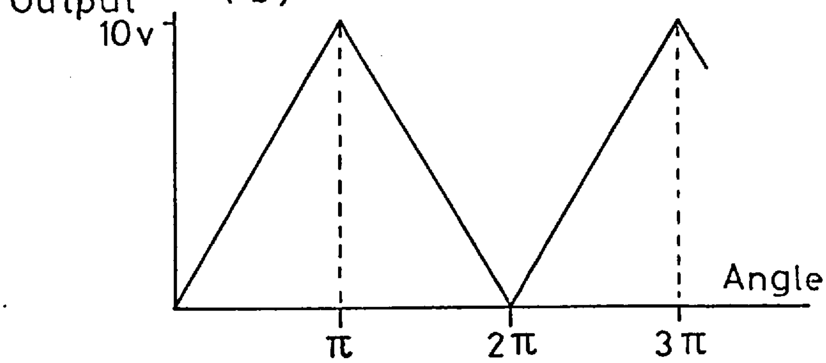

(c)

Fig. 3.10 Rotor Angle Meter - Principles and Circuit voltage is phase-shifted by 90 degrees using OA 14. The multiplication is then performed using an analog multiplier, M 1 and OA 15; further details of the multipliers are given in appendix A. The product is then passed through a low-pass filter, whose time constant is adjusted to reduce the ripple component of the signal to less than 5% of its original value. The measured reactive power is then displayed on a front panel meter.

3.2.6 Rotor Angle Measurement.

This circuit measures the angle between a pair of sinusoidal voltages, and the principle of operation is shown in Fig. 3.10(a). The two sinusoids are first converted into TTL compatible square waves by comparators OA 17 and OA 18, and these square waves are then exclusive-ORed together. The output of the exclusive-OR is a series of pulses whose width is proportional to the time between the zero-crossings of the two waveforms, and thus the average value of this waveform is proportional to the phase angle between them. The variation of the output with phase angle is shown in Fig. 3.10(c), and in the actual circuit, the signal is scaled and filtered by OA 19 and OA 20. One disadvantage of this kind of circuit is that it gives no indication of which voltage leads which, but under steady state conditions, it is known that the rotor angle will lie in the range 0 to 90 degrees.

3.2.7 Interconnection and Layout.

The whole generator unit is arranged to fit in standard 19" racks, and the front panel, shown in Fig. 3.11, carries all the metering and manual controls. The electrical interconnection of the units which make up the main chassis is shown in Fig. 3.12, and the function of the unit bus is shown in Table 3.1, which also gives the magnitudes of the various signals.

In addition to those circuits already described, there are two additional parts of the main chassis unit. The first of these is the selection

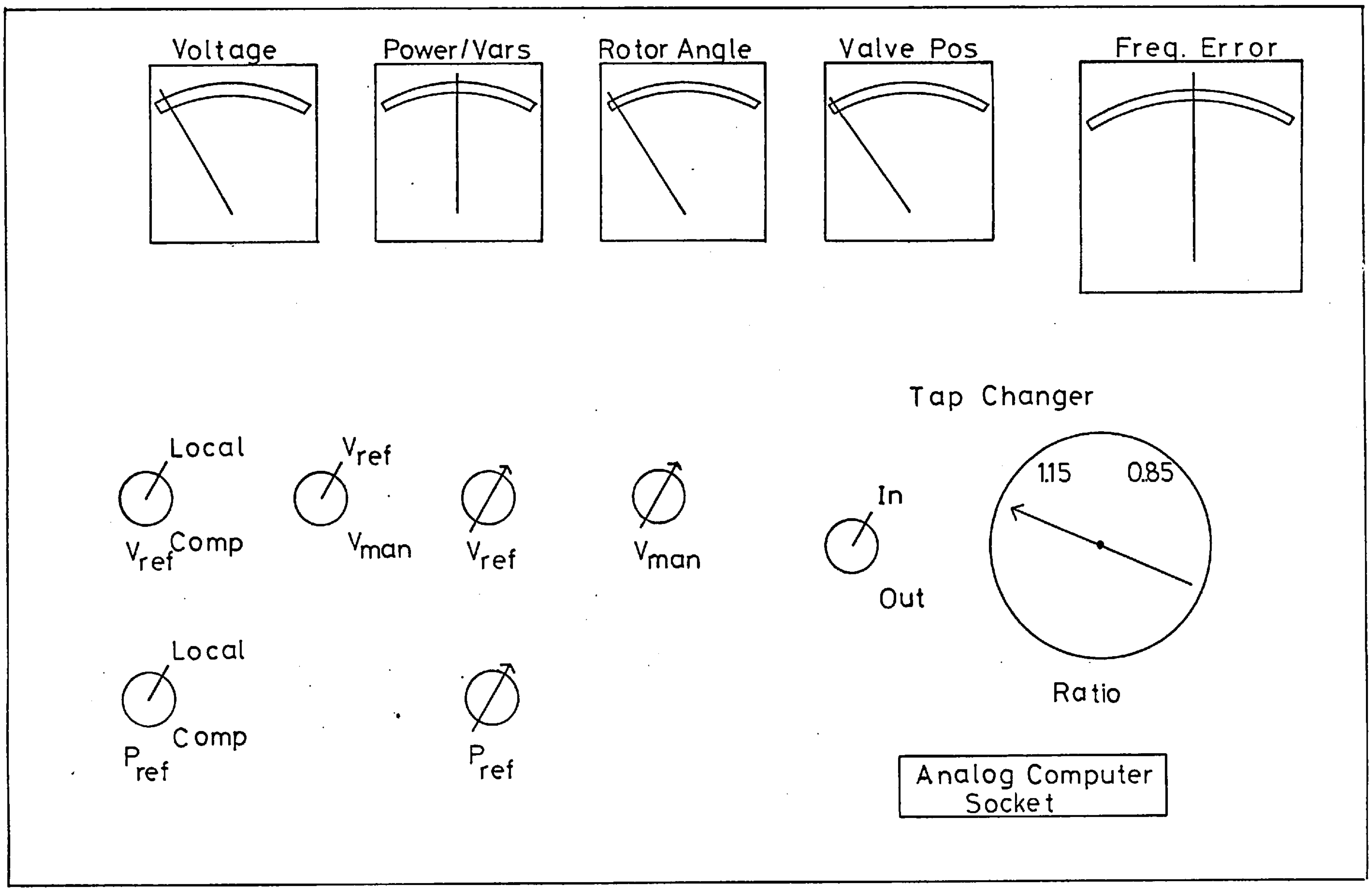

Fig 3.11 Front Panel Layout.

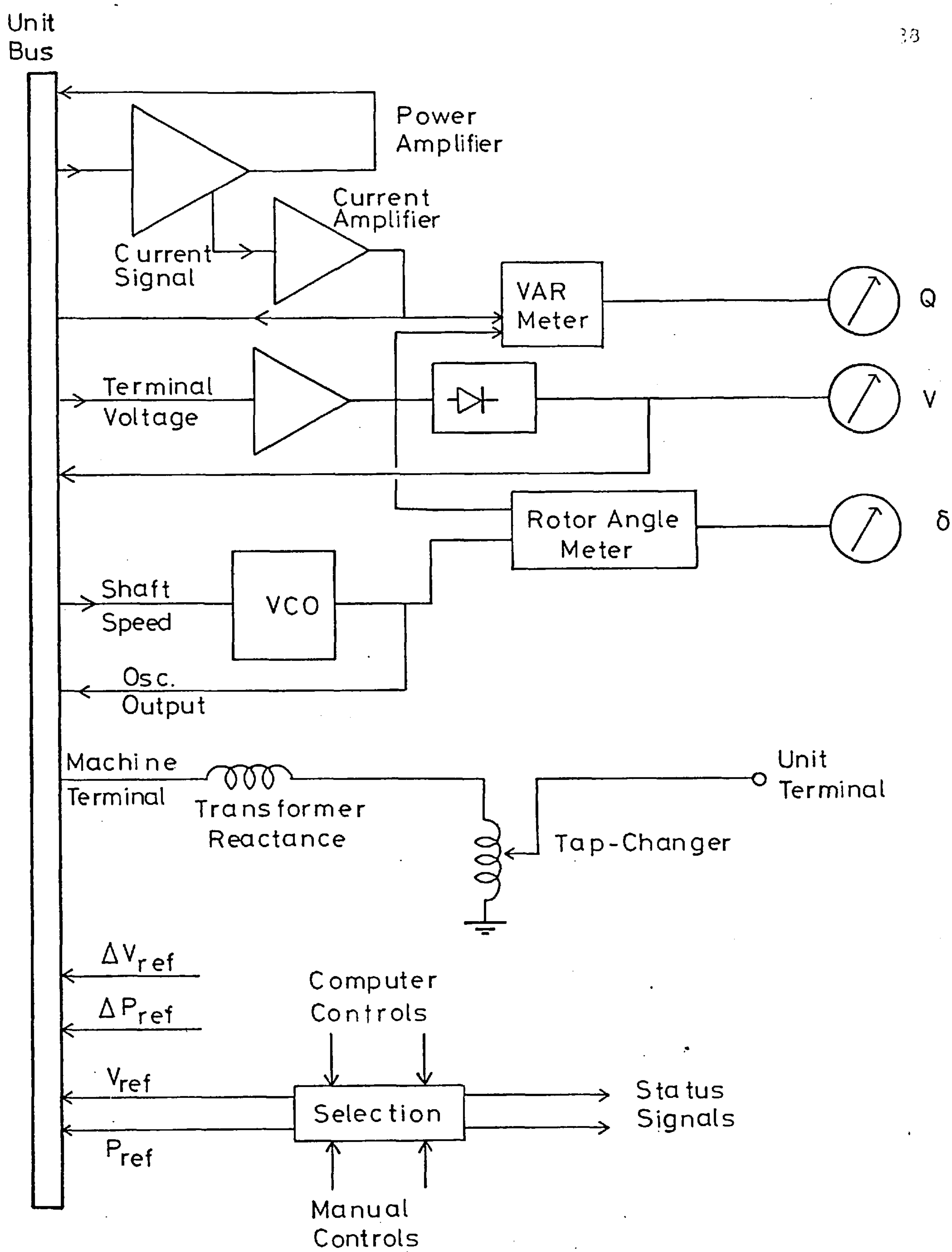

Fig. 3.12 Main Chassiss Configuration.

Table 3.1.

The Unit Bus and its Connections.

Pin No.	Function	Signal Level
1	Earth	
2	+15 v Supply	From Regulators in Unit
3	+12 v Supply	
4	-12 v Supply	
5	-15 v Supply	
6	-20 v Supply	
7	Reference Power Setting	-5 v = Full Load
8	Δ Reference Power Setting	
9	Electrical Power	5 v = 1 p.u.
10	Reference Voltage Setting	-5 v = 1 p.u.
11	Δ Reference Voltage Setting	
12	Terminal Voltage Magnitude	5 v = 1 p.u.
13	Amplifier Input	
14	Machine Terminal	20 v = 1 p.u.
15	Current Signal	8 v pk-pk for 1 p.u.
16	Oscillator Output	10 v pk-pk
17	Frequency Signal	5 v = 50 Hz
18	AVR Output	1 v gives rated voltage on open-circuit
19	Amplifier Output	
20	Spare	
21		
22		
23		
24		

of the voltage reference and the speeder gear setting, which can be supplied either manually or as an output from the computer, and there is a corresponding status signal which indicates to the computer whether or not a particular control signal is provided manually. The second additional circuit is the inclusion of an inductor, X_T, which represents the generator transformer reactance, and also a tap-changing transformer whose ratio goes from 0.85 to 1.15 in steps of 0.02. The output of this transformer is the point which connects the generator unit to the rest of the network, and this point is taken to the generator patching panel.

3.3 The Automatic Voltage Regulator.

A typical voltage regulating system is shown in Fig. 3.13(a), and the section of it which is simulated in the AVR unit comprises the comparator, the amplifiers, the exciter and the stabilizing transformer. There have been many proposals for representing voltage regulators[40 - 43], but the method adopted here is that suggested by the IEEE Working Group of the Excitation Systems Subcommittee as their Type 1 model[40]. This is shown in Fig. 3.13(b), and typical parameters are given in Table 3.2. This representation is designed for simulating continuously acting systems, with rotating exciters, but by a suitable choice of parameters, it can be made to represent almost any type of excitation scheme.

The conversion of the block diagram of Fig. 3.13(b) into an electronic circuit presents no great difficulty, except for the process of rectifying the terminal voltage waveform. The high loop gain and the number of poles in the system demand that the time constants associated with the rectification and filtering of the terminal voltage waveform should be as small as possible.

3.3.1 Filtering the Rectified Waveform.

In a real system, the terminal voltage is measured using a three phase full-wave bridge rectifier, whose output can be expressed as

$$V_r = \frac{3\hat{V}}{\pi} - \frac{6\hat{V}}{\pi}\sum_{\nu=6,12}^{\infty}\left[\frac{(-1)^{\nu}}{\nu^2-1}\right]\cos(\omega\nu t)$$

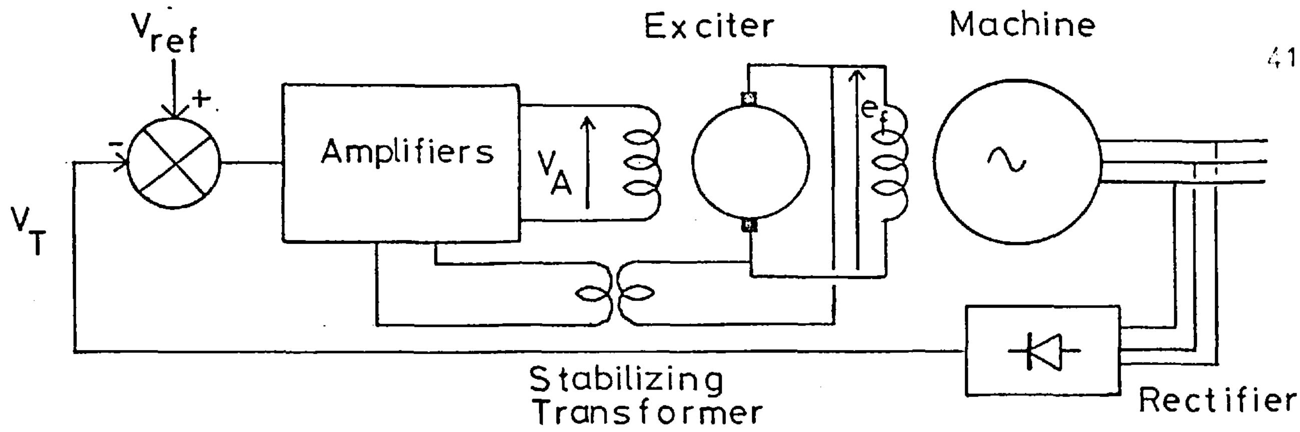

Fig. 3.13(a) Typical Voltage Regulating System.

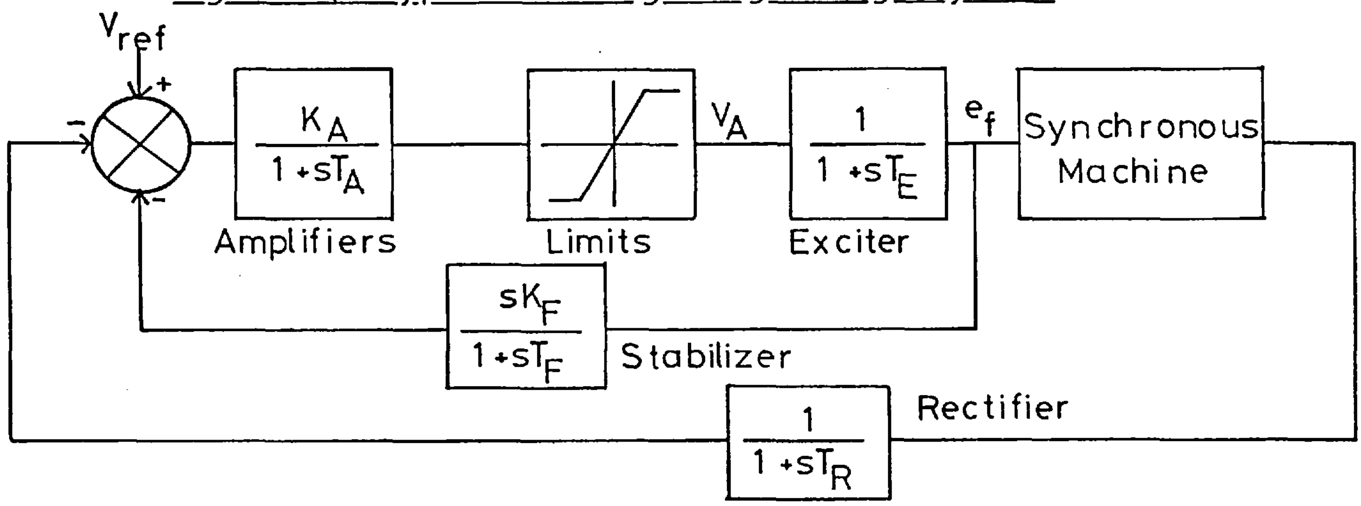

Fig. 3.13 (b) IEEE Type1 Representation

Table 3.2 Typical AVR Parameters.

K_A	50 – 600
T_A	0.02 – 0.2 sec
T_E	0.25 1.5 sec
K_F	0.01 - 0.08
T_F	0.35 - 1.0 sec
T_R	0.0 – 0.6 sec
Ceiling Limits	3–7 x Rated

where $\hat{V}$ is the peak value of the waveform. The first harmonic is at 300 Hz, and its magnitude relative to the dc component is 0.057. In the model, a single phase representation is used, and the rectified version of the terminal voltage can be expressed as

$$V_r = \frac{2\hat{V}}{\pi} - \frac{4\hat{V}}{\pi} \sum_{\nu=2,4,6}^{\infty} \left[\frac{(-1)^{\nu/2}}{\nu^2 - 1} \right] \cos(\omega \nu t)$$

The first harmonic here is at only 100 Hz, and its magnitude relative to the dc component is 0.66.

Thus it can be seen that the problem of removing the harmonics from the measurement of the terminal voltage is much more severe in the case of the single phase model. The reason why the harmonics must be removed is that the output from the amplifier stage, V_A, must be reasonably free from ripple. If a 10% ripple is permissable, then with an amplifier gain of 400, the ripple on the input signal must be less than 1/4000 of the dc component of the input. If the excitation limits are set to $\pm$ 5 x rated field voltage, then if the ripple is greater than 1.2% of the dc component, the output of the amplifier will be driven between the two saturation levels. A simple filtering scheme to remove the harmonics rendered the whole AVR system unstable, and the method finally adopted is shown in Fig. 3.14. A pair of twin-tee notch filters remove respectively the 100 and 300 Hz components, and an extra pole is also included. The effect of this pole is then cancelled out by the inclusion of a coincident zero as part of the exciter transfer function. This is quite satisfactory provided that one of the amplifier limits is not reached, but even in that eventuality the errors were found to be quite tolerable.

The circuit diagram is shown in Fig. 3.15; the rectified terminal voltage V_T is applied to OA 21, which represents the filter and rectifier time constants, and is then filtered by the pair of twin-tee filters. These eliminate the 100 and 300 Hz components, and are buffered by OA 22. The next amplifier, OA 23, acts as the comparator, and also serves to produce

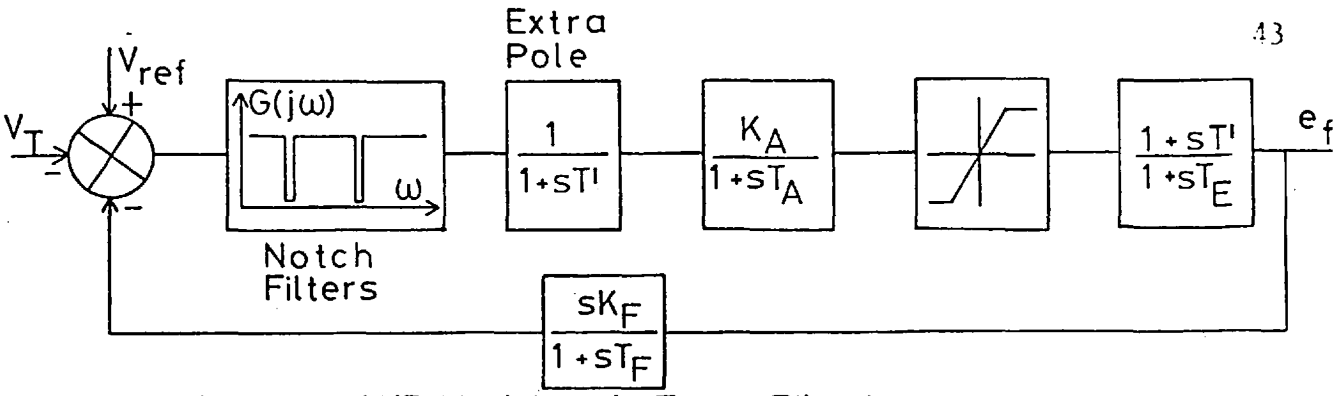

Fig. 3.14 AVR Model with Extra Filtering.

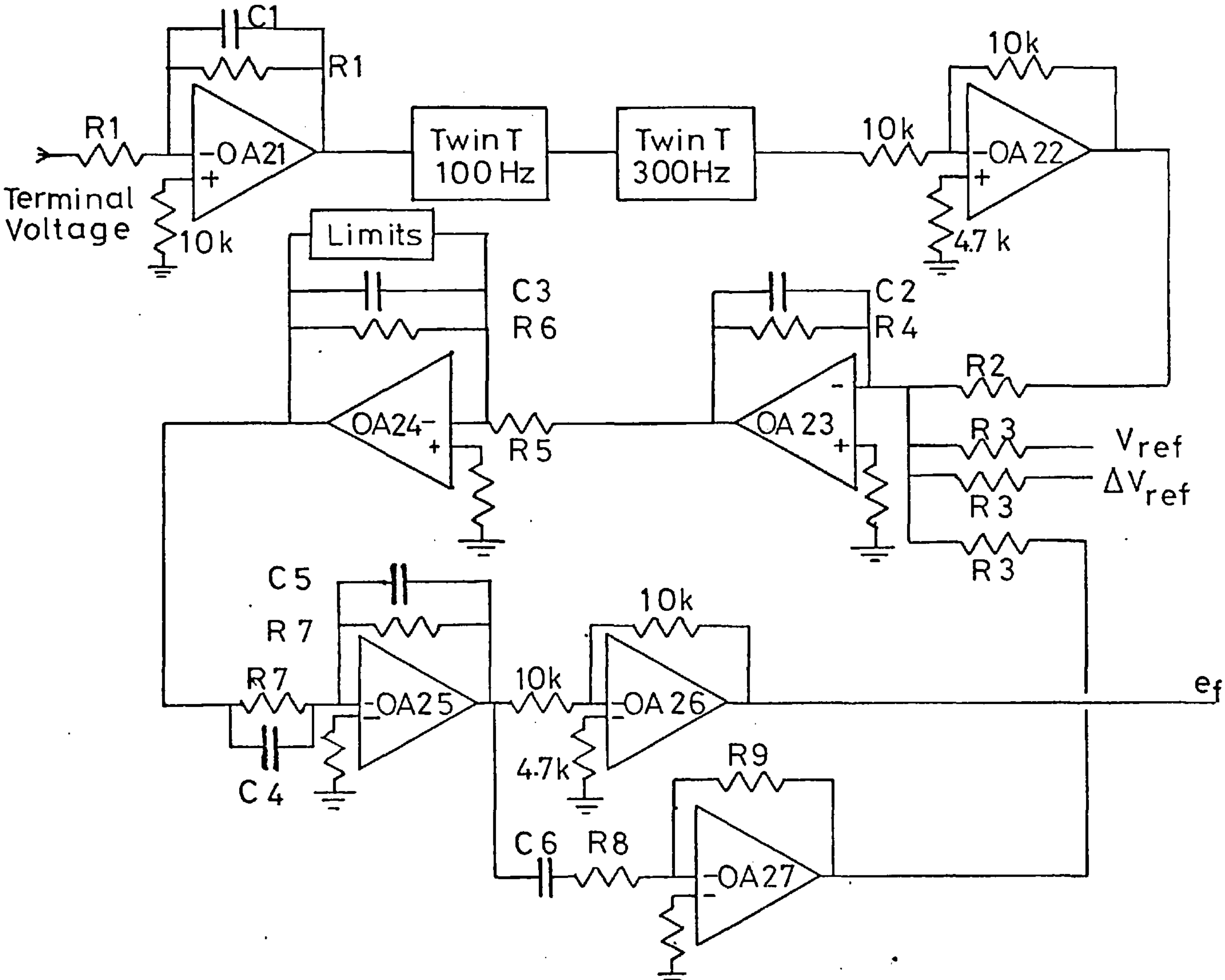

Fig. 3.15 AVR Circuit Diagram.

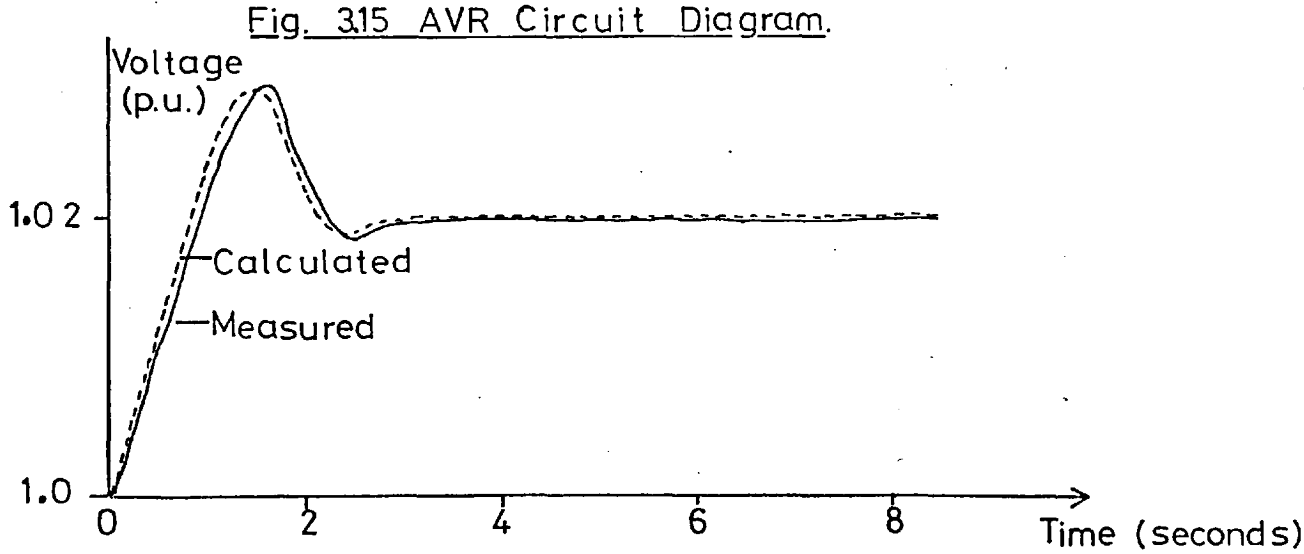

Fig. 3.16 AVR Step Response.

the extra pole which is required for the filtering. The gain, K_A, is divided between this stage and the next, OA 24, which includes the limits and the amplifier time constant. OA 25 represents the exciter, and also the additional zero, while the signal is finally inverted by the unity gain OA 26; this signal is the synchronous machine field voltage. The stabilization signal is produced by OA 27 and fed back to OA 23. The relationship between component values and the system parameters is given by the following equations:

$T_R = C_1R_1$ sec $\qquad R_2/R_3 = 2\sqrt{2}/\pi$

Extra pole = C_2R_4 = Extra zero = R_7C_4 sec

$K_A = (R_4R_6)/(R_3R_5)$ $\qquad T_A = R_6C_3$ sec

$T_E = R_7C_5$ sec

$K_F = R_9 / R_8$ $\qquad T_F = R_8C_6$ sec

As constructed, the AVR had the following parameters:

$T_R = 0.01$ sec

$K_A = 400$ $\qquad T_A = 0.04$ sec

$T_E = 1.0$ sec

$K_F = 0.04$ $\qquad T_F = 1.0$ sec

Fig. 3.16 shows the response of the system to a 2% change in reference voltage, with the synchronous machine on open circuit, with a time constant $T'_{do} = 6.0$ sec. The predicted value is also shown, and the agreement between the two is good. Steady-state tests showed that the AVR behaves in a linear fashion over the working range.

3.4 Governor and Turbine Simulation.

The prime movers employed in generation plant are almost exclusively hydro or steam turbines, and electronic representations of both these types of plant have been developed. The system devised for modelling the hydro turbine and governor will be discussed first, although practical experience has shown that the simulation of a hydro turbine in this way leaves much to be desired.

3.4.1 The Hydro Turbine and Governor.

The speed sensing device in the governor may be a pair of flyballs, as in the mechanical-hydraulic governor[44,45], or an ac tachometer may be used, as in the electro-hydraulic type[46]. The speed of response of the latter kind of governor is better, but a satisfactory representation involves a complicated transfer function. In consequence, and because they are fitted to the majority of hydro turbines, it was decided to simulate a governor of the mechanical-hydraulic type; the basic layout is shown in Fig. 3.17[47]. The shaft speed of the machine is measured by the height of the flyballs, and the displacement of the link, n_s, is fed to the top floating lever. The left end of this goes to the lower floating lever, whose left-hand end is connected to the pilot valve and servo. The right-hand end of this lower lever is connected to the follow-up linkage from the speed adjuster, and the linkage from the main servo actuator. The right-hand end of the upper lever is connected via the transient droop dashpot to the servo actuator. The following equations can be written:

$$a = n_r - \sigma z - n_s - c$$

For the dashpot, it can be shown that

$$c = \frac{s\,\delta T_r}{1 + sT_r} . z$$

While for the pilot servo and the main servo respectively:

$$b = \frac{K_1}{1 + sT_p} . a \qquad\qquad z = \frac{K_2}{s} . b$$

Which gives

$$z = \frac{a}{T_g s(1+sT_p)}$$

T_g is equal to the time in seconds for a 1 p.u. change in shaft speed

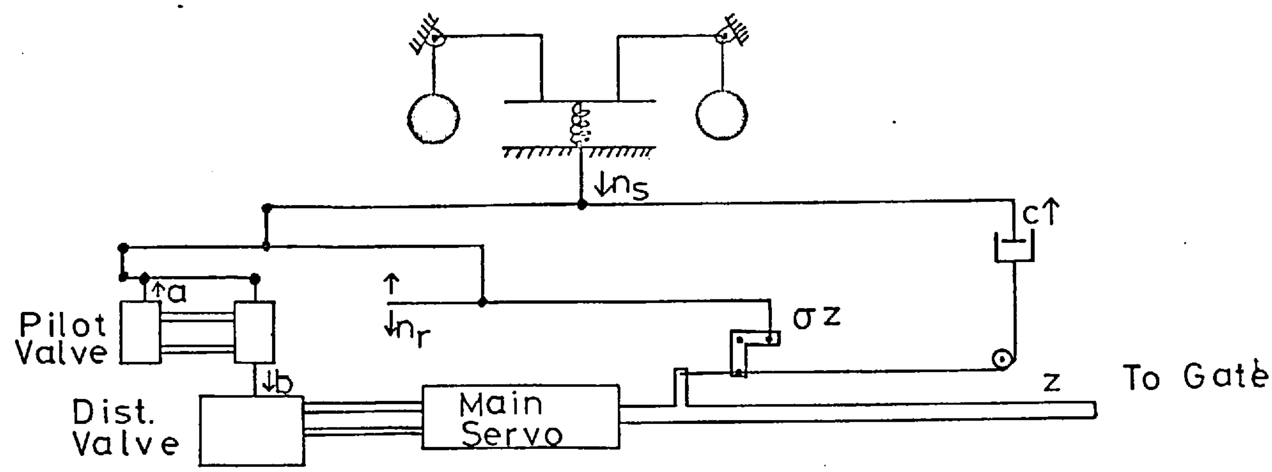

Fig. 3.17 Basic Hydro Governor

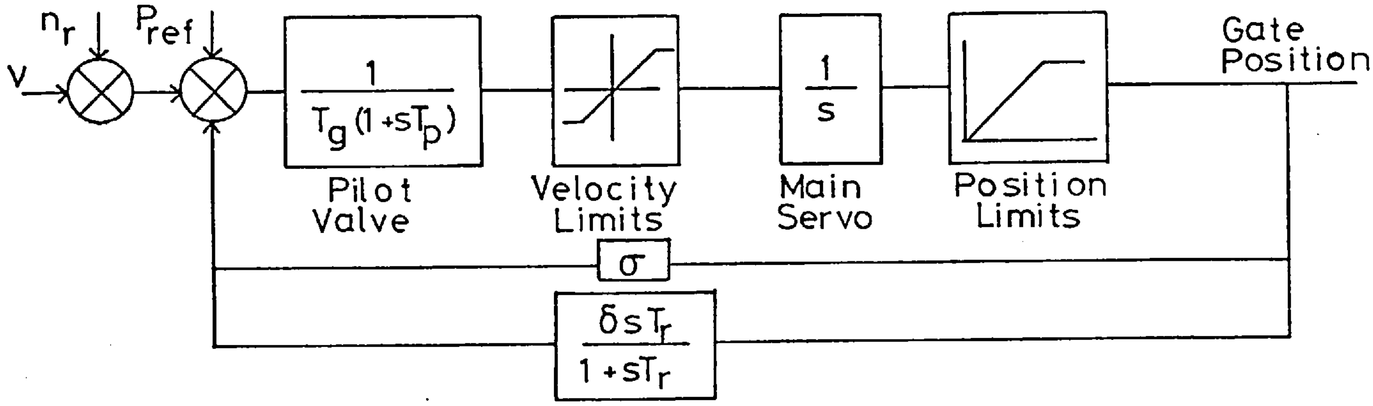

Fig. 3.18 Governor Model.

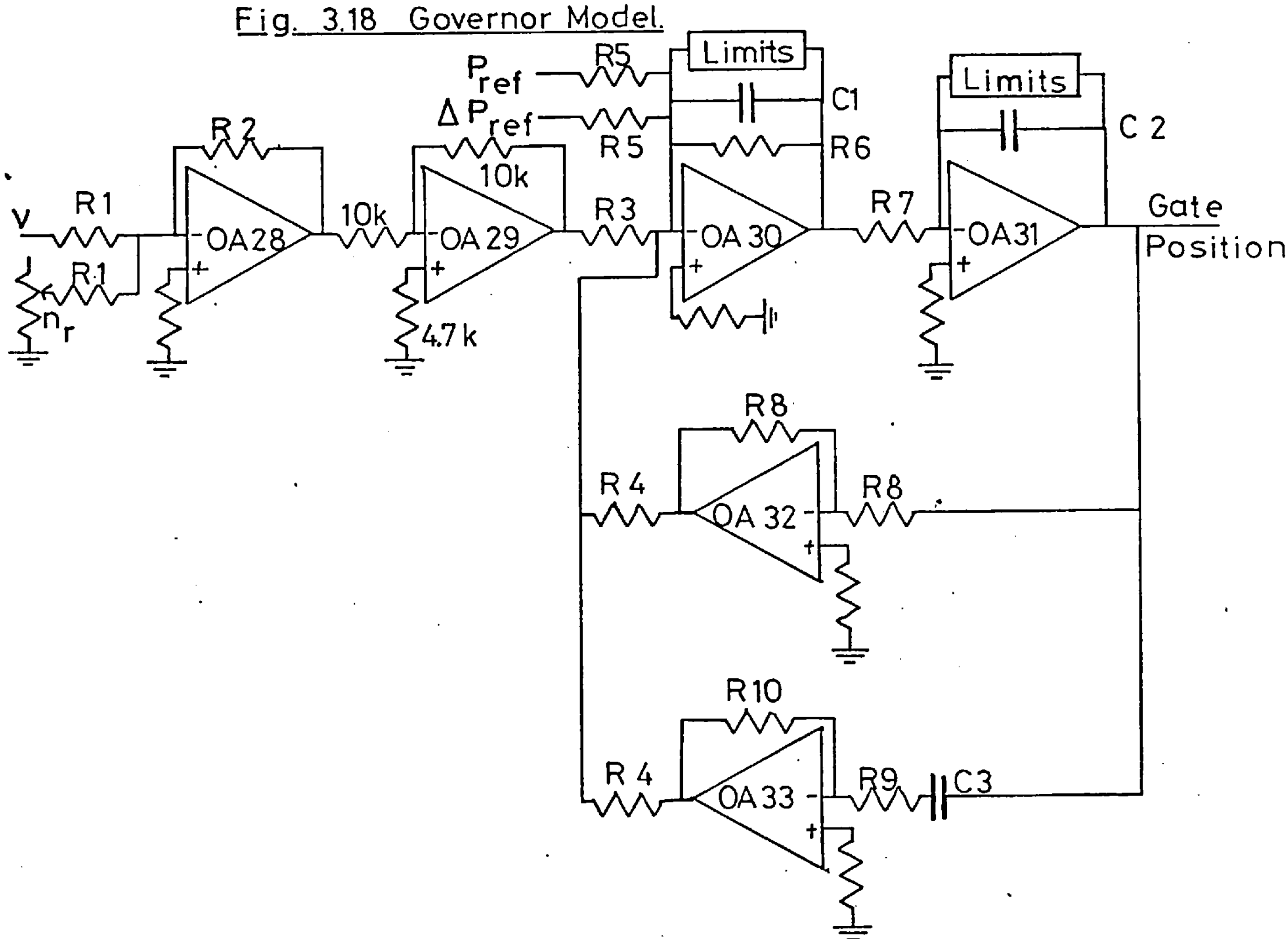

Fig. 3 19 Governor Circuit Diagram.

to produce a 1 p.u. change in gate position, and is related to the gate closing time T_c by $T_g = \beta T_c$, where T_c is the closing time in seconds, and β is the per-unit speed deviation required to saturate the pilot valve. Additionally, limits are placed on the maximum rate of travel of the gate by the saturation of the distributing valve.

However, the displacement of the top link, n_s, is not only due to the speed, as the flyball position is also determined by the speeder gear setting, which operates on the lower end of the spring, such that $n_s = \vee - P_{ref}$, where $\vee$ is the shaft speed and P_{ref} is the speeder gear setting. This can all be reduced to block diagram form, as shown in Fig. 3.18. This can be simulated in a straight-foward manner using analog equipment, and the circuit diagram is shown in Fig. 3.19.

The first amplifier, OA 28, produces a signal proportional to the speed deviation, $\vee - n_r$, and this signal is then inverted by OA 29. The next amplifier, OA 30, represents the pilot valve, summing the speed error, the speeder gear setting and the two droop signals; it also includes the gate velocity limits. This velocity is integrated by OA 31 to give the gate position, which is limited between fully open and fully closed. The output of this amplifier is then fed to OA 32 and OA 33, which produce the permanent and transient droop signals respectively.

Given that the signal levels are:

Speeder gear setting:	-5 V $= 1$ p.u.
Maximum gate velocity:	± 2 V
Gate position:	0 to 10 V

The component values to produce the desired parameters can be obtained as:

Permanent droop, σ, $= (R_1 R_5)/(R_2 R_3)$ when $R_4 = 2R_5$

Pilot valve time constant, T_p, $= R_6 C_1$ sec

Transient droop / permanent droop $= R_{10}/R_9 = \delta/\sigma$

Washout time constant, T_r, $= R_9 C_3$ sec

The chosen values were

$T_g = 0.25$ sec $\quad T_p = 0.03$ sec $\quad \sigma = 0.04 \quad \delta = 0.30$

$T_r = 5$ sec $\quad T_c = 5$ sec.

Fig. 3.20(a) shows the steady state calibration of the governor, for values of $\sigma = 0.04$ and $\sigma = 0.08$, and Fig. 3.20(b) shows the dynamic performance, with zero initial gate opening, and with a speed change of 0.5 Hz. The performance, both static and dynamic, is quite accurate enough for the intended purpose.

The requirement for a model of a hydro turbine for the simulator is that it should operate over the whole range of power output, without parameters having to be changed. The great problem is that a hydraulic turbine is very non-linear[48,49], and any model which purports to be accurate must take into account the fact that all the parameters are a function of the operating conditions, such as the head, the gate position and the blade angle. Several compromise solutions have been developed for use in analog computations, but these all employ several multipliers and square-rooters, and such an implementation is not suitable for a low-cost model. It was decided, therefore to use the classic water starting time model[50], which is frequently employed in transient stability studies. This relates the output torque T_m to the gate position according to the transfer function

$$T_m = \frac{1 - T_w s}{1 + 0.5\, T_w s} \cdot Z$$

where T_w is called the water starting time constant, and is a function of the flow conditions in the conduit; it is given by

$$T_w = \frac{lv}{h_r g}$$

where
l = length of the conduit
v = water velocity
h_r = rated head of turbine
g = acceleration due to gravity.

Under steady flow conditions, the water velocity is proportional to the gate opening, so that v can be written as KZ and the expression for

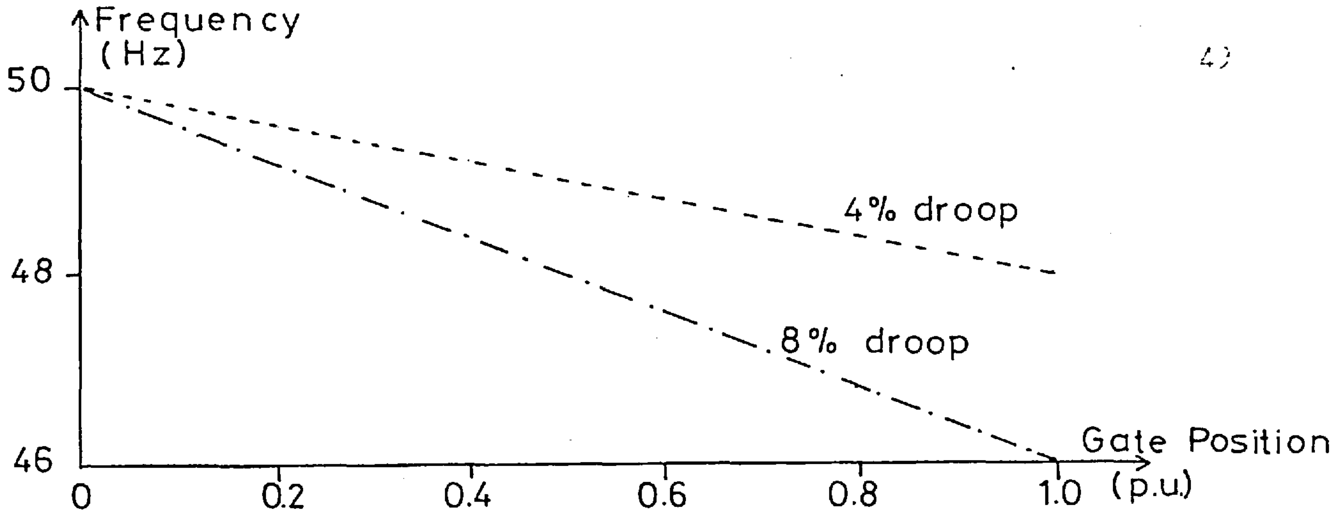

Fig. 3.20 (a) Governor Droop Characteristics.

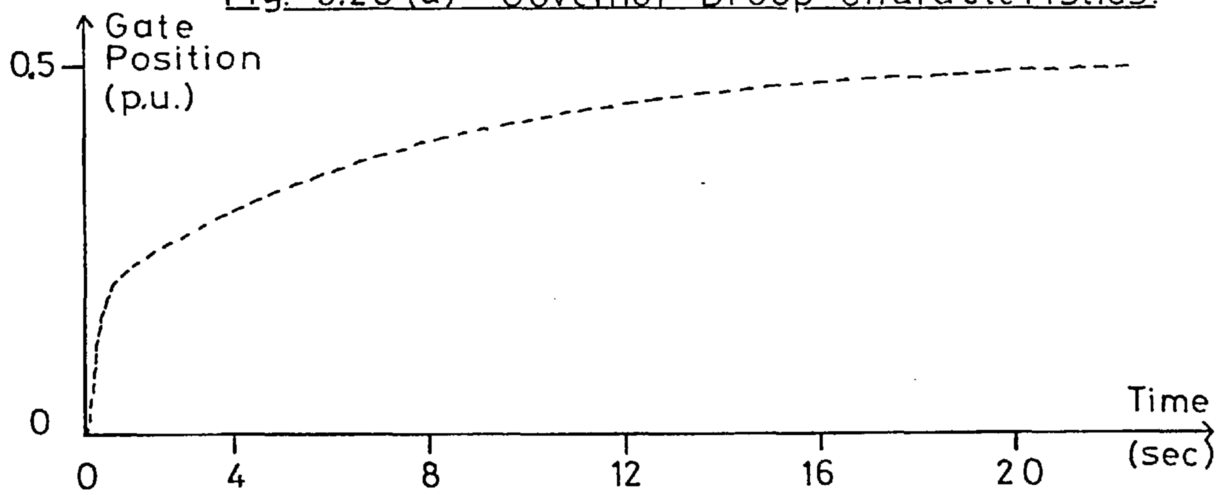

Fig. 3.20 (b) Governor Step Response.

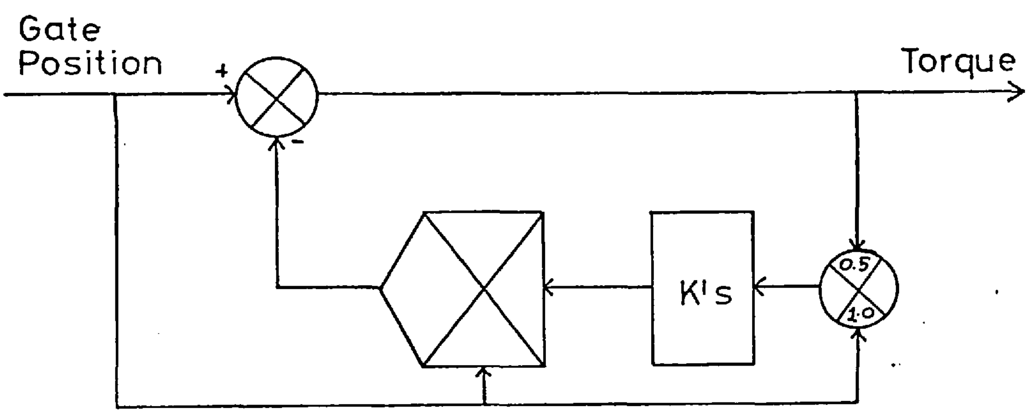

Fig. 3.21 Hydro Turbine Model.

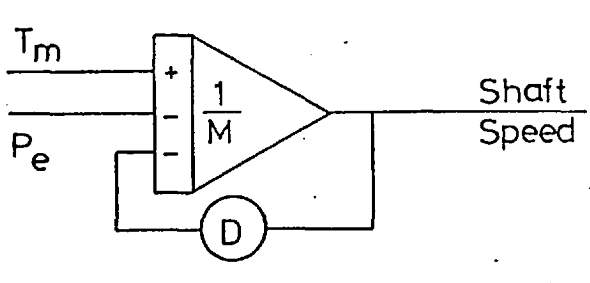

Fig. 3.22 Equation of Motion Integrator.

torque as

$$T_m = \frac{1 - sK'Z}{1 + 0.5sK'Z}.Z \qquad \text{where } K' = \frac{T_w}{Z}$$

This can be expanded as

$$T_m = Z - (K'Z).sZ - (K'Z/2).sT_m$$

and can be organized in block form as shown in Fig. 3.21. This includes the use of a differentiator, which is rather undesirable, but as the changes in gate position are limited by the maximum gate velocity, the differentator can be made to have a small bandwidth, and this overcomes the main objection.

The turbine model must also represent the mechanical dynamics of the shaft, to produce a signal proportional to the shaft speed V. Writing an equation for the motion of the shaft, we have

$$\dot{V} = \frac{1}{M} \left(T_m - \frac{P_e}{V} - DV \right)$$

where T_m is the mechanical torque
P_e is the electrical power
DV is the frictional loss
and M is the moment of inertia

This can be integrated as shown in Fig. 3.22, which assumes that the shaft speed changes are sufficiently small to be neglected when calculating the electrical torque term.

The circuit diagram of the whole turbine simulation is shown in Fig. 3.23. The summation of the gate position and torque signals and their differentiation is performed by OA 34 and OA 35 respectively, and this signal is then multiplied by a filtered gate position signal. An RC network is included to filter the gate position signal to enable the constant T_w to change only slowly, and not to follow rapid fluctuations of the gate position. The multiplier output is added to the position signal by OA 37, whose output is the torque signal. This is inverted by OA 38, and then fed to the equation of motion integrator OA 39. This sums the mechanical and electrical torque signals, which are of opposite polarities, and also includes the effect of frictional damping. The

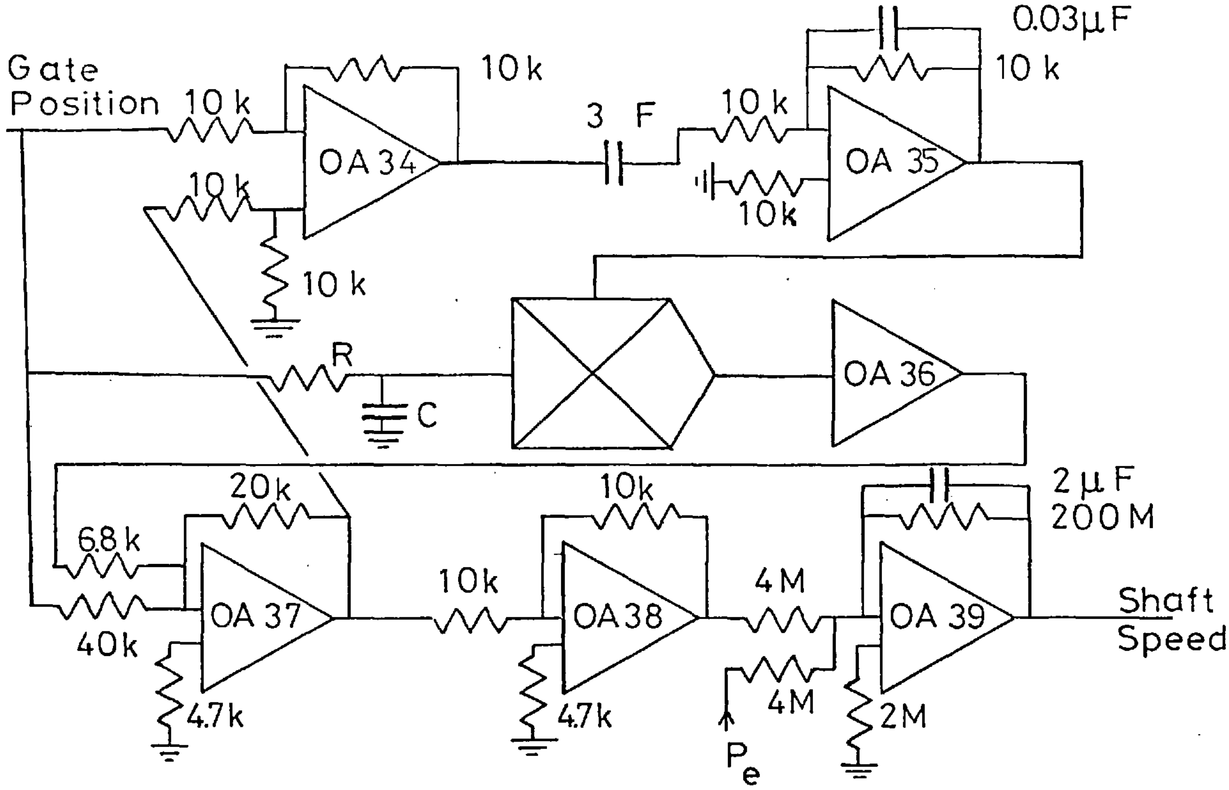

Fig. 3.23 Hydro Turbine Circuit Diagram.

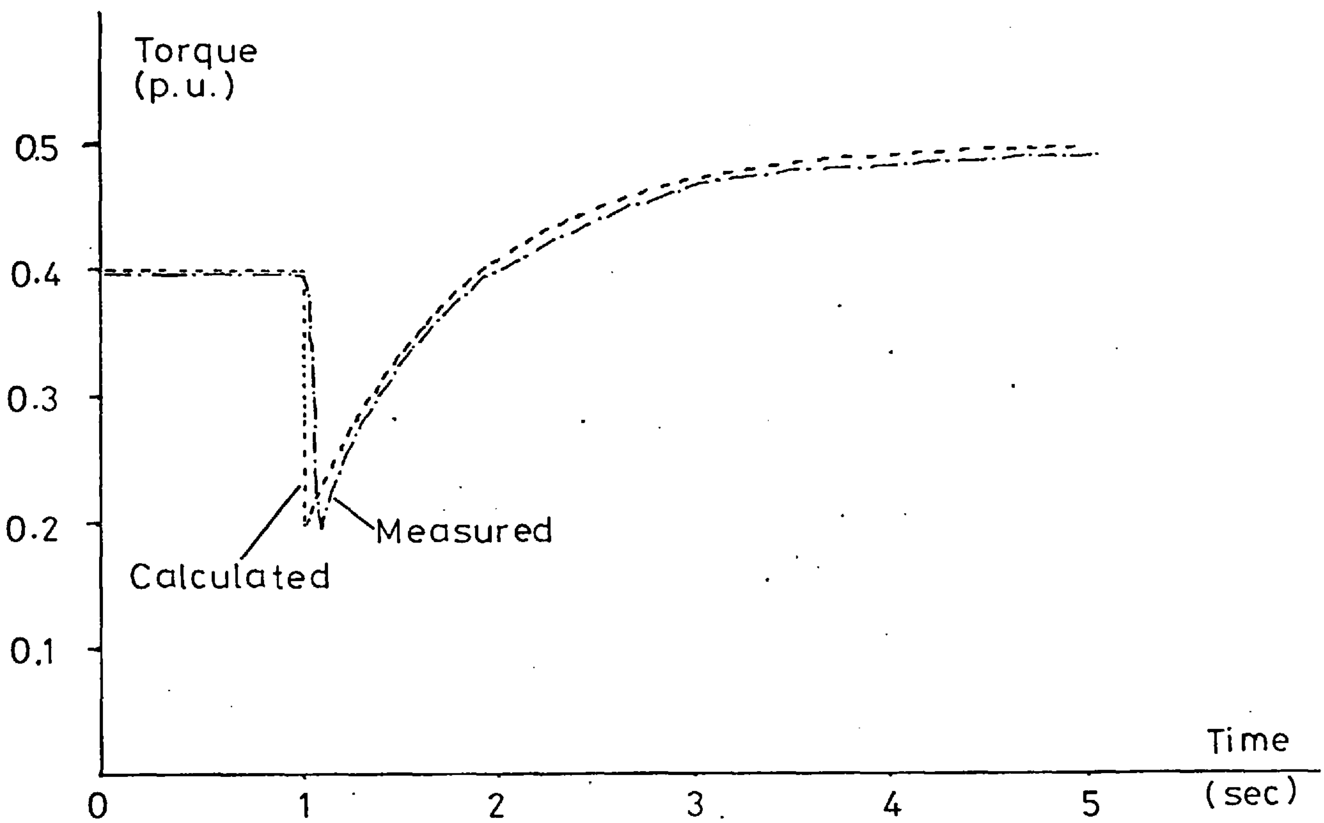

Fig. 3.24 Hydro Turbine Step Response.

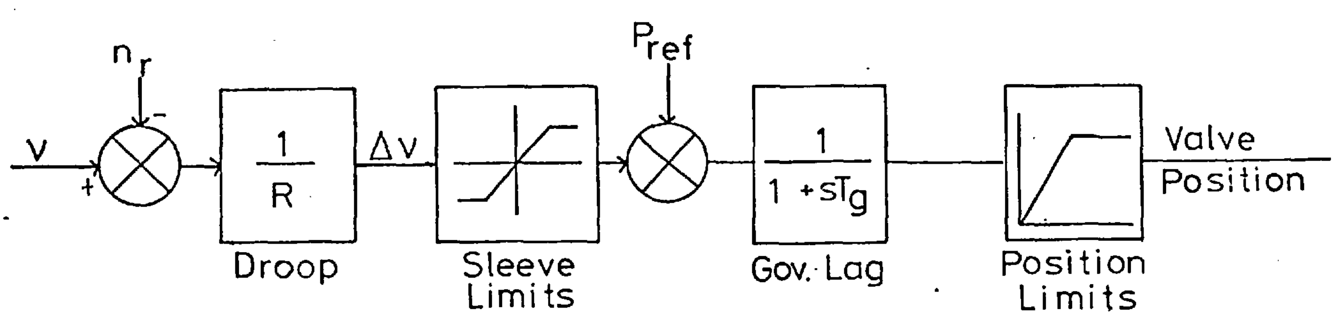

Fig. 3.25 Steam Turbine Governor Model.

inertia constant, H, is given by $\frac{R_1C_1}{2}$, and the damping coefficient, D, by R_1/R_2. Fig. 3.24 shows the effect of a step input in gate position, from 0.4 to 0.5 p.u., and the agreement with the predicted response is shown to be good, except for the initial edge, where the differentiator roll-off produces an error. However, in the whole simulation, the rate of change of gate position is limited by its maximum velocity, and can never be discontinuous.

3.4.2 The Steam Turbine and Governor.

In many respects, a simple representation of a steam turbine is much easier to implement, for there are many possible models[51,52,53] which have been proven, of varying degrees of complexity. Additionally, a linear model has applicability over a wide range of operating conditions. As has been explained previously, the bolier plant is simulated digitally, and provision must be made for the interfacing of such a digital model with the analog representation of the turbine. The way in which this is accomplished will be explained here, but the details of the actual boiler simulation will be given in Chapter 9.

A block diagram of the governor representation is shown in Fig. 3.25, and it can be seen that it is much simpler than the one used for the hydro turbine. By ignoring the velocity limits, it is possible to eliminate the droop feedback, and to produce an open loop system. A speed error signal is produced, and multiplied by $1/R$, where R is the droop, and it is then limited, to represent the limits of the flyball sleeve movement. This is then added to the speeder gear setting, P_{ref}, and a low pass filter is included to represent the dynamics of the hydraulic relays and valves. The output signal is then limited, to represent the fully open and fully shut positions of the main throttle valve.

A simple model for a re-heat turbine is shown in Fig. 3.26(a); a single delay represents the h.p. cylinder, and another the i.p. and l.p. cylinders, while the coefficients K_h and K_{il} represent respectively the proportion of the power from the h.p. and the other two cylinders. this

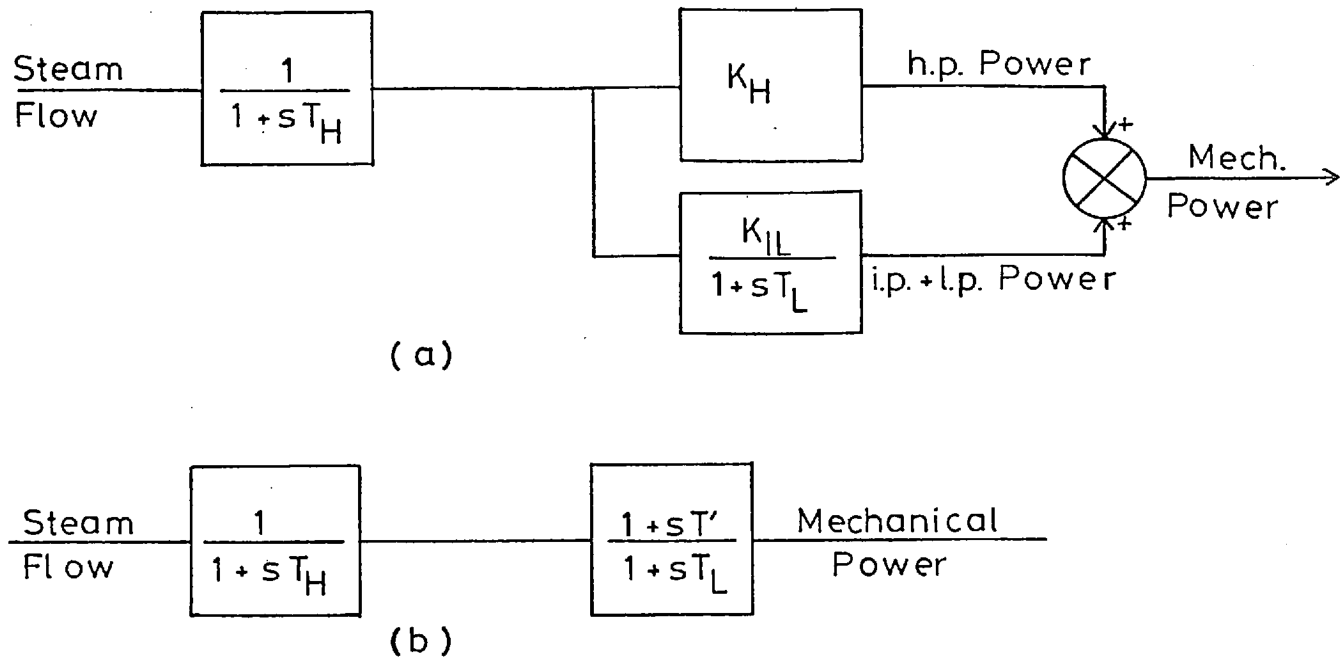

Fig. 3.26 Steam Turbine Model.

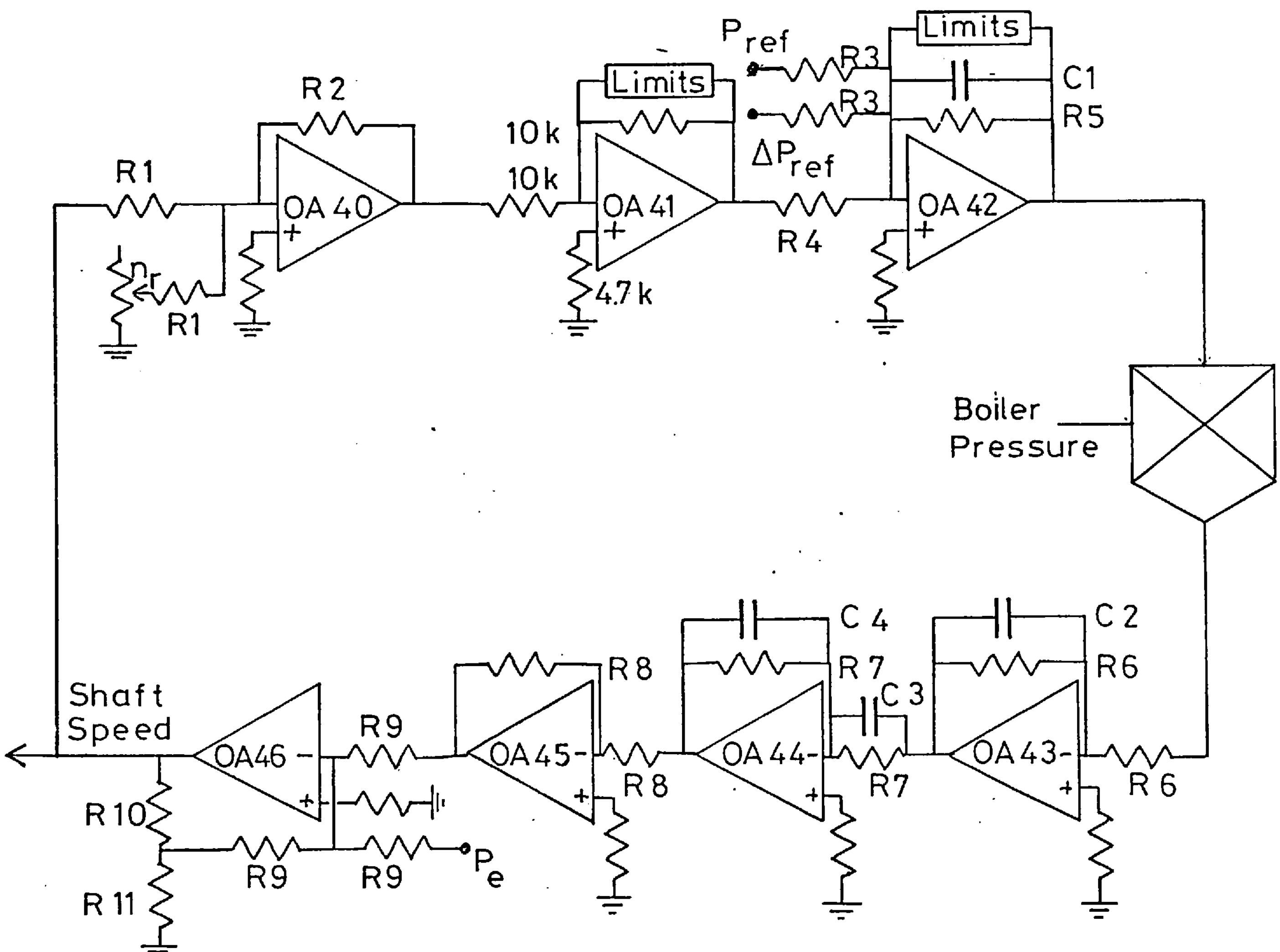

Fig. 3.27 Steam Turbine Circuit Diagram.

can be reduced, for ease of simulation to the system of Fig. 3.26(b), where T' is given by $T' = K_h . T_1$. The input of the turbine model is a signal representing steam flow, while the governor produces a signal proportional to valve position, so it is assumed that

Steam flow = Valve position x Boiler pressure.

In the cases when no boiler simulation is used, the per-unit values of valve position are the same, but if a boiler simulation is required, a multiplier must be included at this point. The solution of the mechanical equation of motion is the same as in the case of the hydro turbine.

The complete circuit diagram is shown in Fig. 3.27. The speed error signal is produced by OA 40, and is inverted and limited by OA 41. The next amplifier, OA 42, sums the speeder gear setting and the speed error, simulates the governor delay and also includes the limits on the valve position. Between OA 42 and OA 43, the boiler pressure multiplier must be included, if a boiler simulation is to be used, for OA 43 represents the h.p. stage of the turbine. OA 44 represents the i.p. and l.p. stages, and sums the power contributions from the various stages. The power signal is inverted by OA 45, while OA 46 is the equation of motion integrator. The component values are related to the parameters by the following expressions:

Droop, R, $= (R_1 R_4)/(R_2 R_3)$

Governor time constant, T_g, $= C_1 R_5$ sec

H.p. time constant, T_h, $= C_2 R_6$ sec

I.p. and l.p. time constant, Til, $= C_4 R_7$ sec

H.p. power fraction, K_h, $= C_3 / C_4$

I.p. and l.p. power fraction, K_{il}, $= 1 - K_h$

Inertia constant, H, $= R_9 C_5 / 2$

Damping constant, D, $= R_{11}/(R_{10}+R_{11})$

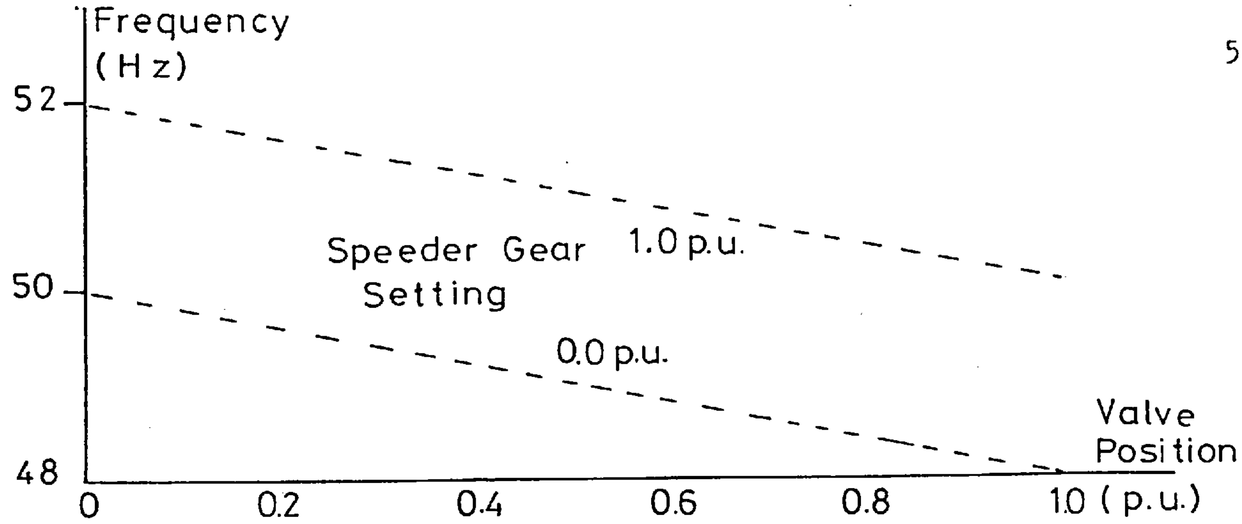

Fig. 3.28 Governor Droop Characteristic.

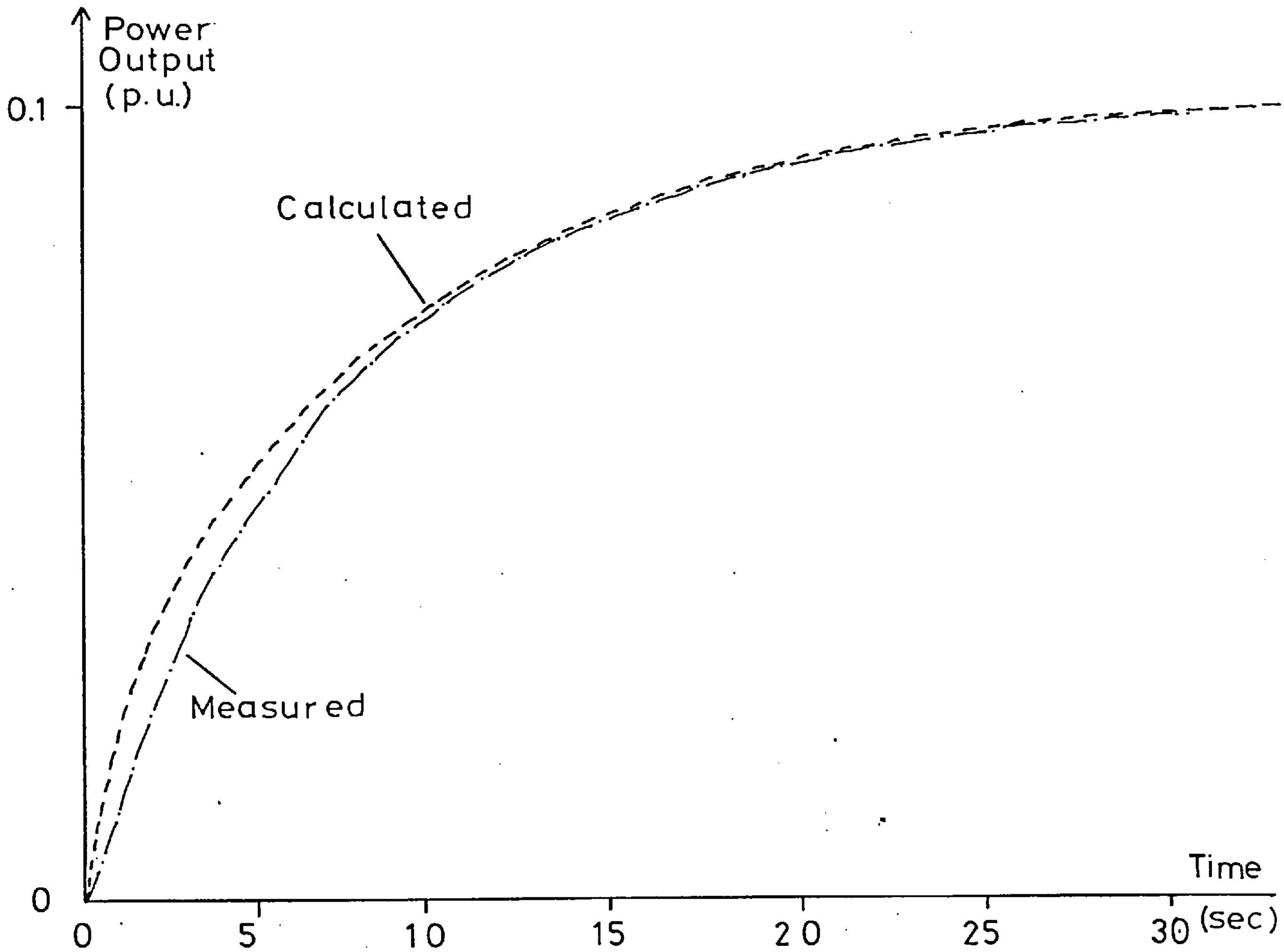

Fig. 3.29 Turbine Step Response.

The chosen values were

$R = 0.04 \qquad T_g = 0.25$ sec $\qquad T_h = 0.5$ sec $\qquad T_{il} = 10.0$ sec

$K_h = 0.28 \qquad K_{il} = 0.72 \qquad H = 4 \qquad D = 0.05$

Fig. 3.28 shows the valve position for different speed errors and speeder gear settings, while Fig. 3.29 shows the transient response of the turbine section of the simulation to a 10% change in steam flow. The static accuracy of the governor is good, as is the dynamic response of the turbine section, although the latter could be improved by using better feedback capacitors.

3.5 Conclusion.

This chapter has described some of the models which have been produced for use in the modular generator unit, and some of the problems involved have been discussed. While the transformation from block diagrams of transfer functions to circuit representation may look simple, it is by far the most complex part of the operation, when, as in this case low grade components are used. However, satisfactory models have been developed and have proved to be reliable in use.

CHAPTER 4 THE SYNCHRONOUS MACHINE ANALOG

4.1 Introduction.

Although the purpose of this simulator is not to study the fast electrical transients which occur in a power system, the model which is used to represent the synchronous machine proves to be a very important factor in the performance of the whole system. The nature of an analog simulation demands that the representation of a generator includes sufficient damping as to ensure stability in the presence of noise; such problems do not affect the designers of transient analysers, for in that instance the duration of the simulation is only a few seconds. This means that if it is to work satisfactorily, the machine model must give a closer approximation to the real behaviour of the machine than is really required. The work done by Sheldrake[27] employed a simple model of a voltage behind a synchronous reactance, and the problems associated with this will be discussed. As a result of these difficulties, it was decided to build a model employing a 2 axis representation of the machine, this being believed to be the first published use of such a model in a continuous real-time simulation. The dynamic and static characteristics of this machine representation will be examined. and its superiority over previous models established.

4.2 The Reactance Model.

The simplest method of representing the static electrical behaviour of a synchronous machine is to use the model of a constant voltage behind the synchronous reactance of the machine[54]. The way in which this can be included in the power system model is shown in Fig. 4.1. The sinusoidal output of the VCO is taken to be in-phase with the internal voltage E_i, whose magnitude is proportional to the current in the field winding. If the VCO output is multiplied by a dc signal proportional to i_f, the field current, then it can be taken to represent E_i. This signal is then passed

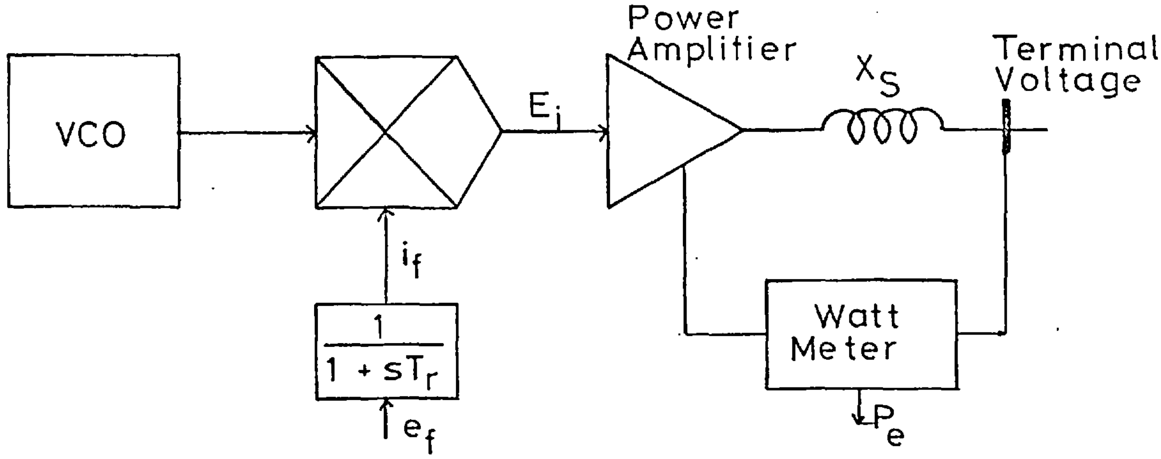

Fig. 4.1 Reactance Machine Model.

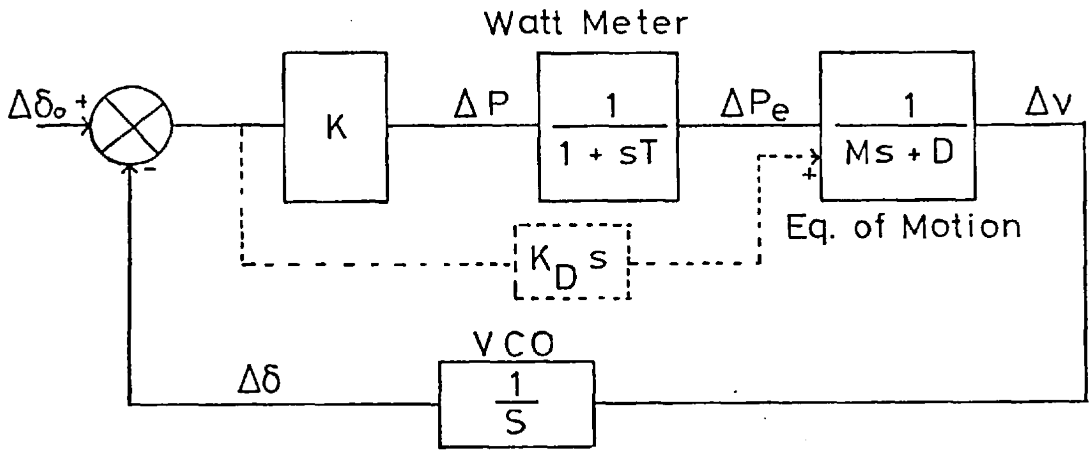

Fig. 4.2 Linearized Model of the Electrical Power Loop.

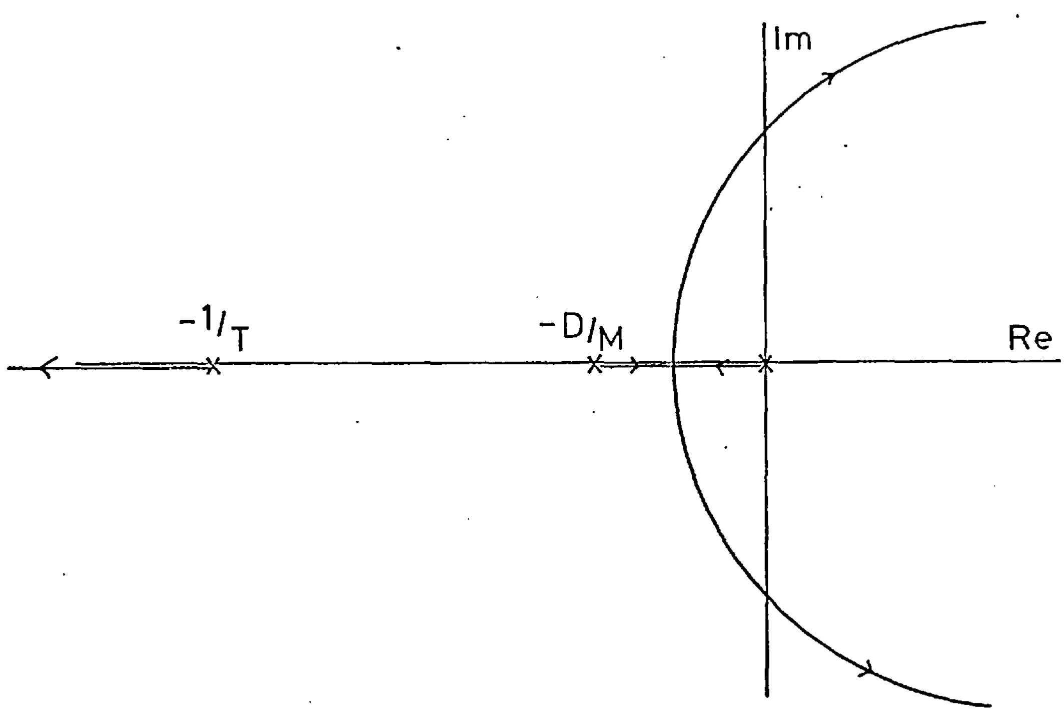

Fig. 4.3 Root Locus of the System of Fig. 4.2.

through a power amplifier, and a large choke is used to represent the synchronous reactance X_s. The effect of the inductance of the field winding may be taken into account by passing the signal which represents the field voltage e_f through a simple lag circuit to give the field current i_f. The electrical power is measured by averaging the product of the terminal voltage and current.

This simple model will work adequately in a single machine - infinite bus system, but will not do so in a two machine arrangement. This has been found to be due to a lack of damping in the machine model, and the only reason why it works in a single machine system is because the terminal voltage is held constant, and the limitations of the electronics for some reason prevent instability. A linearized model of a machine model of this type, with its terminal voltage held constant, is shown in Fig. 4.2. It is arranged as a disturbance model, to examine the damping of the system when a small change in rotor angle occurs.

This change in rotor angle $\Delta\delta_o$ produces a corresponding change in the actual electrical power, ΔP, given by $\Delta P = K\Delta\delta_o$, where $K = \frac{\partial P}{\partial \delta_o}$, $= \frac{E_i V_T \cos\delta_o}{X_s}$. The measurement of this change of power introduces a lag term, represented by the time constant T; this is due to a combination of the filters associated with the electronic wattmeter, and also to the fact that in a single-phase system, the instantaneous power is not invariant, as it is in a 3 phase system, and this introduces an inherent delay into the measurement of electrical power. This measured signal is then introduced into the mechanical equation of motion, producing a change in shaft speed. The effect of the voltage-controlled oscillator is to integrate changes of frequency to give a change in angle relative to the infinite bus, $\Delta\delta$, which will be in such a direction as to oppose the disturbance of the initial angle $\Delta\delta_o$.

The stability of this system can be examined using the Routh-Hurwitz criterion, and this shows that for the system to be stable,

$$T + \frac{M}{D} \geqslant \frac{K M T}{D^2}$$

Typical values are

$$M = 8 \qquad D = 0.02 \qquad K = 1$$

which means that for stability, $T \leqslant 0.02$ seconds; the root locus is shown in Fig. 4.3.

This shows that for the loop to be stable, the time constant associated with the electrical power measurement must be less than one period of the system frequency. This is difficult to achieve, and to ensure stability additional damping must be included. Sheldrake[27] provided this extra damping by including an additional term in the equation of motion which was proportional to the rate of change of rotor angle. This is shown dotted in Fig. 4.2. Suitable choice of the coefficient K_D provides an adequate representation of the effects of the interaction of the positive-sequence air-gap field with the rotor damper circuits. However, this coefficient is very dependent on the operating condition of the machine and it was found in practice that this caused problems of small amplitude oscillations. The effect of this damping term is to introduce two additional zeros into the system, and their loci for different values of K_D is shown in Fig. 4.4(a), while for a typical value of K_D, the root locus of the system is shown in Fig. 4.4(b). The location of the zeros ensures stability, and this has been found in practice to be true for a wide range of values of K_D.

Although this simple model of the machine can be made to work, there are several other objections to its use. The use of a fixed reactance introduces a number of problems, for in a real machine the reactance is a function of the dynamic state of the fluxes and currents. For the investigation of the short term transients, which involve voltage effects, the reactance which is used should be the transient reactance, while for

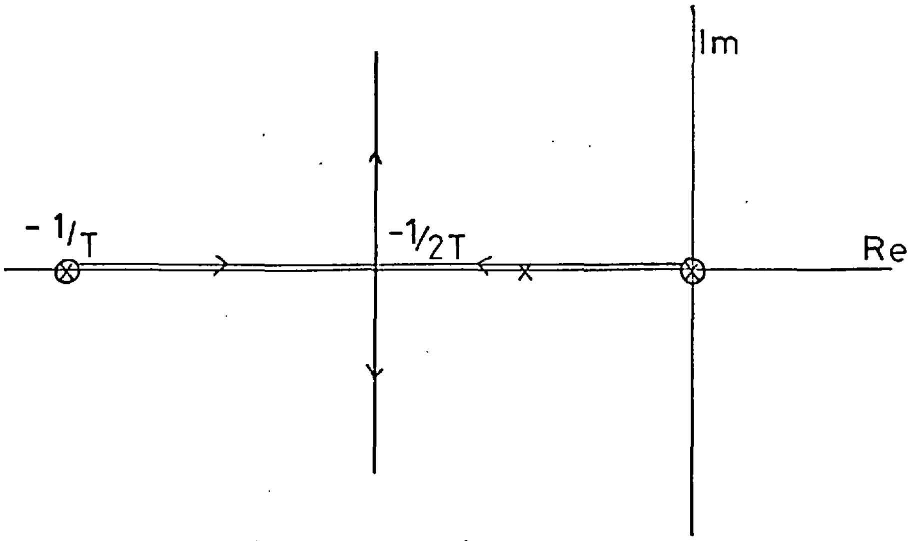

Fig. 4.4(a) Locus of Zeros as K_D Increases.

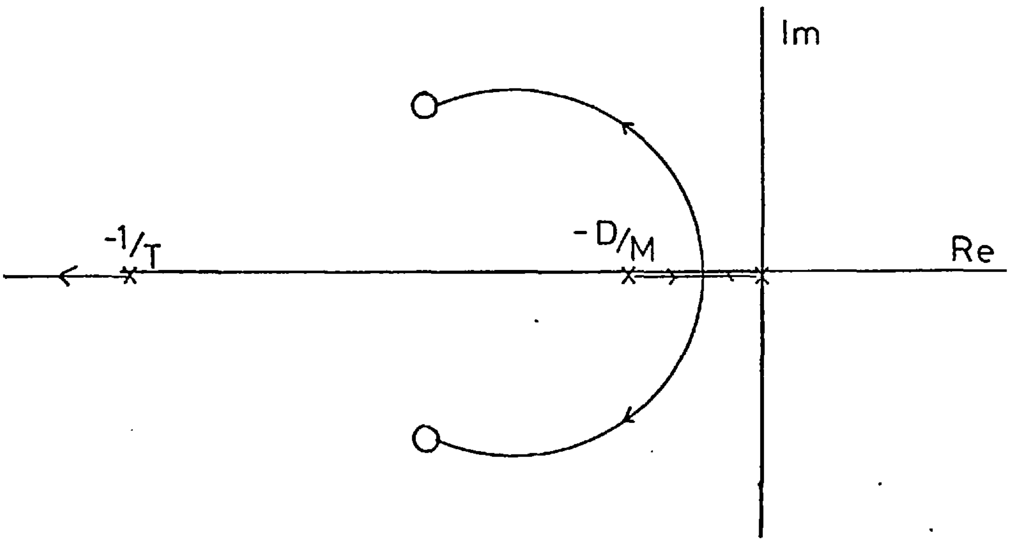

Fig. 4.4(b) Root Locus of the System with Damping.

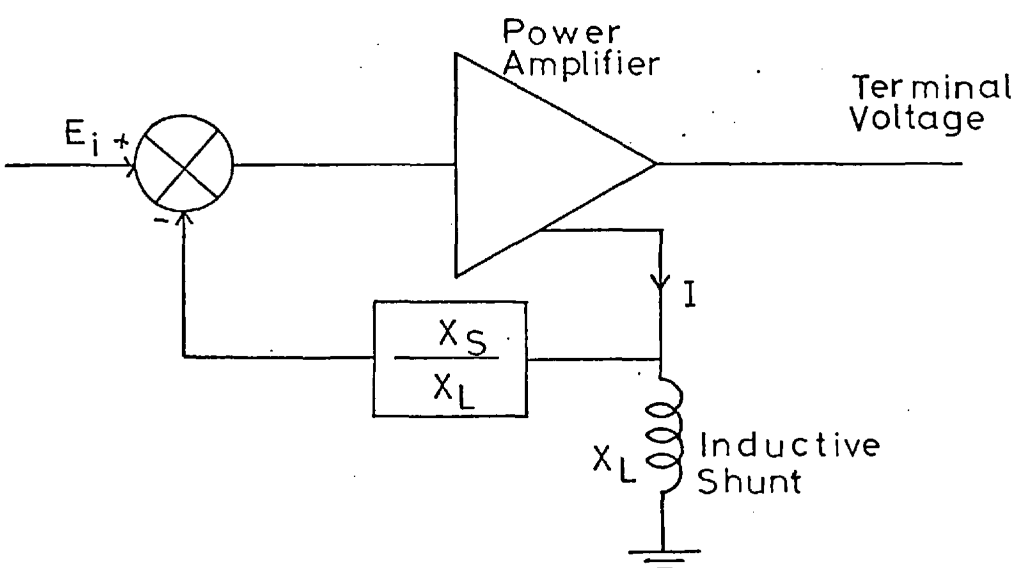

Fig. 4.5 Machine Model without a Reactance Choke.

the steady state condition, the synchronous reactance is required, so that the field voltage is the correct value. The choice of the synchronous reactance by Sheldrake[27] means that under changing conditions, the model moves from one steady state to another, while what happens in between is uncertain. In this model, a change of load produces a large instantaneous change in the terminal voltage, and hence in the measured electrical power, while in a real machine the voltage changes occur with lags of the transient and sub-transient time cinstants. The problem of changing time constants occurs in the lag term associated with the field circuit, for on open circuit this should be the open circuit transient time constant while as the loading increases, it should tend towards the short circuit transient time constant.

These are the main technical disadvantages of the model, the lack of damping and the need for changing reactance and time constant with operating condition, but there are also two practical objections to this method. First, a large high-Q iron cored choke is required to represent this synchronous reactance, and secondly the power amplifier must be able to supply several times the base voltage of the system, for when the generator is supplying lagging load, the internal voltage is much greater than the terminal voltage. A suggested method for overcoming these two problems is shown in Fig.4.5. An inductive shunt X_1 is included in the terminal current path, and the voltage developed across it, jIX_1, is amplified and subtracted from the signal representing the internal voltage E_i. However, this involves the effective differentiation of the current by the inductive shunt, which produces noise which in turn distorts the terminal voltage.

Thus it can be seen that this simple model which at first sight offers many advantages due to its simplicity, in fact presents severe difficulties for a sucessful practical implementation, which is why it was decided to construct a more complex 2 axis model of the synchronous machine.

4.3 The Two Axis Model.

The representation of a synchronous machine using an analog 2 axis model is well established for use in transient stability studies[55,56], but such a model does not appear to have been used in a continuous frequency simulation. The problem can be broken down into three main sections, which are:

(i) Transform the terminal currents into the axis currents

(ii) Solve for the fictitious axis coil voltages

(iii) Produce the terminal voltage by inverse transformation from these coil voltages.

The first and third stages of this operation present no great difficulty, but it is the middle stage which gives scope for different methods of solution. A basic review of 2 axis theory is necessary to understand the operation of the adopted model.

4.3.1 Basic 2 Axis Theory.

All the results stated here are derived in Ref. 57, but they are given here to facilitate the derivation of the model equations. Fig. 4.6 shows the arrangement of the axis coils, and for these the flux linkage equations may be written as:

$$\psi_d = L_{md}\, i_f + L_{md}\, i_{kd} + (L_{md} + l_a)\, i_d \tag{4.1}$$

$$e_f = (r_f + s(L_{md} + l_f))\, i_f + sL_{md}\, i_{kd} + sL_{md}\, i_d \tag{4.2}$$

$$0 = sL_{md}\, i_f + (r_{kd} + s(L_{md} + l_{kd}))\, i_{kd} + sL_{md}\, i_d \tag{4.3}$$

$$\psi_q = L_{mq}\, i_{kq} + (L_{mq} + l_q)\, i_q \tag{4.4}$$

$$0 = (r_{kq} + s(L_{mq} + l_{kq}))\, i_{kq} + sL_{mq}\, i_q \tag{4.5}$$

and the voltage equations for the axis coils as

$$e_d = s\psi_d + \nu\psi_q + r_a i_d \tag{4.6}$$

$$e_q = -\nu\psi_d + s\psi_q + r_a i_q \tag{4.7}$$

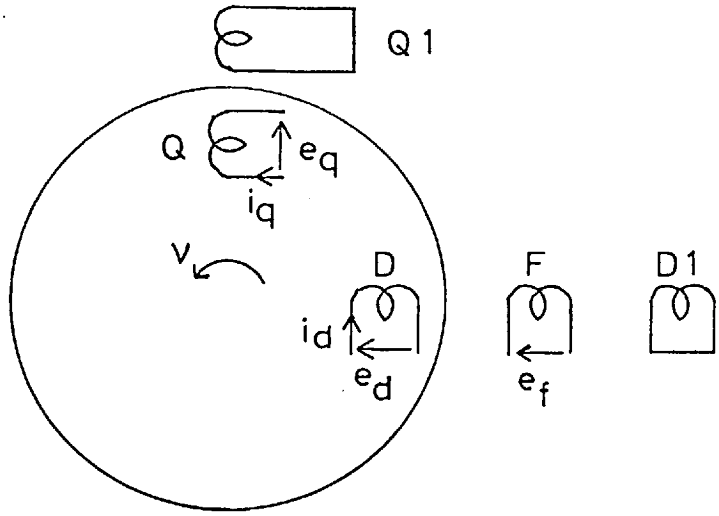

Fig. 46 Coil Arrangement for the 2 Axis Model.

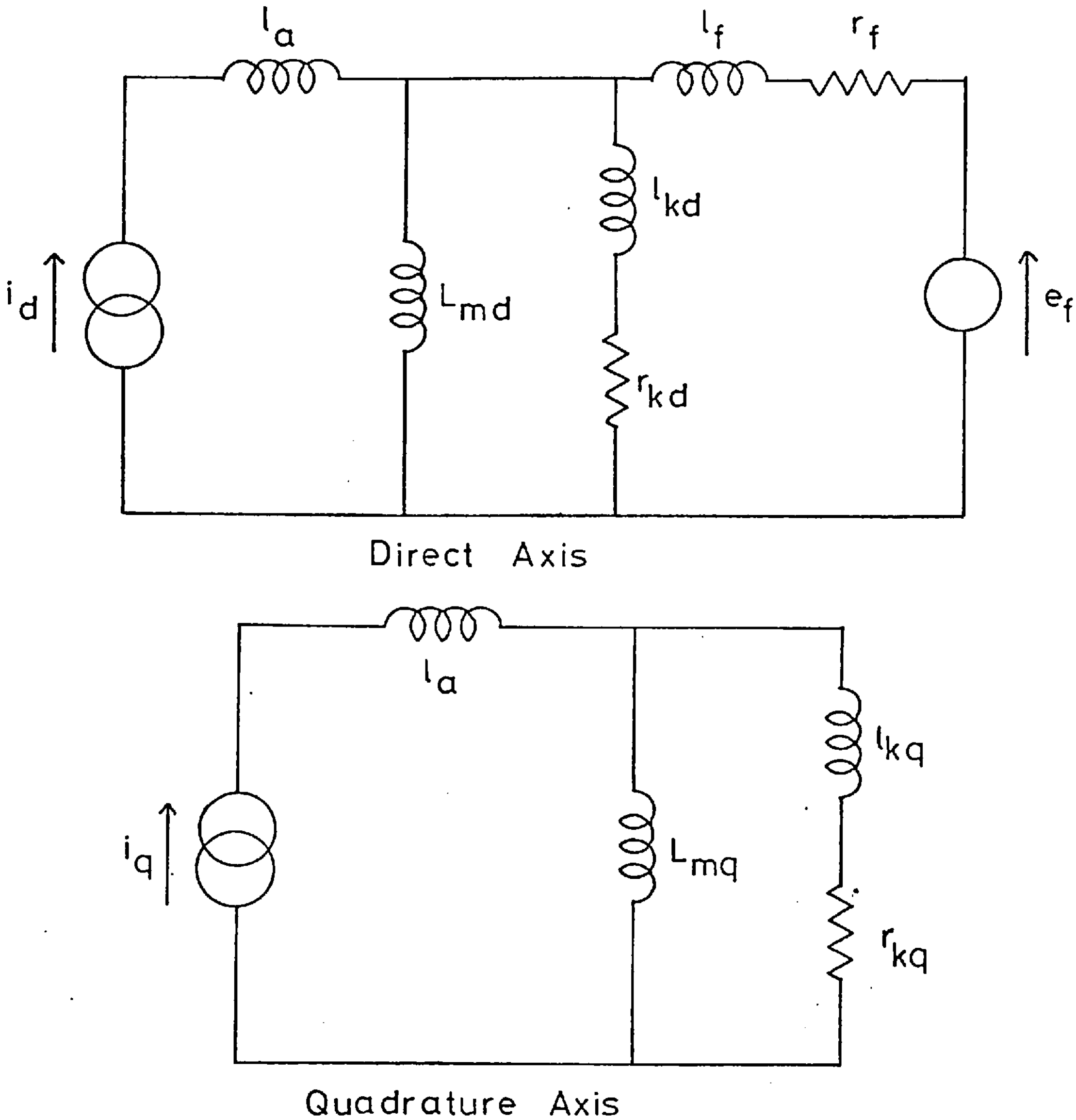

Fig. 47 Axis Equivalent Circuits.

The main problem is to solve for the axis fluxes in terms of the axis currents and the applied field voltage. The simplest solution in many respects is to use the operational impedances, which give the fluxes directly as

$$\psi_d = \frac{x_d(s)}{\omega}\, i_d + \frac{G(s)}{\omega}\, e_f \qquad (4.8)$$

$$\psi_q = \frac{x_q(s)}{\omega}\, i_q \qquad (4.9)$$

where

$$x_d(s) = \frac{(1 + sT_d')(1 + sT_d'')}{(1 + sT_{do}')(1 + sT_{do}'')}\, x_d \qquad (4.10)$$

$$G(s) = \frac{(1 + sT_{kd})}{(1 + sT_{do}')(1 + sT_{do}'')}\, \frac{x_{md}}{r_f} \qquad (4.11)$$

$$x_q(s) = \frac{(1 + sT_q'')}{(1 + sT_{qo}'')}\, x_q \qquad (4.12)$$

This method of solution has several disadvantages, however, for an analog representation, since the time constants are complex functions of the basic machine parameters. Thus if it is desired to change one value, say the quadrature axis reactance, then several coefficients must be altered. Also the use of this technique means that the only outputs are the total flux linkages of the coils, and no information is available about, for example, the damper winding currents. An alternative method of solution, which is particularly suitable for digital computation work, is based on the use of the axis equivalent circuits, which are shown in Fig. 4.7. If these networks are fed with the axis currents and the field voltage, then solutions for the differentials of the fluxes are given at the terminals, and the other currents may be measured in the network. However, straight modelling of these circuits is not practicable, as they demand the use of pure inductors, and of ideal integrators to integrate the derivatives of the fluxes. By suitable manipulation of the circuits,

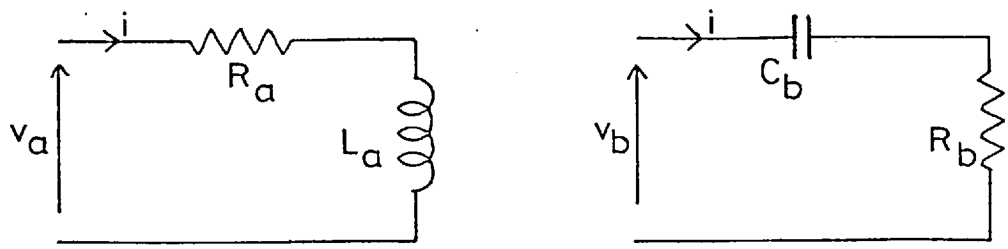

(a) (b)

Fig. 48 Simple Networks.

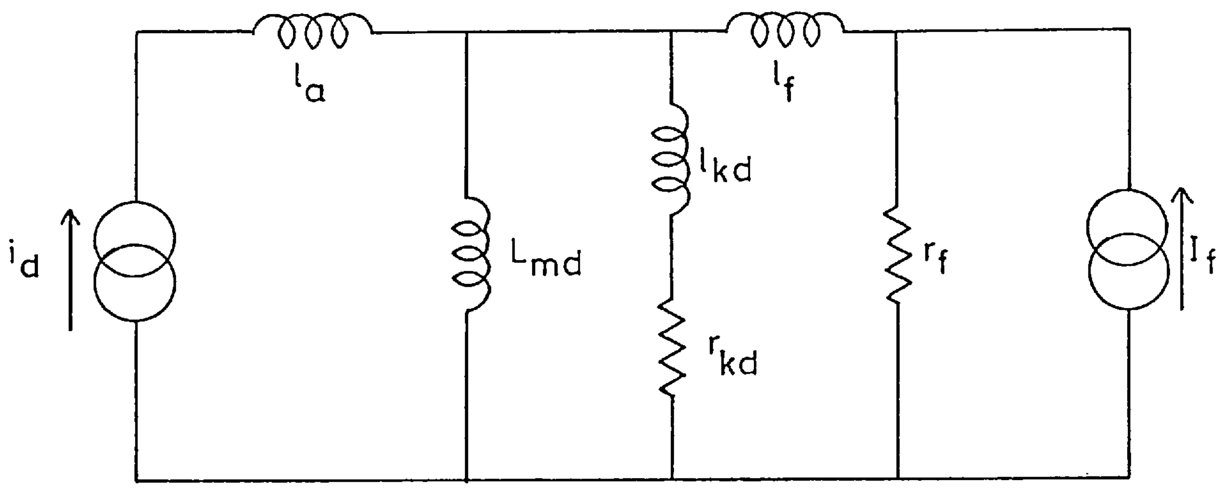

Fig. 49 Modified Direct Axis Circuit.

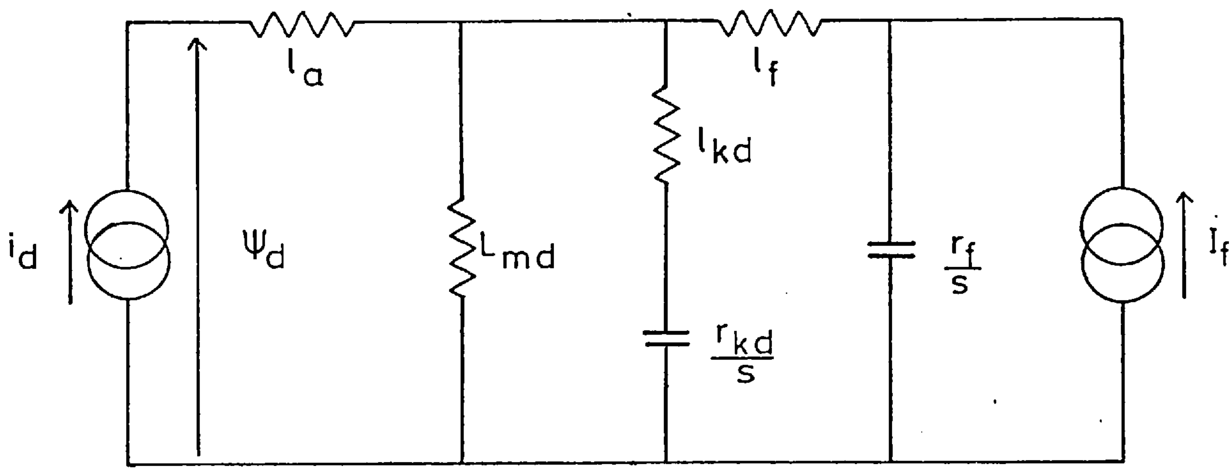

Direct Axis

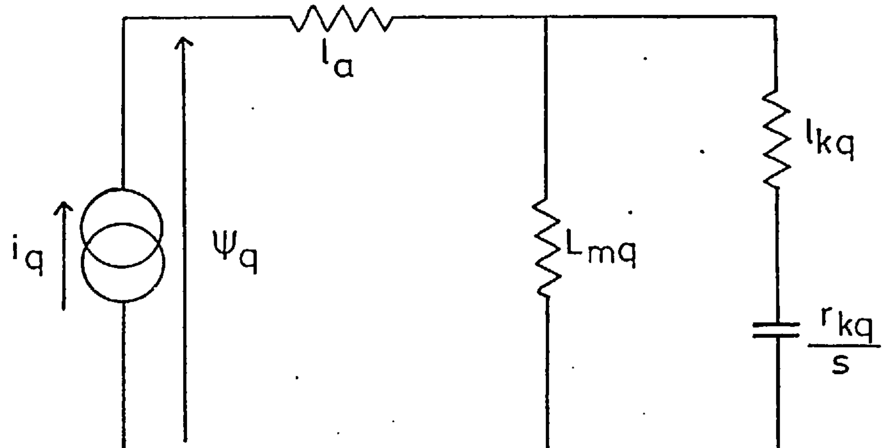

Quadrature Axis

Fig. 410 Converted Equivalent Circuits.

it is possible to arrive at a system which is very suitable for analog modelling.

4.3.2 Manipulation of the Equivalent Circuits.

Consider the simple circuits shown in Fig. 4.8; for each of them the voltage equations can be written

$$\text{(a)} \quad v_a = i.R_a + s\, i.L_a$$

$$\text{(b)} \quad v_b = i./(s\, C_b) + i.R_b$$

Now if $R_a = 1/C_b$ and $L_a = R_b$, then it is evident that $v_a = s.v_b$. Thus it can be seen that by changing the inductors in a circuit into resistors, and the resistors into capacitors, the voltages in the second circuit will be the integral of those in the initial circuit. This can be applied to the original axis equivalent circuits, to yield a system which gives the fluxes directly. First, however, the applied field voltage must be converted into an equivalent current source, using Norton's theorem, as shown in Fig. 4.9. Equation (4.2) may be rewritten as

$$0 = (r_f + s(\,L_{md} + l_f\,))\, i_f + sL_{md}\, i_{kd} + sL_{md}\, i_d - I_f\, r_f \quad (4.13)$$

where I_f is the equivalent injected current, equal to e_f/r_f. The two axis circuits may now be converted to the resistive-capacitive form, as shown in Fig. 4.10. It can be shown that these networks satisfy equations (4.1) and (4.4) as well as equations (4.3),(4.5)and (4.13) when they have been integrated.

The circuits shown in Fig. 4.10 are suitable for modelling as they stand, but further simplification can be achieved by making use of the relationships

$$\psi_d = \psi_{md} + l_a\, i_d$$

and

$$\psi_q = \psi_{mq} + l_a\, i_q$$

By solving for ψ_{md} and ψ_{mq} it is possible to eliminate two of the constant current sources, and the first stage is shown in Fig. 4.11 for the direct axis. This involves eliminating the resistor which represents

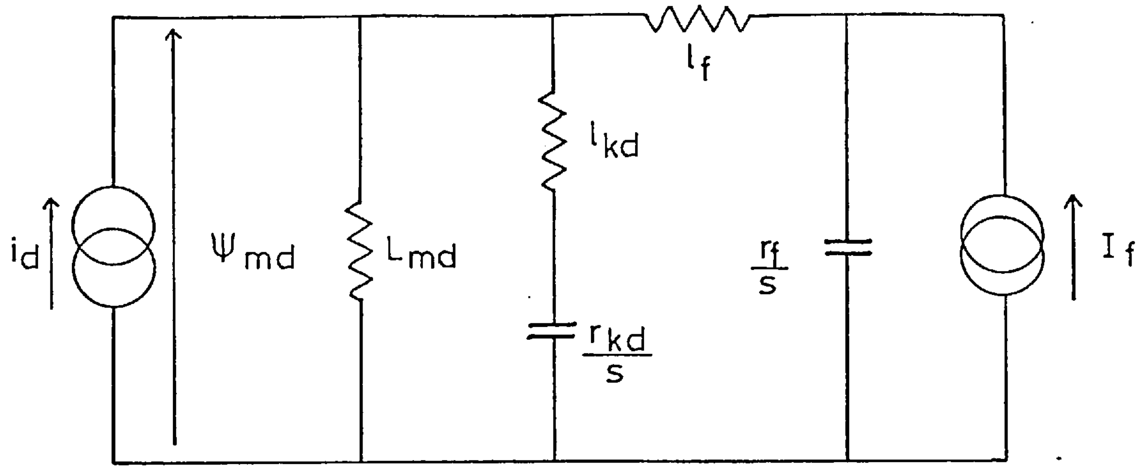

Fig. 411 Direct Axis Circuit to Solve for Ψ_{md}.

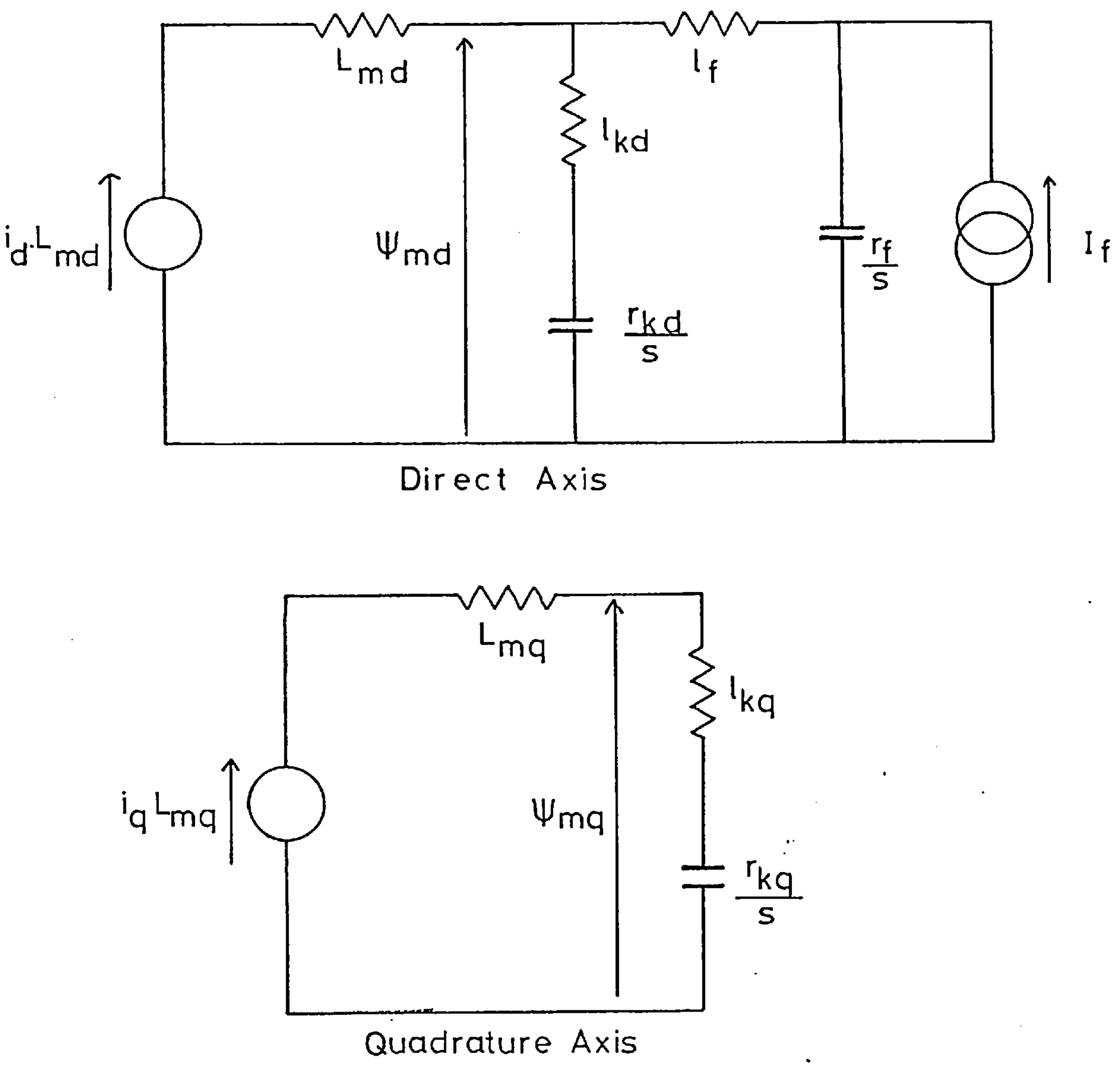

Fig. 4.12 Final Model Circuits.

the armature leakage reactance, and it is then possible to change the current source and the shunt resistance L_{md} into a voltage source and a series resistance. This is shown in Fig. 4.12 for both axes, and these are the networks which are employed in the model.

This method of representation was used by several people[19,58,59,60,61] during the late 1950's, but only for transient machine problems; this is the first use of this technique in a continuous simulation. It offers several advantages, including a clear insight into the effect of the damper windings, and also illustrates the build-up of current in the field windings. Furthermore, with no excitation applied, the model becomes that of a simple induction machine, with the inductances correctly represented, and the effect of slip on the rotor circuit resistances accounted for. Practice has shown that the model will run as an induction generator, with a reactive power demand of the right order of magnitude.

The total system required for a machine representation is shown in block form in Fig. 4.13, and consists of four sections:

(i) Current Resolvers

(ii) Equivalent Circuits

(iii) Component Modulators

(iv) Electrical Power Measurement

Each of these blocks will be considered in turn, and its performance examined. The model will be shown to perform accurately under both steady state and transient conditions, and to be suitable for inclusion in the whole system model.

4.4 Realization of the 2 Axis Model.

The synchronous machine model which has been built is designed to work with the rets of the modular generator unit, and consequently all the signal levels have been made compatible with those used in the unit bus.

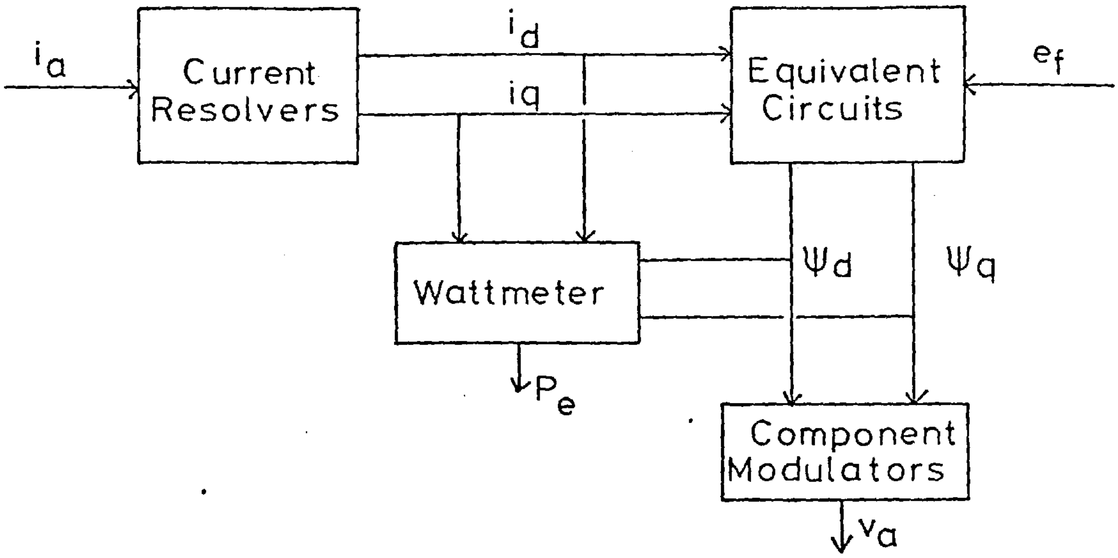

Fig. 4.13 Total System for the Machine Model.

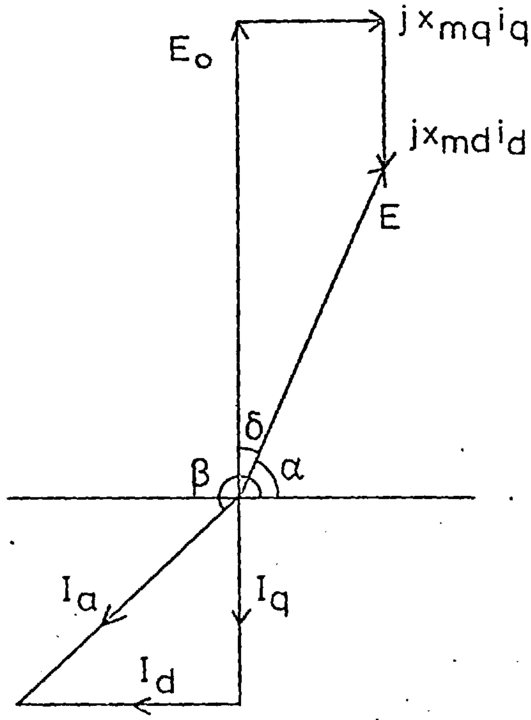

Fig. 4.14 Phasor Diagram.

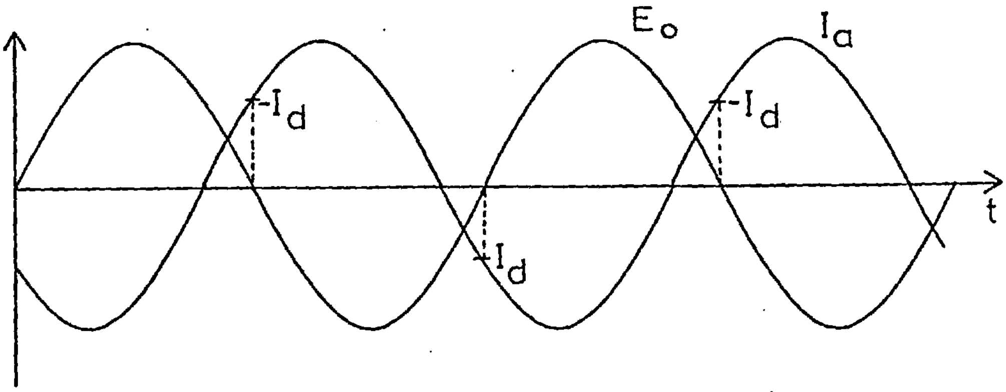

Fig. 4.15 Sampling of I_a to Give I_d.

4.4.1 The Current Resolvers.

The phasor diagram for a synchronous machine operating under steady conditions is shown in Fig. 4.14. The reference phasor is the voltage E_o, whose magnitude is proportional to the field current. For resolving the terminal current I_a into its two components I_d and I_q, it is only necessary to know the phase of E_o. This is therefore taken as being the sinusoidal output of the voltage-controlled oscillator, and it is with respect to this voltage that the direct and quadrature components of the various signals are established. The conventional method of electronic signal resolution is to use synchronous switching in a phase-sensitive detector, but with this method, the output signal contains many harmonics, and the filtering required to obtain a dc signal introduces unacceptable delays into the system.

The technique employed is based on a sampling system, and may be understood by referring to the phasor diagram, fig. 4.14, and the waveforms shown in Fig. 4.15. When the projection of E_o on the direct axis is zero, then the instantaneous value of I_a will be I_d, which may be sampled and held at this instant. The measurement may then be updated when the projection of E_o again passes through zero in the same direction. From Fig. 4.15, it can be seen that when E_o goes through zero from negative to positive, $\uparrow$, then the value of I_a sampled is I_d, but if it passes through zero in a negative direction, $\downarrow$, then the sampled value would be $-I_d$. A system shown in Fig. 4.16 enables two measurements of the components to be made per cycle, by arranging to sample either I_a or $-I_a$, depending on whether E_o passes through zero $\uparrow$ or $\downarrow$.

By determining the sampling instants from the zero crossings of a waveform in quadrature with E_o, the sampled values will be I_q instead of I_d.

The sampling switches are FET analog switches, and they are closed for 10 microseconds, which is sufficient time for the capacitor C to charge up to the required voltage. A complete circuit diagram is given in Fig. 4.17.

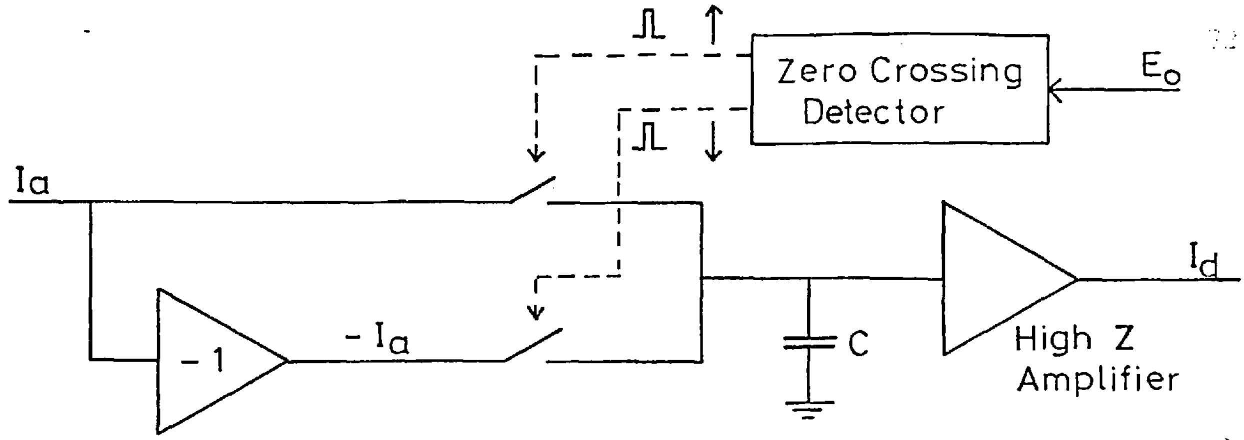

Fig. 4.16 Principle of the Sampling Unit.

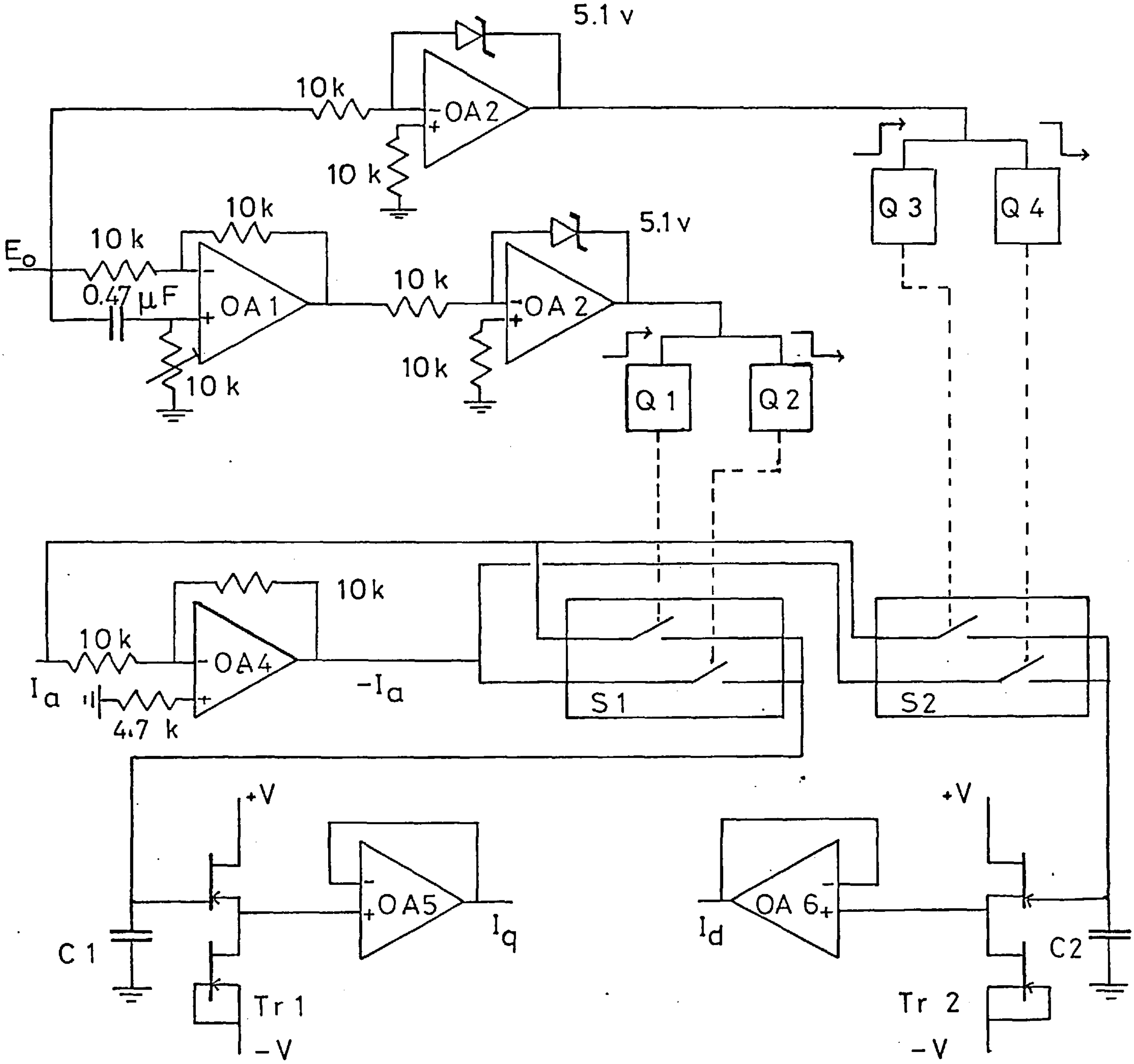

Fig. 4.17 Circuit of the Current Resolvers.

The input voltage E_o is phase-shifted through 90 degrees by OA1, and this is then converted into a square wave by OA 3, while OA 2 squares E_o. These square waves are used to trigger the monostables Q 1 and Q 3 when there is a positive transition, and Q 2 and Q 4 when there is a negative transition. These monostables generate sample pulses of 10μs duration, and these close the respective paths in the dual analog switches, S 1 and S 2, and thus charge up the two capacitors C 1 and C 2 which hold the two signals, I_d and I_q. These analog switches are buffered by dual FETs, Tr 1 and Tr 2, which are connected as source followers. These FETs themselves are buffered by voltage followers OA 5 and OA 6, and the outputs of these amplifiers drive the equipment directly.

During the sampling period of 10μs, the 50 Hz sinusoid changes by less than 0.3%, and the total offset introduced by the analog switch and the source followers is less than 10 mV. The range of the measured signal is $\pm$ 4 volts, and so the accuracy of the whole measuring system is of the order of 0.5%, which has been verified by test measurements.

4.4.2 <u>The Equivalent Circuits.</u>

This section of the machine model comprises three main sections, which are:

(i) Field voltage to equivalent current conversion

(ii) The networks themselves

(iii) The scaling of the network outputs to give the coil voltages and flux linkages.

The scaling of the voltage signals and of the component values in the equivalent circuits require a per-unit system to be devised. There is only one constraint, and that is that time constants must remain unchanged in the transformation from the conventional axis circuits to the new equivalent circuits. Choosing a value to represent 1 p.u. reactance, and a voltage to represent the magnetizing flux* fixes all the values to be used. In this model, it was decided that

$$1 \text{ p.u. reactance} \;\hat{=}\; 200\ \mathrm{k}\Omega$$

and

$$\text{Magnetizing flux} \;\hat{=}\; 2 \text{ volts}$$

This gives 1 p.u. (1/ Resistance) = $1/(2.10^5.314)\ \mu F = 0.01592 \mu F$

From a knowledge of these parameters, it is simple to compute the equivalent field current I_f, and the applied voltages $i_d x_{md}$ and $i_q x_{mq}$ once the machine parameters are known. They are given by the expressions:

$$I_f \text{ (rated)} = 10/x_{md}\ \mu A$$

$$i_d x_{md} = 2.\ i_d(\text{p.u.}).\ x_{md} \quad \text{volts}$$

$$i_q x_{mq} = 2.\ i_q(\text{p.u.}).\ x_{mq} \quad \text{volts}$$

The machine to be represented had the following parameters,and the model equivalents are also given:

x_{md}	2.0 p.u.	400 k Ω
x_{mq}	1.33 p.u.	266 k Ω
x_a	0.14 p.u.	
x_{kd}	0.04 p.u.	8 kΩ
x_{kq}	0.04 p.u.	8 kΩ
r_{kd}	0.0125 p.u.	1.28μF
r_{kq}	0.0125 p.u.	1.28μF
r_f	0.00107 p.u.	15.0μF
x_f	0.14 p.u.	28 kΩ

The resultant equivalent circuits are shown in Fig. 4.18, and it can be shown that for the chosen parameters the voltage sources on the direct and quadrature axes have values of 4 V and 2.66 V respectively, for 1 p.u. current on that axis. The measured voltages which represent the flux linkages are buffered using the same high-impedance circuits which are used in the current resolvers.

* The term magnetizing flux is given to that flux which on the direct axis will produce rated voltage on open circuit. This equals 1 p.u. flux/314.

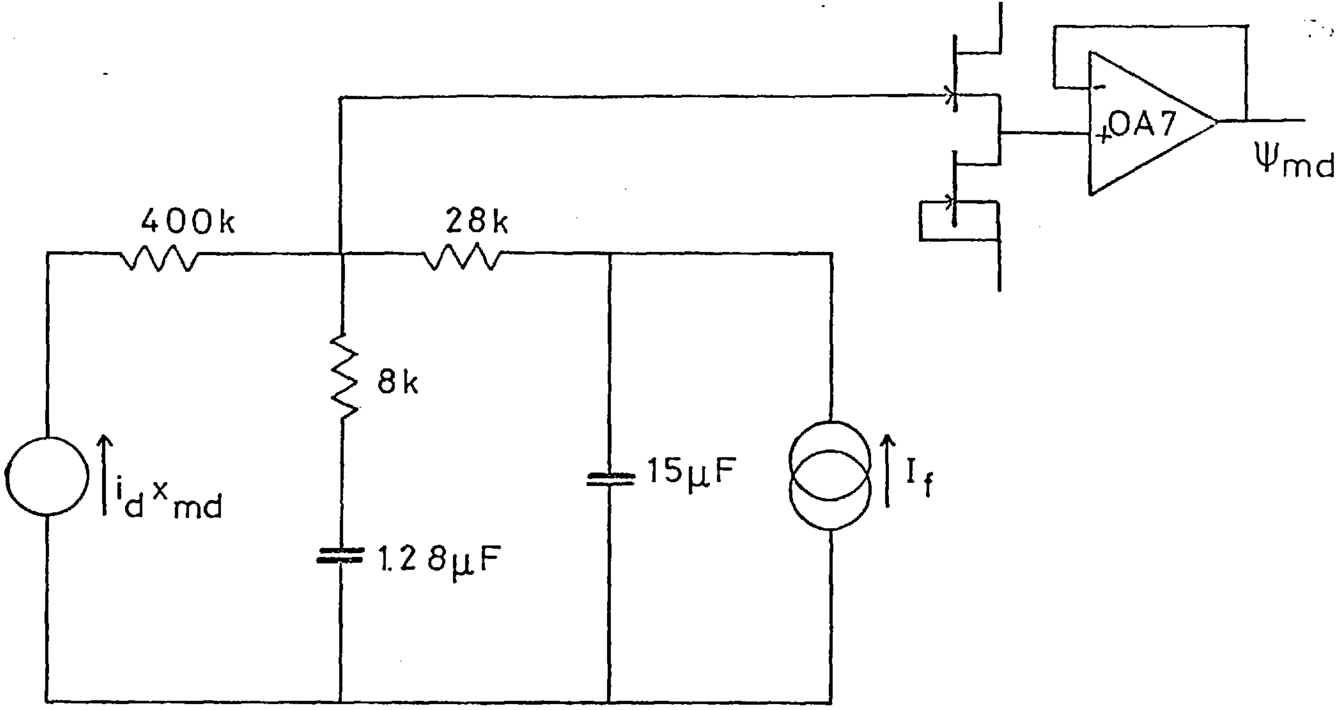

Direct Axis

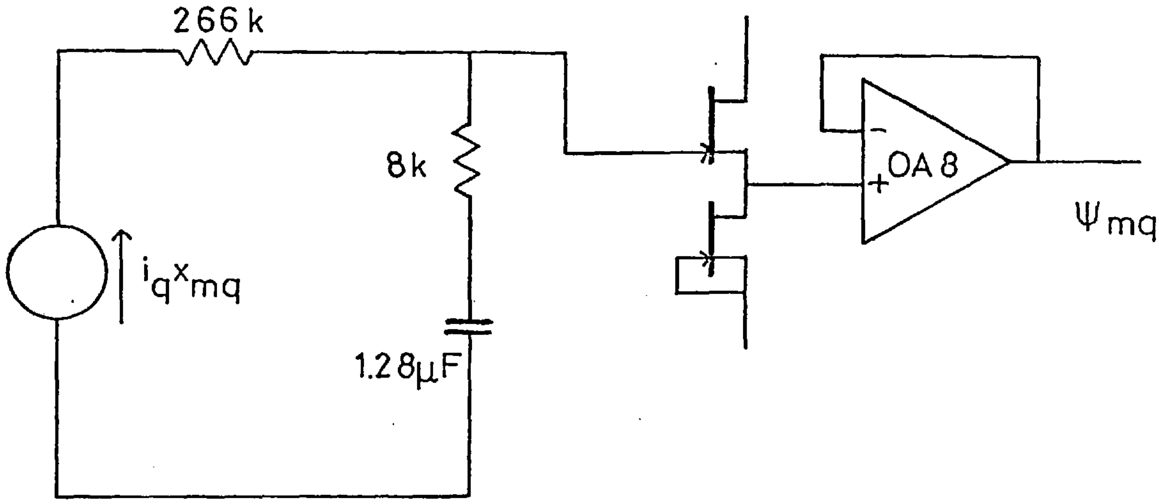

Quadrature Axis

Fig. 4.18 Final Equivalent Circuits.

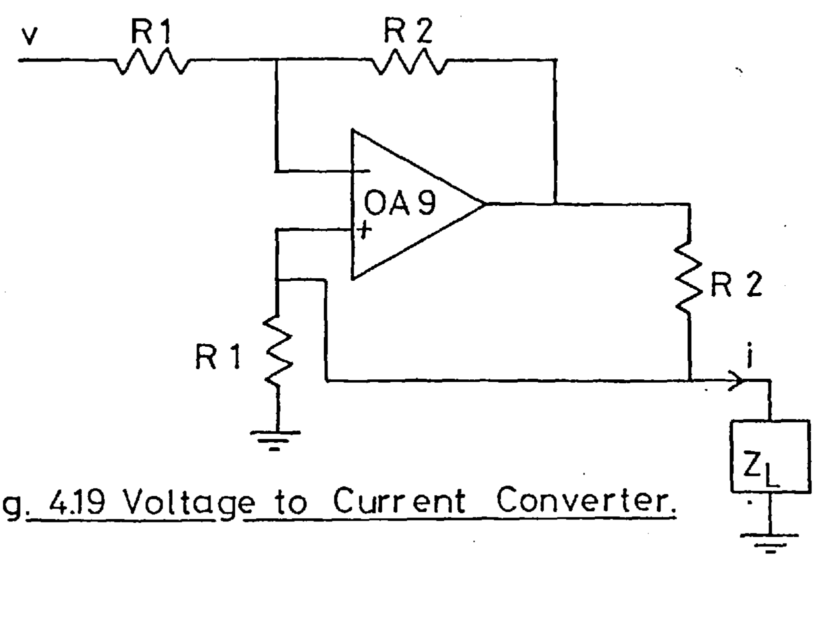

Fig. 4.19 Voltage to Current Converter.

The equivalent field current source must produce 5μA to give rated voltage on open circuit, and the circuit which is used is shown in Fig. 4.19. This is a voltage to current converter, which produces 5μA output for 2 V input. With the resistor ratios shown, the current is given by $i = -v/R_2$, and when tested the circuit was found to perform linearly, and it was not possible to measure its output impedance. The current was measured using a moving spot galvanometer, and within the accuracy of the instrument, about 1%, the circuit was linear, even when working into an active load of complex impedance.

The equivalent circuits provide signals to represent ψ_{md} and ψ_{mq}, but it is necessary to produce ψ_d and ψ_q, as well as the two axis coil voltages, e_d and e_q. These are related by simple equations

$$\psi_d = \psi_{md} + l_a i_d$$

$$\psi_q = \psi_{mq} + l_a i_q$$

and
$$e_d = s\psi_d + \nu\psi_q + r_a i_d$$

$$e_q = -\nu\psi_d + s\psi_q + r_a i_q$$

The resistance of the armature windings, r_a, is neglected, and the shaft speed, ν , is assumed to be constant. To include these terms would greatly increase the complexity of the circuitry, involving the use of another two multipliers. These equations may easily be solved, and the circuit employed for this purpose is shown in Fig. 4.20. The amplifiers OA 10 and OA 11 produce respectively the ψ_d and ψ_q signals, the armature leakage reactance l_a being determined by the ratio of the input resistors. The next amplifiers produce the coil voltages, including the derivative terms; the resistors R_x are to provide high frequency roll-off for this signal, to reduce noise.

This concludes the section of the synchronous machine model which solves the dynamic equations for the fluxes and coil voltages, and it can be seen that it provides insight into the behaviour of the machine by being able to observe the damper winding currents and other internal effects of the machine.

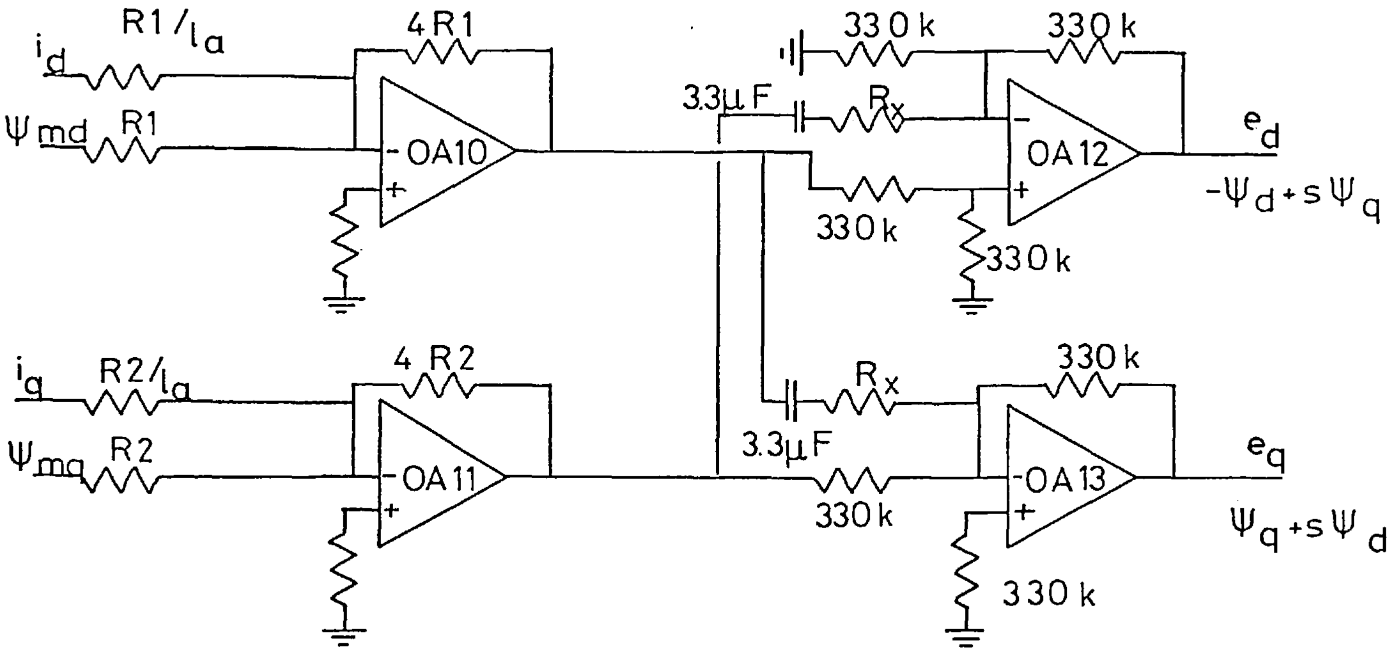

Fig. 4.20 Flux and Coil Voltage Scaling Circuits.

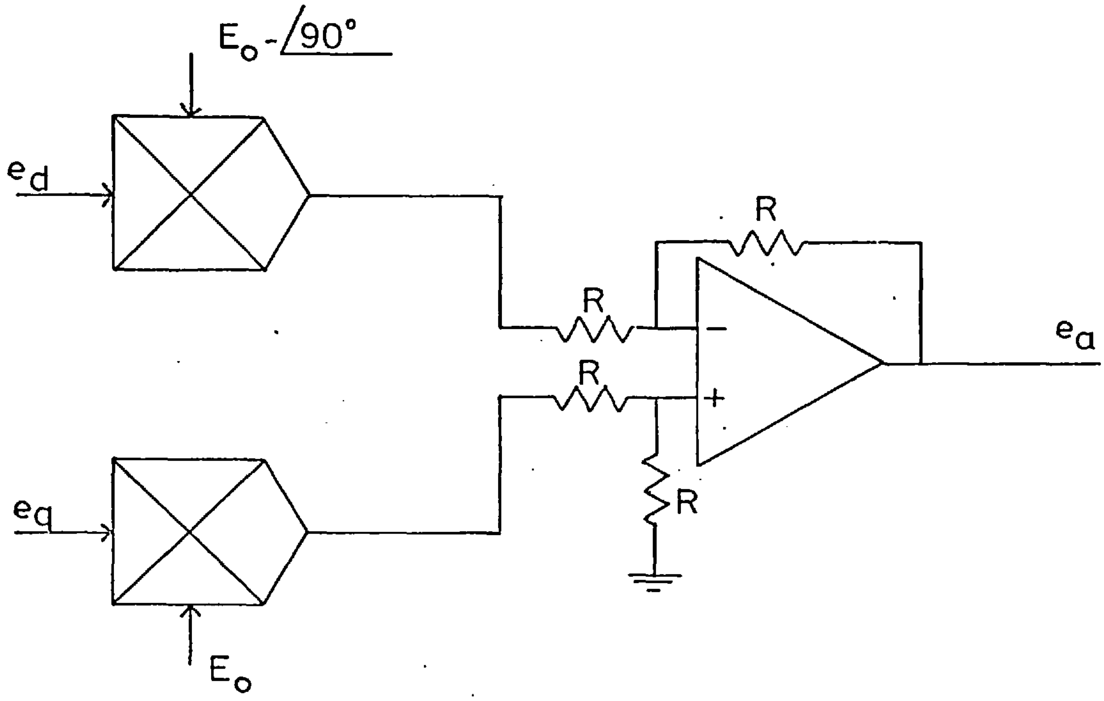

Fig. 4.21 Component Modulators.

4.4.3 The Component Modulators.

The two coil voltages e_d and e_q must be converted into a sinusoidal voltage which is the terminal voltage of the machine. The phase voltage is related to these coil voltages by the expression

$$e_a = e_d \cos\omega t + e_q \sin\omega t.$$

This can be accomplished by using the signals e_d and e_q to amplitude modulate a pair of orthogonal sine waves, one of which is in phase with E_o. These waveforms are already available from the current resolving circuit, and need not be duplicated. The diagram of the system is shown in Fig. 4.21, where the outputs of the two low-cost multipliers are summed to give a signal proportional to the terminal voltage of the machine.

4.4.4 Power Measurement.

There are two main ways in which the electrical power of the machine can be measured, and each method has certain advantages. If the power is measured at the terminals of the machine, by averaging the product of the voltage and current signals, this does not take into account the effect of damping power flows, and consequently supplementary damping signals must be included. This system, however, only requires the use of one multiplier. The alternative method is to sum the products of axis currents and flux linkages, according to the relation

$$P_e = \frac{V^2}{2} (\psi_d i_q - \psi_q i_d)$$

If the power is measured in this way, the effect of the damper windings is included, and thus a better representation of the machine is achieved, but at a greater expense in hardware. By neglecting changes in shaft speed, it is possible to implement this scheme with only two multipliers, but the power signal is the difference of two other signals.

It was decided to adopt this latter scheme, using better quality multipliers than those used in the component modulators. The arrangement used is shown in Fig. 4.22, and with the multipliers used, the accuracy is of the order of 1%.

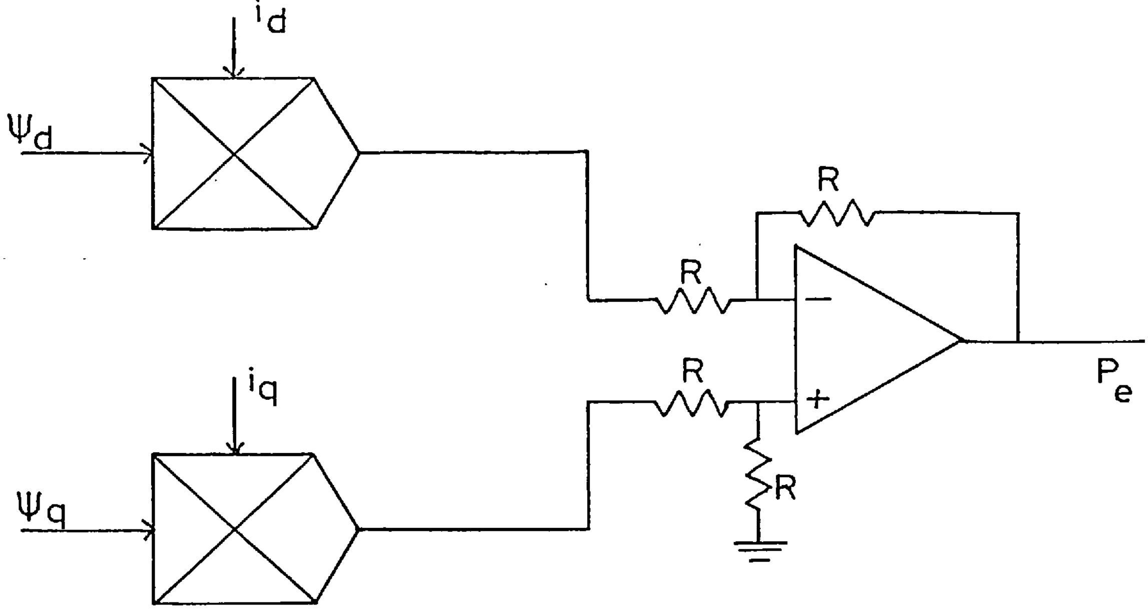

Fig. 4.22 Electrical Power Measurement.

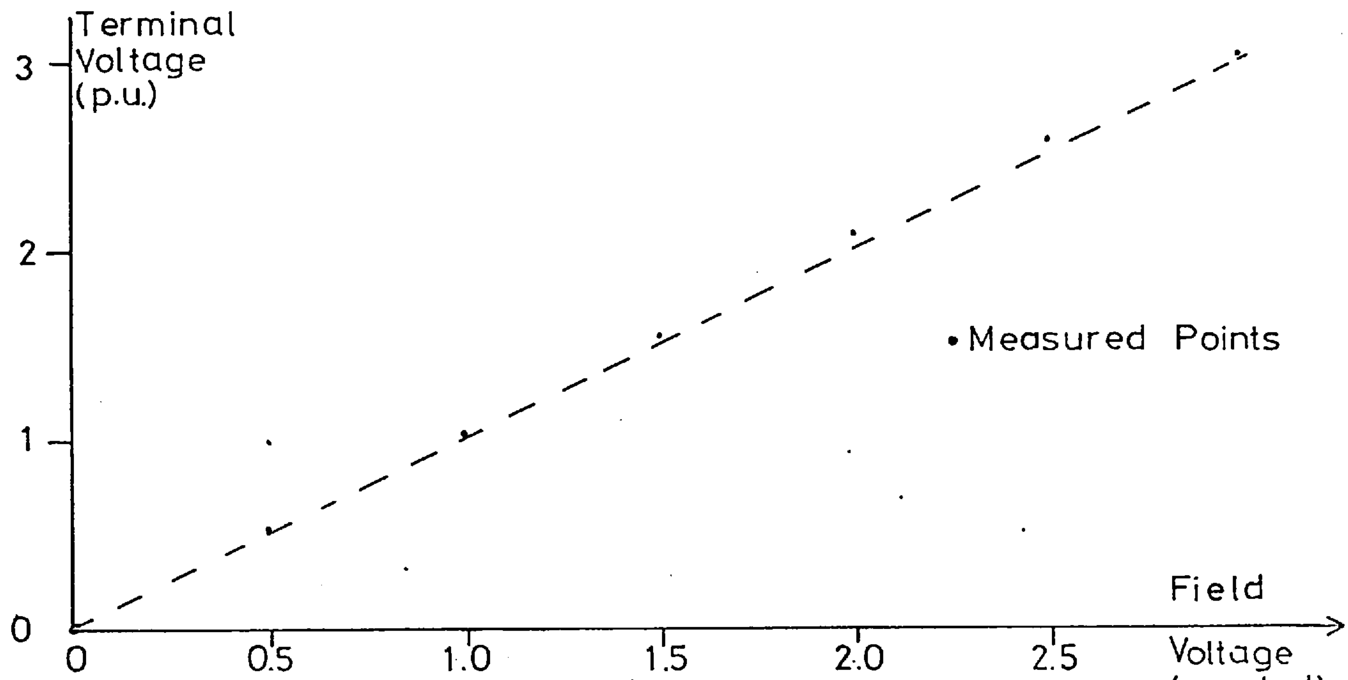

Fig. 4.23 Open Circuit Test.

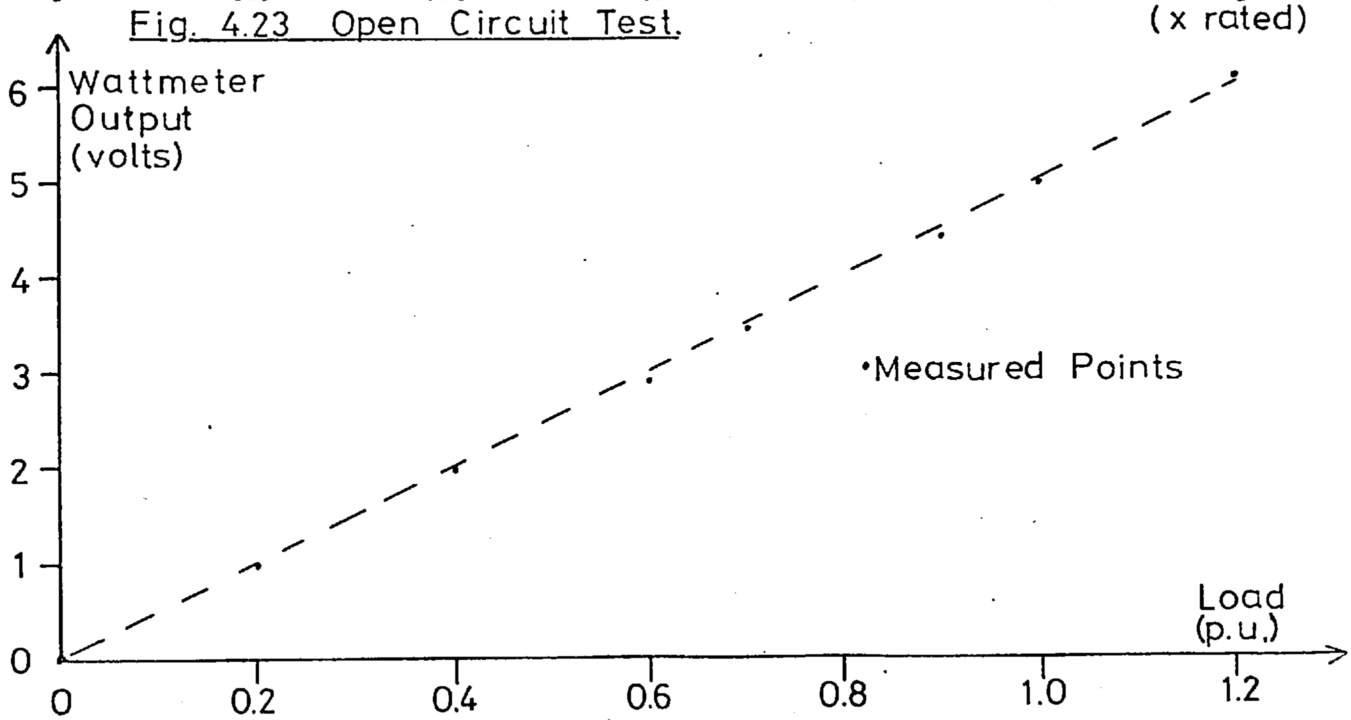

Fig. 4.24 Wattmeter Test.

4.5 Testing of the Synchronous Machine Analog.

The tests performed on the analog fall into two groups, those associated with the static characteristics, and those concerned with the dynamic aspects of the operational impedances.

4.5.1 Static Characteristics.

These tests are concerned with the linearity of the various circuits when they are interconnected to form the whole analog. The first test is the measurement of the open circuit terminal voltage against the applied field voltage, and the results are shown in Fig. 4.23. The analog was operated at fixed frequency, with the power amplifier connected, and this test examined the linearity of the voltage-to-current converter, the scaling circuits and the quadrature voltage component modulator. The results show good linearity, within 1½%, and this error can be ascribed to the multiplier used in the modulator. A similar test was also performed on the other modulator, by injecting a signal to represent quadrature current, and this was found to have an accuracy similar to that of the quadrature voltage multiplier.

The second static test was one performed on the wattmeters, under conditions of both fixed terminal voltage and also fixed excitation. The results shown in Fig. 4.24 are for the constant terminal voltage test, using a variable resistance load. The graph is plotted for wattmeter output against the reciprocal of the load resistance, and it can be seen that the accuracy is of the order of 1% of full-scale reading. The other tests performed on the wattmeter were the measurement of the power/angle curve, and these tests were done with the steam turbine simulation connected, and were obtained by connecting the generator unit to the infinite bus, and by then adjusting the excitation and the electrical power. This also enables the limit of stability to be found. The results are shown in Fig. 4.25, and show that the unit performs as required. The

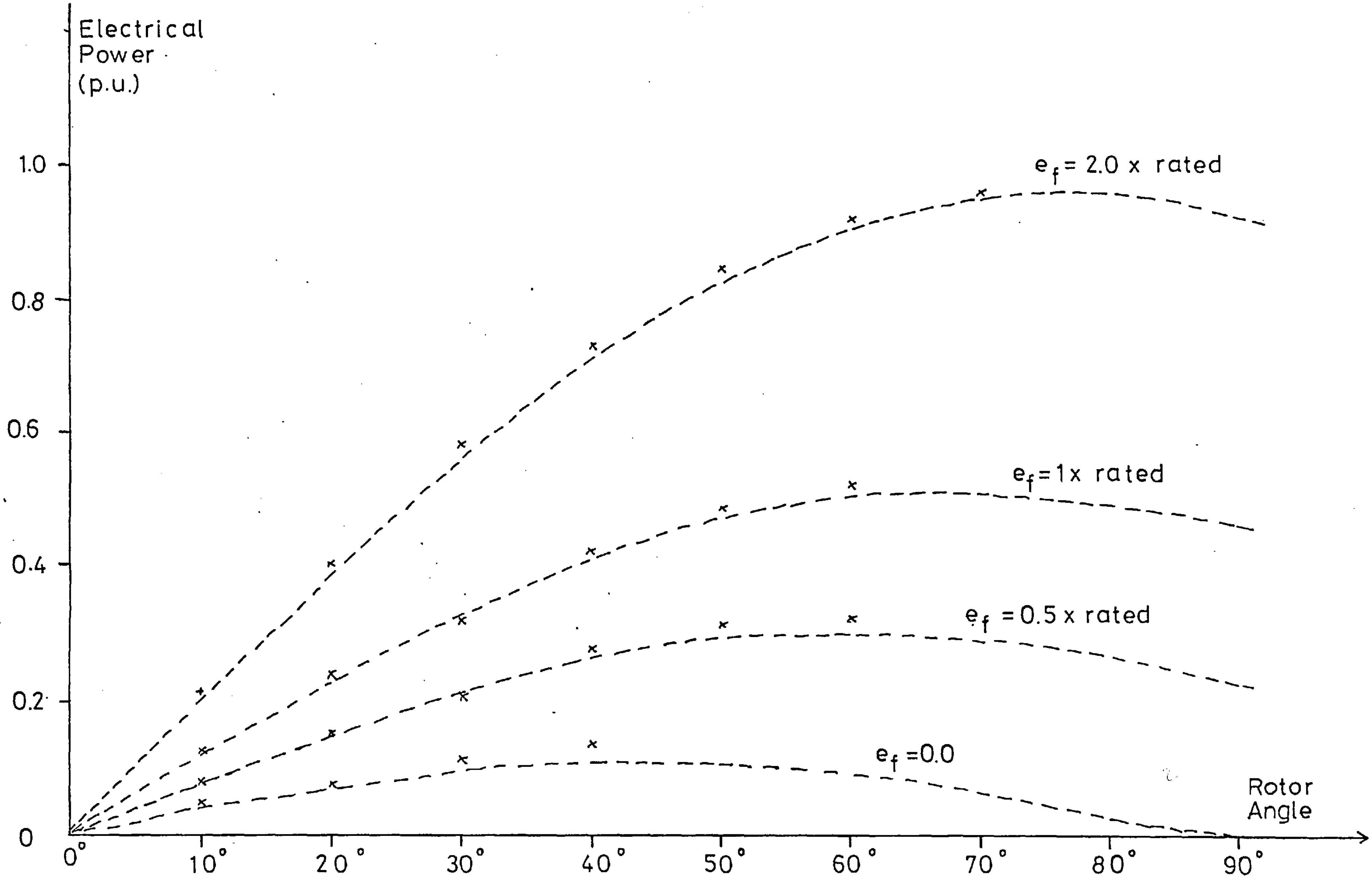

Fig. 4.25 Torque - Angle Characteristic.

decrease in accuracy as the limit of stability is reached is due to the difficulty in making measurements at this point because of the oscillatory nature of the operating point. The salient structure of the machine means that with no excitation, the machine should run on reluctance torque, and this is clearly shown.

4.5.2 Dynamic Tests.

Three main sets of tests were performed on the synchronous machine model in order to assess its dynamic performance. The first set of tests were to measure the operational impedances $x_d(j\omega)$ and $x_q(j\omega)$ as functions of frequency. The measurements were made with the aid of a transfer function analyser, which was synthesised on an EAL analog computer. For constant amplitude sinusoidal signals introduced into the i_d and i_q amplifiers, the resulting axis fluxes were measured, both in amplitude and phase. The measurements, together with the predicted response, are given in the Nyquist plots of Figs. 4.26 and 4.27. The agreement is good, except at low frequencies, and this can be ascribed to the problem of measuring the two components of the output signal, together with the drift in the analyser oscillator.

The second dynamic test was done with the machine running with no excitation, as an induction generator, connected to the infinite bus. The axis currents and fluxes both have sinusoidal variations, and measurement of their respective magnitudes and phase angles enables measurements to be made of the impedances under these operating conditions. The trace is shown in Fig. 4.28, and the points are plotted on the main operational impedance graphs. The agreement is shown to be good. The ability of the machine to run asynchronously is also a useful validation of its performance. Such phenomena as pole-slipping can also be demonstrated, but limitations of the power amplifier preclude short-circuit tests being performed.

The final test is that of voltage response, following removal of an

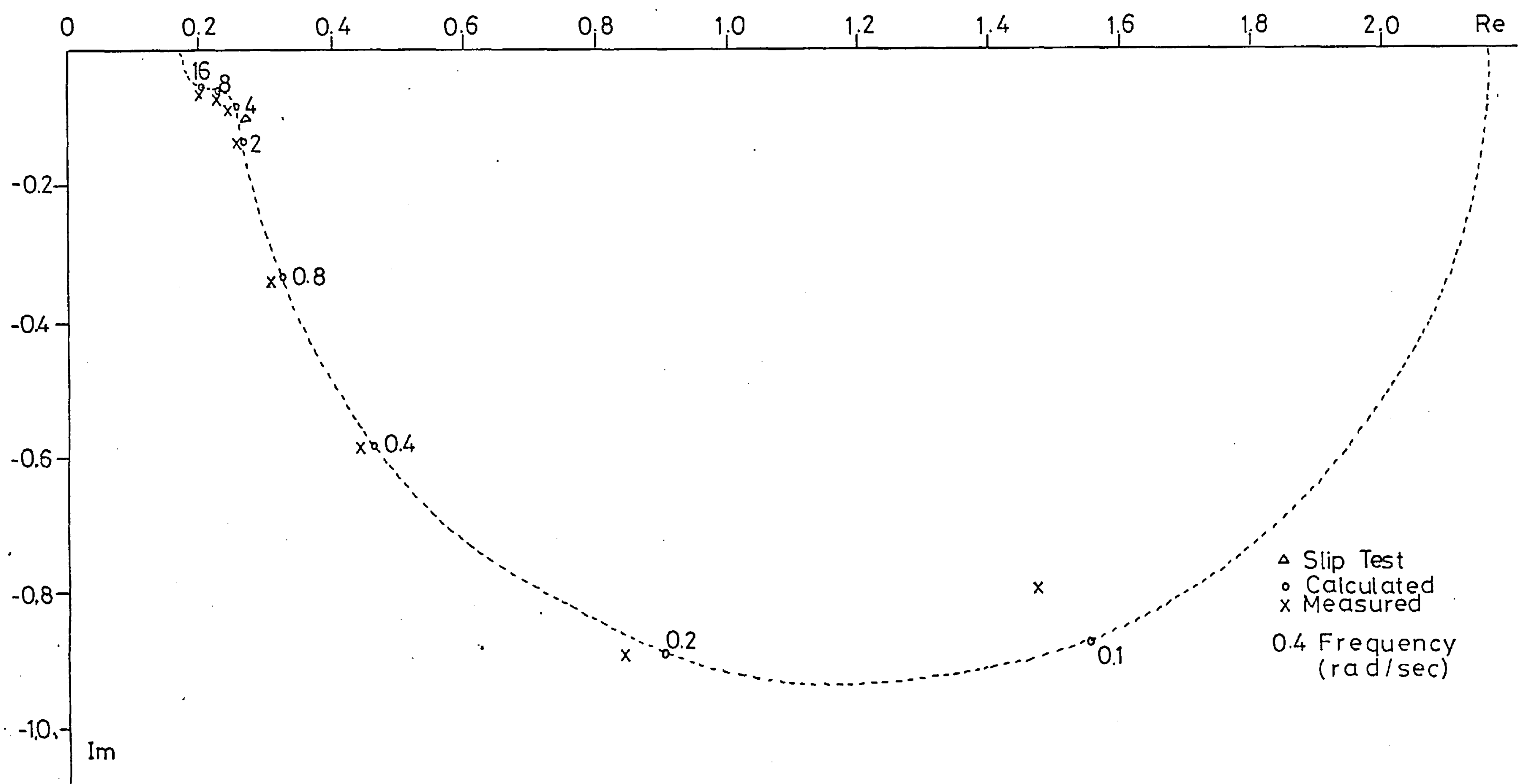

Fig. 4.26 Direct Axis Operational Impedance.

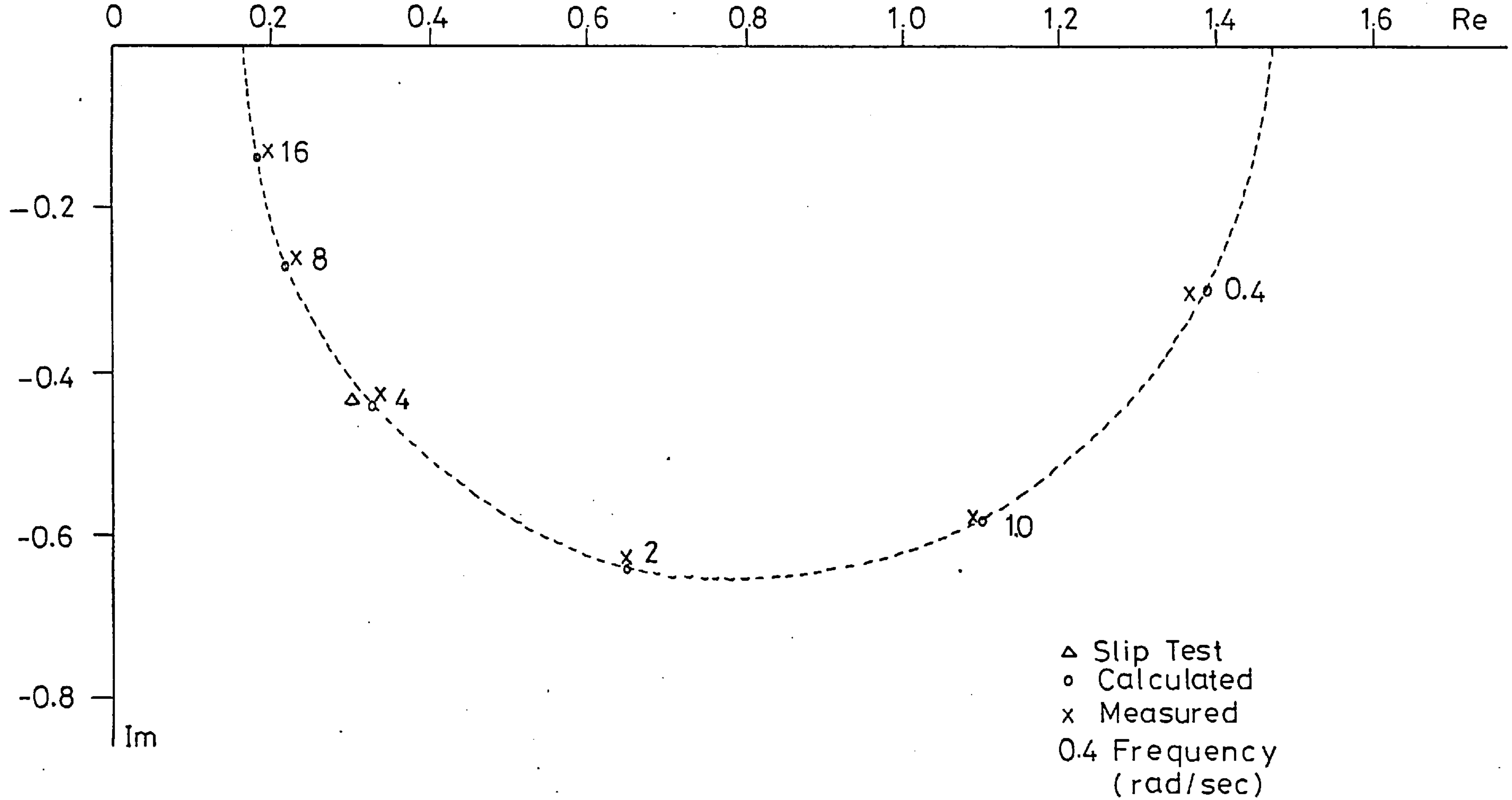

Fig. 4.27 Quadrature Axis Operational Impedance.

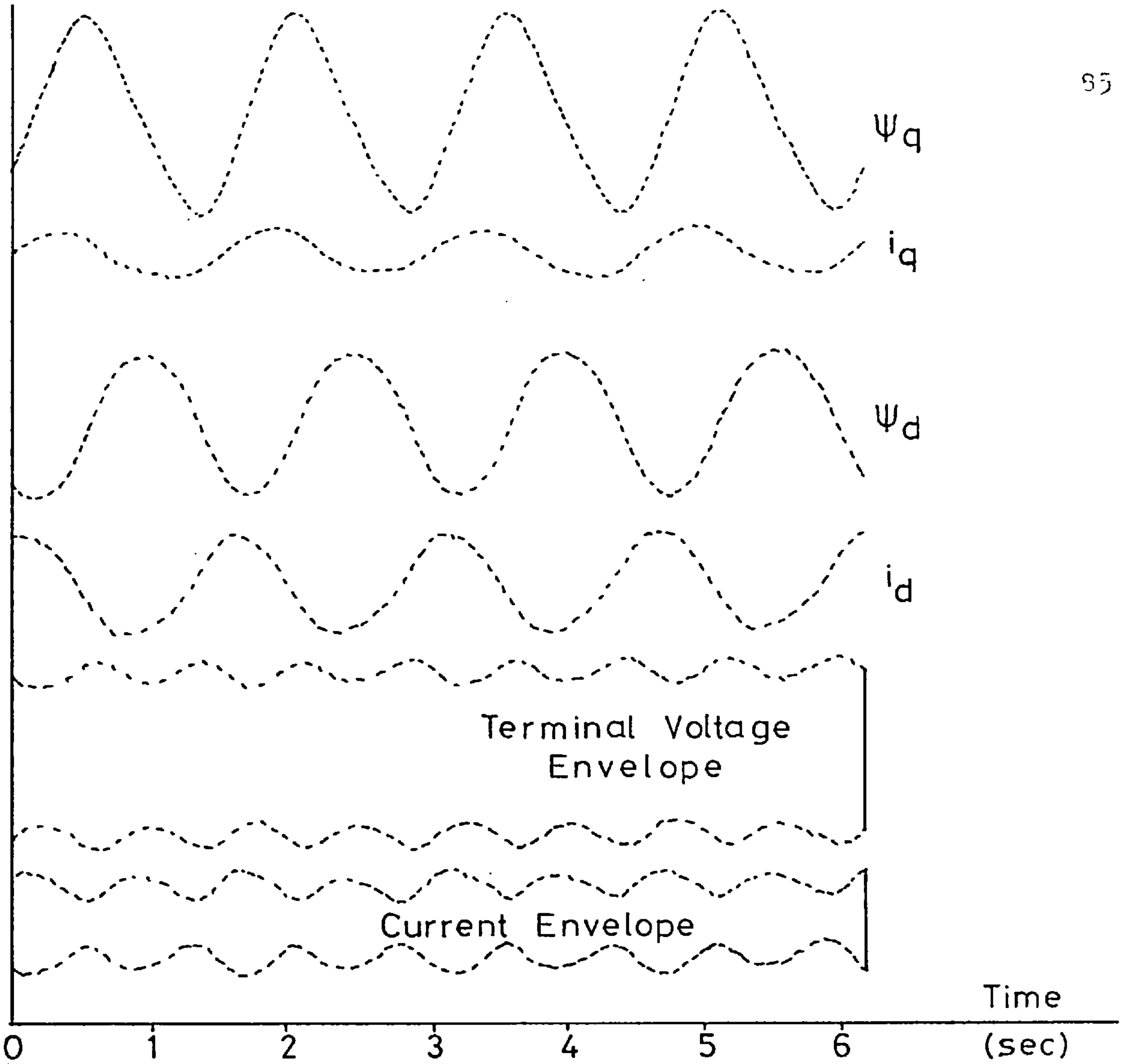

Fig. 4.28 Asynchronous Operation. Slip Freq. = 4.0 rad/sec.

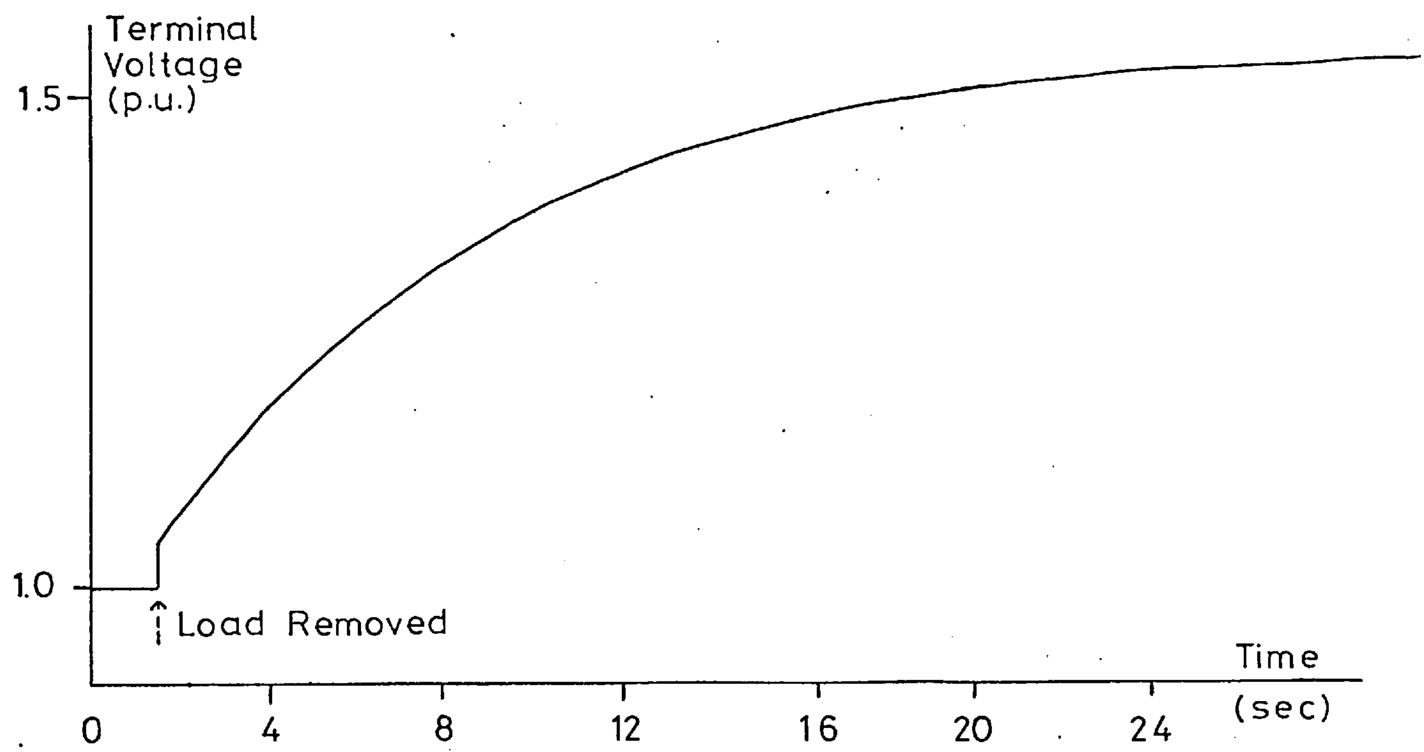

Fig. 4.29 Terminal Voltage Response following removal of a 0.25 p.u. Inductive Load.

inductive load, with fixed excitation. The terminal voltage response is shown in Fig. 4.29, and from this can be estimated the sub-transient reactance, x_d'', and the open-circuit transient time constant, T_{do}'. The measured values and the calculated ones are:

	Measured	Calculated
x_d''	0.19 p.u.	0.17 p.u.
T_{do}'	7.0 sec	6.55 sec

This shows reasonable agreement for the voltage response with no quadrature axis flux, and other tests have shown that with the rejection of resistive load, the response also agrees with the predicted values.

4.6 Conclusion.

The synchronous machine analog has been described, and it has been demonstrated that both its static and dynamic characteristics are in agreement with theoretical predictions. It has been found to work well under all conditions of operation, except that it will not simulate adequately a short-circuit, due to limitations of the power amplifier. Since it is a single phase model, it only represents balanced operation of the machine, but there is no reason why a 3 phase version could not be built, to investigate unbalanced operation, and with a good power amplifier it would be possible to study unbalanced short-circuits. In conclusion, therefore, it has been shown that this analog is a good representation of a real machine, and thus it provides a degree of insight into what is happening inside the machine, in terms of fluxes and currents.

5.1 Introduction.

For maximum simulator flexibility,the representation used for loads on the system must allow the load at a given node to be infinitely variable,both in magnitude and power factor,and the load should also be controllable either manually or by the computer. This precludes the use of switched resistances, inductors and capacitors, such as are employed in network analysers, and indicates that electronic representation is required. The original CERL model used such a representation, where a load unit acted as a programmable power sink, and as a source or sink of reactive power. This representation was initially employed, but was found to be unsatisfactory for use in small systems and had to be abandoned. However, a similar scheme has been developed using the load as a constant current sink, rather than a power sink, and this has been found to be satisfactory for all conditions of operation with the rest of the simulator.

In this chapter,the two approaches to load unit design are examined and their stabilities are analysed. Calibration and dynamic response data are also provided for the load unit which has been finally adopted for use in the simulator.

5.2 Fundamental Concept.

The concept underlying the design of both types of load unit is illustrated in Fig.5.1(a), and by its companion phasor diagram Fig.5.1(b). The resistor,R, is connected between the load busbar of voltageV, and the electronic load unit, which produces a voltage E. Clearly, by changing the magnitude and phase of this voltage E, the current I can be made to have any magnitude and phase with respect to the load busbar voltage V. The internal voltage, E, can be resolved into two components, e_p and e_q;

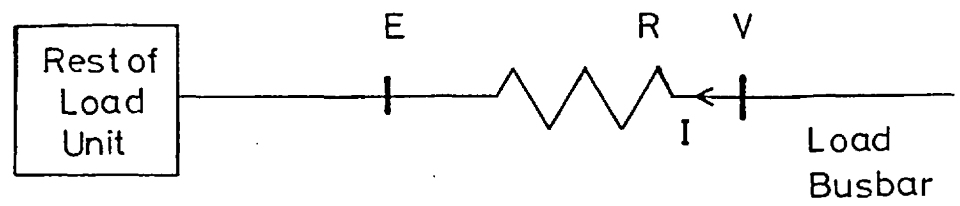

Fig. 5.1(a)

Principle of the Load Unit.

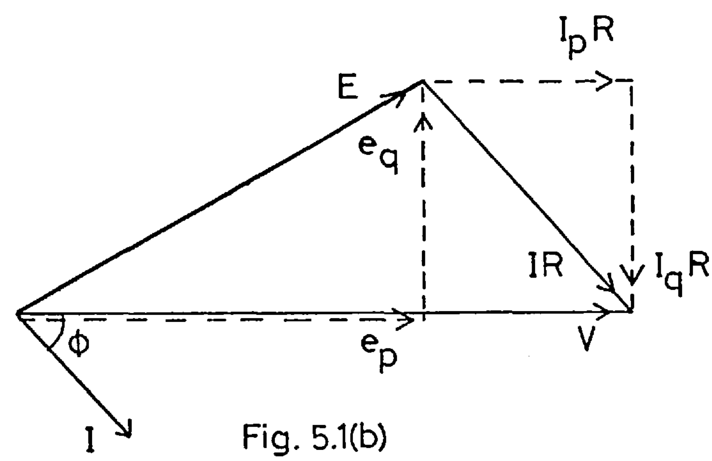

Fig. 5.1(b)

Load Unit Phasor Diagram.

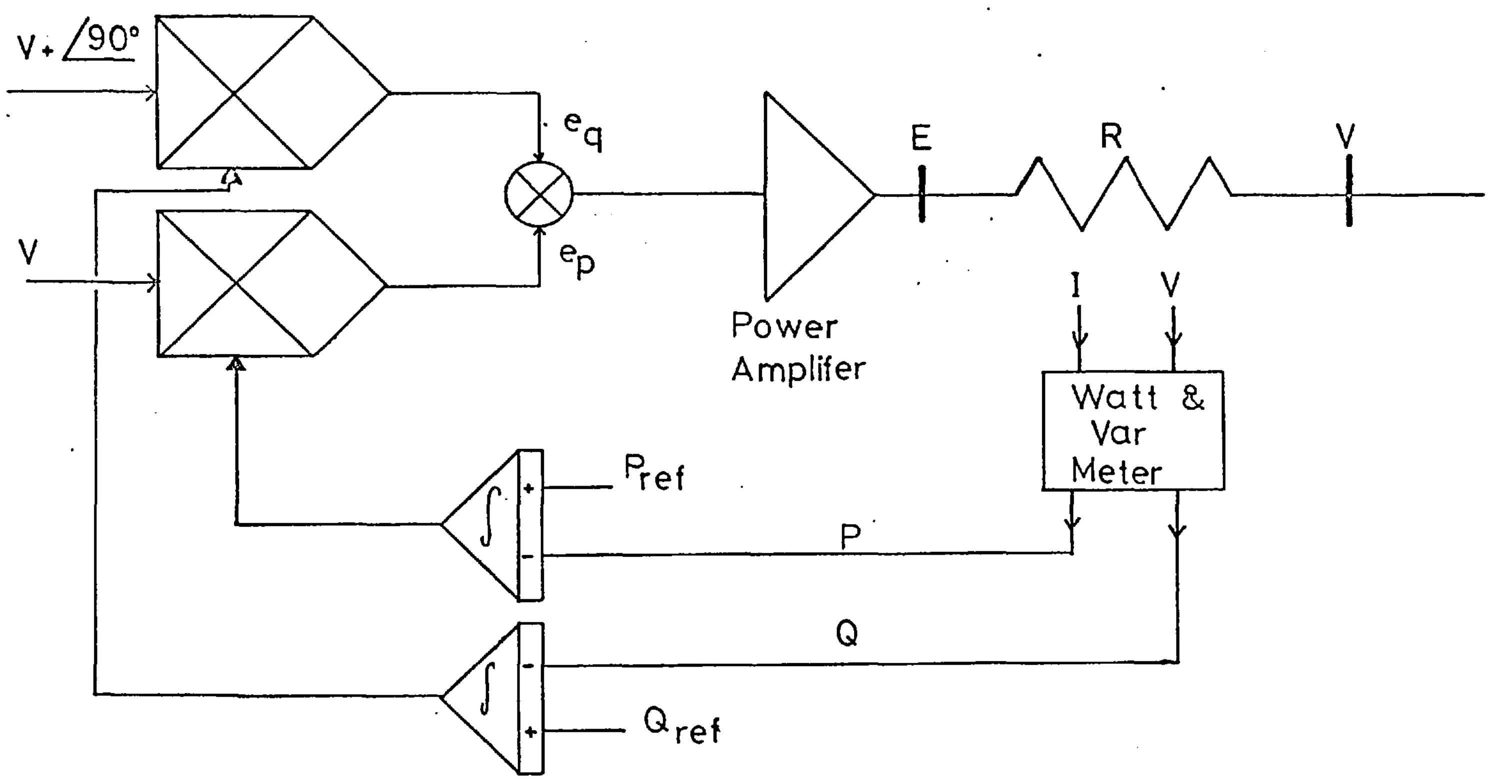

Fig. 5.2

Block Diagram of Constant Power Load.

similarly the load current can be resolved into components I_p and I_q. From the phasor diagram it can be seen that

$$V - e_p = R.\ I_p$$

and $$e_q = R.\ I_q$$

Thus it is possible to control independently the in-phase and quadrature components of the current, I_p and I_q, by varying the two components of the internally generated voltage, e_p and e_q with respect to the load busbar voltage V.

In the constant power and reactive power model, it is desired to maintain the products $V.I_p$ and $V.I_q$ constant, whereas in the constant current unit, only the magnitudes of I_p and I_q must be held to the required value. This can be achieved as shown in Fig.5.2. The internal voltage E is produced by summating its two components e_p and e_q, which themselves are derived from two amplitude modulators. These modulators have as their respective inputs voltages in-phase and in quadrature with the terminal voltage V and these are amplitude modulated by d.c. signals derived from integrators which integrate $(P_{actual} - P_{ref})$ and $(Q_{actual} - Q_{ref})$, the two error signals. This description applies to the constant power model, but if the power and reactive power signals are replaced by signals representing the two components of current, then the unit becomes a constant current load.

Since the two control loops operate on signals 90 out of phase, they are completely independent provided that the terminal voltage does not change. Additionally, if the terminal voltage remains constant then the behaviour of the constant current model will be exactly the same as that of the constant power model.

5.3. The Constant Power Load Unit.

A constant power and reactive power load unit was constructed as described in the previous section, and when connected to a low impedence source

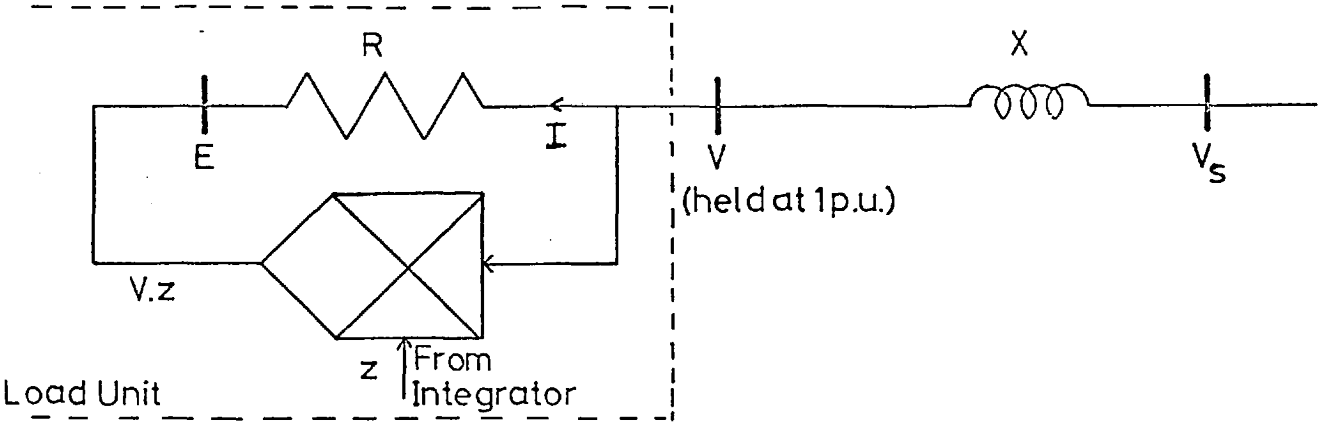

Fig. 5.3 Steady-State Stability Model.

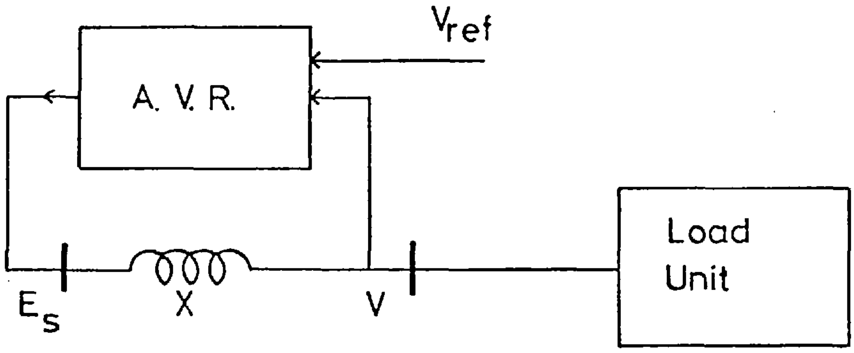

Fig. 5.4(a) Dynamic Stability Model.

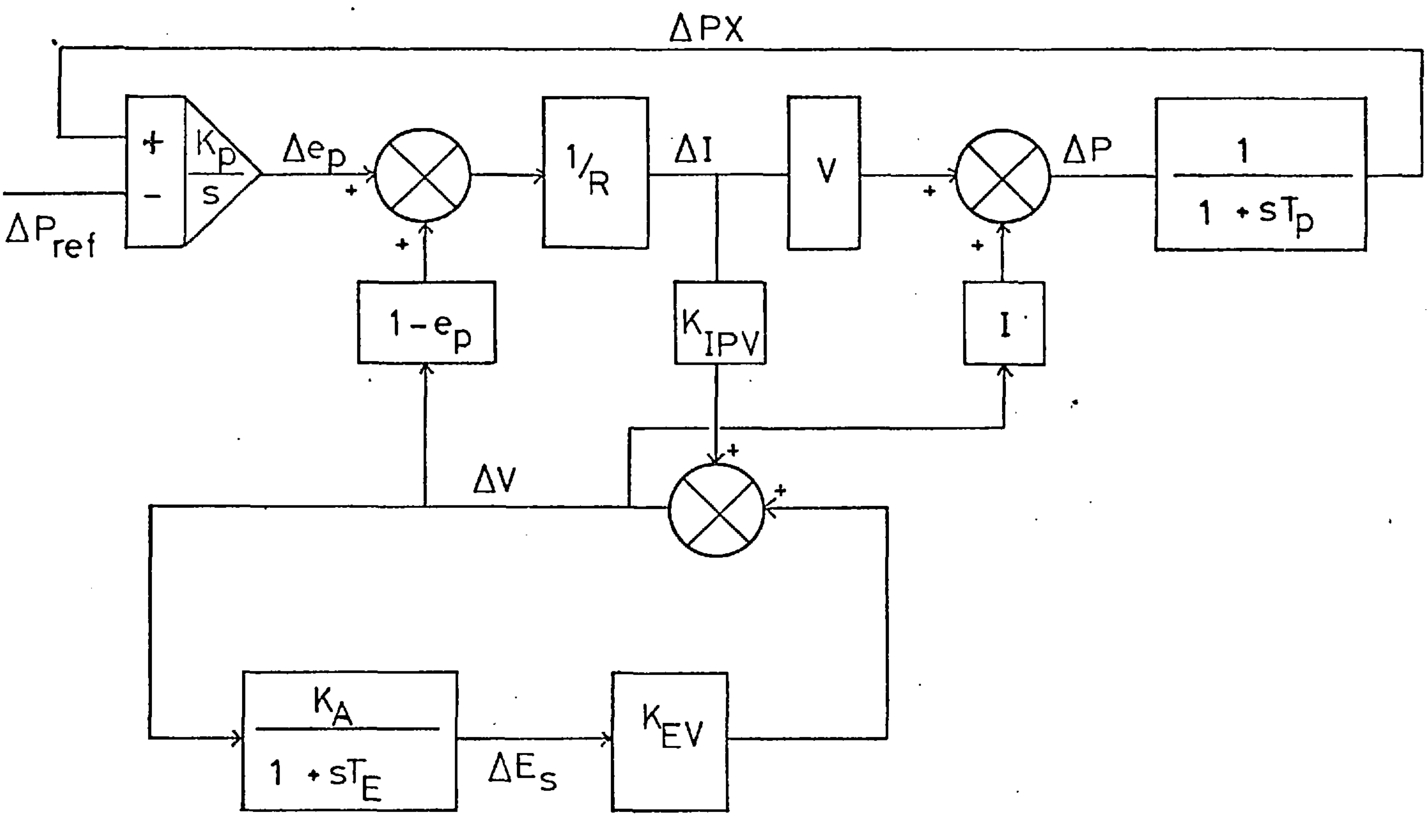

Fig. 5.4(b) Linearized Model for Dynamic Analysis.

its performance was stable, but when connected to a generator unit of the type designed by Sheldrake , it proved to be unstable for large values of absorbed power. Analysis showed that this instability was caused by the large series reactance used in the synchronous machine representation. For a series combination of inductance X, and resistance R, the maximum power is dissipated in the resistance when X=R. Now consider the system shown in Fig.5.3: Z is the controlling voltage from the output of the integrator and the internal voltage E is then V.Z. The following equations can be written :

$$I = V(1-Z)/R$$

$$P = V^2(1-Z)/R$$

also $V^2 = V_s^2 - I^2X^2$ and $I^2 = V_s^2/(R_{eq}^2 + X^2)$

where R_{eq} is the equivalent resistance of the load unit.

$$R_{eq} = R/(1-Z)$$

Thus
$$P = \frac{(1-Z)}{R} \quad E^2 - \frac{E^2X^2}{R_{eq}^2+X^2}$$

$$= \frac{E^2(1-Z)}{R} \quad \frac{R^2}{R^2 + X^2(1-Z)}$$

For the system to be controllable $\frac{\partial P}{\partial Z}$ must be negative, for otherwise the integral control will act in the wrong direction as it tries to maintain the current at the desired value. The limit of stability can be found by considering the turning points of the function P(Z). If this function is differentiated, then it can be shown to have roots

$$Z = 1 \pm R^2/X^2$$

whence $X = R/(1-Z) = R_{eq}$

This shows that the limit of power transfer in the steady state is reached when the equivalent resistance of the load unit equals that of the reactance through which it is fed. In the case of a machine represented by its synchronous reactance, which may be 2 p.u.,this means that a load unit will not work above 0.5 p.u. power, which reduces its usefulness.

Clearly, in the original CERL model, the system was of such a size that the network reactance seen by a given load unit was small enough for the unit to work satisfactorily, and it is only in small systems that this problem manifests itself. It was thought, however, that the presence of a voltage regulator on the machine might tend to improve the stability, for as the terminal voltage dropped, as the load unit took more power, the voltage regulator would tend to increase this voltage. To examine the dynamic interaction of a load unit with a voltage regulator, the system shown in Fig. 5.4 was considered.

The equations describing the system have been linearized, and the effect of the reactance has been reduced to two parameters K_{IPV} and K_{EV}, which describe the way in which the terminal voltage V changes with alterations in the in-phase load current and the synchronous machine internal voltage E_i, respectively. The equations for the system can be written:

$$K_{IPV} = \frac{\partial V}{\partial I_p} \qquad \Delta P = V.\Delta I + I.\Delta V$$

$$\Delta I = \frac{1}{R}(\Delta e_p + (1-e_p)\Delta V)$$

$$K_{EV} = \frac{\partial V}{\partial E_i} \qquad \Delta V = K_{IPV}.\Delta I_p + K_{EV}.\Delta E_i$$

$$\frac{\Delta E}{\Delta V} = \frac{K_A}{1 + sT_E} \qquad \frac{\Delta P_x}{\Delta P} = \frac{1}{1 + sT_p}$$

These can be arranged in state variable form as

$$\begin{bmatrix} \Delta \dot{e}_p \\ \Delta \dot{P}_x \\ \Delta \dot{E}_i \end{bmatrix} = \begin{bmatrix} 0 & -K_p & 0 \\ K_1 & -1/T_p & K_2 \\ K_3 & 0 & K_4 \end{bmatrix} \begin{bmatrix} \Delta e \\ \Delta P_x \\ \Delta E_i \end{bmatrix} + \begin{bmatrix} K_p \\ 0 \\ 0 \end{bmatrix} \begin{bmatrix} P_{ref} \end{bmatrix}$$

The parameters K_{1-4} are given in Appendix B, as are the coefficients K_{IPV} and K_{EV}.

The roots of this system were then determined by finding the eigenvalues of the above matrix, for different values of load unit gain, K_p, reactance

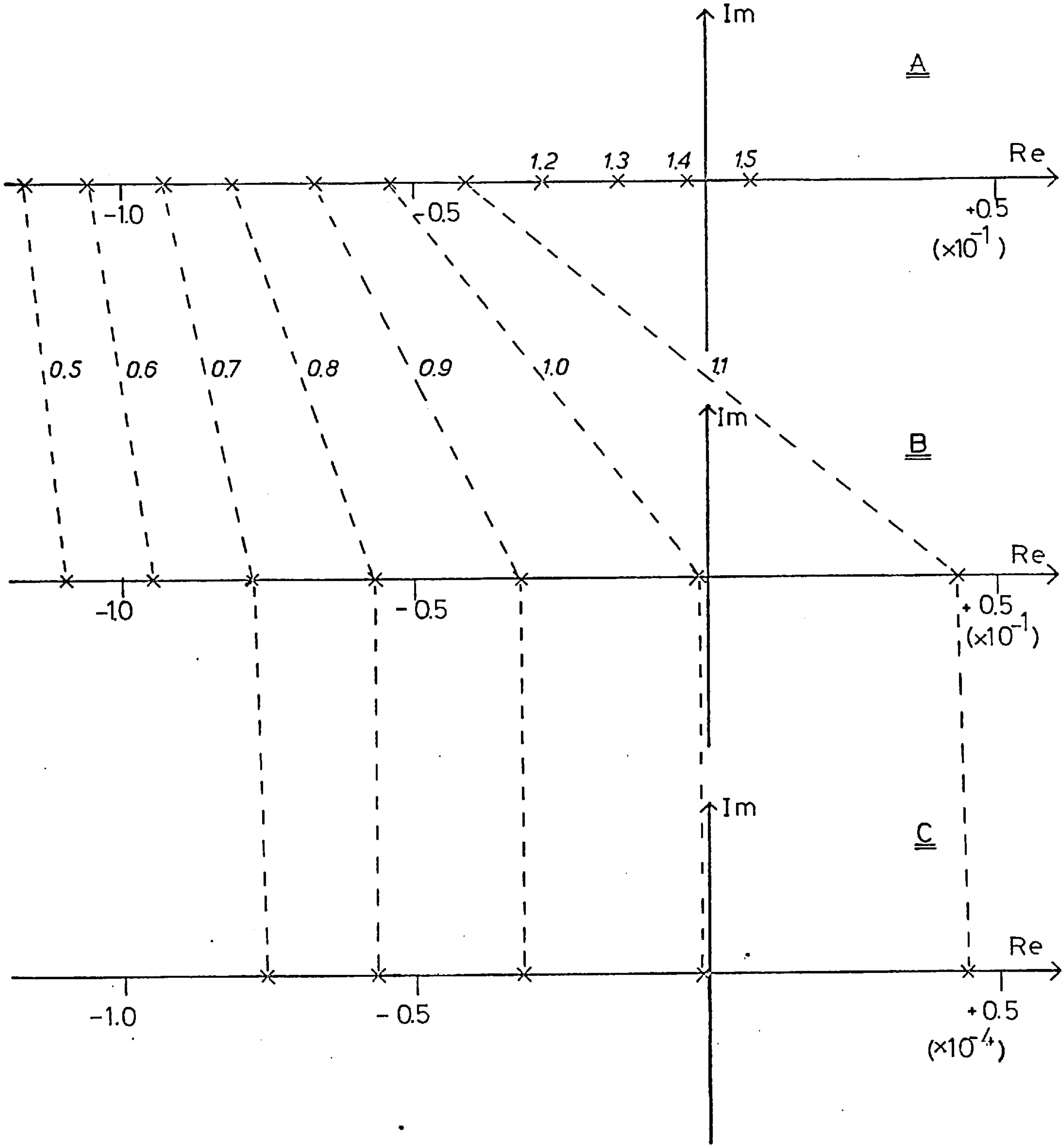

A – No AVR

B – With AVR $K_p = 1.0$

C – With AVR $K_p = 0.001$

--- *1.2* --- *Line Reactance*

Fig. 5.5 Root Loci for Different Line Lengths of the Model of Fig. 5.4.

and voltage regulator gain. Some of these results are shown in Fig. 5.5, for a terminal voltage of 1 p.u., and a power absorbtion of 0.7 p.u., giving an equivalent load resistance of 1.43 p.u.. Root loci are plotted for the following three cases:

(a) No voltage regulator $T_p = 0.02$ sec $K_p = 1.0$

(b) With AVR $K_A = 400$ $K_p = 1.0$ $T_p = 0.02$ sec $T_E = 5.0$ sec

(c) With AVR $K_A = 400$ $K_p = 0.001$ $T_p = 0.02$ sec $T_E = 5.0$ sec

In the first case, A, the stability limit should be $X = R_{eq} = 1.43$ p.u. and this can be seen to be the case. If, however, a high speed voltage regulator is included, then the critical reactance decreases, B, and even if the dynamics of the load unit are slowed right down, C, then although the magnitude of the poles decreases, the reactance for instability remains the same as that for case B. Further studies showed that the stability becomes worse as the AVR gain falls over the normal range of such gains, only to rise to the calculated reactance value as the gain tends to zero. The poor performance of this type of load unit led to its being abandoned in favour of a constant current type, which is described below.

5.4 The Constant Current Load Unit.

Once the problems of the constant power load unit had been ascribed to voltage instability, it was realized that a constant current load unit would not suffer from the same problems, and it was decided to construct a prototype. The block diagram is shown in Fig. 5.6. Several of the circuits employed have already been described in connection with the generator unit and will only be briefly mentioned here. Each section of the unit will be considered in turn, and finally the performance of the whole system will be considered.

5.4.1 The Current Resolvers.

It is necessary to measure the two components of the current at the terminals of the unit, and it is on the accuracy of these measurements that the whole unit depends. It would be possible to use resolving circuits of

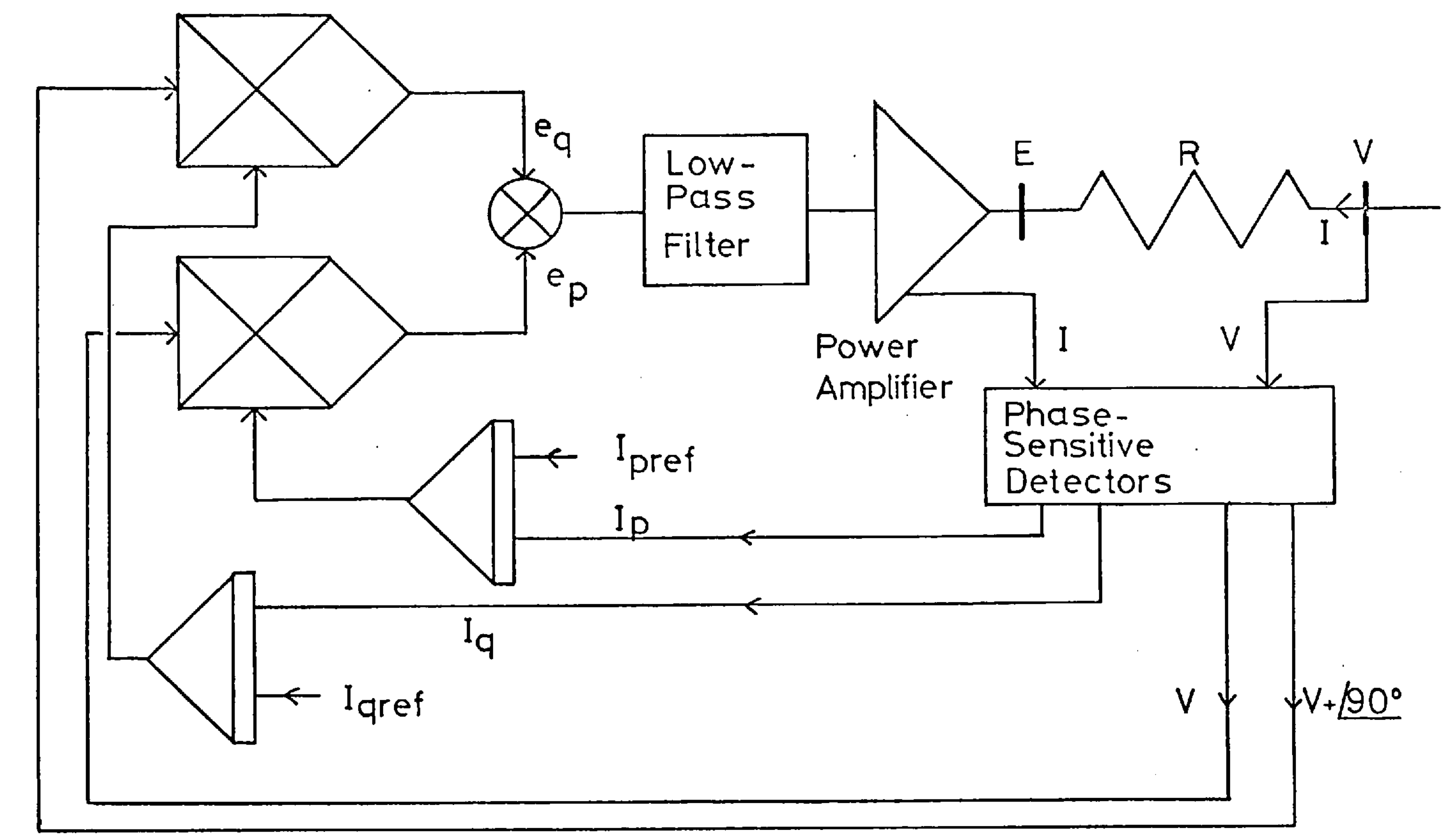

Fig. 5.6 Constant Current Load Unit.

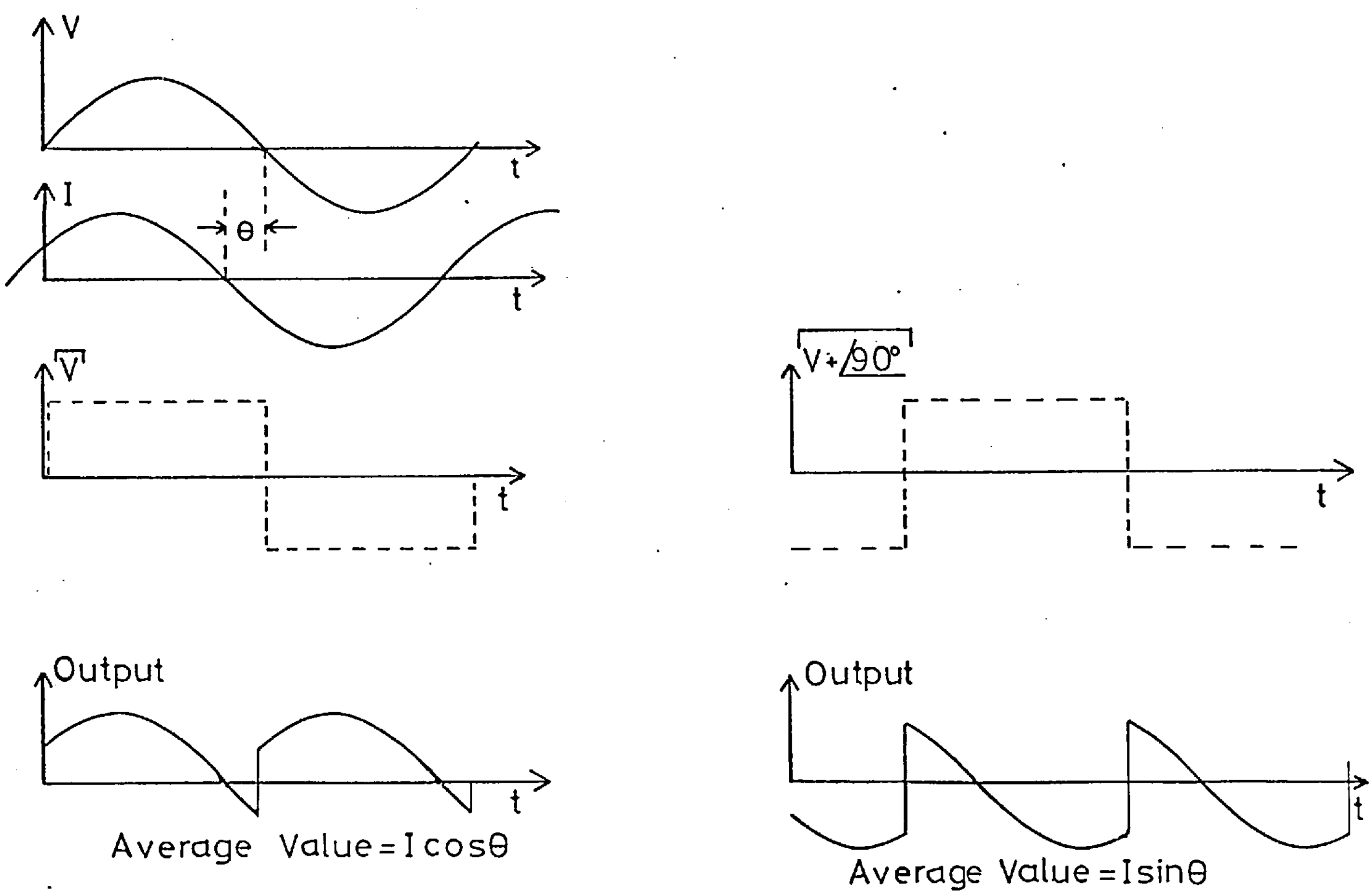

Fig. 5.7 Principle of the Phase-Sensitive Detectors.

the sampling type, such as are employed in the generator unit, but in this case it was decided to use phase-sensitive detectors. These produce a signal whose average value is proportional to the magnitude of the component of the input signal which is in-phase with a switching waveform. Since an electronic watt and var meter had been built for the constant power load, this was modified as shown in Fig. 5.7 to work as a pair of phase-sensitive detectors. The principle of operation is that the current signal is fed to both multipliers, and in one case it is multiplied by a squared version of the terminal voltage, while in the other it is multiplied by a square wave in quadrature with the terminal voltage. If there is an angle between the terminal voltage and current waveforms, then the average output over half a cycle is

$$\frac{2\,V}{\pi}\, I \cos\Theta$$

and for the square wave shifted by 90°

$$\frac{2\,V}{\pi}\, I \sin\Theta$$

Since the signals are fed into integrators, only a small amount of filtering is necessary, and this allows the use of this type of detector. The circuit diagram of this section of the unit is shown in Fig. 5.8.

The amplifier OA 1 takes the current signal, derived from a resistive shunt in the power amplifier output, and amplifies it to a suitable level to be fed to the two multipliers M 1 and M 2. These are the low-cost MC 1495 type. The terminal voltage is fed through a high resistance potential divider, and is then buffered by a voltage follower OA 2. It is then fed to the first multiplier via a squaring circuit, OA 3, while it is fed to the second multiplier via a phase-shifter, OA 4, and another squarer, OA 5. The two multiplier outputs are then fed to two low-pass filters, OA 6 and OA 7 respectively, each with a time constant of 0.02 sec. This removes the highest harmonic components, and these signals are then used to provide the integrators with the measured currents, and also to drive the front panel meters. Further filtering is done on these signals

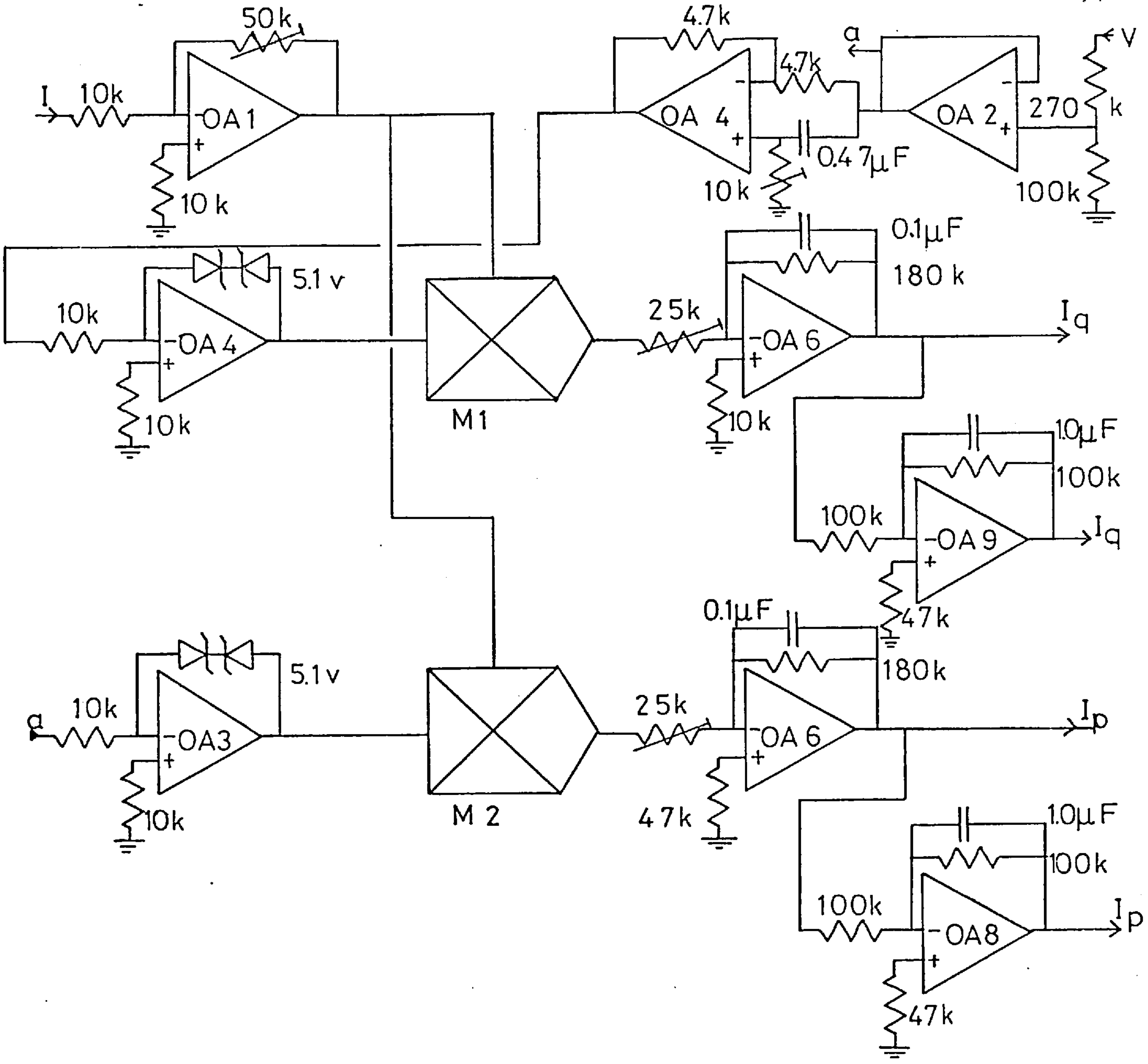

Fig. 5.8 Current Resolvers.

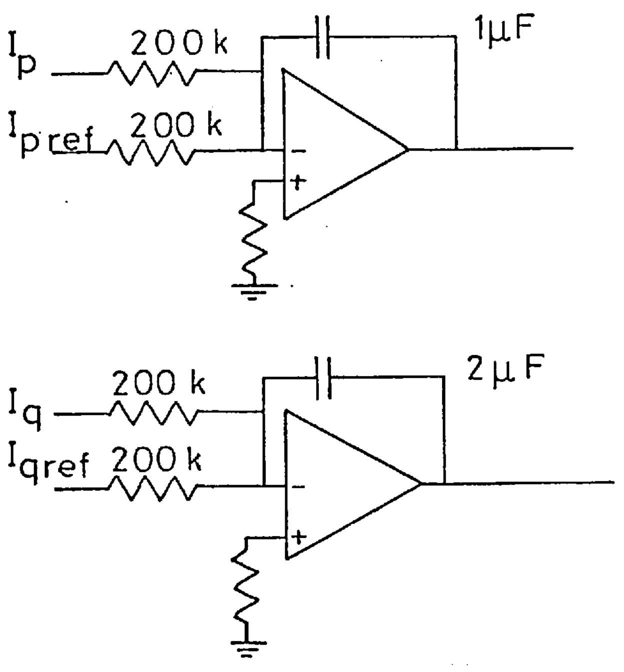

Fig. 5.9 The Integrators.

by OA 8 and OA 9, to reduce the ripple to less than 1%, so that these signals are suitable for direct A/D conversion by the computer. The outputs are calibrated to give the following signals:

$$1 \text{ p.u. } I_p = -10 \text{ volts}$$

$$1 \text{ p.u. } I_q \text{ lagging } = -10 \text{ volts}$$

$$\text{leading } = +10 \text{ volts}$$

To determine the accuracy of this section of the load, on which everything else depends, a test was carried out using an RC series network to act as a load of 0.85 power factor, and the current components were measured when this was fed from an ac source. The results are shown in Fig. 5.10. The worst error ocurs in the middle of the range, where it is of the order of 2%. This error is produced entirely by the multipliers, and the only remedy is to use more expensive multipliers. This was not done since twenty multipliers are required for all the load units.

5.4.2 <u>The Integrators</u>.

The integrators are the main elements in the feedback loops, and they provide the principal control of the loop gains, which determine the system performance. The circuit is shown in Fig. 5.9. The demand signal and the measured signal have opposite signs, and the integrator is driven in such a direction as to reduce the sum of these two signals to zero. Since these integrators are used in feedback loops, they may be constructed using low cost operational amplifiers, as any offset or drift is automatically cancelled. The feedback capacitors are chosen to give the desired value of loop gain.

5.4.3 <u>The Amplitude Modulators</u>.

The circuit employed here is identical to that used in the synchronous machine analog, and will not be discussed further.

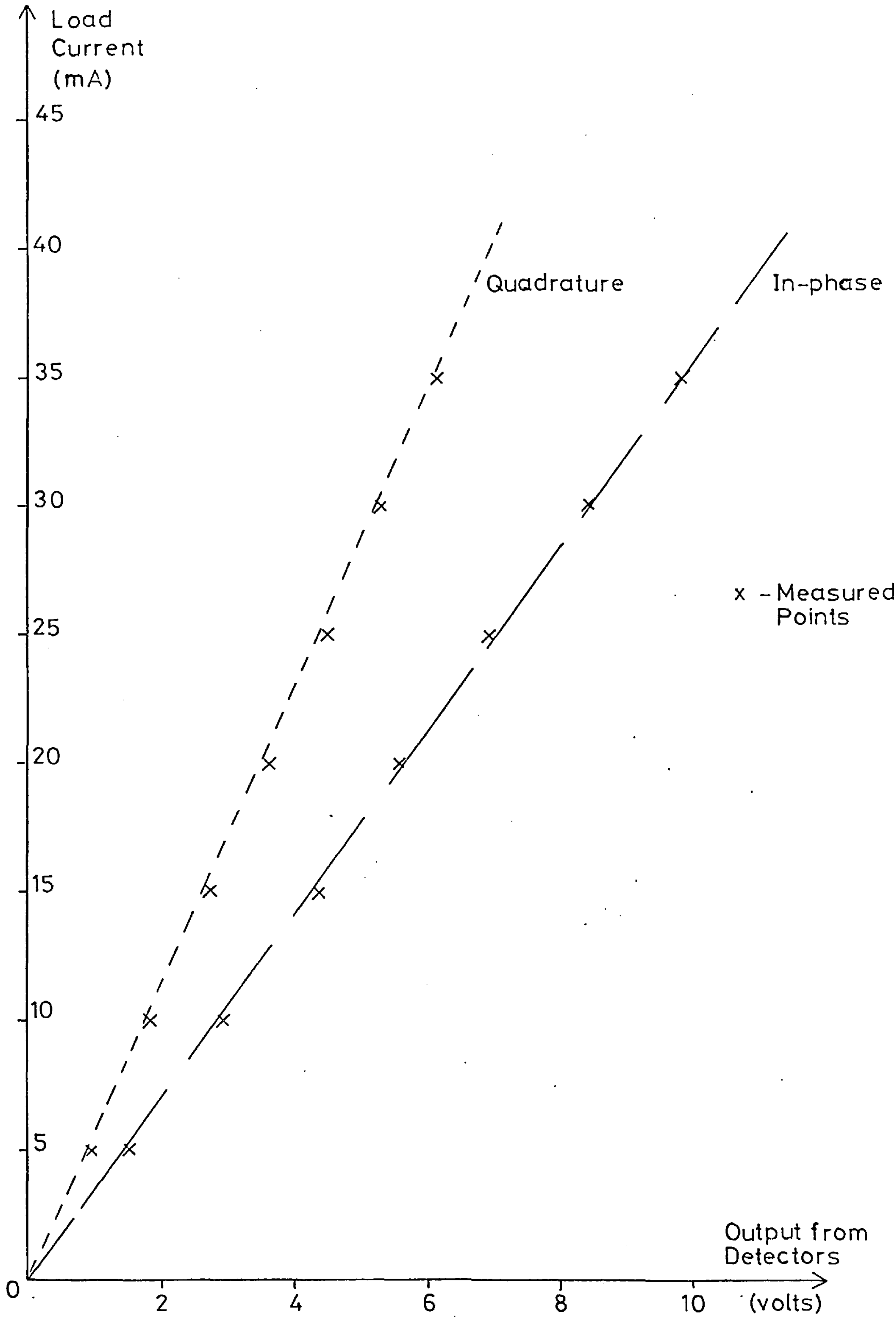

Fig. 5.10 Phase-sensitive Detector Calibration. Load p.f. = 0.85 lagging.

5.4.4 The Filters and Power Amplifier.

If the voltage applied to the load unit by the network is a pure sinusoid, and the internal voltage, E, contains harmonics, then the resultant current will also contain harmonics. For the whole simulator to operate accurately, it is important that all the voltages and currents should be sinusoidal, and for this reason, great care must be taken to ensure that the units which comprise the simulator should introduce the smallest amount of harmonic distortion. In the amplitude modulators, distortion is produced in the waveforms. owing to imperfections in the multipliers, and a filter, shown in Fig. 5.11, is included before the power amplifier.

The first stage, OA 10, sums the two components, e_p and e_q, and drives a two pole filter, OA 11. This is arranged to have both poles coincident, with a cut-off frequency of 80 Hz, and its phase-shift at 50 Hz is compensated by the phase adjusting circuit, OA 12. It is important that there is no overall phase-shift between the multiplier outputs and the power amplifier output, for this ensures that there will be minimal interaction between the real and reactive current loops. This is adjusted when the amplifier is operating under zero load conditions.

The amplifier itself has the unusual requirement that it must be able to absorb power at its output terminals, as well as being able to operate at any power factor. The power amplifier used in the generator unit was found to be unsatisfactory, and required redesigning. Financial considerations led to the retention of the existing output transformer, power transistors and heavy duty power supply, but these all introduced constraints into the design. The circuit finally adopted is shown in Fig. 5.12.

The push-pull transformer coupled output stage has output transistors Tr 3 and Tr 4 resistively biased, and they are driven by the phase-splitter Tr 2. This in turn is driven by the preamplifier, comprising OA 13, OA 14 and Tr 1, and there is a feedback path from the secondary of the transformer to both of the operational amplifiers. Regulation tests showed that the amplifier could absorb up to 1 p.u. current with a change of less than

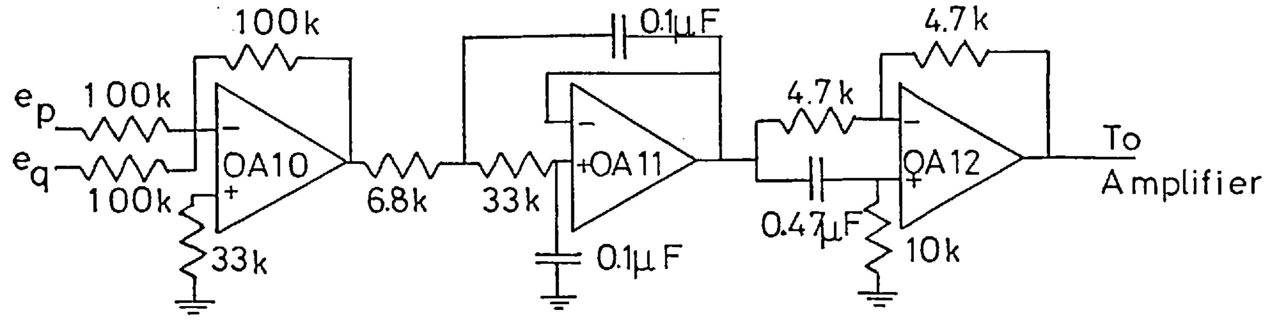

Fig. 5.11 The Filters.

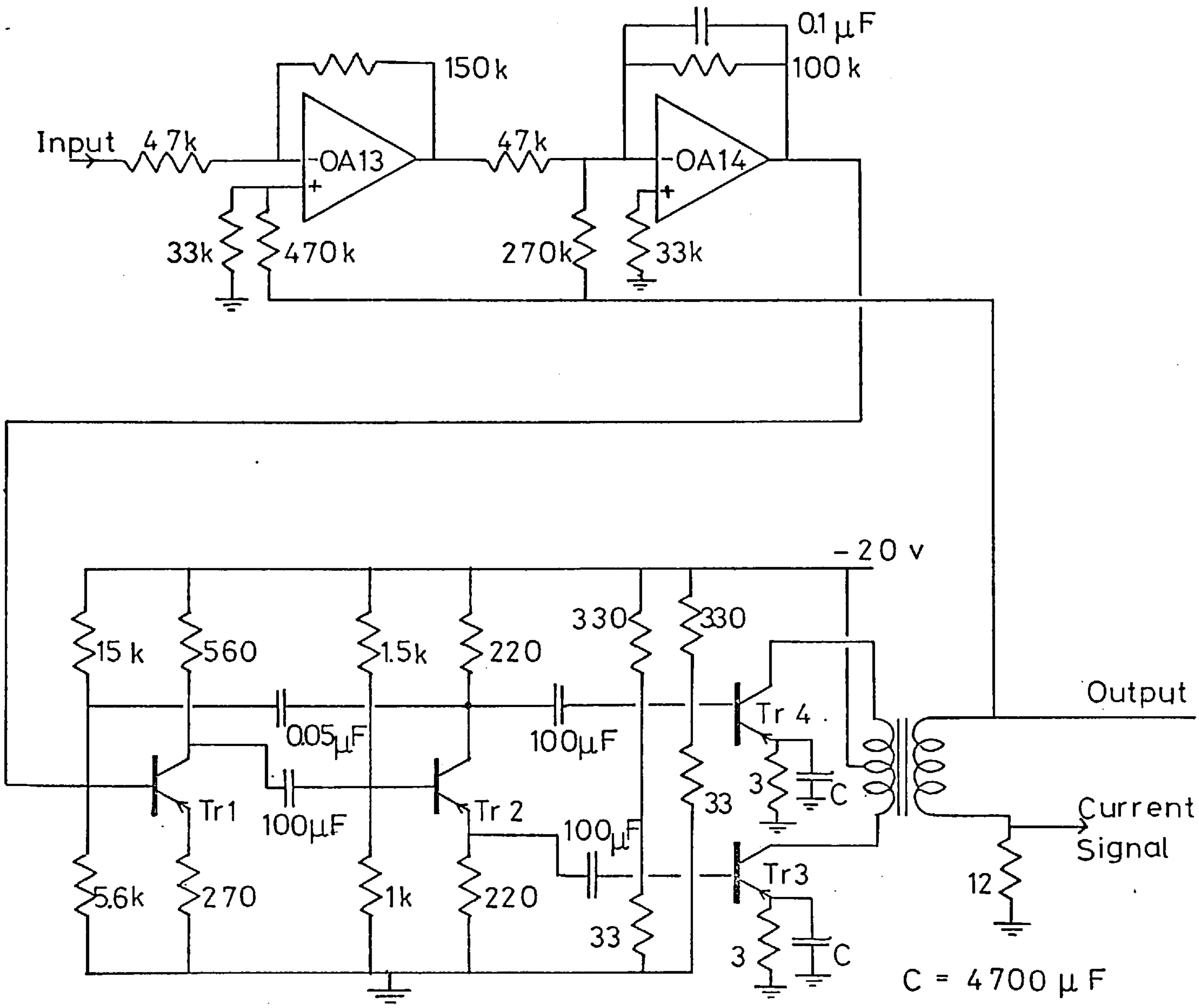

Fig. 5.12 The Power Amplifier.

2% in the secondary voltage. Currents of up to 5 p.u. could be absorbed, but then the regulation fell to 15%. However, the amplifier gain is not critical, since the integral feedback reduces the steady-state error to zero.

5.4.5 Control and Auxiliary Circuits.

In addition to those parts of the load unit which have already been described, there are additional circuits for control and measurement. These comprise:

(i) Voltage regulators

(ii) Terminal voltage measurement

(iii) Control signal routing

The voltage regulators, shown in Fig. 5.13, are used to provide stabilized voltages for the phase-sensitive detectors, and also for certain zero adjusting circuits. The zener diode acts as the reference element, and the series regulation is done by a Darlington pair, with a single transistor acting as a comparator.

The terminal voltage is measured using the circuit of Fig. 5.14, which provides two outputs. The first drives the front panel meter, with an absolute measurement of the voltage, while the second provides the computer with a signal which indicates the voltage deviation from 1 p.u.. The input signal is fed through a potential divider, and buffered by a voltage follower, OA 15. The next pair of operational amplifiers, OA 16 and OA 17, form a perfect full-wave rectifier, and the final stage subtracts the measured value from a reference, to provide a signal proportional to the voltage deviation; this stage also includes a low-pass filter to remove the harmonic components from the waveform.

The control signals come either from potentiometers mounted on the front panel, or from the computer, and a manual change-over switch is provided. This switch also provides a status signal to the computer, to indicate whether control is manual or from the computer. An additional

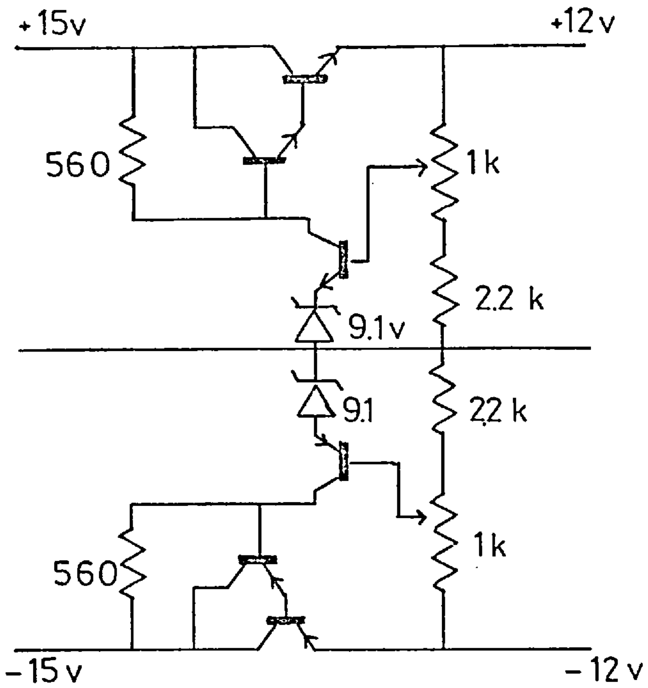

Fig. 5.13 Voltage Regulators.

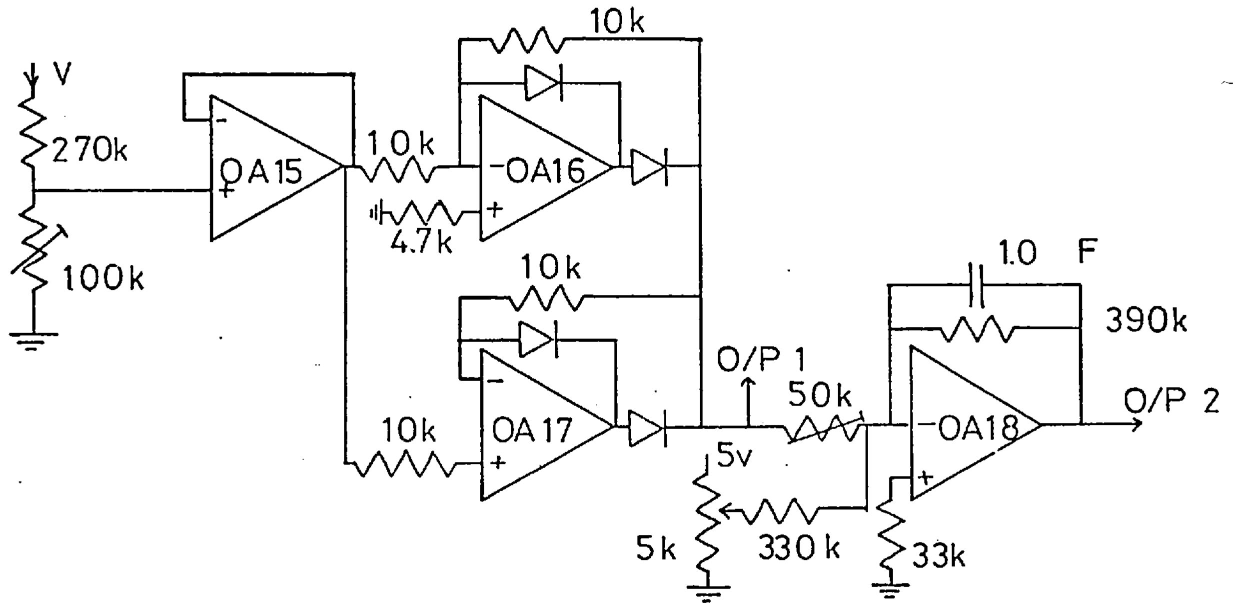

Fig. 5.14 Voltage Measuring Circuit.

Signal	Min. Value		Max.Value	
I_p meas.	-10 v	1 p.u.	0 v	0 p.u.
I_q meas.	-10 v	1 p.u. lag	+10 v	1 p.u. lead
V meas.	-10 v	0.8 p.u.	+10 v	1.2 p.u.
I_p cont.	-10 v	1 p.u.	0v	0 p.u.
I_q cont.	-10 v	1 p.u. lag	+10v	1 p.u. lead

Table 5.1

status switch is also incorporated, and this can be used in conjunction with the computer to provide control over a load simulation program. Details of the signal levels, for both measurement and control, are given in Table 5.1.

5.5 Choice of Loop Gain.

When a unit had been constructed and tested, its dynamics were analysed in order to select the best value of loop gain for both real and reactive current loops. A linearized model of the unit was derived, and is shown in Fig. 5.15. The effect of the transmission line is represented by the two parameters K_{IPV} and K_{IQV}, which give the change in receiving-end voltage for a change in the two components of current at the receiving-end. These parameters are derived in Appendix B. The following state equations can be derived, and the coefficients Z_{A-D} are also given in Appendix B.

$$\begin{bmatrix} \Delta \dot{e}_p \\ \Delta \dot{i}_{px} \\ \Delta \dot{e}_q \\ \Delta \dot{i}_{qx} \end{bmatrix} = \begin{bmatrix} 0 & -K_p & 0 & 0 \\ Z_D/T_p & -1/T_p & Z_C/T_p & 0 \\ 0 & 0 & 0 & -K_q \\ Z_B/T_q & 0 & Z_A/T_q & -1/T_q \end{bmatrix} \begin{bmatrix} \Delta e_p \\ \Delta I_{px} \\ \Delta e_q \\ \Delta I_{qx} \end{bmatrix} + \begin{bmatrix} K_p & 0 \\ 0 & 0 \\ 0 & K_q \\ 0 & 0 \end{bmatrix} \begin{bmatrix} I_{pref} \\ I_{qref} \end{bmatrix}$$

As can be seen from the figure the only coupling between the two loops is that due to changes in terminal voltage, and an examination of the eigenvalues of the matrix for various lengths showed that even for large reactances, the coupling effect is small, and that the two loops are nearly independent, and can be regarded as second order systems.

To avoid the possibility of hunting phenomena, it was decided to make the response of the in-phase current loop twice as fast as that of the other loop, and convenient values of gain are $K_p = 12.0$, $K_q = 6.0$. This gives real current loop poles at $\pm\ 25 \pm j13$, and the reactive current

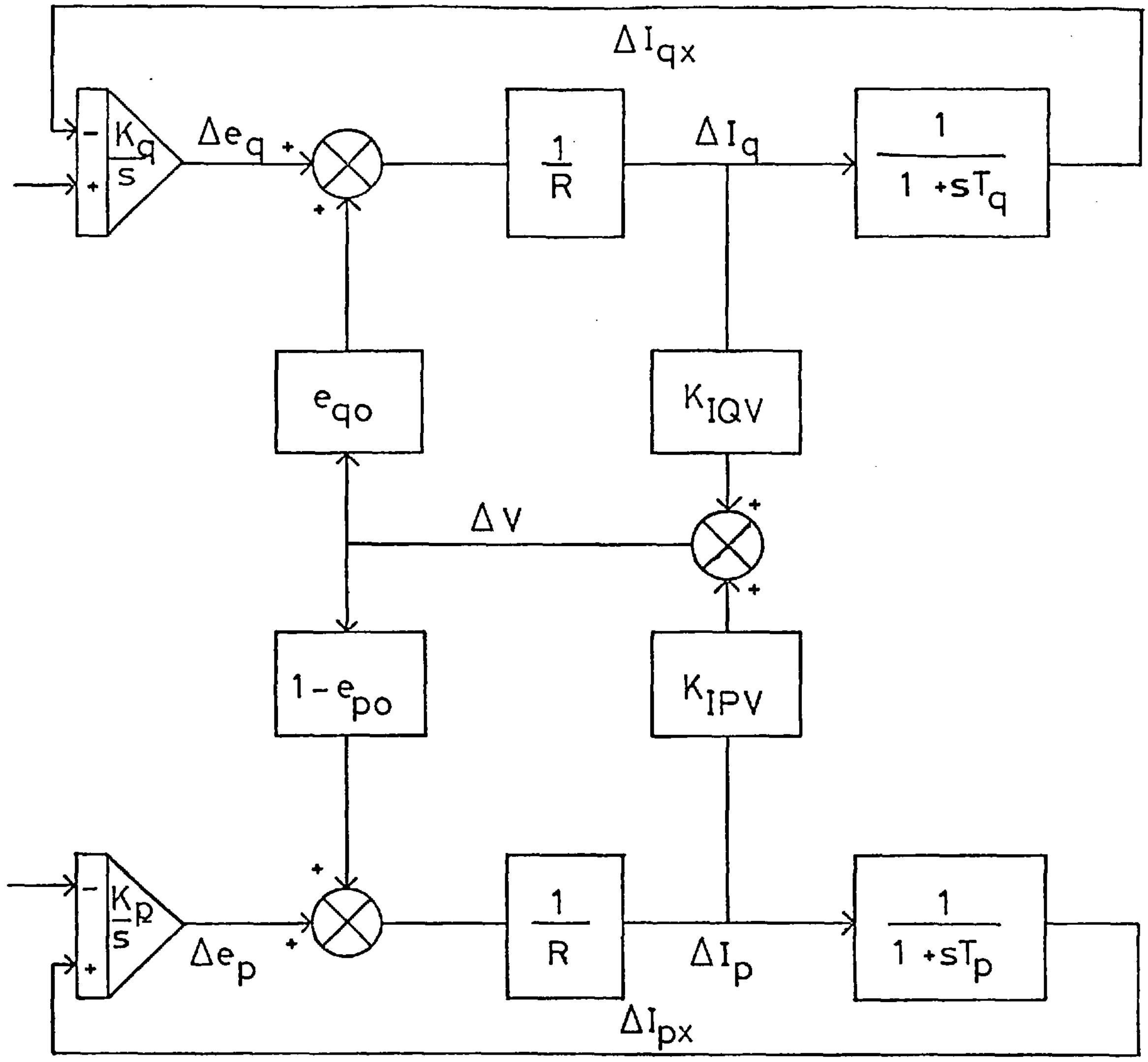

Fig. 5.15 Linearized Model of a Constant Current Load Unit.

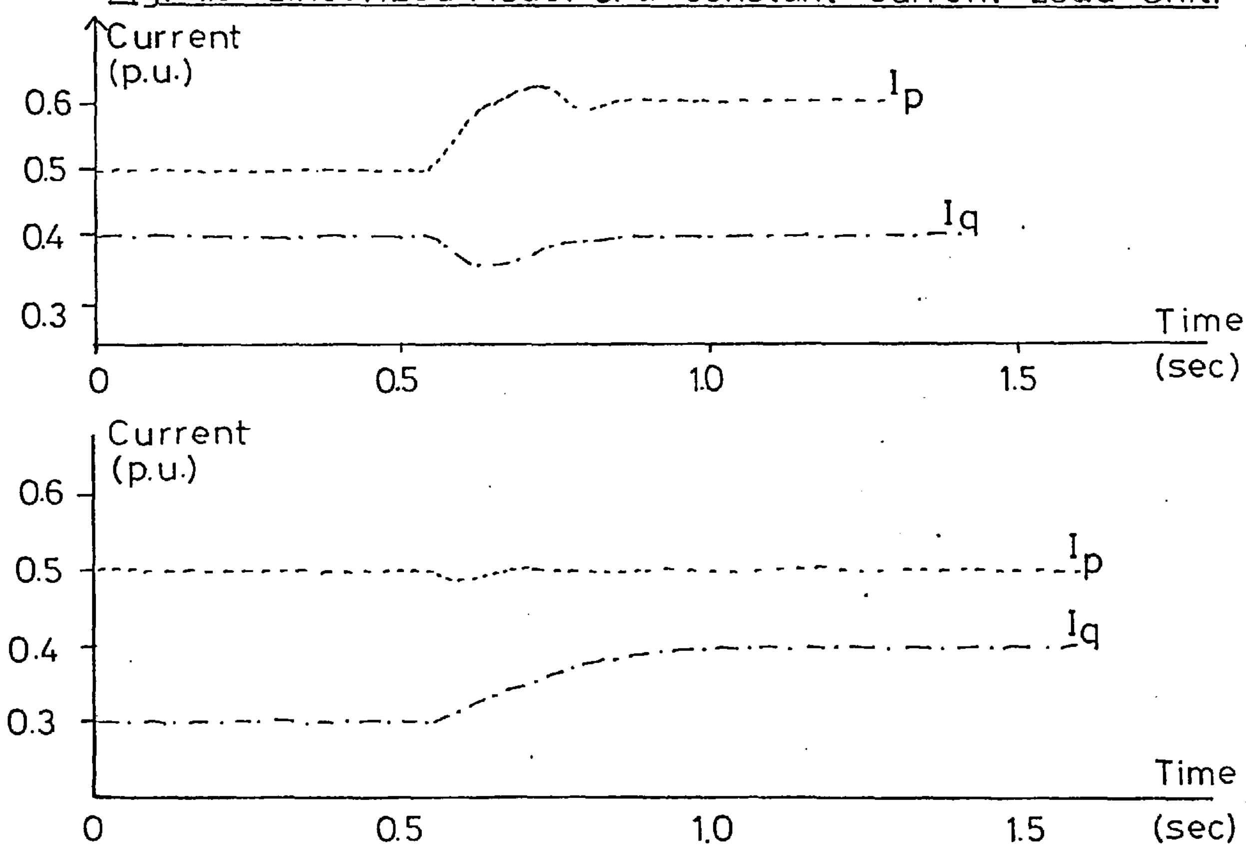

Fig. 5.16 Load Unit Step Response.

loop poles at -40, -10. This should give a damped response to changes in I_{qref}, and a slightly oscillatory response to a change in I_{pref}. Two test responses are shown in Fig. 5.16, one for a change in I_{pref}, the other for a change in I_{qref}. The results show that the response is of the form indicated by the equations, and that the unit has an acceptable transient response. Coupling between the loops through changes in terminal voltage manifests itself as a change in the other component when one reference signal is changed.

5.6 Conclusion.

The final version of the load unit has been shown to have good linearity and an acceptable transient response. Five of these units have been constructed, and their performance is similar in standard to that of the prototype. The present design is satisfactory, but it would be beneficial to redesign the power amplifier and to improve the quality of the multipliers used in the phase-sensitive detectors.

6.1 Introduction.

The major sections of the power system model, namely the generator and load units, have been described, and this chapter will deal with the interconnections of these units by the network, and also with the connection of the model to the computer interface. The network section of the model comprises the lines, the grid tap-change transformers, and circuit breakers to connect the various items of plant together. Both the lines and the transformers are fitted with current transducers, to enable measurements of the line flows to be made, and there is also provision for measureing nodal voltages. The network interconnections are made in a patching area, and a patching scheme is also used for the routing of control signals and measurements between the model and the interface. Fig. 6.1 shows the basic arrangement of the whole system, and each section will be described in turn, in three main groups: (1) Network and network patching, (2) AC signal processing, and (3) signal patching and the general operation of the interface.

6.2 The Network and Network Patching.

The elements which comprise this part of the model have already been listed, and their physical layout is shown in Fig. 6.2. A system has been adopted whereby the network configuration can be easily changed. The original system proposed by Sheldrake[26] employed a system of busbars, to which any item of plant could be connected, and hence the whole network set up, but this method used a very large matrix of several hundred switches. While this gave complete flexibility, without the use of patching leads, it is not a simple task to produce programs for the digital computer to convert a change in switch status to a change in, say, the nodal admittance matrix. The method which has been adopted employs a small number of switches to act as circuit breakers, and these are then connected in known places in the

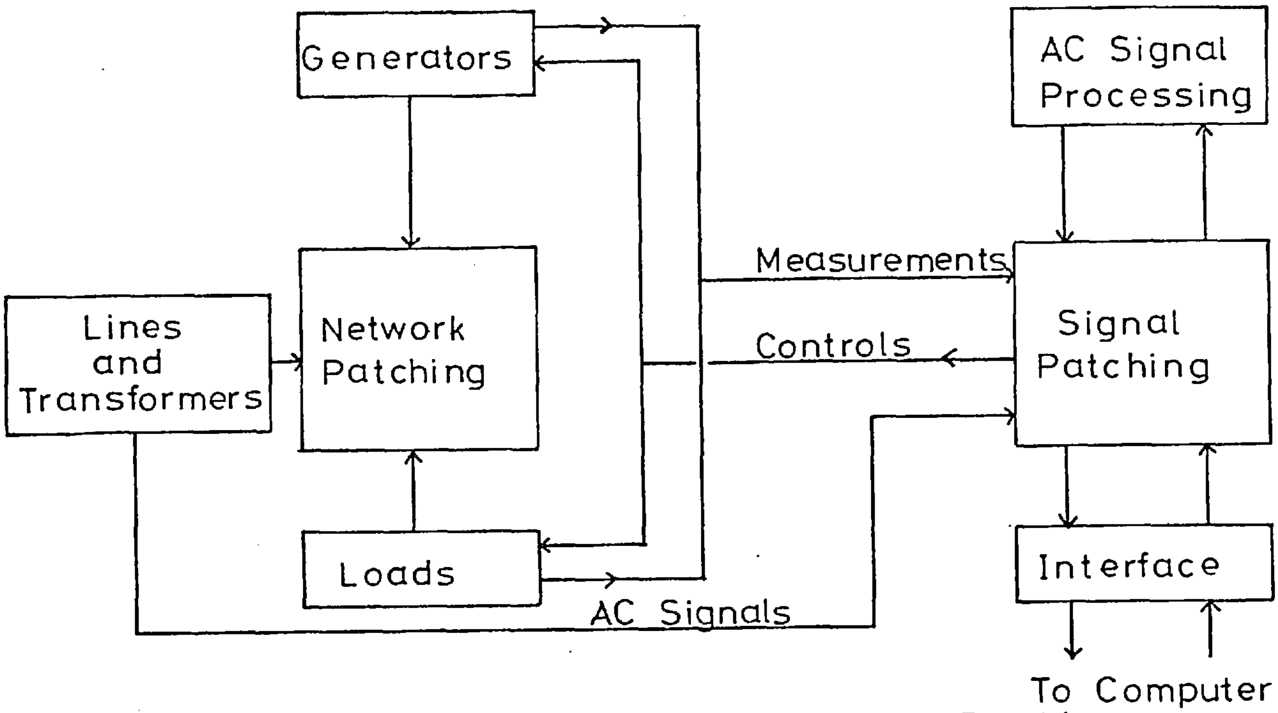

Fig. 6.1 Arrangement of the Simulator Patching.

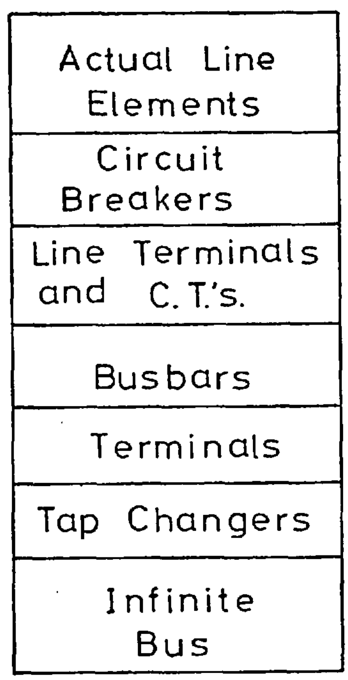

Fig. 6.2 Network Rack Layout.

network. By examining the status of a given switch, which is known to be in series with a particular line, it is an easy matter to determine the exact configuration. Additionally, these switches may also be operated either manually at the front panel, or by the computer. The system has the capability of being expanded indefinitely, but the present capacity is 16 circuit breakers, 10 transmission lines and 4 tap-change transformers.

6.2.1 The Lines and Transformers.

Once the system per-unit values have been decided, the line parameters for the model are fixed. With the inherited base impedance of 667Ω, it was decided to take the lines as being 132 kV single circuit[62], and to select the line lengths according to the available inductors. For a line with a cross-sectional area of 0.4 in^2, the model parameters are

X series inductance	0.00341	p.u./ mile	100 MVA base
R series resistance	0.00072	p.u./ mile	
B shunt susceptance	0.0008	p.u./ mile	

To achieve the necessary linearity, iron-cored inductors are used throughout, and these exhibit less than 10% change in inductance at a current of 270 mA, which is 9 p.u. current. A nominal pi representation is used, and the line lengths provided are 12, 12, 24, 24, 30, 38, 42, 63, 120 and 126 miles respectively, the lengths being determined by the available inductors.

The tap-change transformers were specially wound for the original model, and are auto transformers with ratios from 0.85 to 1.15 in steps of 0.02. The magnetizing current of these transformers is less than 1% of the base current, and the transformer may therefore be considered as an ideal one.

In order to measure line flows in the network it is necessary to have a means of measuring line currents, both in phase and magnitude. There are two main ways in which this can be done, the first of which is to use a small resistive shunt in the line, and to measure the voltage drop across it.

If this is to be done electronically, it means measuring a small differential voltage in the presence of a large common-mode one, and this calls for the use of an accurate differential amplifier, built using precision resistors. The main alternative is to use a current transformer, but the use of a real current transformer is precluded on grounds of cost. It was discovered that for currents up to 500 mA a small Radiospares transistor amplifier output transformer, type T/T 7[63], worked excellently. Using the speech coil as the primary winding, with a 10Ω burden across the whole of the secondary winding, this was very linear, and performed most satiafactorily. In particular, the phase angle error was only about 1° over a wide current range, which is superior to many commercial C.T.'s. This transformer has a ratio of 9.2:1, so the referred primary resistance is 0.118Ω plus the transformer resistance of 0.2Ω. The voltage appearing across the burden when per-unit current flows through the primary winding is therefore 32.6 mV. This is then amplified as shown in Fig. 6.3(a), and the current signal is sent to the signal patching panel. Additionally, a voltage signal is also sent to this patch panel.

The arrangement of the terminals, the current transformers and the tap-change transformers is shown in Fig. 6.3(b), and it can be seen that the line unit can be changed without disturbing the current measuring arrangements. The units all fit in 19" racks, and are interconnected using multi-way plugs and sockets.

6.2.2 The Circuit Breakers.

Small electromechanical relays are used to represent the circuit breakers, and they may be operated either manually or by the computer. The circuit arrangement is shown in Fig. 6.4 for one relay, RLA. This relay may be operated either by the manual switch or by the transistor, depending on the state of RLB. This is a 16 way change-over relay which determines whether conrol comes from the computer or from the local switches. A lamp is provided to show the status, and a digital indication is also produced using an auxiliary set of contacts to indicate to the computer whether the

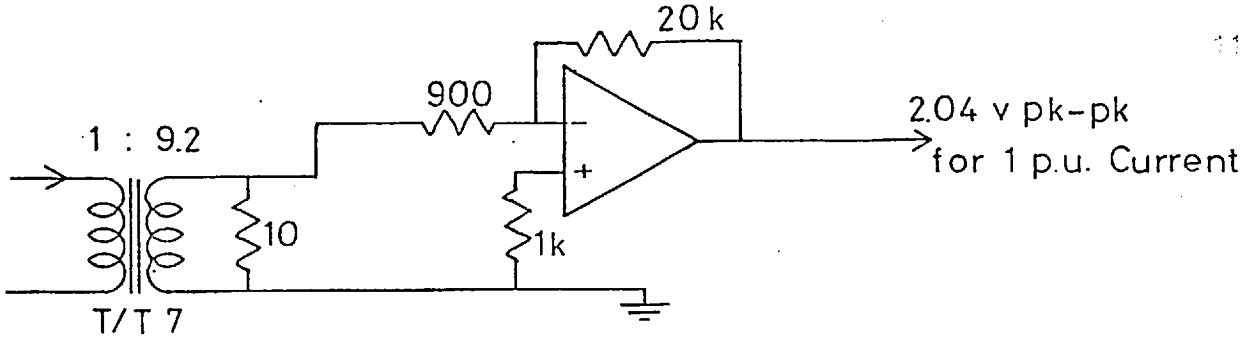

Fig. 6.3(a) Current Measurement.

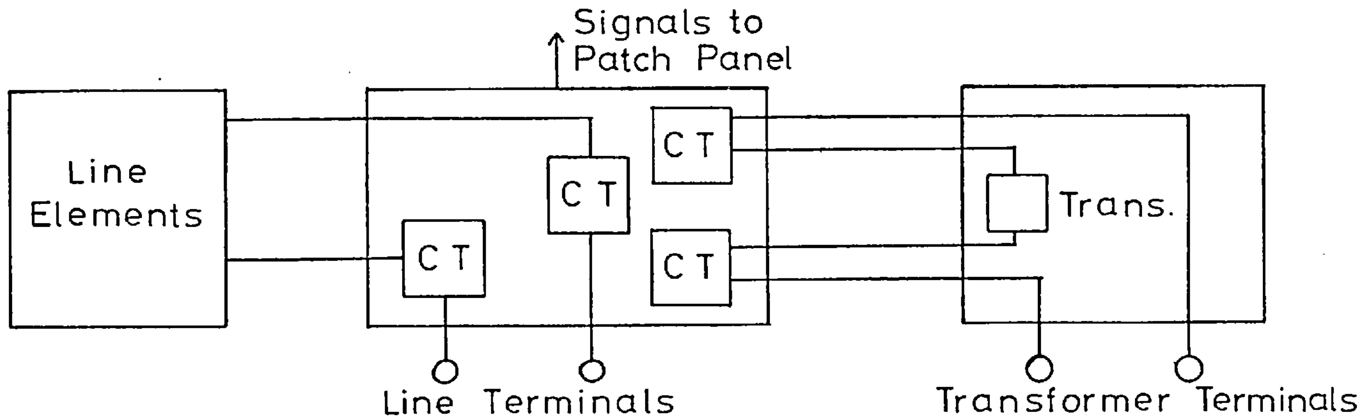

Fig. 6.3(b) Arrangement of the Units.

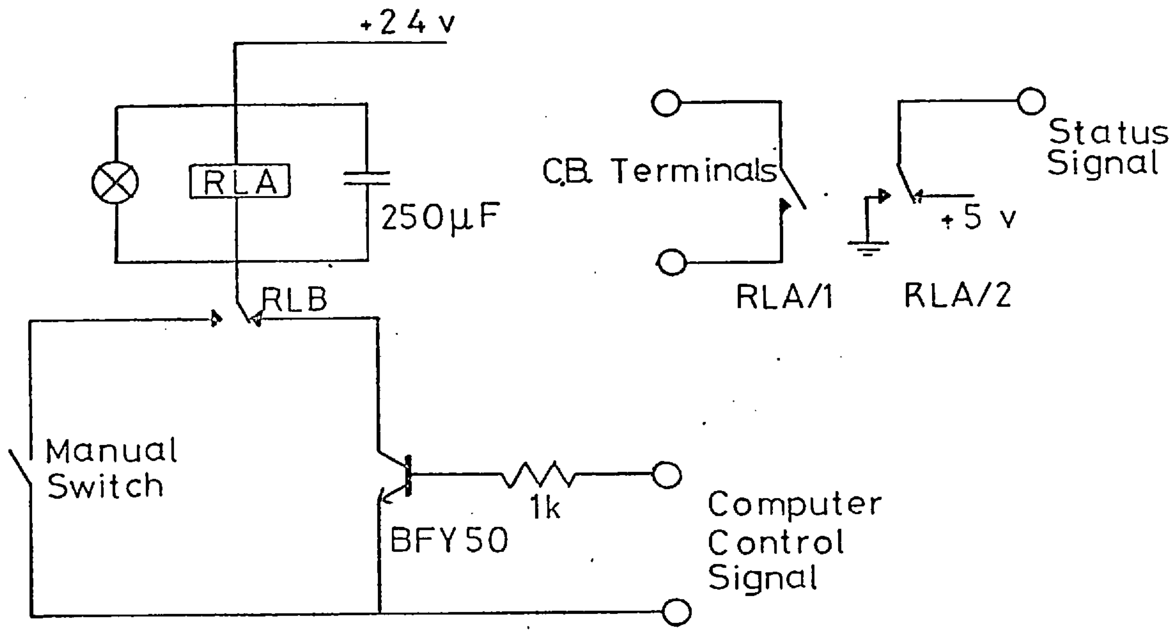

Fig. 6.4 Circuit Breaker Arrangement.

breaker is open or closed. The large capacitor is connected across the relay coil to prevent the relay from operating when the control relay RLB operates.

Although this unit functions satisfactorily, it has given more trouble than any other part of the model, owing to the electromechanical components. An alternative system using a high frequency transistor switch has been tested, and will probably be fitted in the near future. Its only disadvantage is that the high frequency switching waveform will penetrate into the network, but on the other hand, it operates in a few microseconds, and could be used in studying transient problems, where the switching instant is important.

6.2.3 The Infinite Bus and The Busbars.

For certain tests it is desirable to have a source which will function as an infinite busbar, and a unit of this type has been included. It consists of two step-down transformers whose outputs are connected in series, while the primary of one of these transformers is fed from a Variac. This allows fine control of the voltage, and a rectifier meter is included to measure the terminal voltage. This source has a very low output impedance, giving good regulation, but at certain times of the day, notably in the early evening, frequency variations of the mains can interfere with the generator unit governors, and produce spurious results. It is recommended that a stable oscillator driving a power amplifier should be used in place of the present arrangement.

The terminals of each generator and load unit are brought out in the patching area, and to assist with the interconnections 16 busbars are provided, each one consisting of 6 sockets connected together. All the network connections are made using standard 4 mm plugs and sockets.

6.3 AC Signal Processing.

From the AC measurements of voltage and current at various points in the network, it is necessary to produce steady DC signals which correspond to such variables as real and reactive power flow, voltage and line angle, which may be sampled and converted to digital data by the computer. Circuits have been produced for all of these functions, and each will be described in turn.

6.3.1 The Watt/Var Meter.

The measurement of the line currents using the current transformers has already been described, and it is this current signal together with a voltage signal from the same point in the network which are used to measure the line flow. The block diagram of this unit is shown in Fig. 6.5, and it can be seen that the Var measurement section is the same as that used in the generator unit. The unit is calibrated such that 1 p.u. flow will give an output signal of 5 V dc, and the cut-off of the filters is arranged so that the output ripple is less than 1% of the maximum signal. Twenty of these units have been built, and their accuracy has been found to be dependent on the particular batch of multipliers used. The prototype had an accuracy of the order of 2%, but later versions have not met this specification, and an assessment of their errors is being undertaken[64].

6.3.2 Angle Measurement.

A circuit for the measurement of angles has already been described in connection with the generator unit, but it only provides information as to the magnitude of the angle, and not as to which voltage leads which. This can be overcome using a modification of the system of Fig. 3.10, and this is shown in Fig. 6.6. The two input stages, consisting of the RC divider networks[65], give a combined phase-shift of 90°, irrespective of frequency, at their mid-points. By thus effectively adding a phase shift of 90 to one of the input signals, the range of a 0° to 180° angle meter is changed to that of a -90° to +90° meter, thus giving a lead or lag indication.

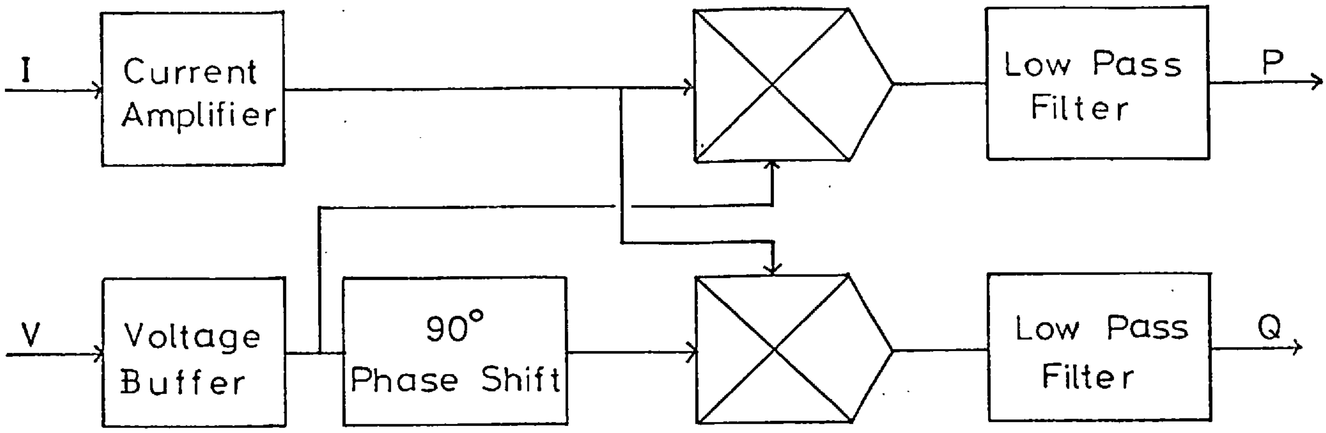

Fig. 6.5 Watt/Var Meter.

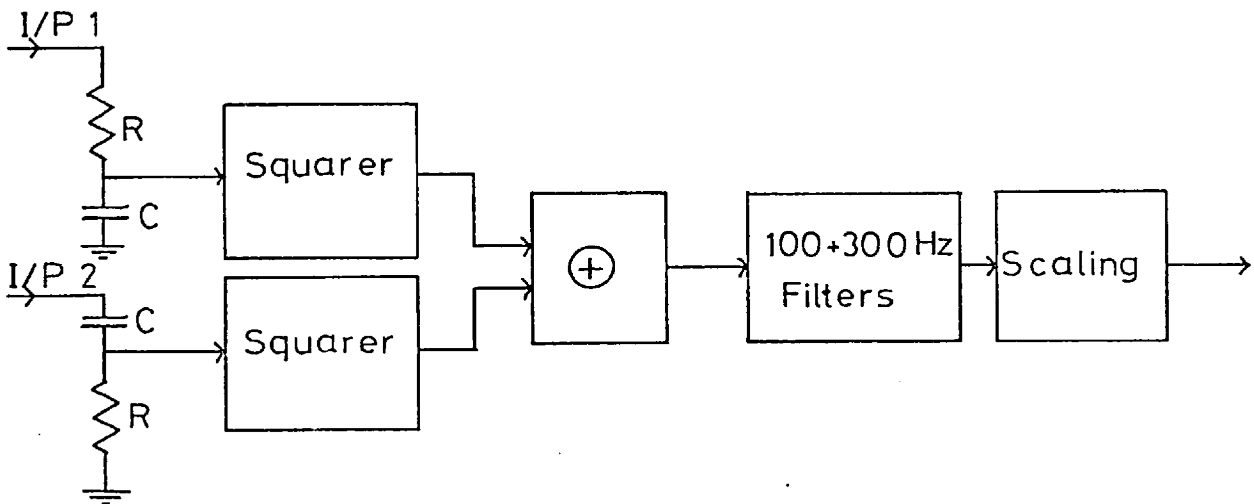

Fig. 6.6 Angle Measurement.

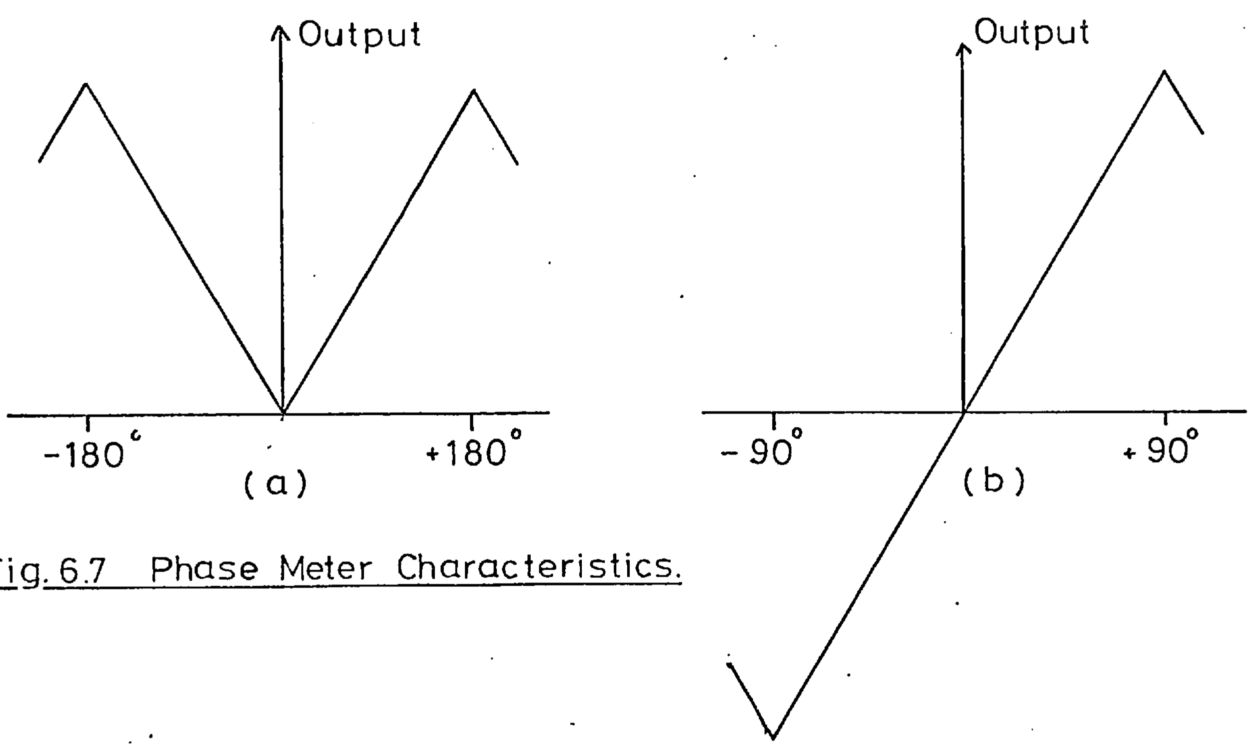

Fig. 6.7 Phase Meter Characteristics.

These respective characteristics are shown in Fig. 6.7. The output of the exclusive-OR gate is a pulse train with a fundamental frequency of 100 Hz, and to eliminate the harmonics while providing a fast response, two twin-tee filters, centered respectively on 100 and 300 Hz, are cascaded. A final stage provides level shifting and filters the higher harmonics. The output ripple is less than ½%, and the accuracy, when compared with a digital phase meter, is better than 1°.

6.3.3 Voltage Measurement.

Ten circuits are provided for the measurement of the voltage at chosen points in the network. The output is proportional to the voltage deviation from 1 p.u., and is heavily filtered to remove the ripple. The circuit is shown in Fig. 6.8, and as can be seen it is most economical on components. The amplifier OA 1 is a buffer, connected to a high resistance potential divider, while amplifiers OA 2 and OA 3 comprise a perfect rectifier, with a gain given by R_1/R_3. This alone would give an output proportional to the actual voltage, but a variable source connected via R_2 is used to null the output for an input of 20V rms. The gain is adjusted to give +10 V output for 1.2 p.u. input, and -10 V for 0.8 p.u.. When set up, the circuit is very linear, but the high gain and the nulling of the output give a coupling between the various controls, and as a result the circuit is very difficult to set up. It is recommended that future circuits of this kind are constructed to the design used in the load units.

6.3.4 Period and Frequency Measurement.

One of the most important quantities to be measured is frequency, and this poses a number of problems. The method used at high frequencies is to count the number of zero crossings of the waveform under examination in an interval of time, this interval being determined by a crystal oscillator. At low frequencies this method is useless if a fast measurement is required, since the measurement of a 50 Hz signal to an accuracy of 0.1 Hz requires an interval of 10 seconds. The main alternative is to measure the period of a waveform, by counting the number of clock pulses which occur between

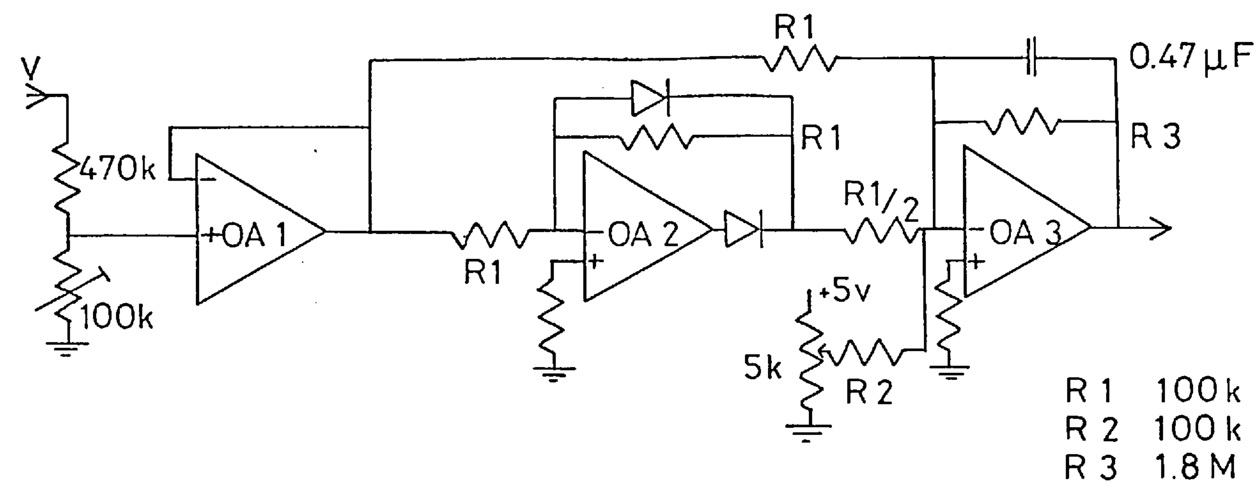

Fig. 6.8 Voltage Measurement.

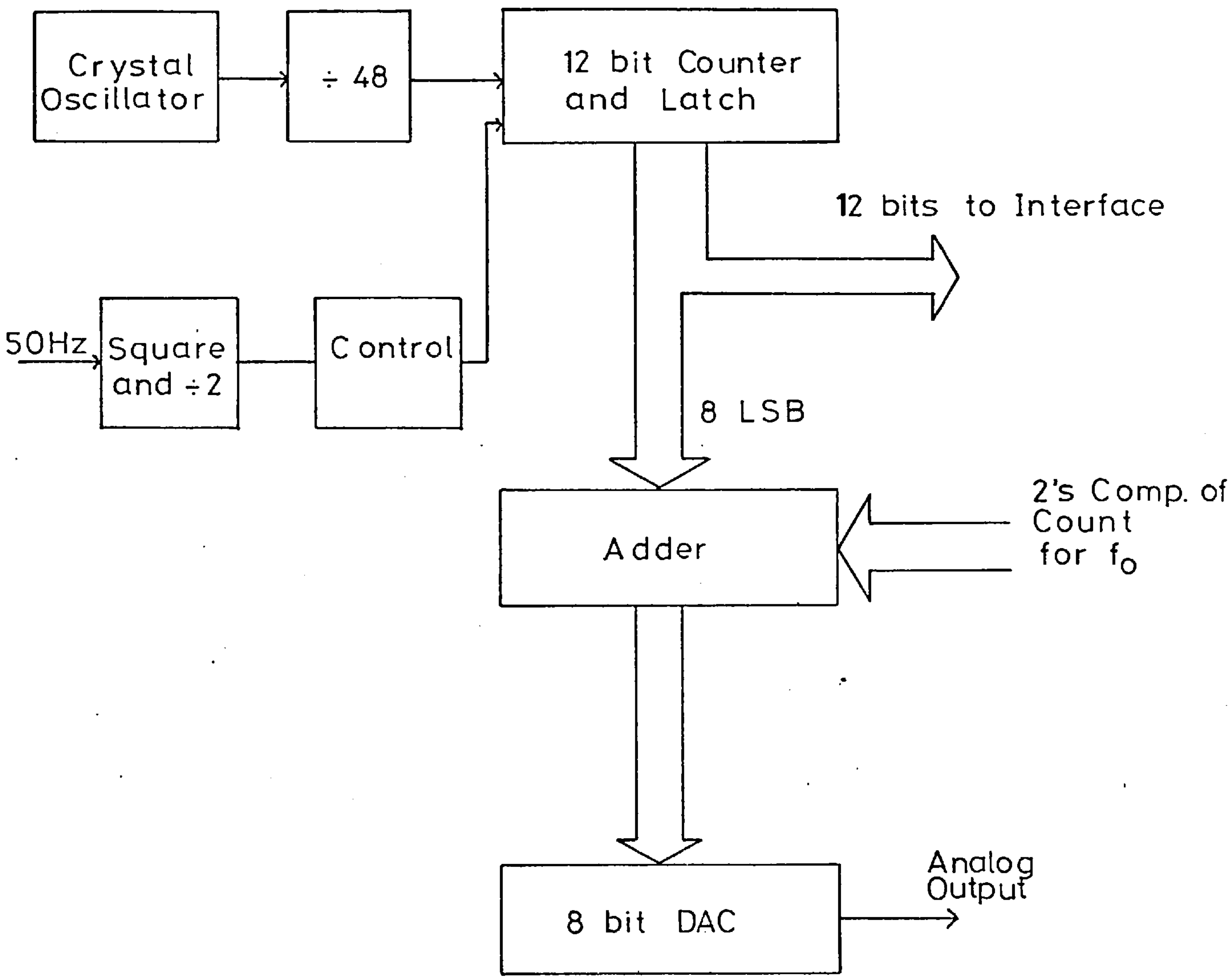

Fig. 6.9 Period / Frequency Meter.

successive zero crossings. Using this method, the digital period count can be fed to the digital computer, and the frequency determined by taking the reciprocal of the period. This method does not give an analog indication and this would be a useful facility for the operator of the model. A system has been devised which provides a digital output of period, and an analog output which is a non-linear function of frequency. The block diagram is shown in Fig. 6.9.

The period meter consists of a crystal oscillator, at 5 MHz, and a divide-by-48 chain. This divided output is counted by a 12 bit counter, the counting period being determined by zero crossings of the input waveform, which is itself divided by 2 in order to remove the effects of any distortion in the waveform. When the count has been completed, the output is strobed into a latch, this number being the binary measurement of period. The timing arrangement is shown in Fig. 6.10. The clock frequency used gives a resolution of 0.025 Hz, and the measurement of period is made 25 times per second.

The relation $P = K/F$ can be written, where P is the period count, F the waveform frequency and K is a constant dependent on the clock frequency. For small changes, $\Delta F = -\frac{F^2}{K}\Delta P$, and by assuming that for very small changes the term $\left(\frac{F^2}{K}\right)$ does not change, a method of measuring small changes in frequency is available. A base frequency, 48 Hz in this case, is chosen and the period count for this frequency is subtracted from the actual period count. The resultant binary number is a measure of the frequency deviation from the base frequency. Thus $(P_{actual} - P_{base}).K' = (F_{actual} - F_{base})$, and the resultant number may be fed into a digital to analog converter to give an analog signal which is proportional to, but a non-linear function of, the frequency deviation.

Since an 8 bit digital to analog converter (DAC) was available only an 8 bit version was built; the least significant bits of the period count are added to the two's complement of the number which represents the count at 48 Hz, using a binary adder. The adder output is fed to the DAC, and

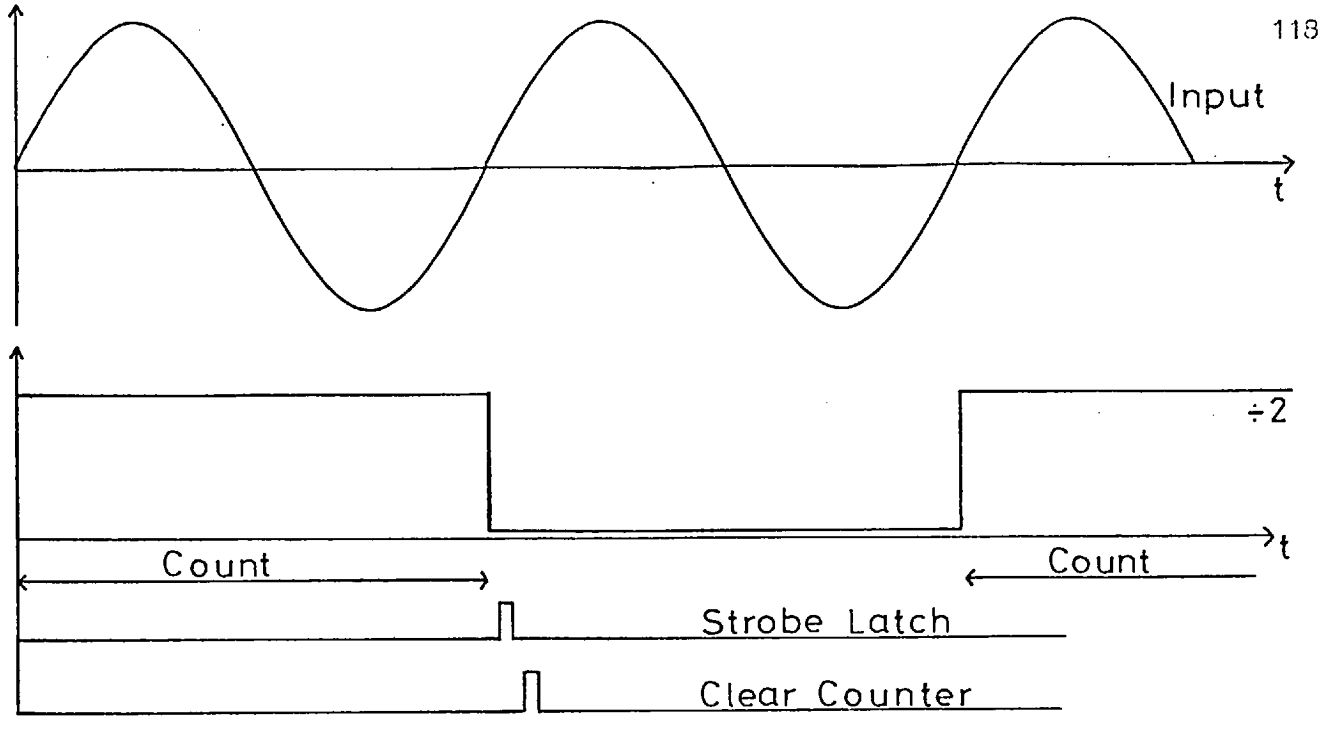

Fig. 6.10 Timing for the Period Meter.

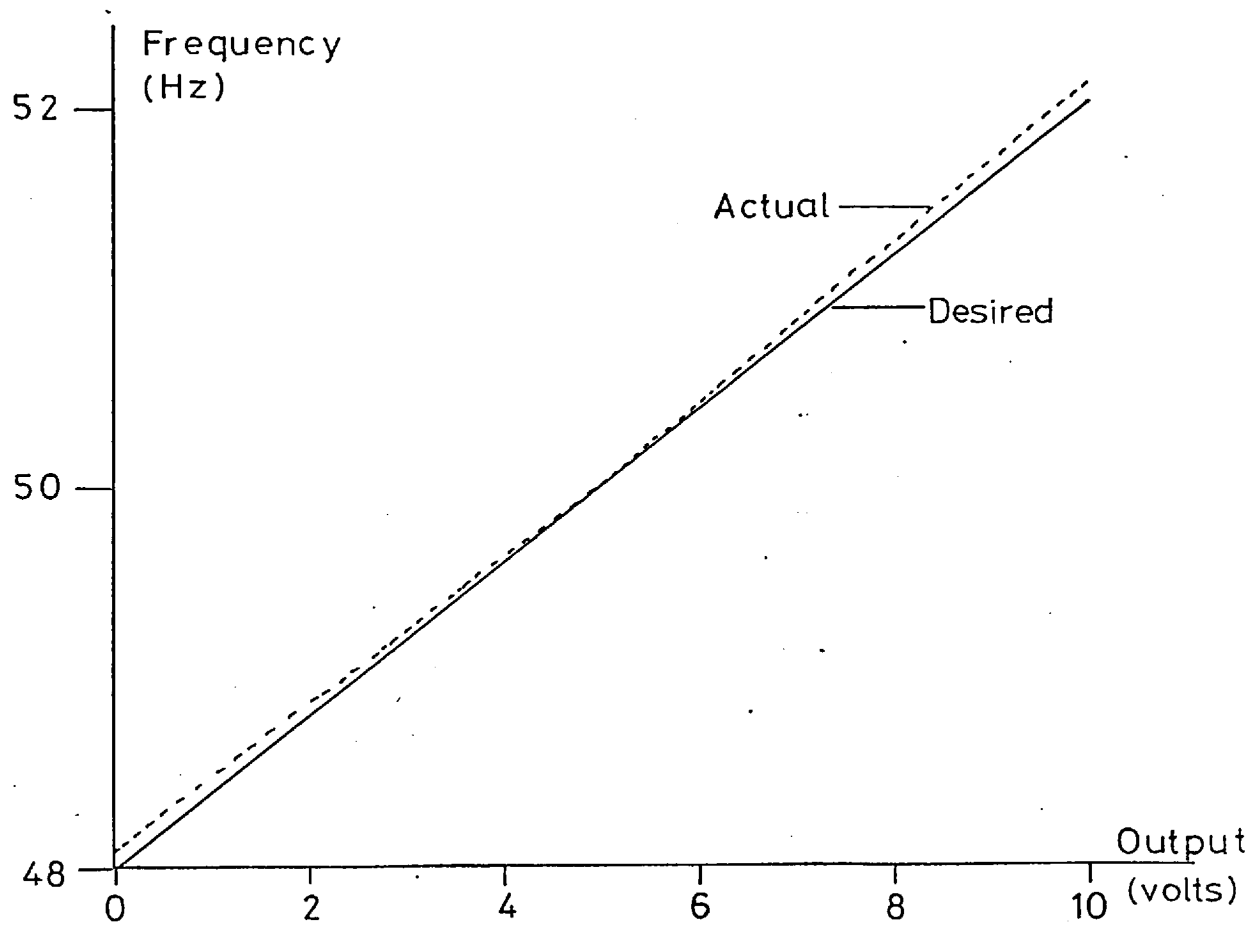

Fig. 6.11 Frequency Meter Calibration.

the output of this is scaled to give the characteristic shown in Fig. 6.11. There is an inherent non linearity in the system, since the term F^2/K changes with frequency, and the error is of the order of 2% of the range of interest, in this case of 4 Hz, giving a direct accuracy of 0.1 Hz. This is, however, a constant non-linearity, and a moving coil meter has been specially calibrated to give a true reading. It can also be adjusted such that the error lies at the ends of the range, or at the centre. The choice of the former region of error was chosen, since most of the time the frequency lies in the region of 50 Hz.

6.4 Signal Patching.

The actual hardware which constitutes the model has all been described, as has the auxiliary circuitry which processes the AC signals of the network. It remains only to describe briefly the wiring which connects the signal inputs and outputs of the interface to the measurement outputs and control inputs of the model. There are four basic types of signal which flow between the model and the interface, and these are:

(1) Analog inputs	measurements on load and generator units outputs of the AC signal processing circuits
(2) Analog outputs	control signals to load and generator units.
(3) Digital inputs	status signals from circuit breakers and load and generator units.
(4) Digital outputs	control signals to circuit breakers computer acknowledgement of status

The terms input and output are relative, and hereafter will be used as those employed by an observer on the computer side of the interface.

Each load and generator unit is provided with four analog input lines and four analog output lines, together with two digital input lines. In a load unit, the inputs will be the two current signals, and the voltage deviation, and the digital input will be the computer/manual status, while the control outputs will be the two current reference signals. In a generator unit the analog inputs can be chosen from many variables, such as power output, valve position, voltage, reactive power, governor sleeve position, or speeder gear setting, while the controls may be the reference voltage and the raise/lower control for the governor. The status signals will be whether the AVR has its reference supplied locally or from the computer, and whether the speeder gear is similarly controlled. All this wiring is permanently connected from the rear of the units to the signal patch panel.

This patch panel is shown in Fig. 6.12, together with the analog inputs and outputs to the interface. The model connections are in three groups, comprising the measurements on the loads and the generators, the controls for the same, and the AC signals from the lines and transformers. The inputs and outputs of the signal processing circuits can be seen. In addition, there are six variable voltage sources which may be used to provide accurate voltages for testing and control purposes, and twelve centre-zero meters are also included for general indication purposes. All the connections are made with 1 mm plugs and sockets, which have proved most reliable in use.

All the digital inputs and outputs are hard-wired to their respective units, to reduce the patching complexity, and they are organized as four 16 bit words. In order that the computer can identify when a digital status has changed, a status discrepancy feature is included. This is initialized by the computer reading all the digital inputs and then transferring these inputs into the output latches. These latches contain the status as the computer believes it to be. The output of the latch and its corresponding status input are fed into exclusive-OR gates, which will produce an output when one input differs from the other. Thus if the actual status changes, the output of the corresponding exclusive-OR will change. If the outputs of all the exclusive-OR gates are then logically ORed together, a signal can be produced if any status changes from that which the computer believes it to be. This can then cause an interrupt, to notify the computer of a

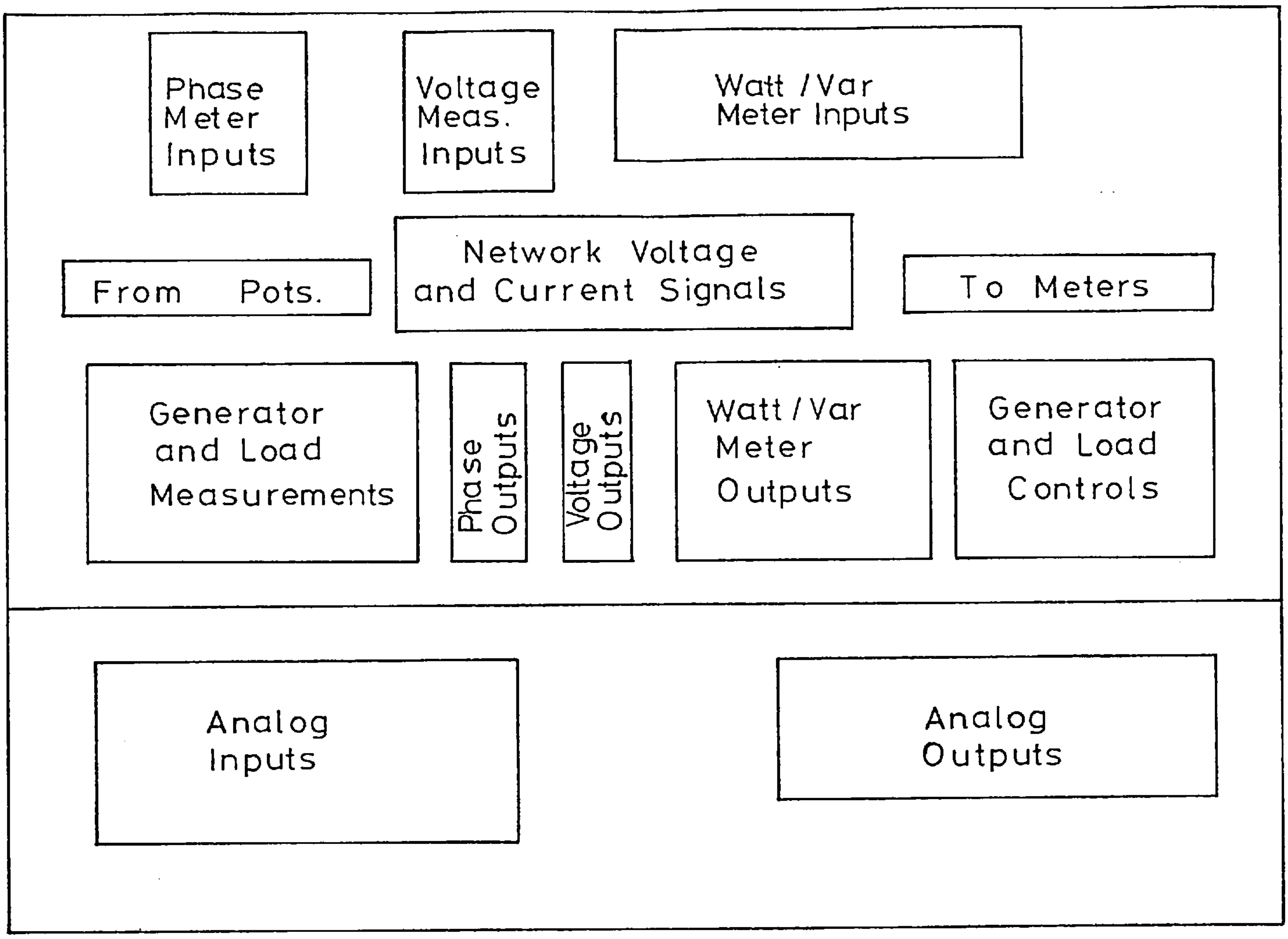

Fig. 6.12 Signal Patch Panel.

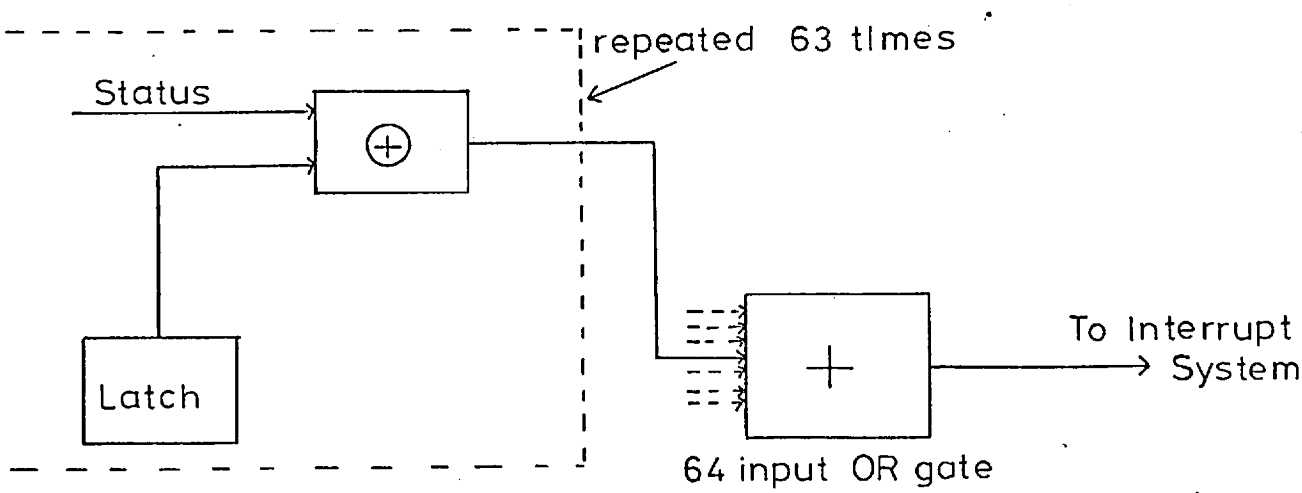

Fig. 6.13 Status Discrepancy.

status change. This is shown diagrammatically in Fig. 6.13. If the use of interrupts is to be avoided, the status discrepancy bit is also included as a digital input, so that the computer only has to check one bit to see if any status change has occurred.

6.5 Conclusion.

The interconnection of the various parts of the model itself have been described, as has the connection of the model to the interface, which is necessary when the model is to be used in conjunction with the digital computer. Circuits for the processing of the AC signals encountered in the network have also been described, and these are available for such functions as line flow, voltage, angle and frequency measurement. The system which has been adopted is very flexible, and enables any configuration within the capacity of the model to be set up. Similarly, there is a wide choice available of the measurements which can be made on the system, and in the way in which these measurements may be fed into the interface.

7.1 Introduction.

It has long been realized by the designers of AC network analysers[66] that it is advantageous to operate with a system frequency higher than 50 Hz. The principle reason for this is that to achieve a given per-unit reactance, smaller, and thus cheaper, components may be used as the frequency increases. The advantages of using a higher frequency in the Imperial College model may be summarised as:

(1) Smaller network components

(2) Simplification of the actual electronics

(3) Simplification of the signal processing

In particular, it is the last advantage which gives the greatest incentive to increasing the frequency, for if the ratio of

$$\frac{\text{Model Frequency}}{\text{Real Frequency}} \times \frac{\text{Solution Time}}{\text{Problem Time}}$$

can be increased, then the difficulties associated with filtering various waveforms in the Avr and the power measuring circuit will become less acute. This can be done either by increasing the model frequency, or by retaining the 50 Hz network signal and increasing the solution time. Both of these methods are used in the design of transient analysers, and while the latter has been employed in dynamic simulators, it means that the simulator no longer works in real time.

The main problem which occurs in a continuous simulation is that it is the actual frequency deviation which is of importance, not the percentage deviation from a nominal value. This can be easily grasped by considering the problem of synchronising two generators, with a speed difference of 1%. At 50 Hz, this corresponds to a 0.5 Hz difference, which would be possible, whereas at 1 kHz it is a 10 Hz difference, which is not feasable. Thus it can be seen intuitavely that it is the actual frequency deviation which is of interest. This problem is not encountered by the designers of transient analysers, for they are only interested in fixed frequency operation, where relative swings between the rotors of the various machines occur.

The implication is that for a continuous simulation it is necessary to have a voltage-controlled oscillator whose output frequency changes from the nominal value by, say, $\pm$ 5 Hz. At 50 Hz this represents a total frequency change of $\pm$ 10%, while at 1 kHz it is only $\pm$ 0.5%. Using elementary techniques it is not possible to build a VCO with stability and linearity of this order of magnitude, and the only solution to the problem would seem to be to synthesise the high frequency signal.

7.2 The Single-Sideband Approach.

Consider the products of two pairs of signals:

$$x = A\sin(\omega_s t + \varphi_a) \qquad\qquad y = B\sin(\omega_s t + \varphi_b)$$

$$z = C\sin(\omega_c t + \varphi_c) \qquad\qquad z = C\sin(\omega_c t + \varphi_c)$$

$$x.z = \frac{AC}{2}\Big[\cos((\omega_c - \omega_s)t + \varphi_c - \varphi_a) - \cos((\omega_c + \omega_s)t + \varphi_c + \varphi_a)\Big]$$

$$y.z = \frac{BC}{2}\Big[\cos((\omega_c - \omega_s)t + \varphi_c - \varphi_b) - \cos((\omega_c + \omega_s)t + \varphi_c + \varphi_b)\Big]$$

These expressions can be recognised as resulting from the balanced modulation of carrier z by signals x and y respectively. Considering the two upper sidebands, it can be seen that there is a phase difference between them of $(\varphi_a - \varphi_b)$, which is the same as that which existed between the original modulating signals. Fig. 7.1 shows the system as originally conceived, where the outputs from existing voltage-controlled oscillators are fed into single-sideband modulators, all of which use the same carrier signal. The upper sideband is then used to feed the remainder of each generator unit; this is the basic principle behind the work which has been done in this area.

7.2.1 Methods of SSB Generation.

There are three conventional methods of producing a single-sideband

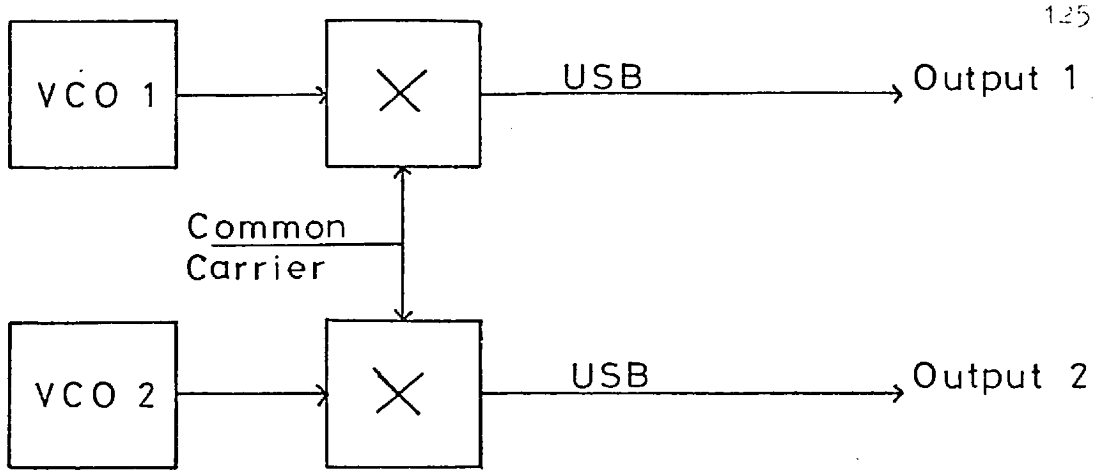

Fig. 7.1 Principle of High Frequency Method.

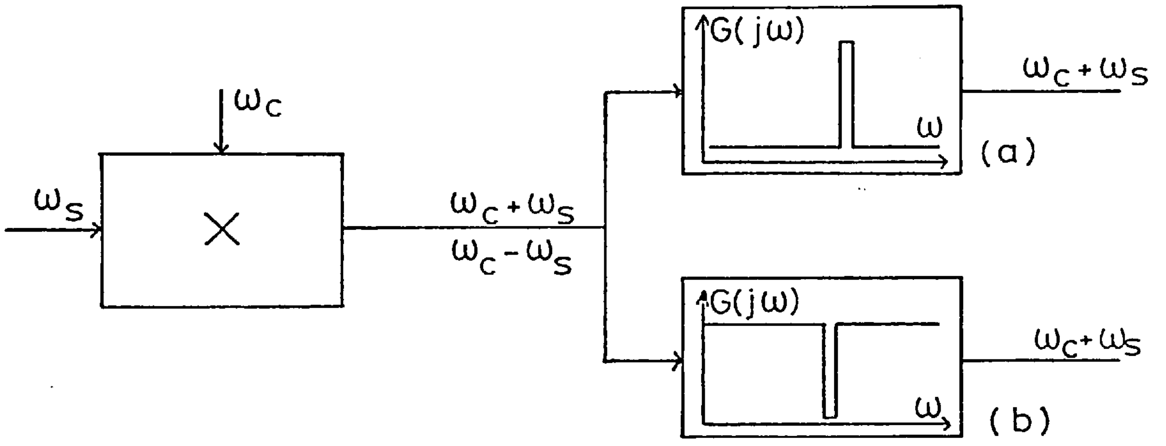

Fig. 7.2 SSB Generation — Method 1.

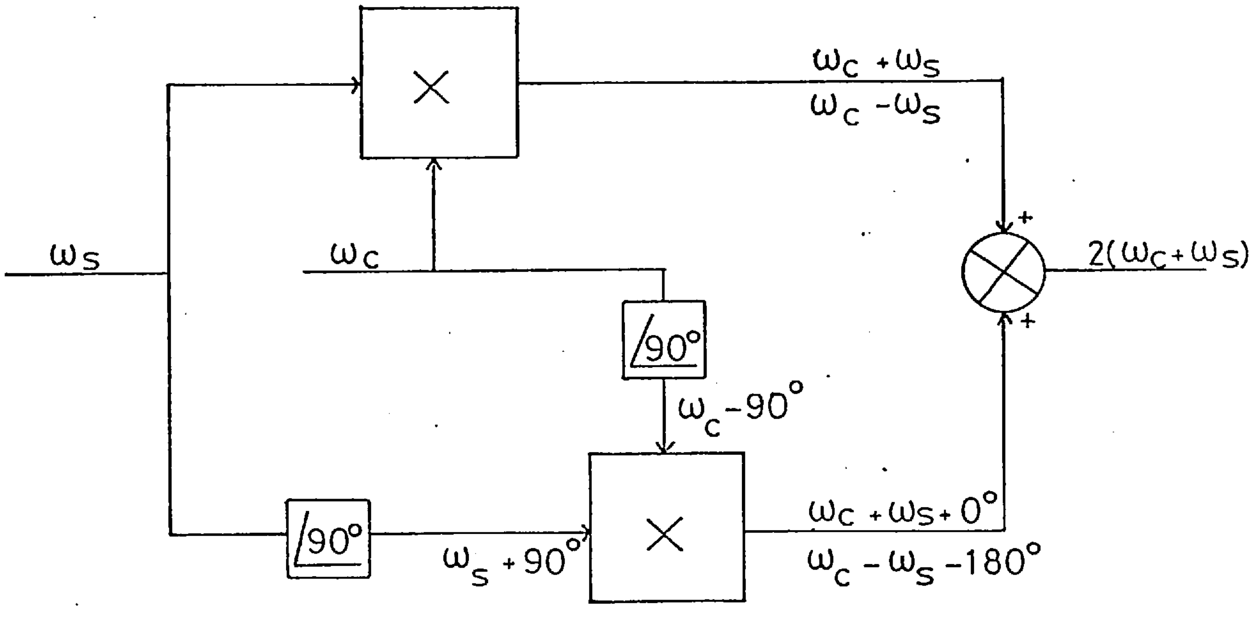

Fig. 7.3 SSB Generation — Method 2.

signal, and these are:

(1) Use a balanced modulator, and filter the product to give the desired sideband.[67]

(2) Use two modulators, with 90° phase shift in the carrier and the signal to one of the modulators, and sum the two outputs.

(3) Use four modulators in a double conversion scheme, with two carriers, each with phase and quadrature components.

The last method is just too complex, and this leaves the first two techniques as possibilities.

7.2.2 Method 1.

This is shown in Fig. 7.2, and employs a balanced modulator of some kind, followed by a filter, which either (a) accepts only the desired sideband, or (b) rejects the unwanted one. The better solution is to use filter (b), as its phase characteristic, $\frac{\partial \varphi}{\partial \omega}$, can be made nearly zero in the region of interest, which will ensure fast response to changes in the signal. With certain types of modulator, such as the Cowan, the output signal contains many harmonics and intermodulation products and in that case a bandpass filter, of type (a) must be used.

7.2.3 Method 2.

Two modulators are used, as shown in Fig. 7.3, and phase shifts of 90° are introduced into the signals which are fed to one of the modulators. When the two outputs are summed, the two lower sidebands cancel out, leaving only the upper sideband. The problem with this system is to design the 90° phase-shifter for the input signal, as it must have exactly 90° shift, and no change in amplitude over the range 45-55 Hz. Considering all the factors involved, it was decided to construct a system using method 1.

7.3 Experimental Work.

The system used to test this new idea is shown in Fig. 7.4, and is based on an existing generator unit and an infinite bus, whose frequency is manually controlled. This requires two single-sideband generators, a carrier oscillator and a 50 Hz oscillator; the carrier frequency was chosen to be 1542 Hz, which gives an operating frequency of 1592 Hz, or = 10,000 rad/sec. Each section will be described in turn, and the overall static performance examined.

7.3.1 The Modulators and Filters.

The first element to be considered is the modulator itself, and a variety of types were tried. The Cowan modulator was quickly rejected, owing to its numerous intermodulation products. The most promising device appeared to be an i.c. balanced modulator, MC 1496, but its performance was not up to its data sheet specification in several respects, and this was probably due to the low frequency at which it was used, as it is an r.f. device. Eventually a low-cost analog multiplier was used and found to be the best solution, as it produced the output with the lowest harmonic content. However, in addition to the two sidebands, various other frequencies were found to be present in the output, and this influenced the design of the subsequent filtering system.

Many different types of filters were tried, and it was decided that the use of notch filters to reject the unwanted sideband would be the most satisfactory solution, for the use of band-pass filters alone would give:

(1) Large variations of gain in the region of interest

(2) A large group delay, tending to reduce the stability of the system.

The simplest form of notch filter is a high-Q LC series combination, and this can be included in an active network[68] as shown in Fig. 7.5. At resonance, $Z = 0$, and if $R_1/R_2 = r_1/R$ then the circuit is a differential amplifier with a common input signal, and there will be zero output. However, at other frequencies, as $Z \rightarrow \infty$, the circuit becomes a follower, with

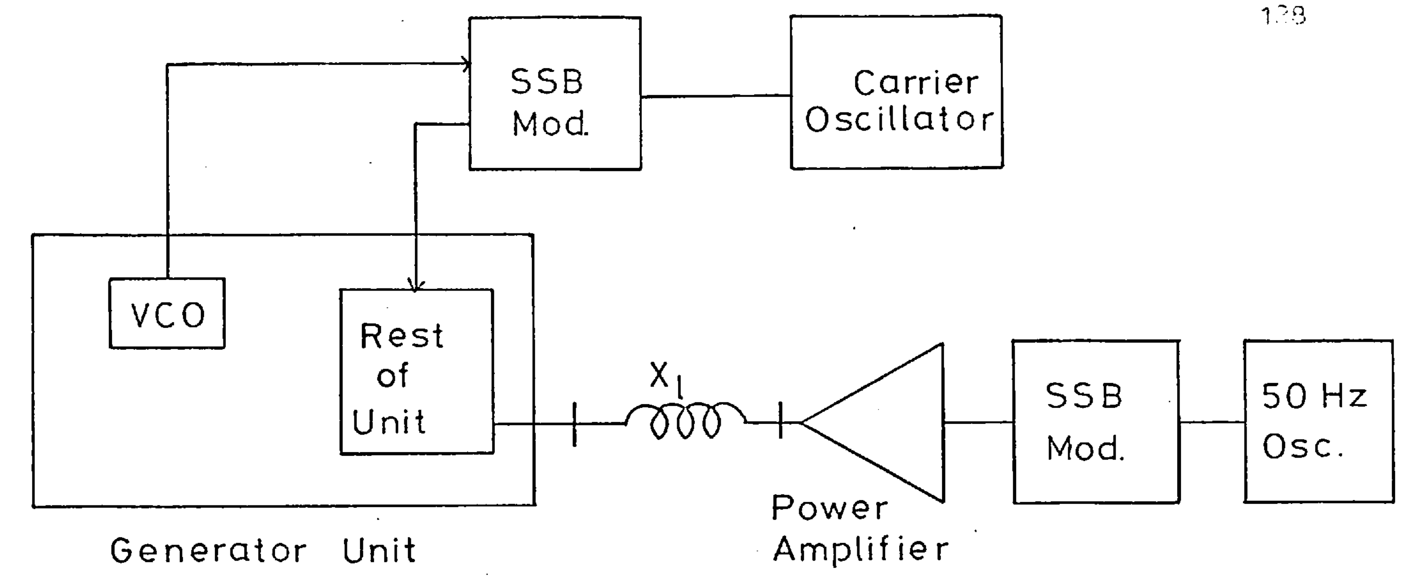

Fig. 7.4 Test System.

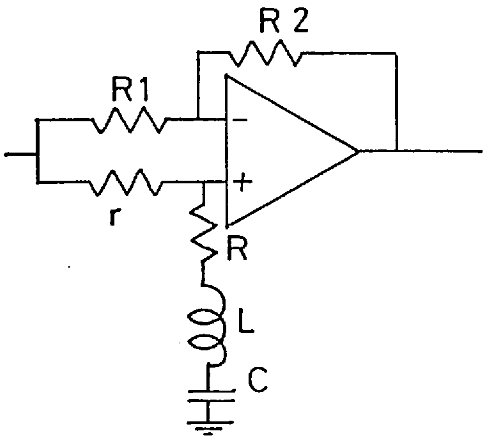

Fig. 7.5 Active Notch Filter.

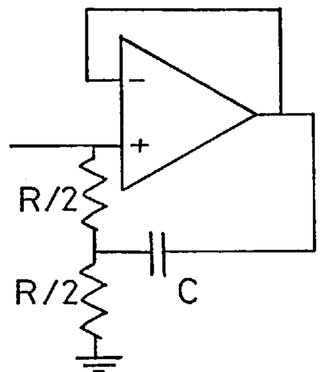

Fig. 7.6 Simulated Inductance.

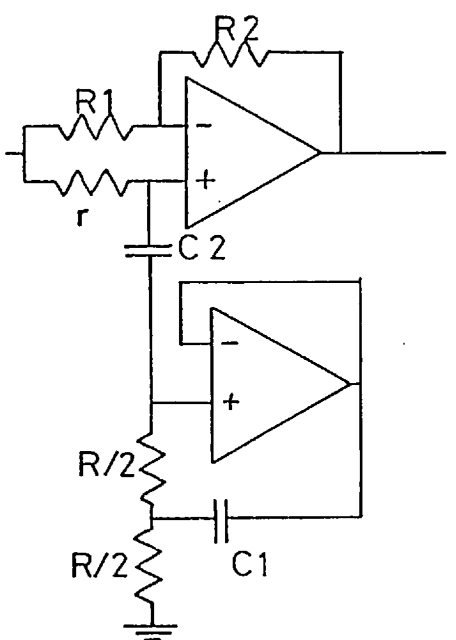

Fig. 7.7 Final Notch Filter.

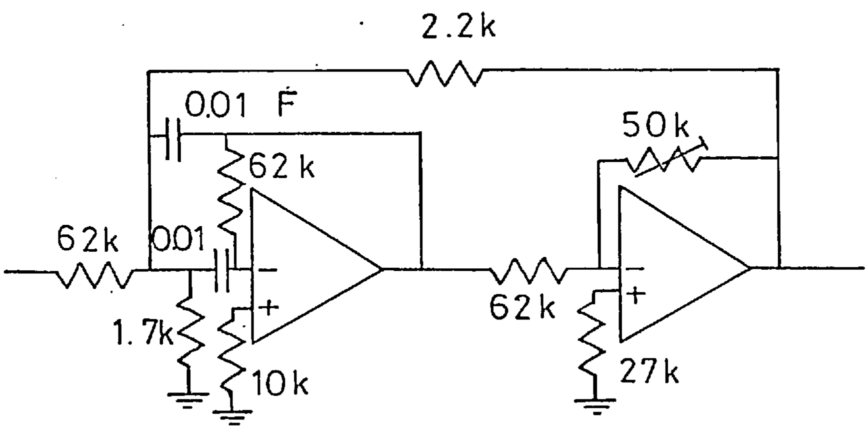

Fig. 7.8 Bandpass Filter.

a gain of 1. The resonant frequency is $1/\sqrt{LC}$, and the Q is $\omega L/R$. To obtain a sufficiently high Q at 1.5 kHz would require a special choke, and to avoid this, the circuit of Fig. 7.6 was used. The effective impedance looking into the input is given by[69] $Z = R + j\frac{R^2}{4}C$, which is the same as that of a grounded inductor with inductance $L = \frac{R^2}{4}C$ and resistance R. Thus the filter can be realized with two amplifiers, as shown in Fig. 7.7, with a resonant frequency given by $= 1/\sqrt{(\frac{R^2}{4} C_1C_2)}$ and with a Q of $\frac{1}{2}\sqrt{\frac{C_1}{C_2}}$.

Two of these filters are cascaded, one centered on 1489 Hz, the other on 1494 Hz. This combination provides adequate rejection of the unwanted sideband, but does nothing to reduce carrier feed-through, and the inter-modulation products. To reduce these spurious frequencies, a band-pass filter[70] of the type shown in Fig. 7.8 is included. The parameters were chosen to give a Q of 40, and the resonant frequency was chosen to be just over 1598 Hz. This means that the gain of the filter is increasing over the range of operation, and this can be adjusted to give an approximation to the change of electrical machine output voltage with a change in shaft speed. Care must be taken however that the phase shift introduced by this band-pass filter is small, otherwise undesirable interactions with the machine analog will occur.

The overall response of the filter system is shown in Fig. 7.9, where log(response) is plotted against the frequency. The rejection of the unwanted sideband, and the sharp discrimination in the region of interest can be seen clearly.

It was found necessary to introduce an extra low-Q bandpass filter after the synchronous machine analog, to remove the slight distortion caused by the component modulators. Measurements of the harmonics of the waveforms were made at points in the system shown in Fig. 7.10, and the results are shown in Fig. 7.11(a)-(e). As can be seen, the upper sideband signal is 48 dB above the carrier, with the lower sideband suppressed by more than 60 dB.

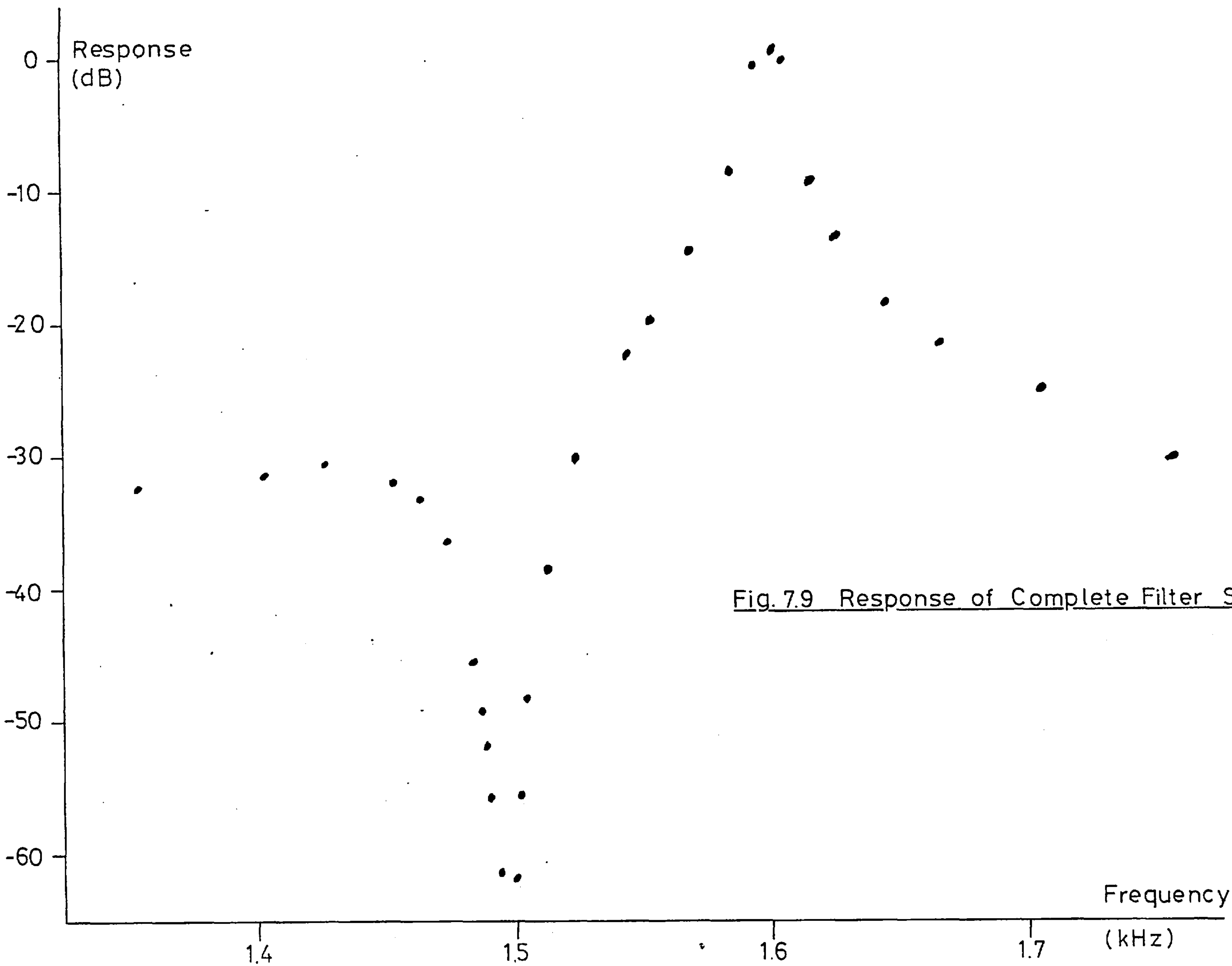

Fig. 7.9 Response of Complete Filter System.

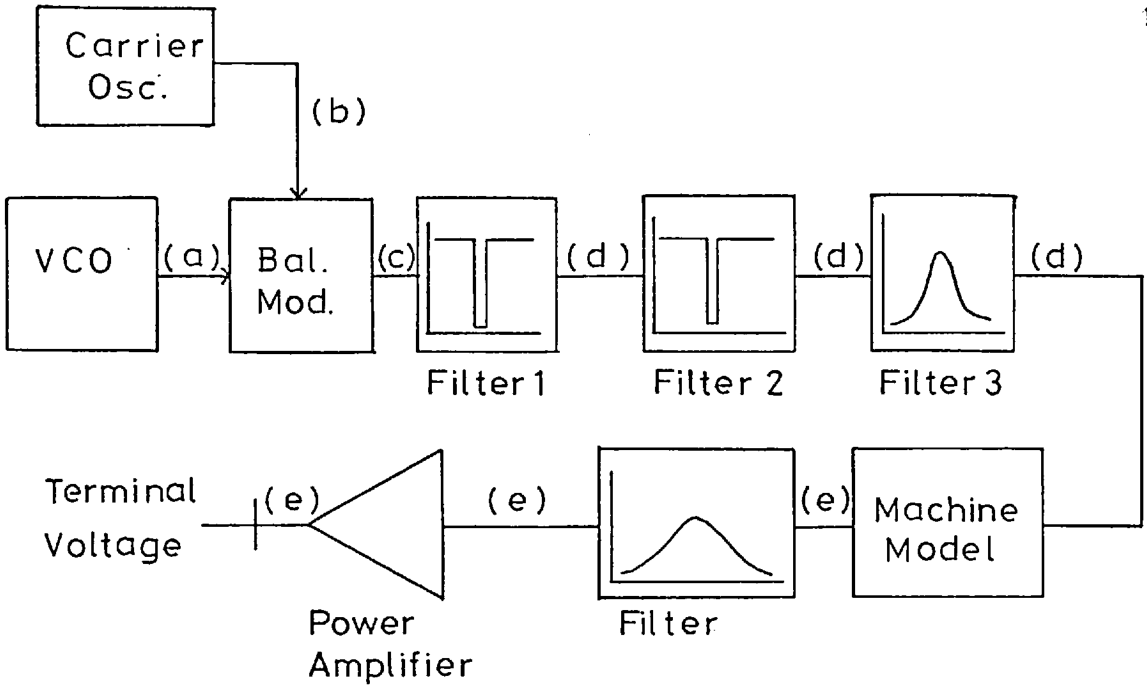

Fig. 7.10 Points of Waveform Measurement.

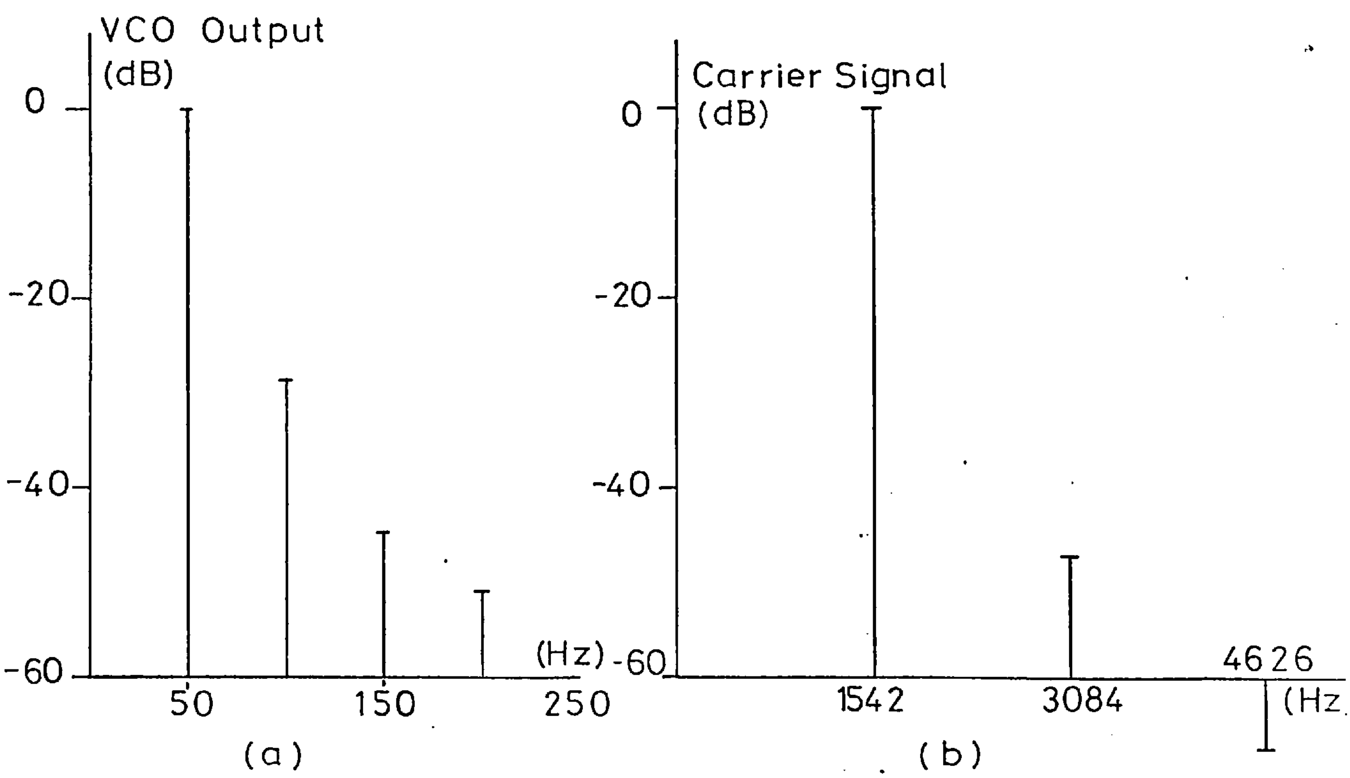

Fig. 7.11 Harmonic Measurements.

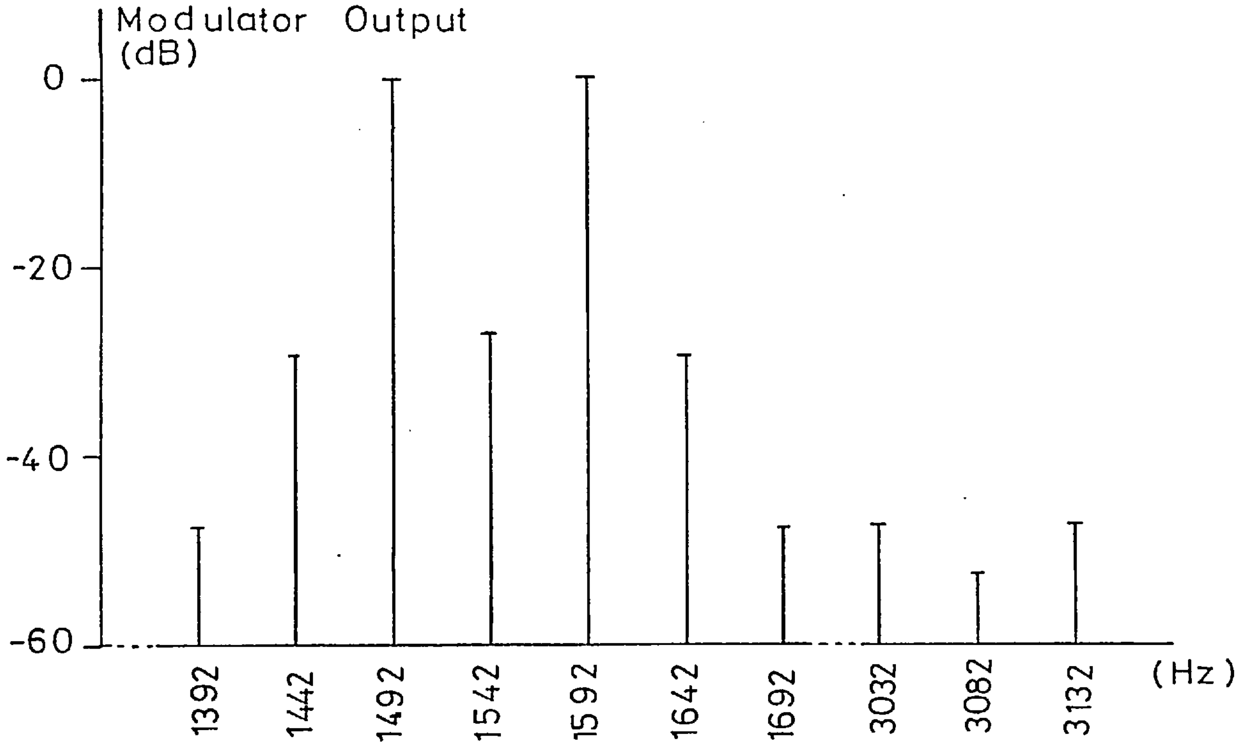

(c)

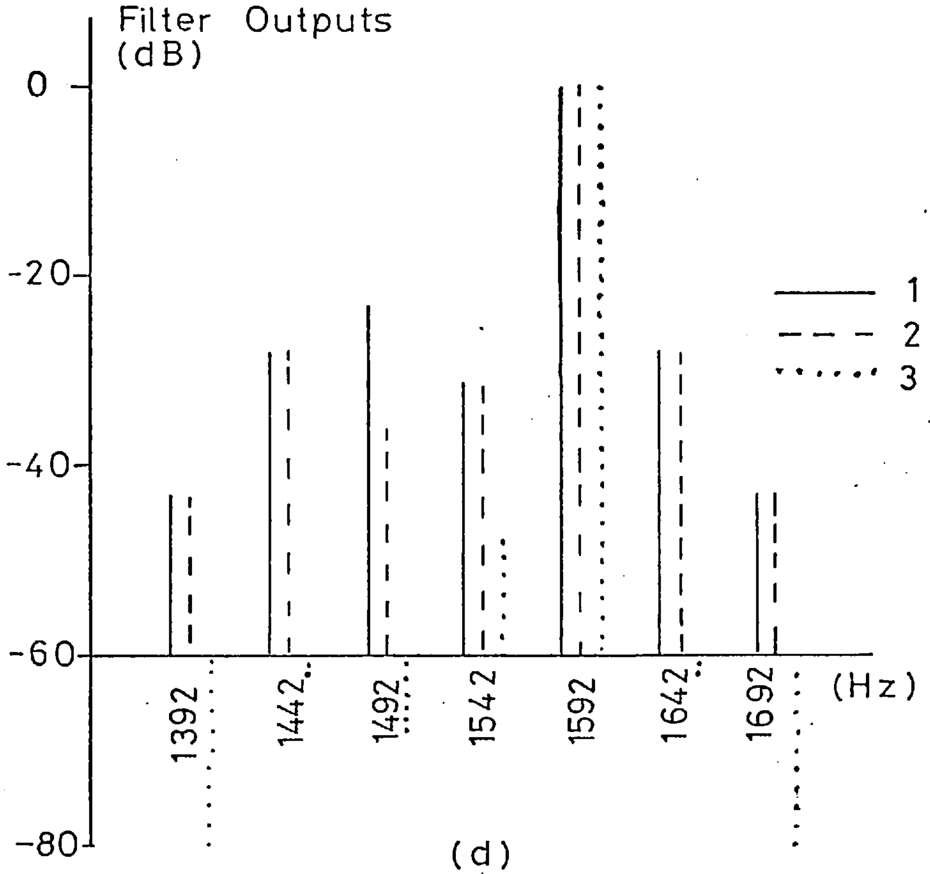

(d)

Fig. 7.11 Harmonic Measurements.

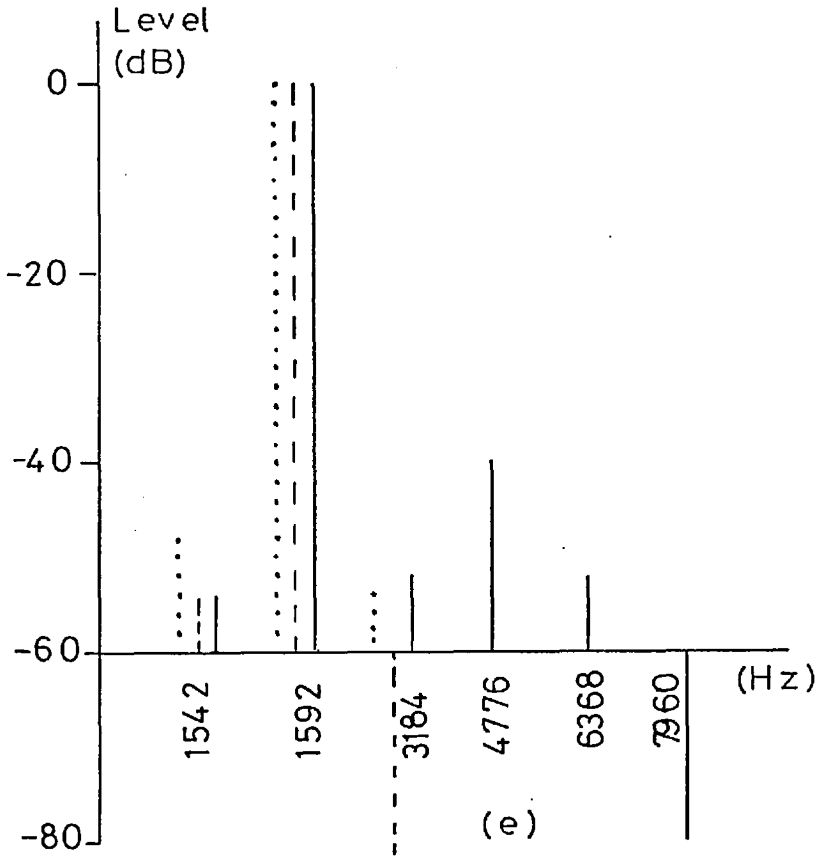

..... Output of Machine Model
– – – Filter Output
—— Terminal Voltage

Fig. 7.11 Harmonic Measurements.

The synchronous machine analog introduces some distortion, which is then largely filtered out, but harmonics appear in the terminal voltage due to the amplifier distortion. This could be corrected in a new design, since the amplifier is not really suitable for operation at 1.6 kHz.

7.4 Performance.

When set up and tested, the system was found to work excellently, and the performance was no different to that at 50 Hz. The synchronous machine analog exhibited better damping characteristics, and the whole operation was more stable; this can be ascribed to the faster measurement of electrical power. However, to try and understand the influence of the modulators and filters on the unit performance some analysis was performed, and the results indicate that the dynamics of this section of the equipment have no real effect on the system.

7.4.1 Transient Performance of the Modulator and Filters.

The process of balanced modulation is essentially a linear one, in that if the modulating signal can be resolved into components of a given frequency, then the output will have components at the appropriate frequencies. Thus the influence on the transient performance of the system comes from the filtering section, and two cases are considered:

(1) Small oscillations in the modulating signal, perhaps due to synchronising oscillations, about a steady operating point.

(2) A sudden change in modulating signal frequency.

7.4.1.1 Small Oscillations in the Input Signal.

In any simulation of power system dynamics, there occur small oscillations in the rotor angles of all the machines, and the form of these oscillations is nearly sinusoidal. If the maximum deviation from the steady state δ_o is α, then the oscillation of the angle may be written as

$\delta = \delta_o + \quad \sin \omega_x t$ where ω_x is the oscillation frequency.

The output of the voltage-controlled oscillator may then be written as

$$v = V \cos(\omega_m t + \delta) = V \cos(\omega_m t + \delta_o + \alpha \sin(\omega_x t))$$

This last expression can be recognised as that characterising an angle modulated carrier, and can be expanded[71] using Bessel functions. For this system, however, α is sufficiently small for all the terms J_n to be ignored, for $n \geqslant 2$. Thus it can be written as

$$v = V\left[\cos(\omega_m t + \delta_o) + \quad (\cos(\omega_m t + \delta_o + \omega_x t) - \cos(\omega_m t + \delta_o - \omega_x t))\right]$$

This is the signal which is the input to the modulator, whose output will contain three frequencies in both the upper and lower sidebands, since the input contains three frequencies. Under steady-state conditions, the filters will give a steady response to each of the components, and assuming that $\omega_x \leqslant \omega_m$, then all of the lower sideband components will be eliminated, while those of the upper side-band will be passed. If the filter has only a small change in phase angle in the range $\omega_c + \omega_m \pm \omega_x$, then the upper sideband group of signals will pass undistorted, and the oscillations which were present in the output of the VCO will appear in the high frequency output.

In the practical system the phase changes associated with the filters are sufficiently small to allow such oscillations as these to pass unchanged through the system.

7.4.1.2 Step Change in Input Frequency.

To study the effect of rapidly changing input signals, the case of a step change in frequency was considered, as this is the simplest case to study analytically. The response of a notch filter to a suddenly applied sine wave can easily be determined using Laplace Transforms. The transfer function of a notch filter is $G(s) = \dfrac{s^2 + \omega_o^2}{s^2 + \frac{\omega_o}{Q} + \omega_o^2}$

where ω_o is the notch frequency. The response to the suddenly applied sine wave can be obtained as

$$v(t) = W e^{-\alpha t}\cos\beta t + X e^{-\alpha t}\sin\beta t + Y\cos\omega_x t + Z\sin\omega_x t$$

where $\alpha = \frac{2\omega_o}{Q}$, and $\beta = \omega_o^2 - \alpha^2$, and W,X,Y and Z are functions of ω_o, ω_x and α. The first two terms are the damped response of the filter's own modes of oscillation, and the second two terms give the steady-state response to the input signal.

The sudden change in input frequency can be produced by considering the removal of a sine wave of one frequency, and its replacement by one of another frequency. The response of the filter will show a transient output, caused by the modes of oscillation of the filter, and also the final steady-state response to the input.

Consider the case with a carrier of 1542 Hz, and a change in modulating signal from 50 to 51 Hz. The lower sidebands do not contribute to the steady-state output, as the filter is tuned to reject 1492 Hz, but it does produce a contribution to the transient response. The transient response has been calculated for two filters, one with a Q of 20, the other with a Q of 100. For a unit amplitude sine wave input, the responses were:

$$Q = 20: \quad V = 0.018\, e^{-250t}\cos\omega_o t$$

$$Q = 100: \quad V = 0.098\, e^{-50t}\cos\omega_o t$$

It can be seen that the contribution to the total response is dependent on the Q of the filter, both in magnitude and also in duration. Even with a Q of 100, the transient dies away with a time constant of 0.02 seconds, which for a severe change such as this is quite adequate.

7.5 Conclusion.

Although the additional complexity of this arrangement to operate at a higher frequency may at first seem to be undesirable, experience has shown otherwise. In return for the inclusion of a balanced modulator and a filtering system, it is possible to simplify the rest of the generator unit. Smoothing requirements of the waveforms associated with measurements are greatly eased, and this would also enable the computer to measure signals which are not as heavily filtered as at present.

Once the equipment was set up, it was found to be perfectly stable, and operated satisfactorily for four months without adjustment. Greater attention must be paid to the layout of the AC parts of the generator unit at this frequency than is necessary at 50 Hz, but there is no reason why the frequency should not be increased still further. The only parts of the generator unit which are affected by the higher frequency are the power amplifier and the synchronous machine analog; the former was not really suitable for use at the new frequency, and lack of time prevented a new design being produced. The machine analog only encounters the AC signal in the current resolvers and the component modulators, and both of these parts will operate up to a frequency of several kiloHertz without modification; all the other sections of the analog use only DC signals, and at the higher frequency it means that the current signals are updated more frequently. This gives a faster response to electrical power measurement, and consequently this accounts for the slightly improved damping performance of the machine analog at this higher frequency.

In conclusion, it can be said that this new method of operating a continuous simulation at a higher frequency is a useful one, and despite the apparent complexity it offers great simplification in signal filtering, and also enables smaller elements to be used in the representation of the transmission system.

8.1 Introduction.

In order to understand how the whole power system model is used, it is necessary to have a knowledge of the way in which the analog section is connected to the digital computer, and also how various computer programs may be run in order to monitor and control the model. Examples of some actual uses of the model will be given in the next chapter, and the space here will be devoted to a discussion of the actual computer and the interface, together with a brief explanation of the Real Time Executive used in the machine. The basic software which is used to acquire data and to dispatch control signals will also be described; this software has been written by two other research students[72,73], and the present writer claims no credit for the detail of it, but it is felt that a short discussion of it will clarify the operation of the digital section of the model. The chapter will be divided into two main sections, one of which will deal with the actual hardware, while the other section will concentrate on the software aspects and the particular features of the model and the computer which influence the approach which has been adopted.

8.2 The Computer and the Interfacing Hardware.

The digital computer which is used with the model is a Digital Equipment Corporation PDP-15, a medium sized machine intended for scientific use. Developed during the late 1960's, it is very large by modern standards and the method of construction reduces its reliability below that of present-day mini-computers. However, it is equipped with many useful peripherals and was available for use in conjunction with the power system model. It is located on Level 5 of the Electrical Engineering Department.

The PDP-15 is a single accumulator machine, using an 18 bit word length and is presently equipped with 24 K of core store. Mass storage is provided by two fixed-head disk units, each with 256 K words of storage, and by a dual DECtape drive. Four of these small DECtapes are required to save an image of the whole disk system. The central processor unit is fitted with a hardware multiply and divide unit, but a floating point processor is not included. The implication of this is that any operations performed which use floating point arithmetic tend to be slow, and this is of considerable importance in the execution of mathematically complex programs.

The peripherals which are attached to the computer comprise:

(1) A local teletype, parallelled by a Tektronix storage type visual display unit.

(2) A teletype controller, type LT 19, which can control up to 5 remote teletypes.

(3) A high-speed paper tape reader.

(4) A high-speed paper tape punch.

(5) A serial printer.

(6) An X-Y plotter.

(7) A 4 channel D to A converter, with a 10 bit word length.

(8) An A to D converter with a selectable word length of between 6 and 12 bits, together with a 16 channel local multiplexer.

(9) A digital input/output unit.

(10) A real-time clock.

The input/output processor in the computer is also fitted with the Automatic Priority Interrupt (API) option, which considerably increases the speed of interrupt handling. Full details of most of these peripherals are given in the relevant DEC manual[74], and they will not be discussed further here. The main items of importance to the use of the PDP-15 with the model are the A/D converter, the D/A converter and the digital I/O unit, since these provide for the transfer of both analog and digital data between the two.

As was explained in the previous chapter, the whole system requires bidirectional transfer of both analog and digital data between the computer and the model, and to achieve this end the digital I/O unit and the Level 8 interface were designed and constructed by M.J.P. Bolton[75,76]. There are two main cables which run between Levels 5 and 8, one of which is a 50 way screened lead used for the analog signals, and the other is a 50 pair twisted cable used for the digital signals. The interface on Level 8 provides for the multiplexing of both analog and digital signals, to give sufficient signal inputs and outputs. It would be more convenient to have the interface adjacent to the computer and its other peripherals, but the cabling cost for this scheme would be very large. The whole system is shown in Fig. 8.1.

A block diagram of the interface is shown in Fig. 8.2, where its facilities may be seen. These include:

(1) 96 analog inputs

(2) 64 analog outputs

(3) 64 bits of digital input and output

(4) A phase-locked loop

(5) Period measurement

(6) An interrupt facility.

The various modes of operation are selected by a digital input word, which may be supplied either by the computer or by a local switch panel. This word may be either an instruction (bit 0 =0) or digital data (bit 0 =1), so once it has been clocked into a register it is decoded to decide on its function. If it is an instruction, it operates the appropriate section of the interface, whereas if it is data it is clocked into an output latch. The instruction format is shown in Fig. 8.3.

The analog multiplexer is connected to six of the inputs of the Level 5 multiplexer, and each line is multiplexed 16 ways, to give a total of 96 analog inputs. The conversion range of the A/D converter is $\pm$ 10 V, so all the input signals must lie within this range. The channel address for the multiplexer is held in its own register, and if bit 1 is set the data

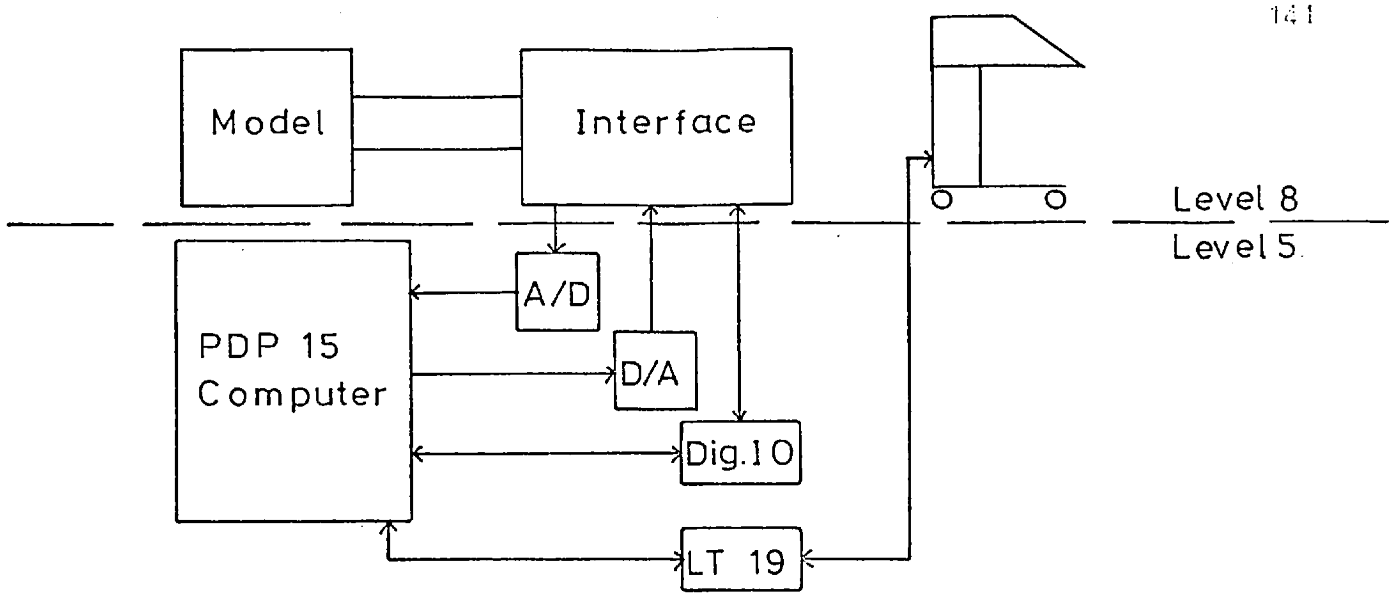

Fig. 8.1 Total System.

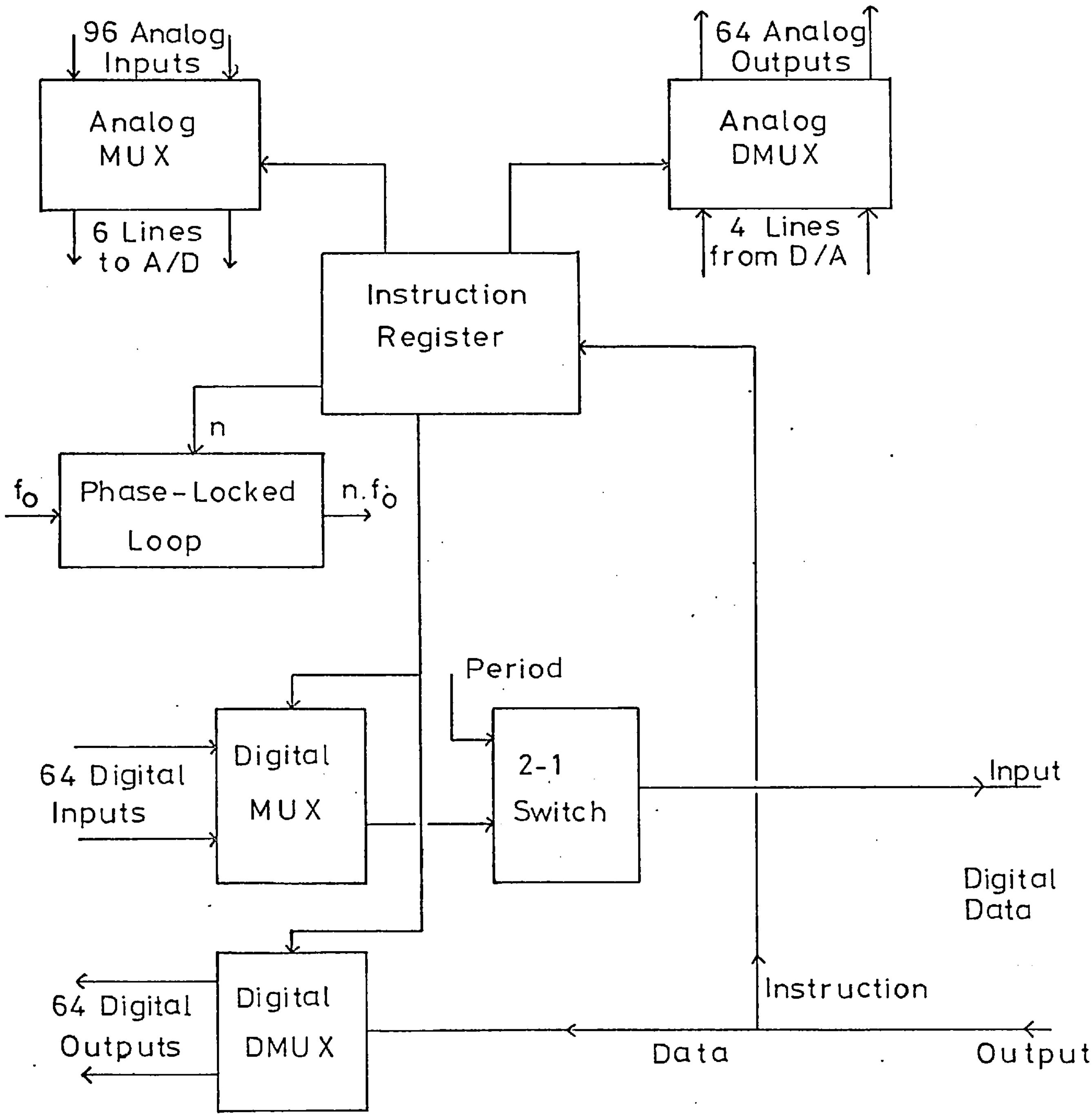

Fig. 8.2 The Interface.

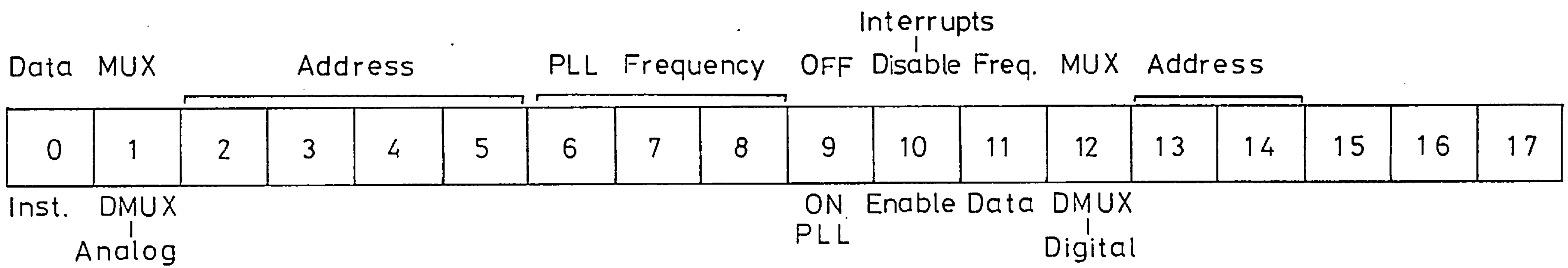

Fig. 8.3 Interface Instruction Format.

word will update this address, which is given by bits 2-5.

The analog demultiplexer uses all four channels of the D/A converter, each channel being demultiplexed 16 ways. The address of the appropriate channel is determined in the same way as that of the multiplexer, but the actual analog switches are only closed for 20μs following an updating of the channel address. Since the analog output is required for use as a control signal, the demultiplexer is followed by zero-order hold circuits, consisting of capacitors which are charged up to the D/A output voltage during the 20μs period when the switches are closed. The capacitors are connected to high impedance buffer amplifiers, and the whole holding system has a droop of about 10 mV per second.

The phase-locked loop is a voltage-controlled oscillator running at 256 times the AC line frequency and locked in phase to it. The output of the oscillator is divided down and fed to the phase comparator with the line voltage. From the frequency division chain various multiples of the input frequency are available, the multiple being determined by bits 6-8. The whole phase-locked loop system is enabled by bit 9. The main use of the loop is to permit sampling of a periodic waveform to be synchronized with that waveform, and since there is no necessity to look at the sinusoidal voltages in the model. this facility is not usually required.

The digital I/O unit is connected to the API system and a line to the interrupt input is brought up to Level 8 to permit interrupts to be generated from the model. The interrupts are enabled by bit 10, and also as a further precaution by a front panel switch, which may be operated to prevent spurious interrupts. The main use of this facility is in conjunction with the status discrepancy system which was described in the last chapter.

Digital data may be input and output from the computer and this data is organised as four 16 bit words. Bit 0 cannot be used as it determines whether a given word is an instruction or data, and bit 17 is also not used. There are, therefore, four channel multiplexers and demultiplexers, the address being determined by bits 13 and 14. The digital inputs go srtaight into the multiplexers, with no double-buffering, while the digital outputs are held in data latches. The system is akin to that used for the analog signals.

The cable connecting Levels 5 and 8 have already been mentioned, and they carry the following signals:

Digital Cable	Analog Cable
18 digital inputs	6 analog inputs
1 interrupt line	
18 digital outputs	4 analog outputs
1 timing pulse	Teletype cable
	Intercom

The digital cable is fitted at both ends with conventional balanced line drivers and receivers, and no trouble has been experienced with this arrangement. The analog cable, however, presented several problems, owing to the capacitive nature of the screened lead. Special driving amplifiers were designed to counteract ringing on the line, and the problem was then overcome. This analog cable also carries the teletype lines from the teletype controller to the second Tektronix VDU which is situated alongside the model, and the lines of the intercom, which is used to facilitate communication between the model and the computer operators.

It can be seen that the whole computer and interface system is well adapted for use with the model, providing as it does the capability of digital and analog data transfer. The VDU situated adjacent to the model is used for both the display of measured data and for the control of programs running in the computer.

8.3 Requirements of the Computer.

There are three main areas in which the computer plays an important role as part of the whole simulator, and these may be listed as:

(1) Monitoring
(2) Simulation
(3) Control

The monitoring section of the problem is concerned with the acquisition of data from the model through the interface, and the preliminary processing of this data. This data must also be displayed to the operator in a convenient form, and also be logged to give a permanent record of the system state. The simulation to be performed by the digital computer is of those sections of the power system which cannot be conveniently simulated using analog equipment for one reason or another. Two simple examples are the simulation of load characteristics, both voltage and frequency dependence and the effects of trends and random fluctuations in demand, and the simulation of boiler plant. The former task poses problems as it requires extra multipliers if it is to bs done using analog circuits, and the latter involves both very long time constants and also pure delays. The control algorithms are likely to be very varied, since it is for the purpose of investigating different control strategies that the whole system has been developed. Typical tasks might be load-frequency control, economic dispatch or security assessment.

It can be seen that when the simulator is operating fully, all the computer programs which perform these tasks must be run at the correct time without intervention from the operator. The data must be acquired, say, every second, and the simulation programs must run at regular intervals. This is not an easy job to arrange, since certain programs must have priority over others, and the running of all programs on a regular basis must be scheduled by interrupts from the real-time clock. Given the complexity of the problem, it was decided to use the Real Time Executive supplied by DEC which is known as RSX phase 1.

8.4 The Real Time Executive.

The usual operating system used with the Electrical Engineering Department's PDP-15 is the Disk Operating System (DOS)[77], and this is a single-user system with a comprehensive range of system software. Facilities include a text editor, a file handling system, an assembler for the MACRO assembly language, a Fortran 4 compiler and a linking loader. All user-generated interrupts must be handled by programs written in MACRO. The loader only executes one program at a time, and if this operating system were to be used in conjunction with the simulator, all the routines for scheduling the running of the separate programs and handling the interrupts would have to be written in MACRO. This would be a complex job, and the problem can be overcome by using the Real Time Executive.

A Real Time Executive is an operating system which enables many programs to be active in a computer at one time, and these programs can then be scheduled to run at regular intervals, or be run on request. The user is spared the problems of dealing with the timing and the interrupts from the real-time clock, and as the programs may be given a specified priority the system will ensure that the most urgent program will be run when the machine is next free.

For the RSX system to be implemented on a PDP-15 there is a certain minimum hardware configuration which is necessary, and among the peripherals which are required are the disk, the API system and the real-time clock. Each seperate program is converted into a Task, which is a binary file containing the program, its priority, its linkages and information as to the section of core in which this program is to run. The production of a task is performed using a utility program, the Task Builder, which is available under a third operating system, Advanced Monitor.

The core of the machine is divided into partitions, and each program is allocated a partition in which it will run; the program may either be resident in core, or stored on the disk and loaded into its partition when it is required to run. Obviously those programs which are required to run frequently must be fixed in core, to avoid an excessive number of disk to core transfers. The size of the partitions must be chosen carefully so that all the various programs required to run in the same partition can be accommodated, and so that even those programs which are not core resident are transferred as infrequently as possible between disk and core. Data may be transferred between different programs, and between successive runs of the same program if it is not core resident, by using variables in common storage areas. These areas are defined in advance, and when a task is built the references of the program to these common areas must be specified.

When an RSX system is running all the possible tasks are stored on the disk, and must be installed in the system. This, and all other communication with the system, is achieved through the Monitor Console Routine, which operates with any teletype connected to the system. This routine provides the following facilities for dealing with tasks:

(1) Installing a task in the system

(2) Fixing the task in core - if this is done, no other task can run in the same partition

(3) Running a task - the task can either be run immediately or at some specified time in the future

(4) Scheduling a task - the task can be requested to run periodically, with the period being variable in steps of 0.02 seconds

(5) Cancelling a task

(6) Removing a task from the system

(7) Changing the priority of a task in the system.

It can be seen that this system performs all the necessary handling of the programs without undue complication for the user, who is not concerned with all the detailed timing arrangements.

8.5 The Basic Software.

The system within which all the programs run has been described, and with an understanding of that, the basic software can now be explained. The original concept was that this basic software would perform all the input and output of data to and from the model, so that the user could run his own control programs without requiring a detailed understanding of the interfacing arrangements. The input program would acquire data from the model and store it in a common storage area, whence it could be accessed by a FORTRAN program using a labelled COMMON statement. It has since become apparent that this was a naïve view to take of the operation of the simulator, owing to the great complexity of the whole system. However similar arrangements for the linking of the programs through COMMON areas have been adopted.

There are three programs concerned with the handling of data, these being the analog input program, the analog output program and the digital data program. The analog input program controls the analog multiplexers and the A/D converter. All 96 channels are converted in turn, and before the results are stored in the COMMON area DATIN, a digital low-pass filter is used to filter the converted value. This is to remove any spurious values and to smooth the measurements made on the system when small hunting oscillations occur. A word length of 10 bits is used with the A/D converter, since this gives a resolution of 19.6 mV on a range of $\pm$ 10 V. The filtered results are stored as 2's complement numbers.

The analog output program takes values from the output signal COMMON area, DATOUT, and controls the D/A converter and the demultiplexer. The data stored in the DATOUT area is in the same format as that used in the DATIN area, even though the A/D and D/A converters use different number representations. This facilitates the use of the system. There are two ways in which the digital data program can operate; first, it could operate on interrupts from the Level 8 interface, which indicate status changes, or secondly it could read the status words frequently, to see if a change had occurred. The former method was initally used, but following changes made to the computer hardware, the interrupt line no longer works reliably, and the second method had to be adopted. The digital data words are also stored in the DATIN and DATOUT areas.

These programs perform all the data handling, and the other main facilities provided by the basic software are the monitoring and logging functions. The monitoring program produces a display on the VDU of certain important variables, such as voltages and the frequency, and the time at which the data was recorded. This display is updated at intervals of about 15 seconds. There are logging programs for making permanent records of system measurements, one program logging the results on the serial printer, the other onto the DECtape for subsequent off-line analysis.

All this software provides a framework within which different control and simulation algorithms may be easily tested. and the use of the Real-Time Executive enables the whole system to operate efficiently, with a minimum of operating system overheads. The following chapter will describe work which has been done using the whole simulator, and the advantages of the software system which has been adopted will become clear.

CHAPTER 9 DEMONSTRATION OF THE CAPABILITIES OF THE SIMULATOR

9.1 Introduction.

The purpose of this chapter of the thesis is to give details of three demonstrations of the capabilities of the whole simulator. The first of these is designed to show how the digital computer can be used for the simulation of processes with long time constants, and how such a digital simulation is accommodated by the analog hardware. The example chosen is the implementation of a simple boiler model, and demonstrates how this is interfaced with the analog governor and turbine model.

The second example shows how the simulator may be used for testing a control algorithm. The example here is a load-frequency control system with a unit scheduling scheme which employs digital compensation to minimize control action. The third demonstration shows how the model can be used to evaluate a proposed method of power system parameter measurement. This involves the identification of the power/frequency characteristic and the determination of the system inertia.

The investigation of these three diverse problems demonstrates the versatility of the whole simulator, and its potential value as an aid to power system studies.

9.2 The Digital Simulation of Boilers.

As has been explained previously, the boiler plant is simulated digitally, and the choice of a suitable model involves a number of compromises. Any real-time simulation demands that the chosen algorithm is numerically stable, an important point in a machine with a short word-length. The algorithm must also be capable of fast execution, especially when it is only one of a number of programs which have to be run sequentially. The technique adopted here not only produces an efficient boiler model, but also demonstrates the principles which should be followed for any other digital simulation which is performed in conjunction with the model.

Traditionally, boiler models can be divided into two main classes, depending on the use to which the model is to be put. In the first class are the very complex models[79], involving perhaps 20 or 30 state variables, which represent each section of the boiler separately. For example, the performance of the super-heater will be calculated in terms of the heat transfer through the tube walls to the steam, and such calculations involve the solution of partial differential equations, whose coefficients are functions not only of the boiler geometry, but also of the steam conditions. In the second class, at the other extreme, are models [49,80] concerned only with the terminal performance of the whole boiler system, and these calculate changes in boiler pressure for changes in the throttle valve position. Such a model is adequate for use with the power system simulator, as great accuracy is not required in this area. Changes in the boiler pressure are usually limited by the pressure un-loading gear to less than 10%, so even if the model itself has an error of 10%, this will only contribute a 1% error to the whole system.

9.2.1 The Boiler Model.

The model which has been adopted is one which has been used by the CEGB[13] in their system response studies, and it is shown in block diagram form in Fig. 9.1. This model can be decomposed into three main sections, one associated with the boiler storage effects, the second representing the pressure control loop, and the last part being the fuel feed and firing systems. The boiler is represented as a steam storage system, in which the difference between the heat input to the boiler and the steam flow out through the throttle valve is integrated to give the change in pressure. The steam flow is assumed to be equal to the product of the valve position and the steam pressure.

The pressure control system is a conventional 3 term controller, with the error signal being the pressure deviation from the set value. The output

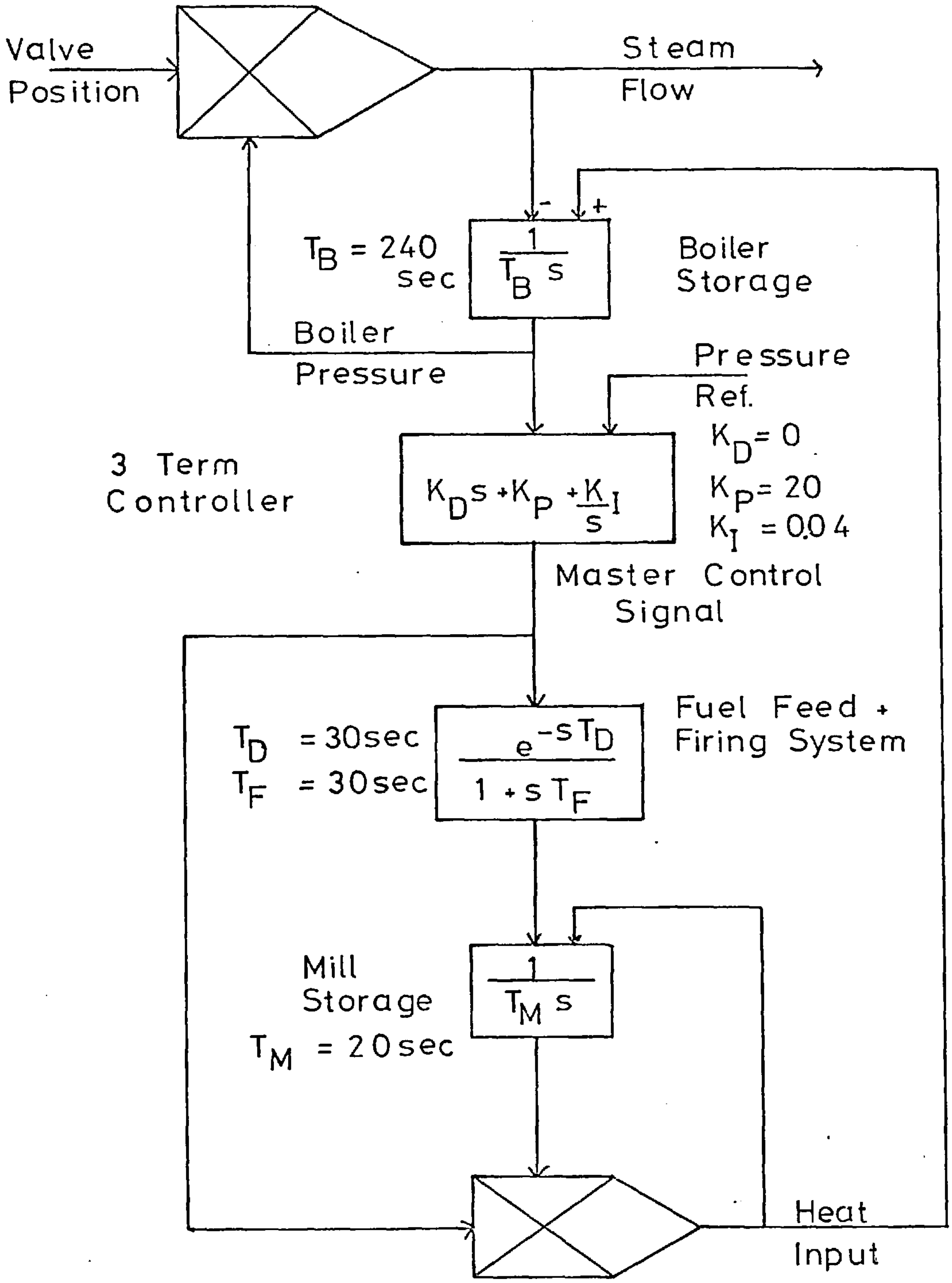

Fig. 9.1 Simple Boiler Model.

of the controller is known as the master control signal, and this acts on both the fuel feed system and the air supply. The heat input to the boiler is given as the product of this control signal and the fuel density. The firing rate is determined by a delayed version of the master control signal, the pure delay and the simple lag representing the transport delay and the lags associated with the firing system. The fuel density is obtained by integrating the difference between the fuel arriving, given by the firing rate, and the fuel consumed, given by the heat input to the boiler.

It can be seen that this is a very simple model, but a suitable choice of the various parameters enables it to represent a wide variety of boiler plant. Typical values of these parameters for a drum boiler are given in Fig. 9.1.

9.2.2 Solution of the Differential Equations.

From a dynamic point-of view, the model described above is a fourth order non-linear system, and a real-time simulation of this system requires the solution of the differential equations. There are many ways in which these may be solved, but in a real-time simulation the execution time of the algorithm must be as short as possible, commensurate with stability of the solution. Conventional numerical methods, such as predictor-corrector or Runge-Kutta algorithms will give satisfactory results, but their execution times tend to be long, owing to frequent ~~constant~~ evaluation of the function, and to the relatively small time increments which must be used to guarantee numerical stability. In recent years much interest has been centered on simpler methods of solution, which are faster in execution. In the power systems area Domel and Sato[81] have recommended the use of the trapezoidal rule in fast transient stability studies, and in the field of space vehicle dynamics success has been achieved using operational methods.[82]

The basic concept behind such operational methods is the development of a discrete integrating operator, which can then be directly substituted in the system transfer function to give a set of difference equations. The best known such operator is that due to Tustin[83], who derived it in terms of "time series". The original manipulation is rather cumbersome, but a useful explanation of its derivation using the foward shift operator, z, is given in Ref. 82. The integrating operator, $\frac{1}{s}$, is given in discrete terms as

$$\frac{1}{s}^{\,m} \qquad \frac{T}{2}\,\frac{z+1}{z-1}^{\,m}$$

where T is the time step. For an integrator with input x and output y,

$$y(s) = x(s).\,\frac{1}{s} \qquad \text{or} \qquad y(z) = x(z).\,\frac{T}{2}\;\frac{z+1}{z-1}$$

or in terms of a difference equation

$$y_n = y_{n-1} + \frac{T}{2}\,(x_n + x_{n-1})$$

which can be recognized as being the familiar expression for trapezoidal integration. All that is required for the solution of a linear system is to derive the transfer function, and to isolate powers of $\frac{1}{s}$, which are then replaced by the appropriate power of the discrete operator, and a difference equation can then be derived.

Once this difference equation has been derived, and its coefficients calculated, the solution of the system is a simple task. A non-linear system may be broken down into a set of linear sections, linked by non-linear equations, and even time-varying parameters may be accommodated by periodic re-evaluation of the coefficients. For feedback systems containing a non-linearity, where an open-loop equivalent cannot be obtained, the feedback path introduces a delay of T, and this can cause problems of stability; various techniques have been devised to accommodate this problem, and these involve matching closed-loop gain and eigenvalues by introducing a digital compensator[84,85].

These methods have given excellent results in the solution of many problems, one of the most interesting being the case of the simulation of a space vehicle, with six degrees of freedom. The use of Tustin operators was found to be the only stable way in which a real-time simulation could be developed, and this offered an execution time saving of over 90% compared with a conventional Runge-Kutta method.

It was therefore decided to use the Tustin operators for the boiler model, in order not only to ensure fast program execution but also to enable a simple trial of these methods to be made. The results have been very satisfactory, and the use of such operators is strongly recommended for any further dynamic simulations which may be required.

9.2.3 Implementation of the Boiler Model and the Results.

Before the boiler model was implemented on-line, tests were carried out to determine the smallest time increment which could be used, and some of these results are shown in Fig. 9.2, for time steps of 0.1, 1.0 and 5.0 seconds. It can be seen that the difference between the 0.1 and 1.0 second step lengths is minimal, and since the whole real-time system could accommodate the boiler program to be run every second, this step length was chosen. The parameters used in this test were those later adopted for the on-line simulation, and these are:

T_B, boiler storage time constant	= 240 seconds
K_D, controller derivative gain	= 0
K_P, controller proportional gain	= 20.0
K_I, controller integral gain	= 0.04
T_D, fuel feed delay	= 30 seconds
T_F, firing system lag	= 30 seconds
T_M, mill storage time constant	= 2.0 seconds

The analog hardware associated with the inclusion of the boiler model is shown in Fig. 9.3. In the actual generator unit, an analog multiplier is used to give the steam flow from the valve position and the pressure signals. A potentiometer is used to provide a manual pressure signal when the boiler simulation is not in use, and this also serves to give the reference pressure to the digital model. The basic software performs the

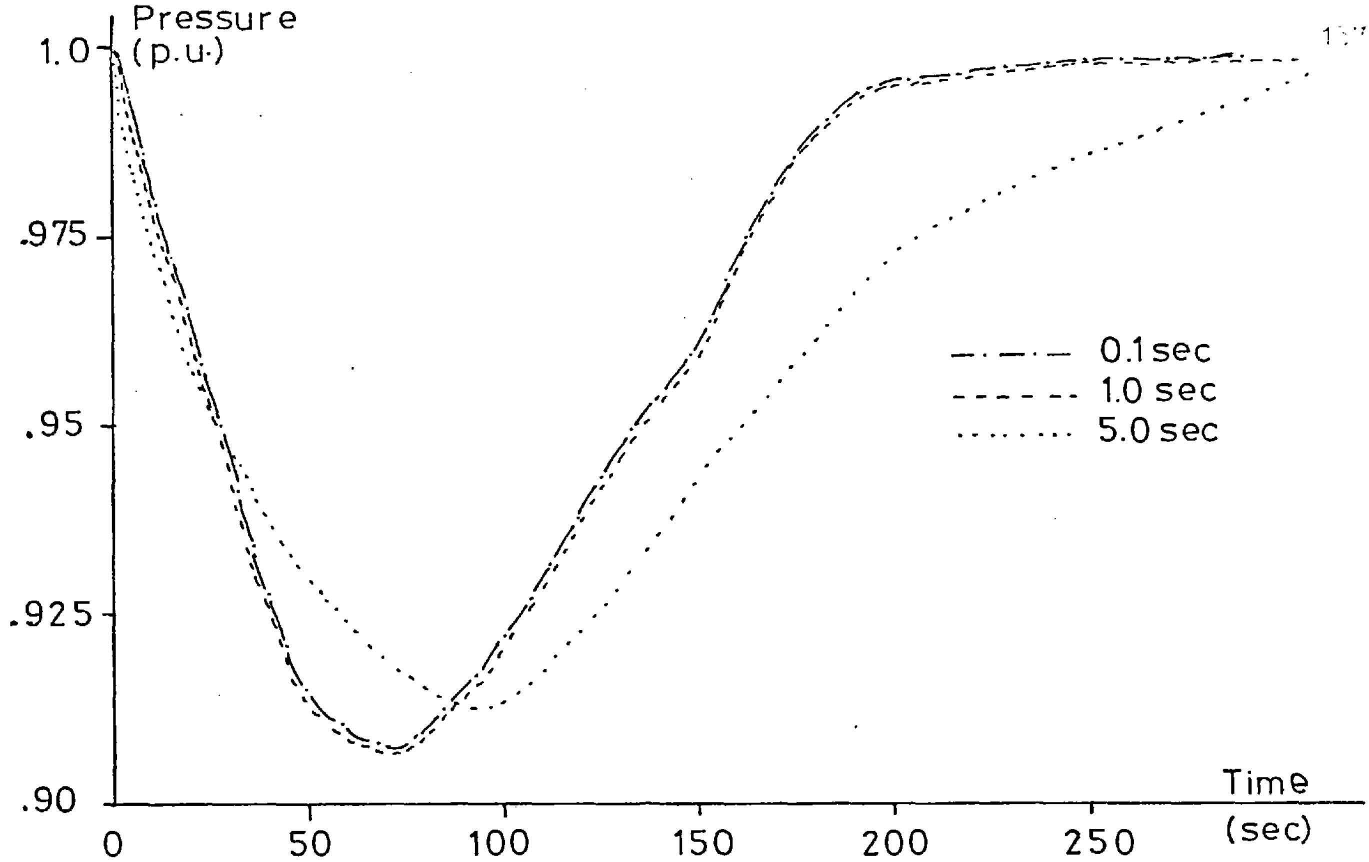

Fig.9.2 Response to 50% Increase in Valve Opening for Different Step Lengths.

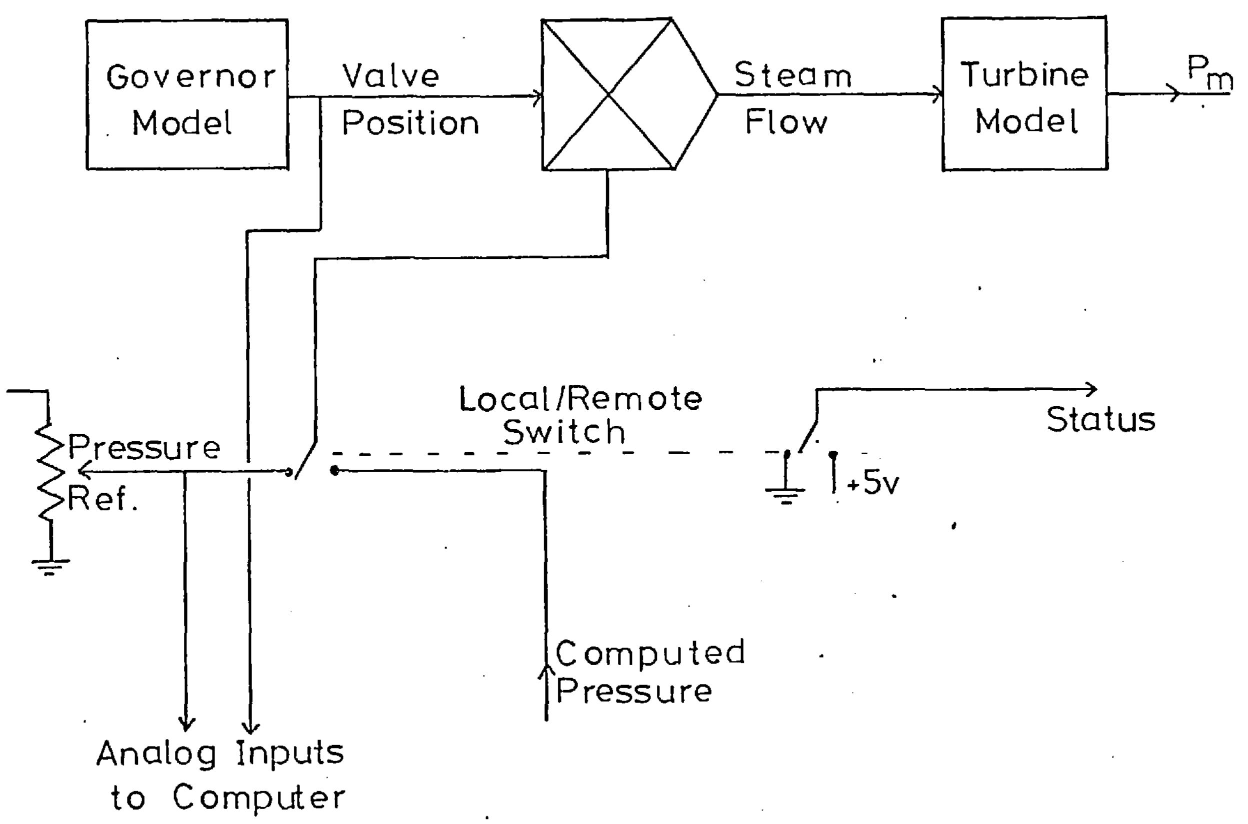

Fig. 9. 3 Hardware for the Inclusion of the Boiler Model.

transfer of the analog and status signals between the model and a COMMON storage area in the computer core. The program examines the status signal, to determine whether the pressure signal is provided locally or by the computer; in the former case the computer pressure signal is updated to be equal to the potentiometer setting. If the boiler model is in operation, at each iteration the valve position and the reference pressure are read and the new boiler pressure calculated and output to the generator unit.

Test results for the model are given in Fig 9.4 for three tests, and the practical results are compared with those produced by an off-line program. The conditions for the three tests were:

	Initial		Final	
	Valve Pos.	Ref. Pressure	Valve Pos.	Ref. Pressure
Test 1	0.5 p.u.	1.0 p.u.	1.0 p.u.	1.0 p.u.
Test 2	1.0 p.u.	1.0 p.u.	0.5 p.u.	1.0 p.u.
Test 3	1.0 p.u.	0.95 p.u.	1.0 p.u.	1.0 p.u.

These correspond to the valve opening, the valve closing and to a change in reference pressure. As can be seen, the results obtained using the simulator bear a close resemblence to those generated by the off-line program, the accuracy being better than 3%. This is due to the A/D and D/A converter offset errors, and subsequent work has reduced these to less than 0.5%.

The aim of developing a boiler model suitable for on-line use in conjunction with the analog hardware has been achieved, and the use of integrating operators has been shown to be convenient in real-time simulation work.

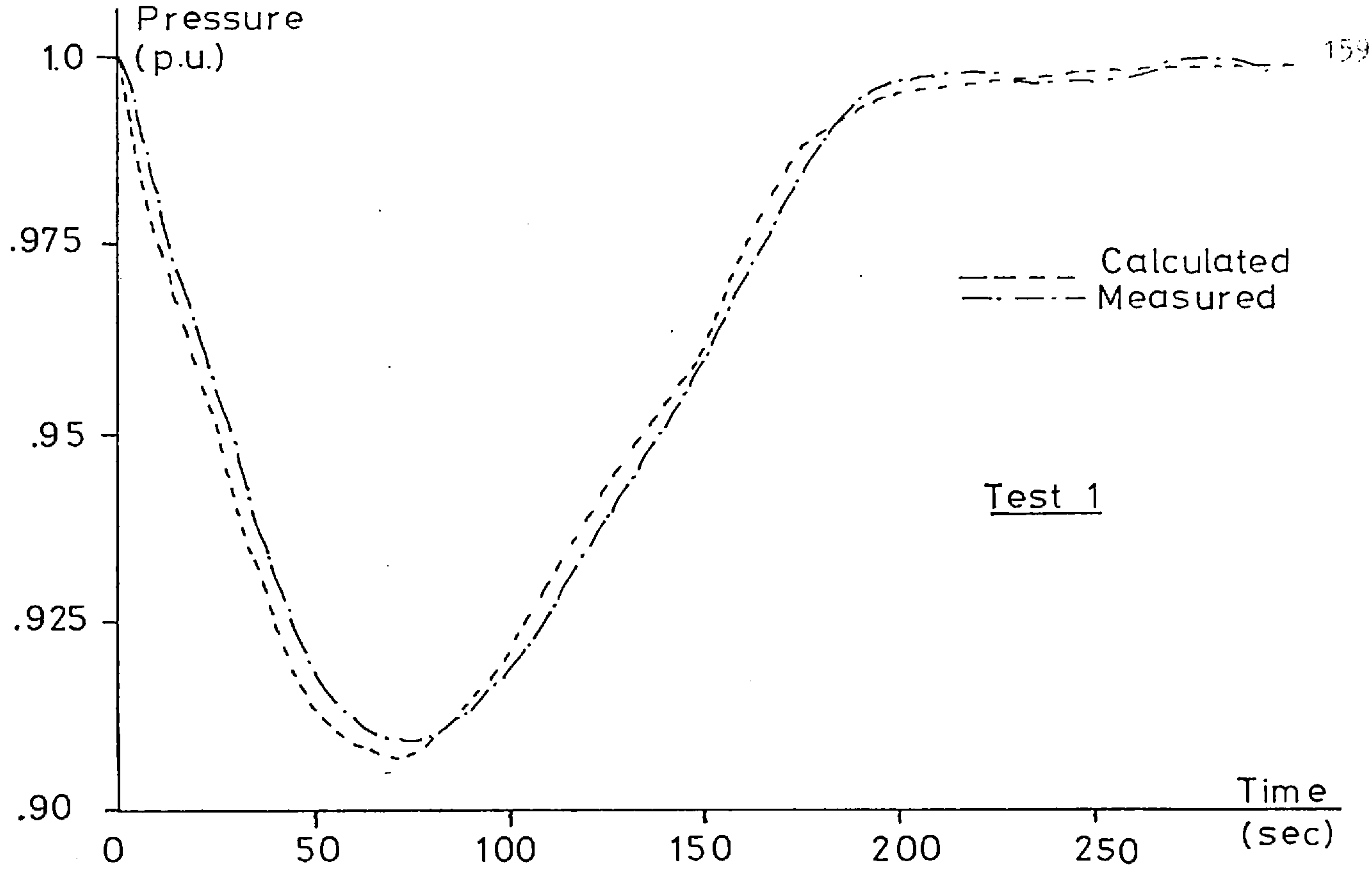

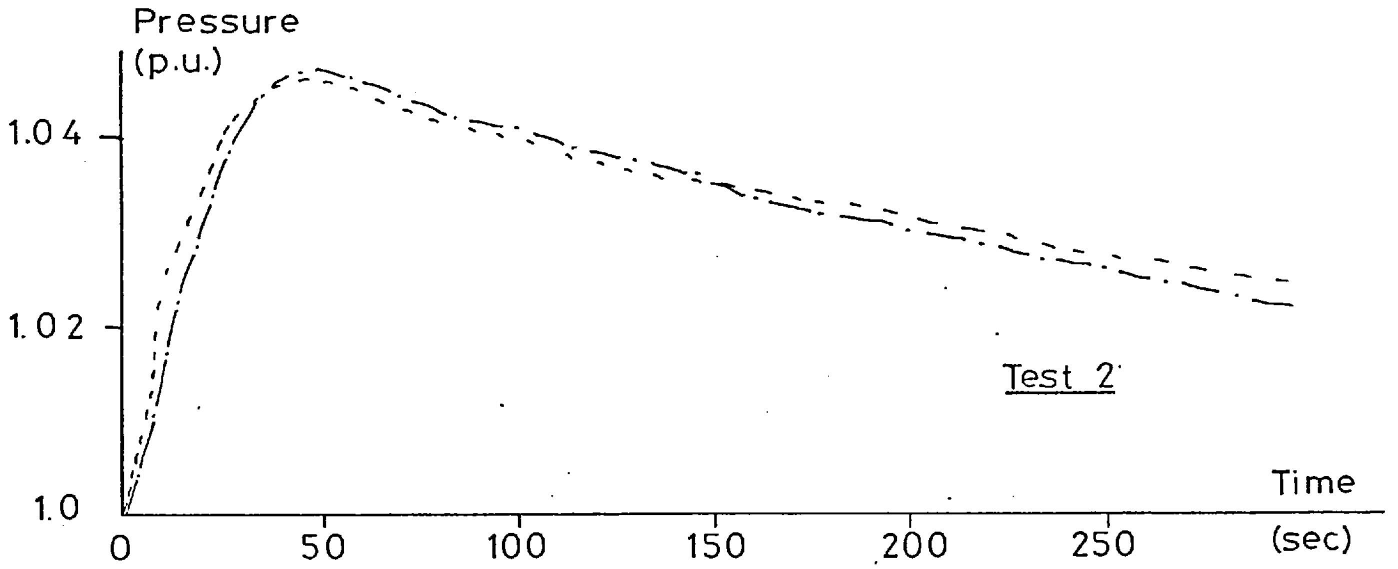

Fig.9.4 Boiler Model Test Results.

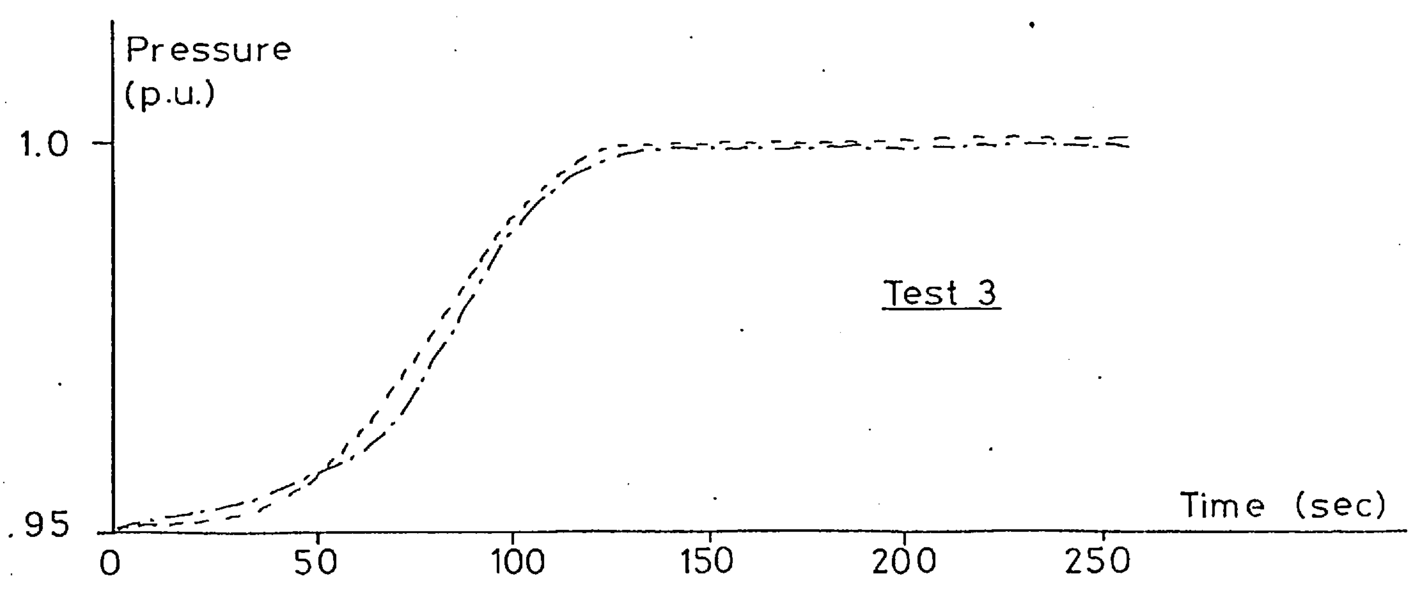

9.3 The Test Load-Frequency Control Scheme.

9.3.1 Introduction.

The basic principles of the various methods of load-frequency control have been understood for the past 40 years, and most modern schemes differ only slightly from these original concepts. Despite considerable activity during the late 1960's, the use of techniques from modern control theory, in the areas of stochastic and optimal control, has found no favour in practical implementations and the design methods employed are largely heuristic. To evaluate the PDP-15 in the role of a digital computer controlling a model power system, it was decided to implement a simple $\Delta p + K\Delta f$[86] controller.

Such a controller consists of five stages:

(1) Measurement of power flows and frequency, and up-dating of the agreed interchange schedule.

(2) Calculation of the area control error (ACE), according to the relationship

$$ACE = \sum_{i=1}^{NTIE} (TLS_i - TLA_i) + K(F_s - F_a) + IPB$$

where NTIE is the number of tie-lines connected

TLS_i is the scheduled flow in line i

TLA_i is the actual flow in line i

F_s is the scheduled frequency

F_a is the actual frequency

IPB is the inadvertant payback, determined by accumulated flow error or time error.

(3) Determination of the total demand, PDT, knowing the actual generation and the area control error

$$PDT = \sum_{i=1}^{NUNIT} PGEN_i + ACE$$

where NUNIT is the number of units on control

$PGEN_i$ is the power generated by the i^{th} unit.

(4) Knowing the total generation requirement, this must be divided between the units available, according either to a previously calculated generation schedule or as calculated by an on-line economic dispatch algorithm. At this stage security considerations must be taken into account.

(5) Control of the individual units, once the target power is known. Control signals must be sent to each unit to indicate whether generation is to be increased, decreased or held constant, and this change should be accomplished in a reasonable time and without introducing oscillations into the system. Since a zero steady-state error is required, a closed loop system must be used, and there are two main methods:

(a) Pulse and Wait Method.

If it has been decided that a unit should increase its generation from 100 MW to 150 MW, the controller will issue a Raise pulse to produce what it believes to be a 50 MW increase. After the prime-mover transients have died away, the controller may look at the output and find it to be only 140 MW. It will then issue a Raise pulse for a further 10 MW, and wait.

Since some of the time constants might be of the order of tens of seconds, this gives a very slow control over the system, but it does mean that no knowledge of the plant dynamics is required, beyond the settling time.

(b) Transient Response Monitoring Method.

If the form of the transient response is known, it is possible to monitor the response of the unit following the issuing of a control pulse, and if it deviates from the anticipated response by more than a certain amount, then corrective pulses can be issued.

9.3.2 The Unit Control Loop.

On a generating unit fitted with a conventional mechanical/hydraulic governor, changes in the reference setting are accomplished by driving the speeder gear motor in the correct direction, and the change which is accomplished is proportional to the time for which the motor is switched on. Thus the speeder gear, to a first order, may be regarded as an integrator of control pulses. However, many factors combine to make this only an approximation to the true behaviour. First, the actual governor characteristics are non-linear, and secondly the motor transmission system will have a certain amount of slack and slip, the motor will take time to accelerate and will continue to coast after the removal of its power supply. All these factors combine to give an uncertainty of perhaps $\frac{1}{2}$ to 2 in the integrator gain figure which is to be used, and hence in the calculation of the duration of the Raise/Lower pulses which are to be sent.

In the light of this gain uncertainty the need for a closed loop control system can be seen. The simplest scheme is shown in Fig. 9.5, where the computer acts as part of a sampled data system, computing a new value of the Raise/Lower pulse every 4 seconds. The gain is assumed to be known, and the turbine dynamics are represented by a simple lag with a 10 second time constant. The behaviour of the closed loop system is shown in Fig. 9.6(a), while the open loop response is given in Fig. 9.6(b). It can be seen that although the closed loop response is more rapid, it has a large overshoot, is poorly damped and gives rise to excessive speeder motor action.

One of the main criteria for a satisfactory control scheme is that it should not cause oscillatory effects in the system and this is not met by the simple closed loop system. Additionally, it is advantageous to reduce control activity to a minimum, as this not only reduces wear on the mechanical components but also reduces disturbances to the system. A better closed loop control scheme can be produced by incorporating a digital compensator in the unit control algorithm, but such a compensator demands a knowledge of the prime-mover transfer function. There are many possible compensation

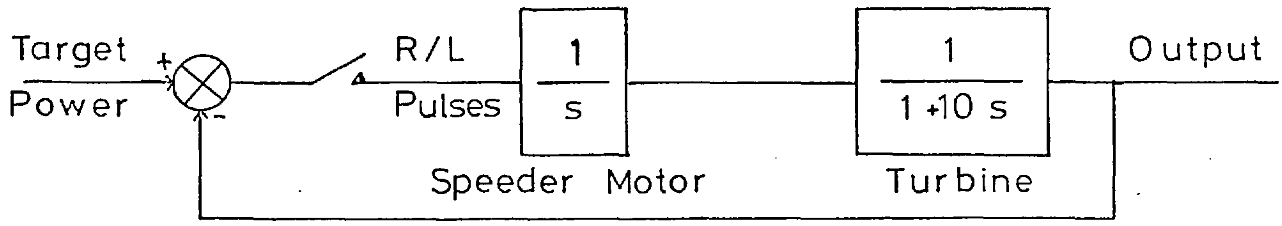

Fig. 9.5 Closed Loop Control System.

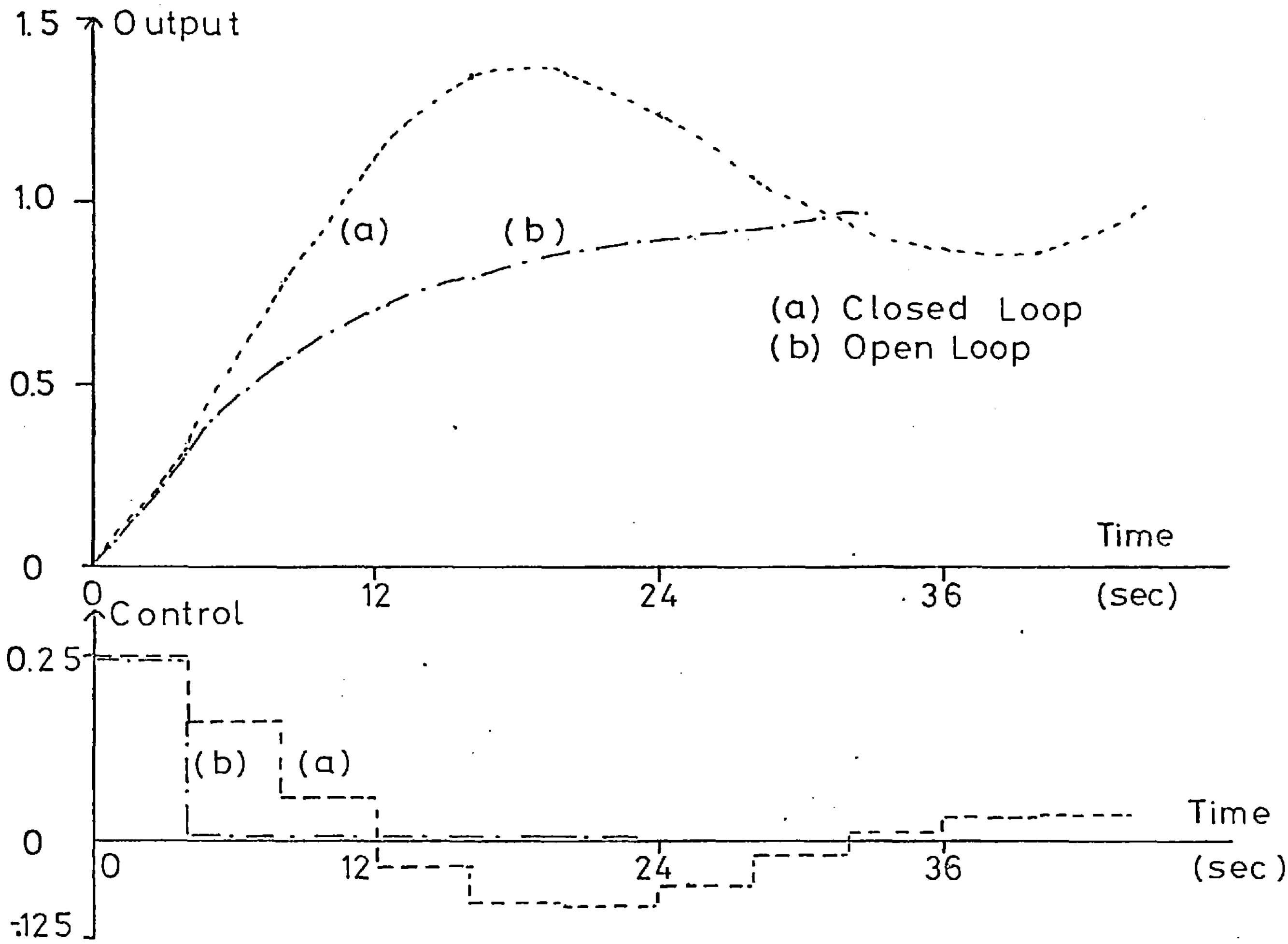

Fig. 9. 6 System Response.

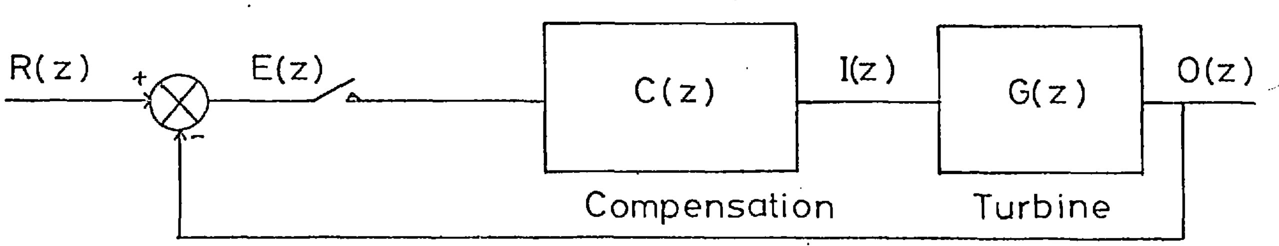

Fig. 9.7 Compensated System.

techniques which could be applied, but the one adopted here aims not to improve on the open loop response of the unit but to correct for the uncertain gain of the system. That is, if an increase in generation is required, a Raise pulse will be issued on the basis of an assumed system gain, and the power output of the turbine at the next sampling instant will be predicted on the basis of this gain and of the system open loop response. Only if the actual response differs by more than a certain amount from the predicted response will additional control pulses be issued. Thus when the gain is exactly known only the initial control pulse will be issued. Knowing this, it is possible to derive an expression for the desired form of the compensation.

Fig. 9.7 shows the control loop in terms of a sampled data system[87,88] with compensation C(z) and a unit transfer function G(z). For a step input, $R(z) = \frac{z}{z-1}$, the control pulse sequence should be of the form 1,0,0,0,0,0...., thus I(z) = 1. From the figure we can write

$$O(z) = R(z).\ \frac{C(z)\ G(z)}{1 + C(z).G(z)}$$

and

$$C(z) = \frac{I(z)}{E(z)} = \frac{I(z)}{R(z)-O(z)}$$

$$C(z) = \frac{I(z)}{R(z)\ \ 1 - \frac{C(z)\ G(z)}{1 + C(z)\ G(z)}}$$

$$= I(z)\ \ \frac{1 + C(z)\ G(z)}{R(z)}$$

For $R(z) = \frac{z}{z-1}$, $I(z) = 1$

so

$$C(z) = \frac{1 + C(z)\ G(z)\ .\ (z-1)}{z}$$

Thus

$$C(z) = \frac{z-1}{z- (z-1).G(z)}$$

Hence knowing the pulse transfer function for the units, it is possible to derive the compensation block C(z). For the generator units in the model, it was assumed that the prime-mover transfer function was of the form $\frac{(1 + sT_1)}{(1 + sT_2)(1 + sT_3)}$, while the speeder gear motor is represented as $\frac{K}{s}$,

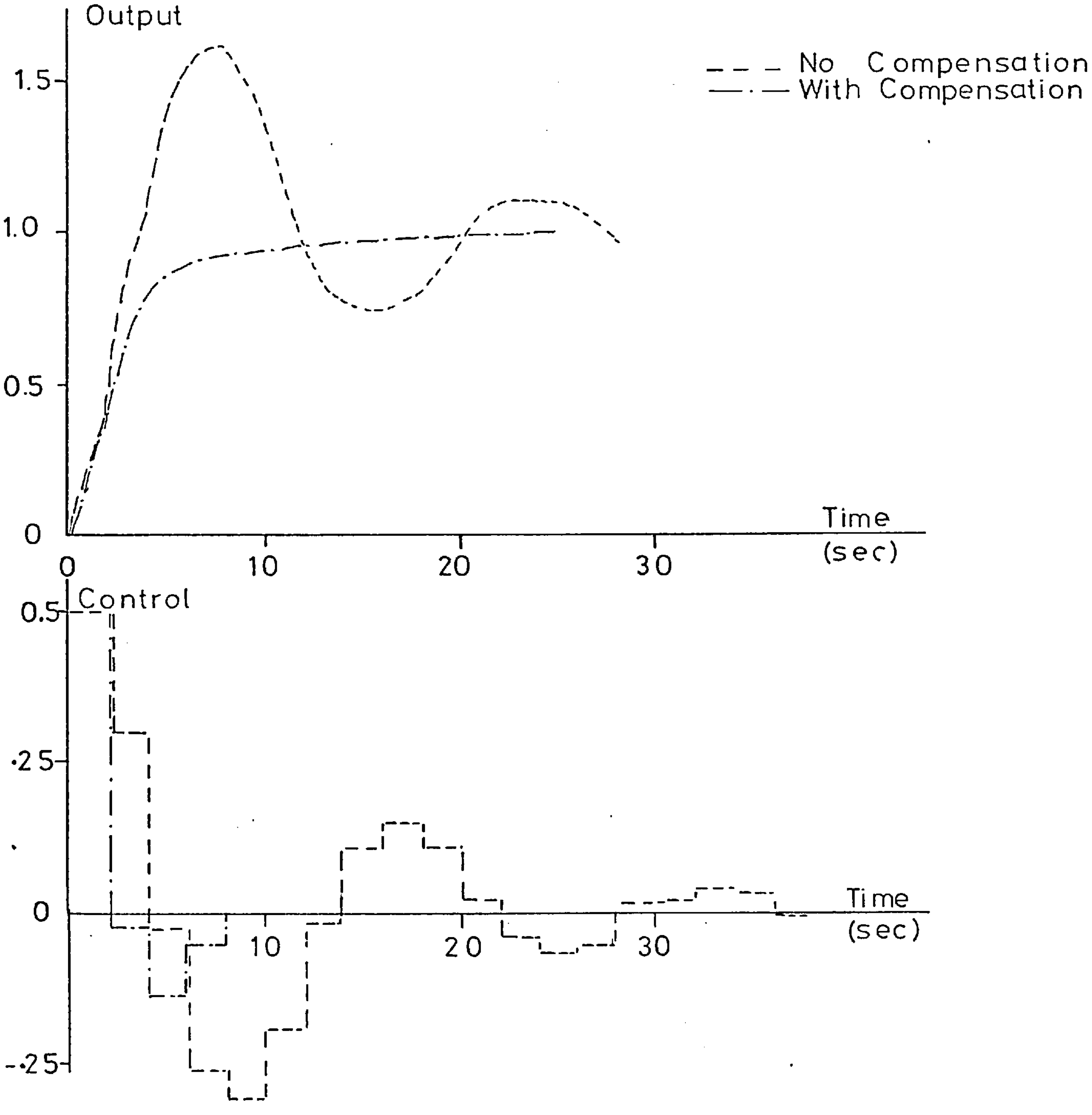

Fig. 9.8(a) Compensator Performance. K=2.

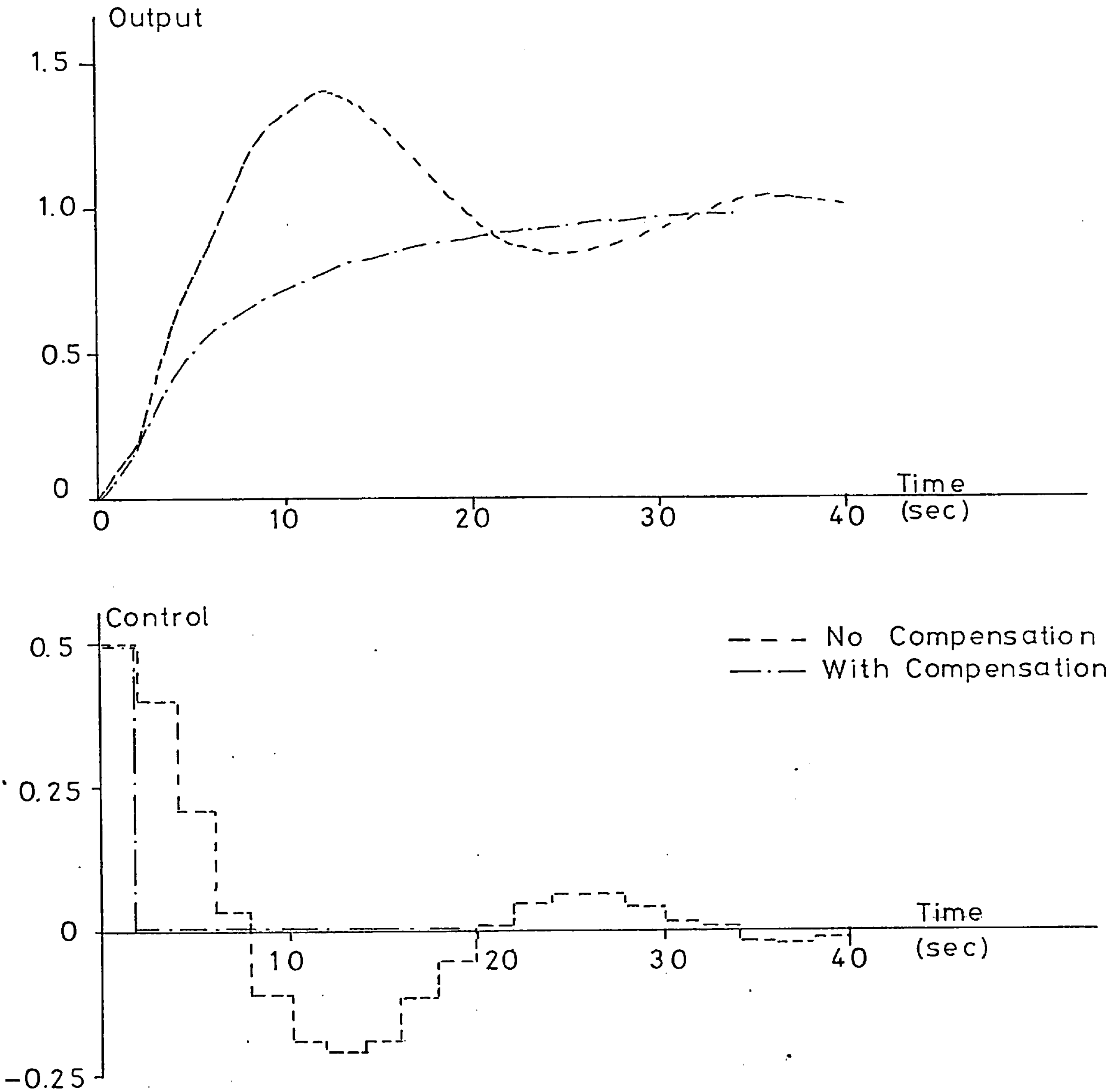

Fig. 9.8(b) Compensator Performance. K=1.

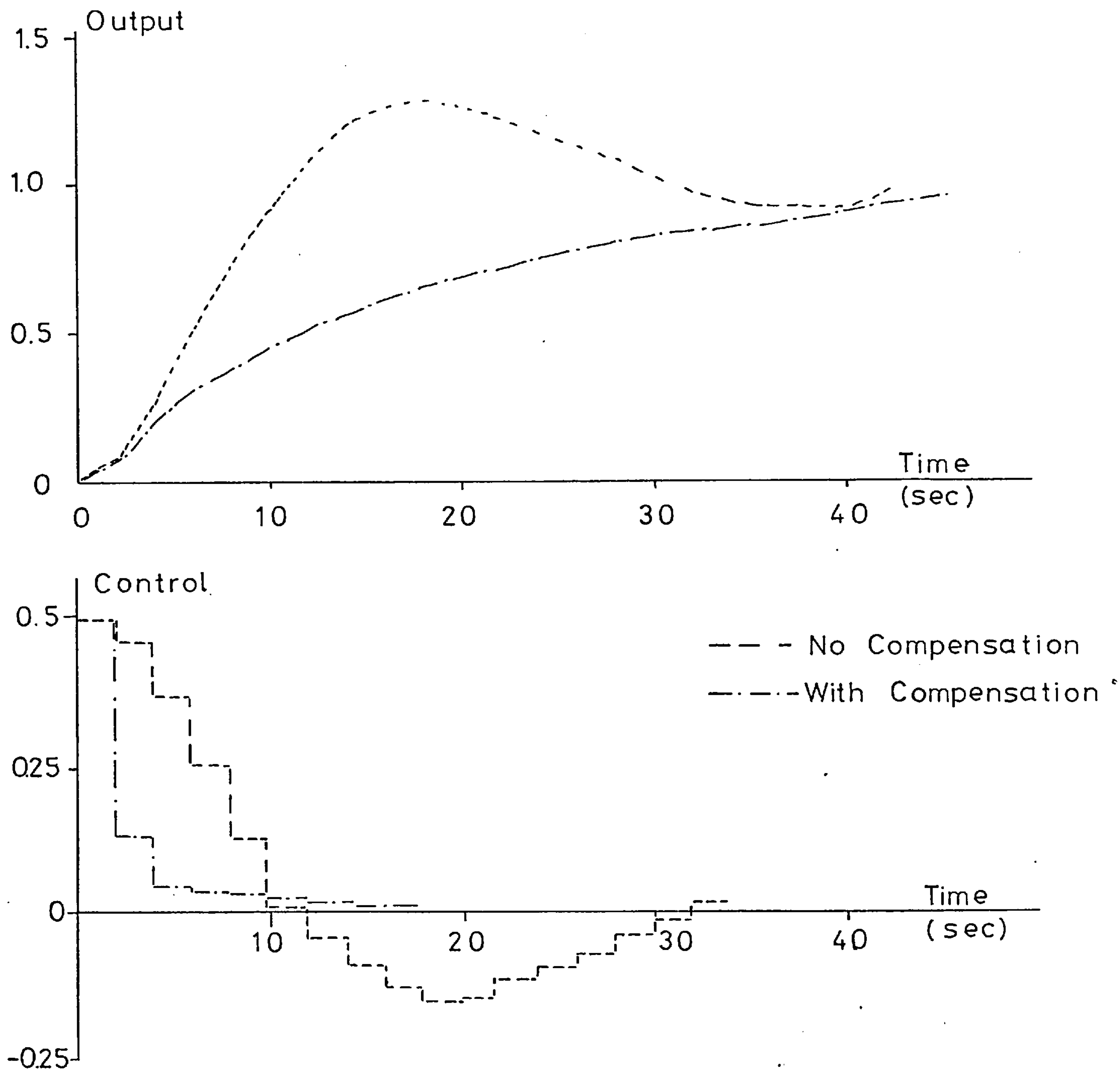

Fig. 9.8(c) Compensator Performance. K = 0.5.

where K is a variable gain. A special hardware unit was constructed to act as a slow integrator, and a dead-band was included so that if the magnitude of the control pulse is less than 5% of the maximum Raise/Lower level, then the integrator is put into its "Hold" mode. The nominal gain of the integrator is such that the full Raise level will drive the valve from fully open to fully closed in 40 seconds. The gain can be changed to see how the control scheme performs under different conditions.

Off-line computations were performed to examine the predicted behaviour of the compensation with different gains, and the results are given in Figs. 9.8(a)-(c). The sampling interval was two seconds, and the prime-mover time constants were T_1=3.0 sec, T_2=1.0 sec and T_3=10.0 sec. The results show the response of both the compensated and the un-compensated systems, with K = 1, $\frac{1}{2}$, and 2, where the controller believes K to be 1. The great reduction in control activity can be seen, and the shape of the response of the compensated system can be seen to be similar under all conditions.

9.3.3 The Control Scheme.

The control scheme which has been implemented is a simple frequency-bias tie-line control scheme, together with the unit control method described above. The flow chart is shown in Fig. 9.9. The problems of data input and control signal output are handled by the basic software, so the actual program is a brief Fortran one, with all its data transfers accomplished through Common storage areas. The test system is shown in Fig. 9.10, and consists of an infinite bus and two generator units, connected by short transmission lines. The section which is to be controlled depends on the nature of the test, for in a fixed frequency experiment the two generator units are controlled in order to regulate the flow into the infinite bus, but in a variable frequency test only one machine is controlled, with the other machine acting as the rest of the system.

The parameters of the mechanical systems of both machines are:

Inertia Constant, H, 4 p.u.

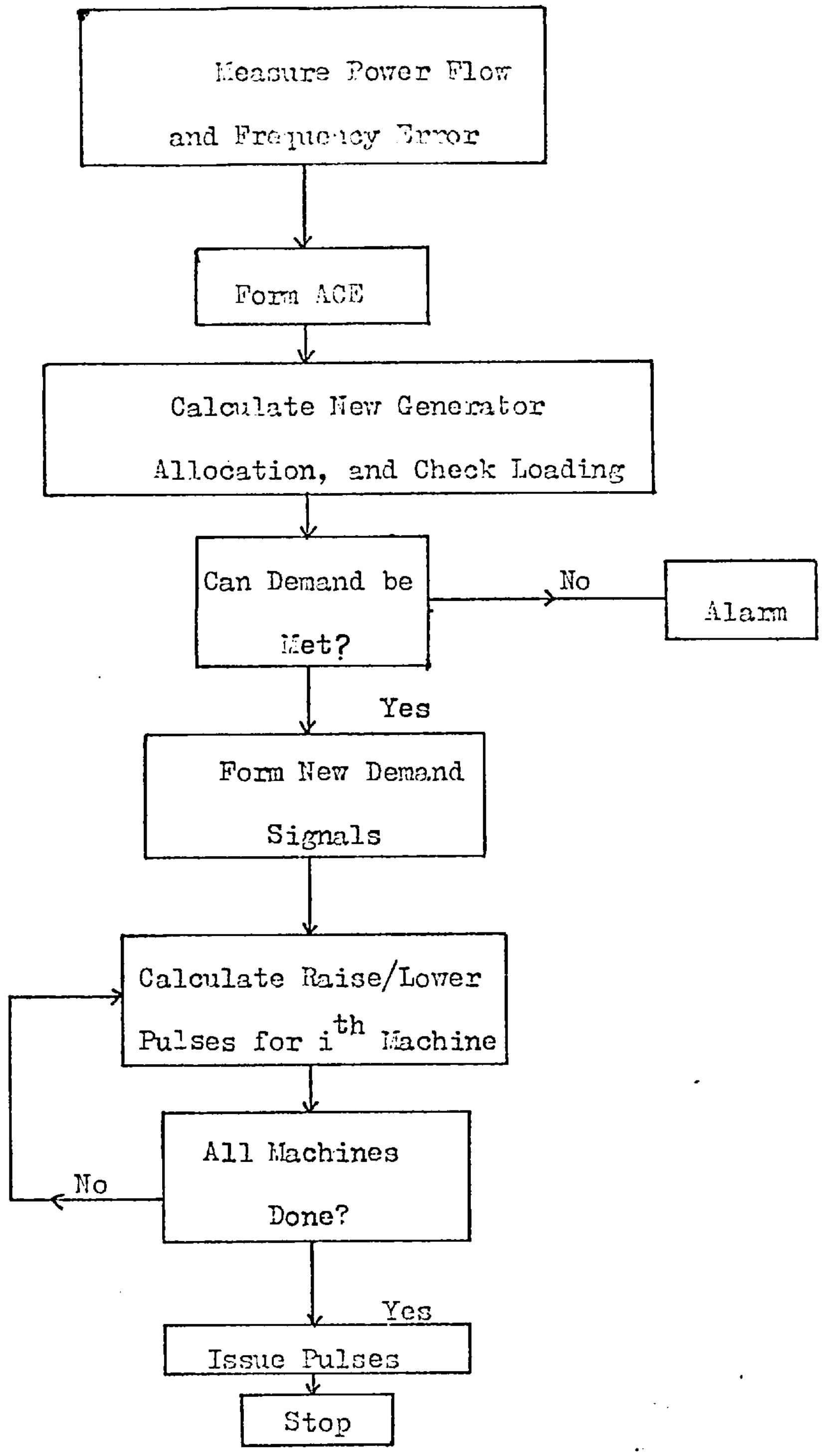

Fig. 9.9 Control Algorithm for Simple LFC Scheme.

H.P. Cylinder time constant	7.0 sec.
I.P. Cylinder time constant	0.5 sec.
H.P. Cylinder power fraction	30%
Governor Droop	4%
Governor time constant	0.2 sec.

A total of four tests were performed, and these are detailed below:

<u>Test 1</u>. System connected to the infinite bus, with a change in reference flow from 0.6 to 0.8 p.u. Fig. 9.11(a)

<u>Test 2</u>. System connected to the infinite bus, with a change in internal load from 1.6 to 1.4 p.u. Fig. 9.11(b)

<u>Test 3</u>. Isolated system with a load change in the uncontrolled half of the system Fig. 9.11(c)

<u>Test 4</u>. Isolated system with a load change in the controlled half of the system Fig. 9.11(d)

In tests 3 and 4 the second generator unit was under manual control, which acted to restore the tie-line flow to its original value.

Test 1 shows that after a step change in reference flow, the controls to increase the generation start to act after a short delay, this being the next time the control program was executed. The tie-line flow is increased steadily to its new value, and this is reached with no overshoot. Since the gain of the speeder motor system was known, only the initial control pulses had to be issued.

Test 2 shows how, following a step change in load, the tie-line flow increases, and after 2 seconds thecontrol starts to bring the flow back to its original value. On this occasion, there is a small overshoot, but this is quickly counteracted. This was probably due to external variations rather than a fault with the control logic.

In Test 3, the controlled machine is No. 1, and no control pulses are sent to it, since the constant K is correctly chosen. The change in power output of this machine is due entirely to governor action, and the restoration of

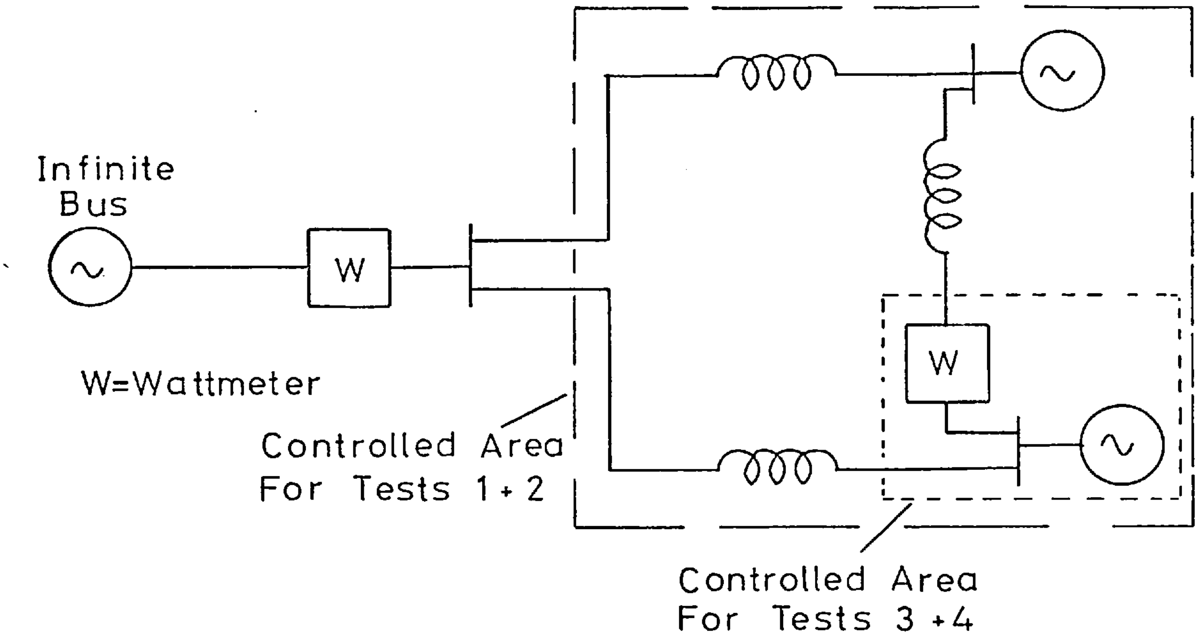

Fig. 9.10 Test System.

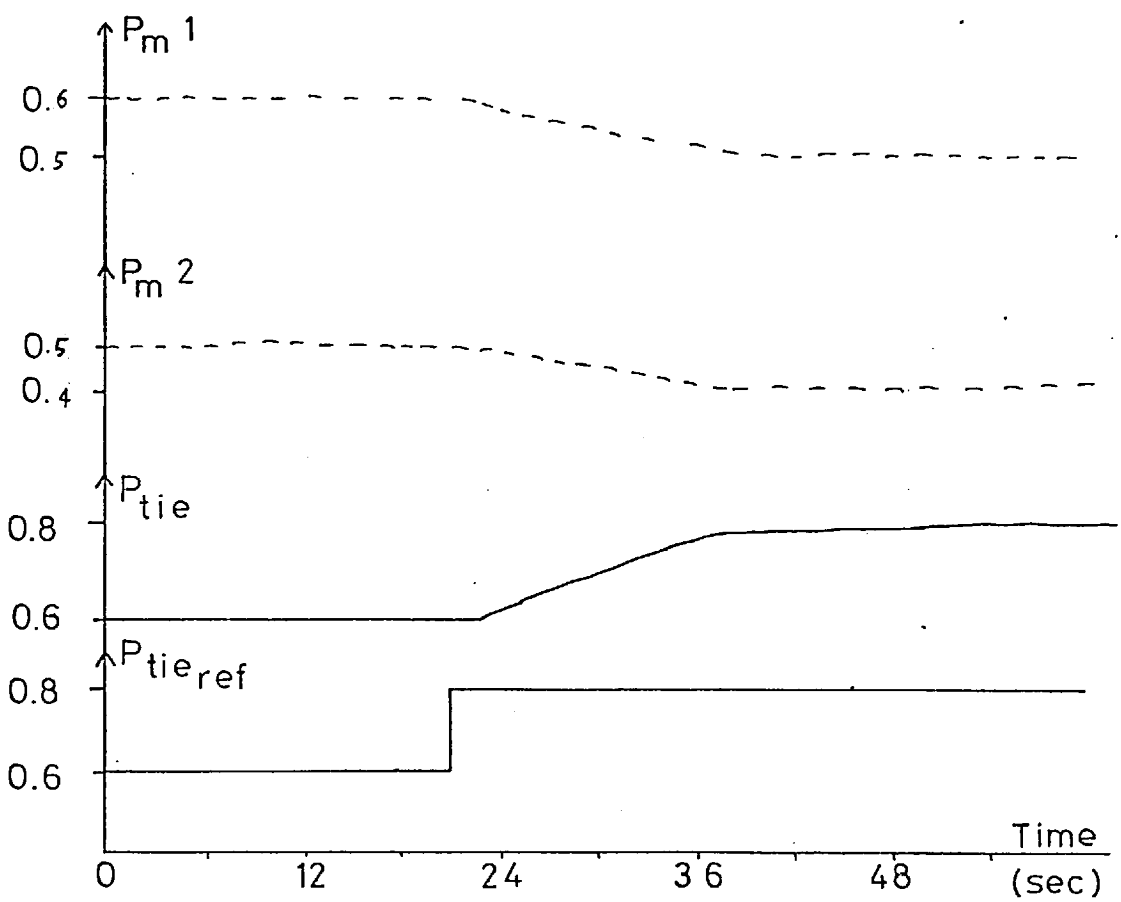

Fig. 9.11(a) LFC Response. Test 1.

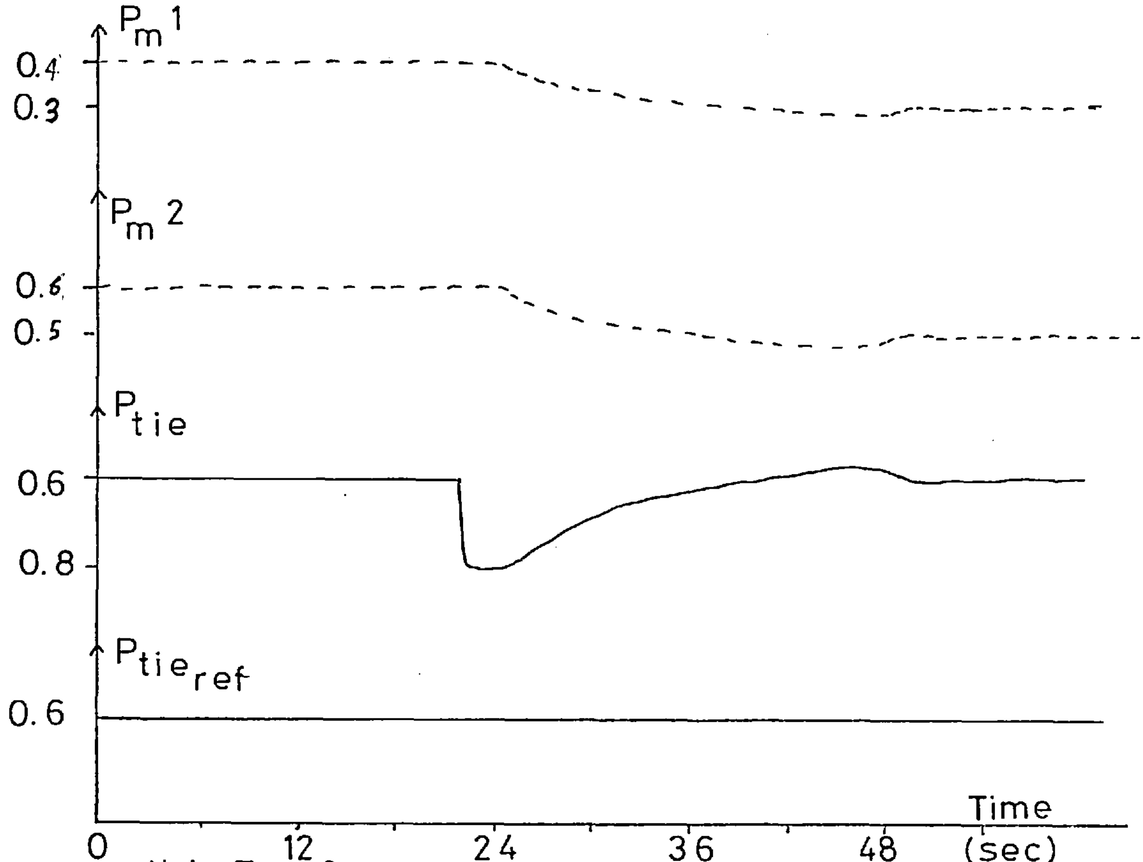

(b) Test 2

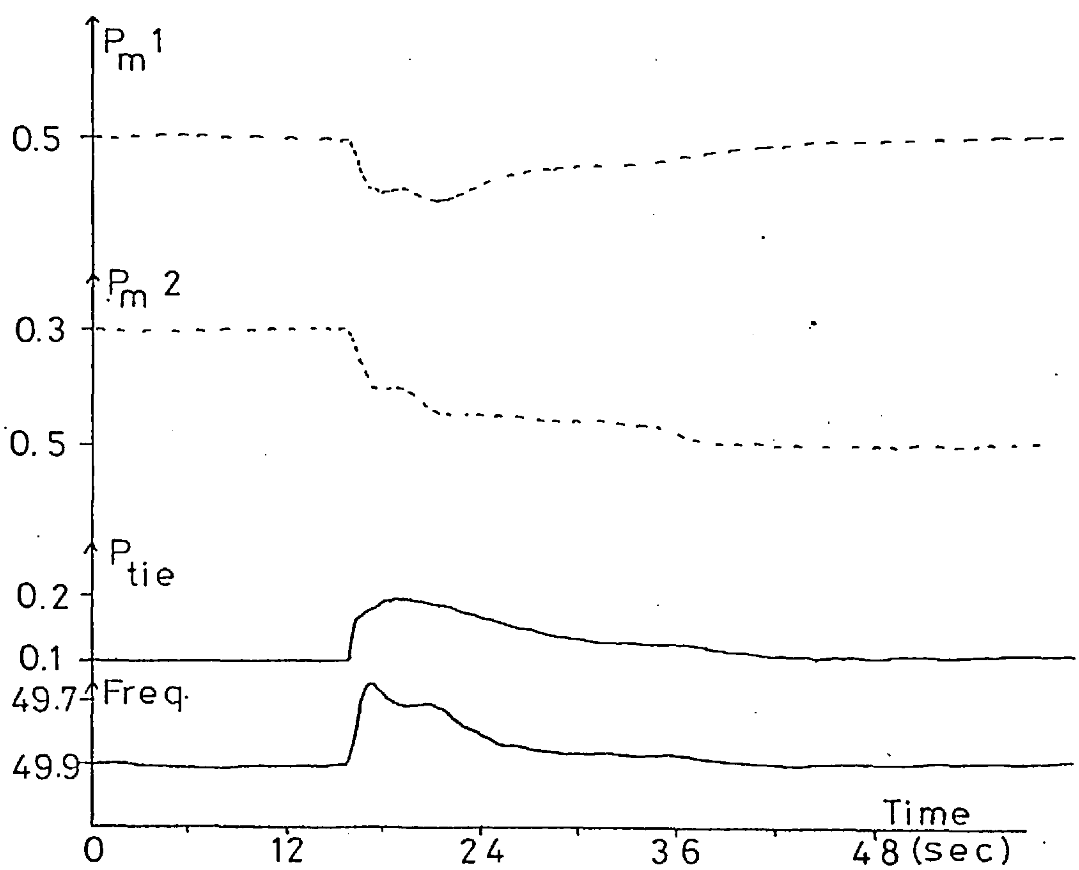

(c) Test 3

Fig.9.11 LFC Response.

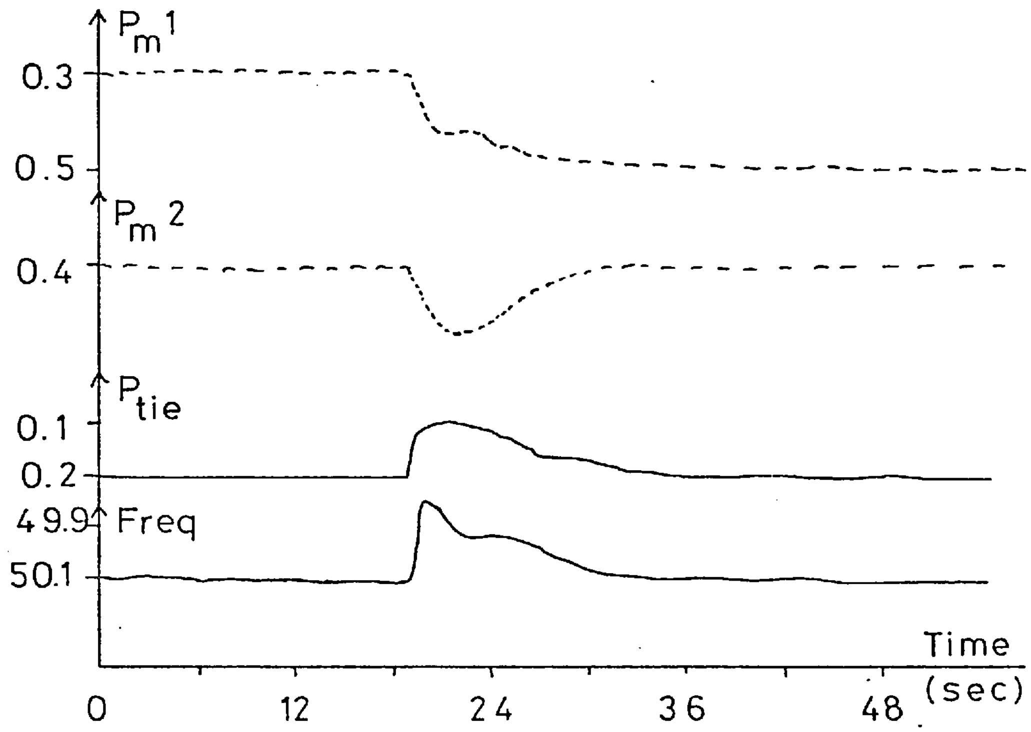

Fig. 9.11(d) LFC Response. Test 4.

the correct tie-line flow and hence the frequency is accomplished by machine 2.

In Test 4, however, the change in load occurs in the controlled area, and hence control action is taken, resulting in the restoration of the correct tie-line flow. No manual action was taken with the uncontrolled machine, No. 2. The similarity between the results of Tests 3 and 4 is because the manual control in Test 3 acted in a very similar way to the computer control of Test 4.

The behaviour of this simple load-frequency control scheme is as expected, and demonstrates that the combination of the computer and the power system model is suitable for further work in this field. In particular, the behaviour of control algorithms in a system with noisy measurements is of interest, and some experiments along these lines were attempted. However, the available noise generator was unable to produce satisfactory noise at a sufficiently low frequency. The noise was centered about 1.5 to 2.0 Hz, and this was effectively filtered by the digital filter associated with the analog input program. However, there is scope for further work, provided that suitable noise sources are used.

9.4 The Measurement of Power System Parameters.

The increasing desire in recent years to understand and to be able to predict the behaviour of power systems has led to a need for accurate measurements of many parameters. Such measurements are frequently difficult or impossible to perform using conventional methods of system testing, and recourse must be made to more sophisticated techniques. This is particularly true in the case of the measurement of power system inertia. This is a most important parameter, as it determines the rate of fall of frequency following a loss of generation. This parameter has in the past been measured by arranging the system into two large areas, connected by a single tie-line which carries an appreciable power flow. By tripping this line, one area will suffer a loss of infeed, while the other will have a surplus of generation and frequency changes will occur.

This method has a number of disadvantages, which may be summarized as:

(1) In order to produce a frequency deviation which can be accurately measured, the power transfer must be of a reasonable magnitude, and it is possible that the tripping of the line may cause stability problems.

(2) It has been found that the long term plant response is different in planned tests from that which occurs following unforseen incidents. This can be attributed to increased operator awareness.

(3) Considerable planning must be undertaken before such tests can be performed.

In recent years much interest has been focused on the identification of control system parameters using random test signals superimposed on the ordinary input[89-91], and then cross-correlating the output with the input. This then gives the system impulse response, from which may be derived its transfer function. It was decided to investigate the use of this method for the determination of system inertia. The principle is shown in Fig. 9.12. A random power infeed is applied to the system, and the frequency of the system is cross-correlated with this random input. Such a variable infeed can be achieved if the system under test is linked to another system by a d.c. line. Small changes in power flow may be used, provided that the experiment is continued for a sufficiently long time.

9.4.1 Theoretical Background.

Consider the system of Fig. 9.13, which shows a linear system whose impulse response is $h(t)$. Its output $y_1(t)$ is contaminated with noise $n(t)$, to give a total output $y(t)$. The cross-correlation function ϕ_{yx} may be written as

$$\phi_{yx}(\tau) = \frac{1}{T}\int_0^T y(t)\, x(t-\tau)\, dt$$

now

$$y(t) = y_1(t) + n(t)$$

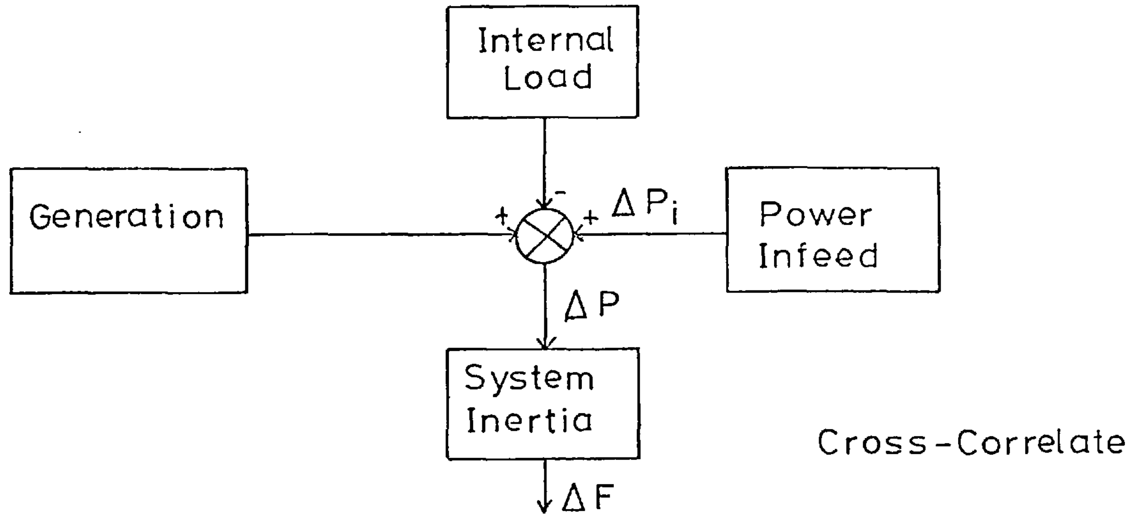

Fig. 9.12 Principle of the Correlation Method.

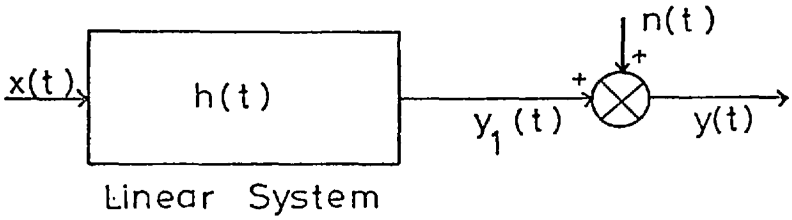

Fig. 9.13 System with Noisy Output.

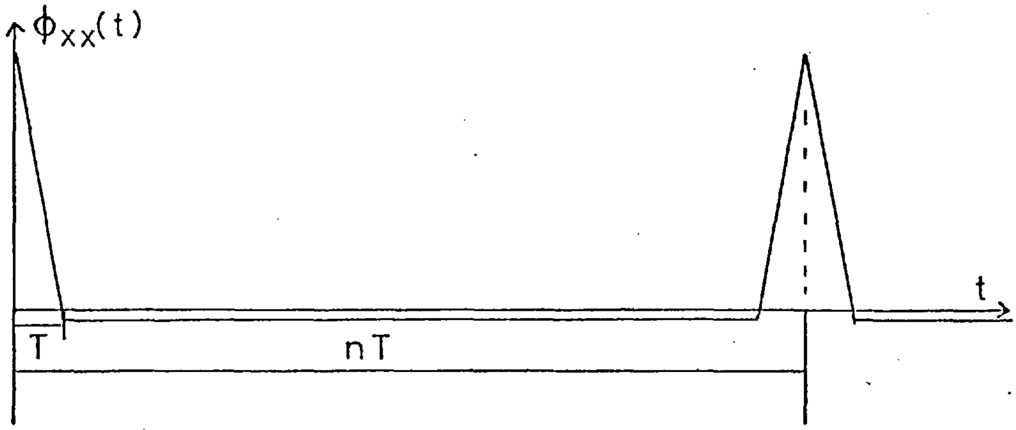

Fig. 9.14 Auto-Correlation of a PRBS.

The system output $y_1(t)$ may be written in terms of the convolution integral:

$$y_1(t) = \int_0^\infty h(z)\, x(t-z)\, dz$$

$$\Phi_{yx}(\tau) = \frac{1}{T}\int_0^T x(t-\tau)\, dt \int_0^\infty h(z)\, x(t-z)\, dz + \frac{1}{T}\int_0^T n(t)\, x(t-\tau)\, dt$$

$$\Phi_{yx}(\tau) = \frac{1}{T}\int_0^\infty h(z)\, dz \int_0^T x(t-\tau)\, x(t-z)\, dt + \frac{1}{T}\int_0^T n(t)\, x(t-\tau)\, dt$$

write

$$\Phi_{xx}(\tau - z) = \frac{1}{T}\int_0^T x(t-\tau)\, x(t-z)\, dt$$

and

$$\Phi_{nx}(\tau) = \frac{1}{T}\int_0^T n(t)\, x(t-\tau)\, dt$$

$$\Phi_{yx}(\tau) = \int_0^\infty h(z)\, \Phi_{xx}(\tau - z)\, dz + \Phi_{nx}(\tau)$$

If the noise and the input are uncorrelated, then $\phi_{nx} = 0$, and

$$\Phi_{yx} = \int_0^\infty h(z)\ \ \Phi_{xx}(\tau - z)\, dz$$

For a random signal Φ_{xx} is the impulse response, and thus

$$\Phi_{yx}(t) = h(t)$$

For practical purposes, the use of a true random input is not convenient, and a pseudo-random binary sequence is frequently employed. Such a sequence has a value of either $\pm$ a, and transitions from one state to another may occur after each clock interval T. The sequence is of fixed length, n, and thus repeats itself every nT seconds. The auto-correlation function is shown in Fig. 9.14 and as $T \to 0$ and $n \to \infty$, then this trends towards the impulse function[92]. Such a sequence may be generated by using modulo-2 feedback around a shift register; for a register with N stages the maximal length sequence occupies $2^N - 1$ clock periods. The sequence generator which was employed in these tests is described in Appendix C.

Since the input test sequence repeats itself, the measured cross-correlation function will also repeat itself every nT seconds, and this means that the sequence length and the clock frequency must be adjusted so that the part of the response which is of interest occurs within this time nT. The fine-ness of the detail in the response is determined by the clock frequency, as the non-ideal auto-correlation of the test signal leads to a smearing of the results. However, a high clock frequency will, in general, only cause very small changes in the system output, which might be difficult to measure. Thus the choice of clock frequency and sequence length must be made with a prior knowledge of the form and duration of the response, and certain compromises must be made.

The longer the period of measurement the more accurate the results will be, and this period is limited only by the equipment used for the test. Analog correlators are prone to drift, whilst in the digital system used here, the limitation is imposed by the storage available.

The use of correlation methods enables system measurements to be made while the system is operating normally, and with a low level of test signal. This causes a minimum of disturbance to the system, and permits measurements to be made in the presence of noise.

9.4.2 Test Results.

The test system is shown in Fig. 9.15, and consists of a single generator unit connected to a small network with fixed loads, and with a switchable load. This latter load is rated at 2% of the base power, and its power factor is adjusted such that when the load is switched in, no change of network voltage occurs. This avoids the introduction of voltage effects, both of the other loads and also of those associated with the voltage regulator. Provision was also made for the contamination of the frequency signal with noise derived from a separate noise source.

In addition to the correlation measurements, step responses were also obtained, in order to demonstrate the ability of the correlation technique to recover signals from noise. The characteristics of the test signal were:

31 bit sequence

2 Hz clock frequency

2 samples/clock cycle

256 samples per test

This enables the first 15 seconds of the response to be examined, and the whole test lasts for four complete sequences. As has been previously explained, the results obtained from the cross-correlation give the system impulse response, and this was numerically integrated using the trapezoidal rule to obtain the step response.

Four different sets of results are given here, with the system operating under the same conditions, but with the frequency measurement signal contaminated with different levels of noise. These noise levels were

Test Number	Signal/Noise Ratio	Figure No.
1	No Noise	9.16(a)
2	20 dB	9.16(b)
3	10 dB	9.16(c)
4	-10 dB	9.16(d)

The results of the conventional step changes are given in Fig. 9.16(a)-(d), and the effect of the noise level can be clearly seen. In particular, in Test 4 the signal/noise ratio of -10 dB means that no information about the system response can be gathered. Fig 9.17 shows a comparison of the step responses of the system obtained using both the correlation method and the ordinary step response, in the "no noise" test. The results can be seen to be almost identical for the first 9 seconds of the response, while after that time the correlation results start to give an error, which can be ascribed to the short duration of the whole test.

Sections of typical test records are given in Fig. 9.18, which shows the

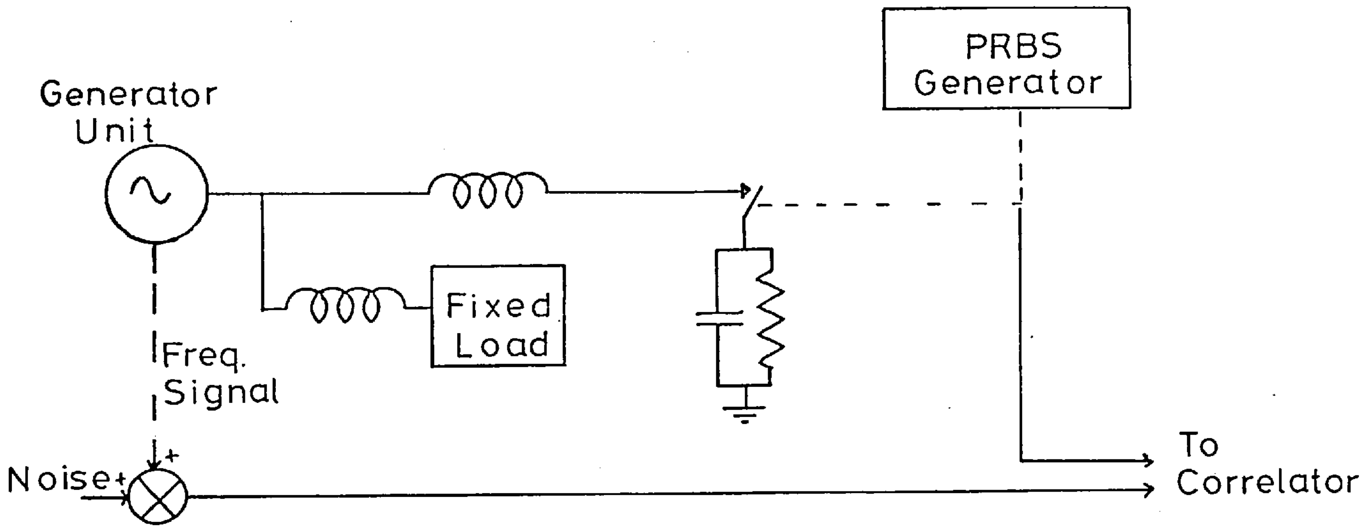

Fig. 9.15 Test System.

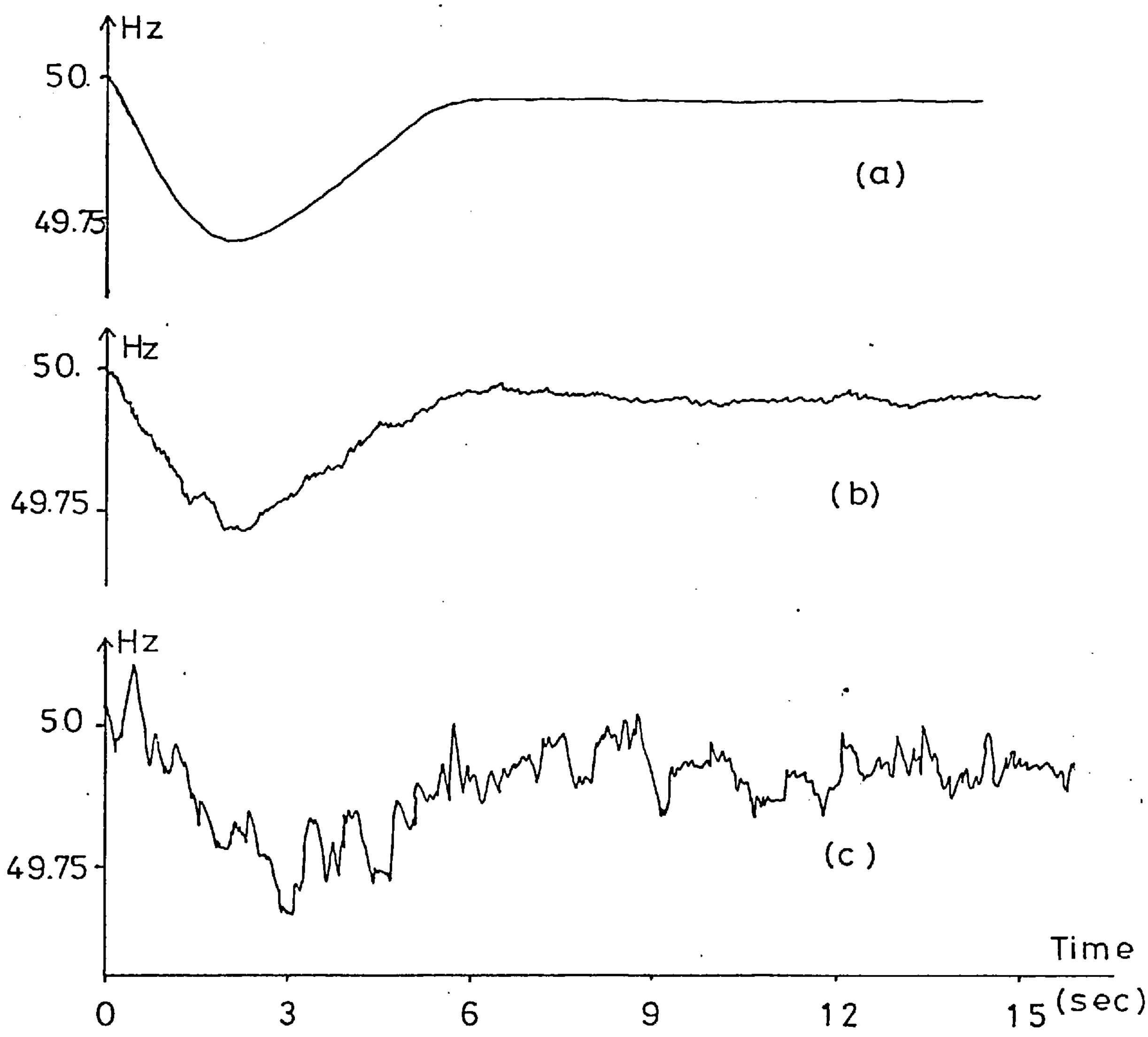

Fig. 9.16(a)-(c) Noisy Measurement of the Step Response.

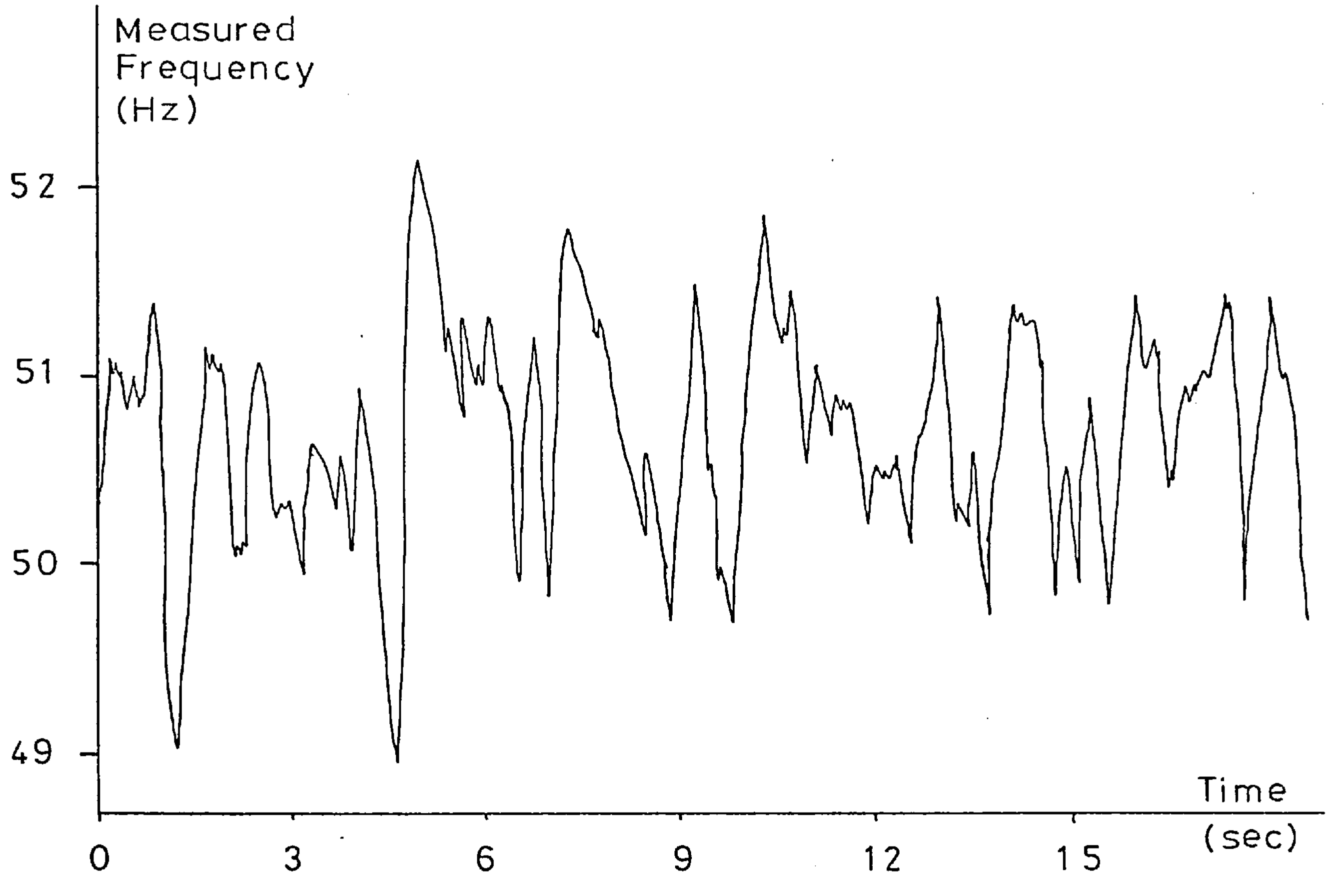

Fig. 9.16 (d) Noisy Measurement of the Step Response.

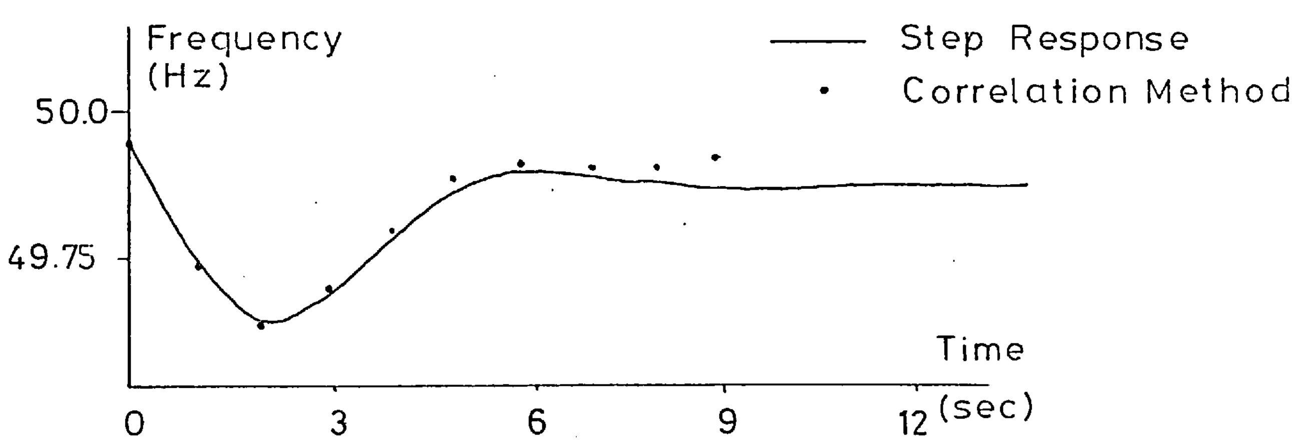

Fig. 9.17 Comparison of Step Response and Correlation Methods.

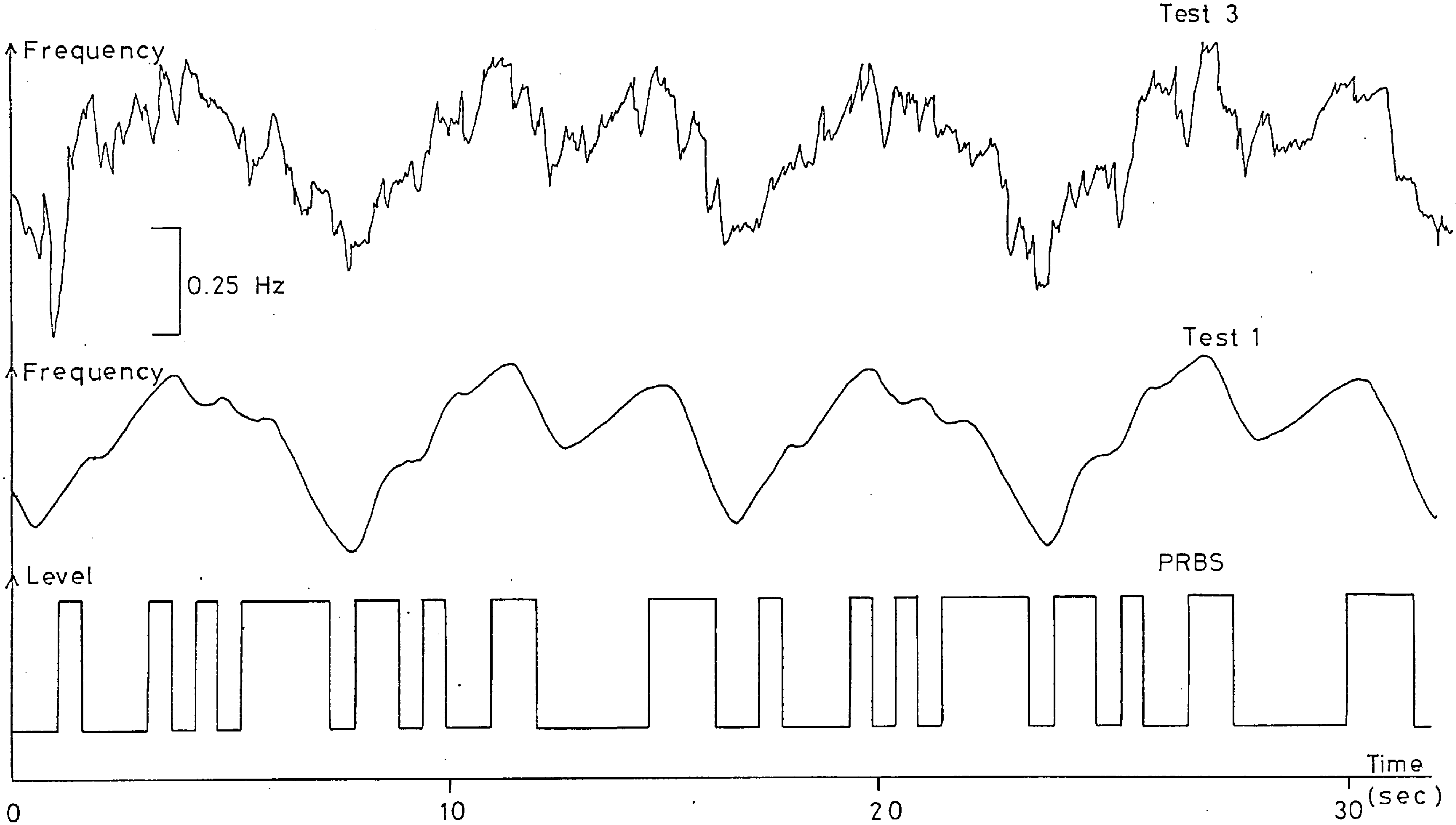

Fig. 9.18 Sample Test Recording.

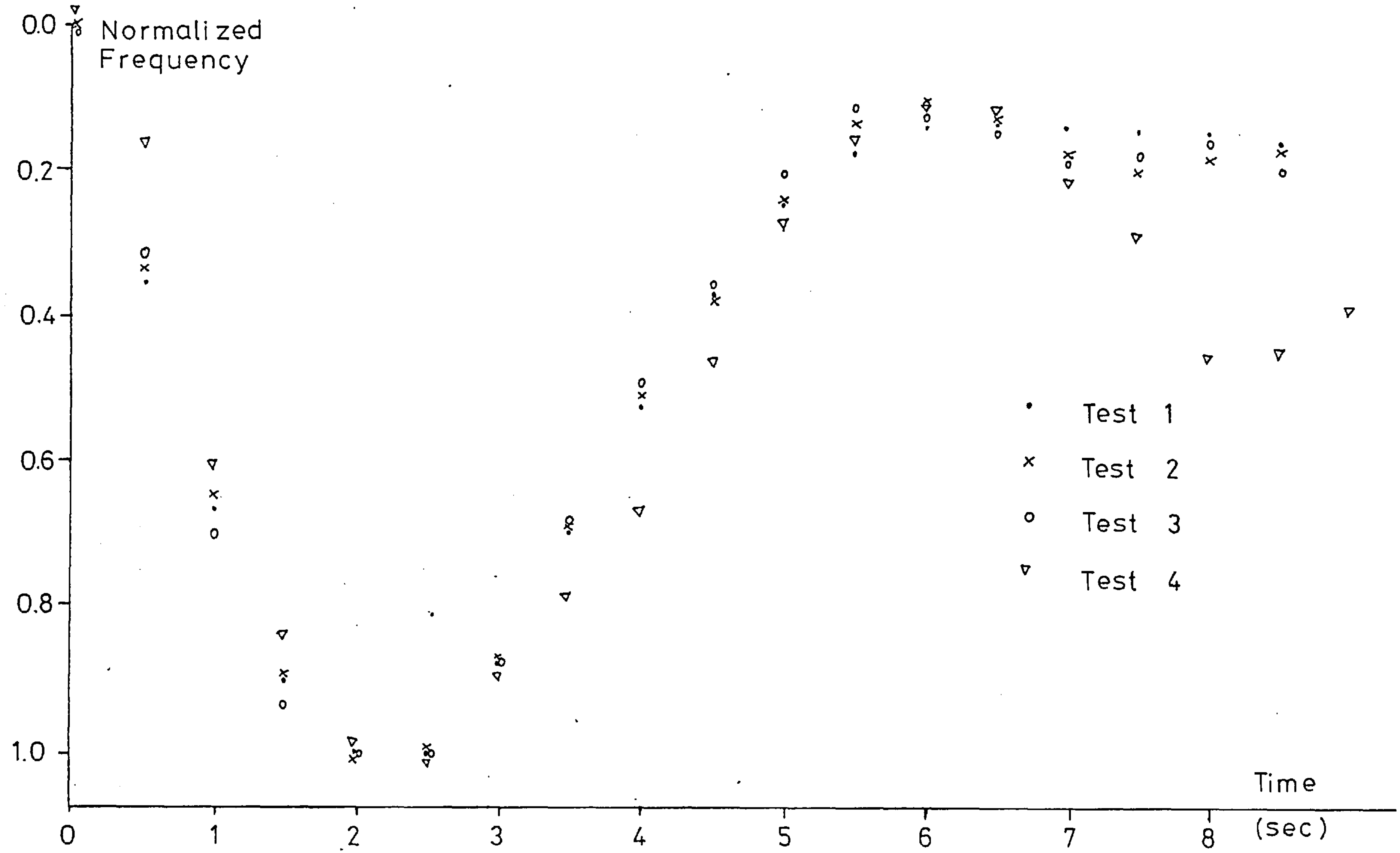

Fig. 9.19 Normalized Correlation Method Results.

test sequence and the measured frequency for Tests 1 and 3; in this figure one complete sequence occurs in 15.5 seconds, and the frequency records can be seen to repeat themselves. The results of Tests 1-4 using the cross-correlation method are shown in Fig. 9.19. These have all been normalized such that the peak frequency deviations for all the tests have the same magnitude. This enables easier comparison of the shape of the dynamic responses, and with a knowledge of the peak deviation, given below, shows the relative accuracies.

Test Number	Peak Frequency Deviation
1	0.165 Hz
2	0.155 Hz
3	0.16 Hz
4	0.14 Hz

The ability of this method to obtain results such as these from such noisy data indicates that there is great potential in such work for the measurement of power system parameters. Having obtained the step response, the system droop and inertia must be determined, and by knowing the final steady-state frequency, the power infeed and the initial rate of change of frequency, this can be done easily.

The droop is given by

$$\text{Droop} = \frac{\text{Final Frequency Change}}{\text{Power Change}} = \frac{\Delta f}{\Delta p}$$

while the inertia is given by

$$\frac{d\,f}{d\,t} = \frac{1}{2\,H}\,.\Delta\,p$$

where H is the inertia constant and $\frac{df}{dt}$ is the initial rate of change of frequency.

From these tests, values of droop and inertia were obtained, and as can be seen, they are close to the design values, which have been validated in other tests.

	Design Value	Obtained From Correlation Test 1
Droop	4%	3.8%
Inertia Constant	4.0	4.5

These measurements have an accuracy of about 10%, and this was obtained during a test which lastel only just over one minute. By increasing the measurement period, the variance of the results will be reduced, since the error is proportional to the square root of the reciprocal of the number of measurements. Similarly, if the behaviour of the system for periods up to minutes was of interest, a longer sequence could be employed, and the test conducted for many hours. This is of particular use, since following a disturbance, the aim is to restore the system to its normal operating condition as quickly as possible, and thus it is not desirable to allow the system to operate with no control, just so that its long-term performance can be observed. With the correlation methods, the disturbance can be made very small, such that the operator will not be influnced by it and consequently will not take any action to counteract the perturbations. Additionally, the ability to recover signals which are buried in noise is a great advantage and in a power system context would prove invaluable.

9.5 Conclusion.

These three examples of the work which has been performed using the simulator show that it is suitable for a wide range of functions. The computer has been found to work adequately in its three roles of data acquisition, simulation and control. The comparative ease with which different experiments can be conducted demonstrates the value of the simulator for the study of power system control methods.

10.1 Summary of the Work.

The first chapter of this thesis described the need for a power system simulator, both for the purpose of control investigations and for educational use. The system which has been developed is capable of meeting these requirements, and thus the basic aims of the project have been achieved.

The general structure of the simulator, with the dynamic plant simulation performed with analog equipment, the network represented by a scale model and the digital computer interfaced for measurement and control purposes, has been described. The concepts behind, and the operation of, both the generator and load units have been explained, and their performance has been shown to be adequate, with errors in the region 1-2%. The interconnect--ions between the different sections of the model and the interface were detailed, as this shows the potential versatility of the whole simulator.

The role of the digital computer was explained, and details given of the basic software, to provide an understanding of the way in which the analog and digital sections may be used together. Finally, three examples of work performed using the simulator were given, to show its uses in the areas of plant representation investigations, control studies and the evaluation of system parameter measurement techniques.

10.2 Original Contribution.

It is the present writer's opinion that the following pieces of work were his own contribution to the project:

(1) The design and construction of a modular generator unit, in which not only individual parameters, but also large sections of the model may be changed by just un-plugging one unit and plugging another one in. In particular the facility for connection with an analog computer is of great convenience. Within this generator unit, the

simple representation of a hydro turbine is also new, since only thermal plant had been considered previously. However, the model is not very satisfactory, and further work could profitably be done in this area.

(2) The inclusion of a 2 axis machine representation in a continuous frequency simulation, rather than in a transient analyser. The model which is used not only gives the correct terminal response, but also the equivalent circuits which form the basis of the solution of the machine equations provides an insight into the internal behaviour of the machine, making it particularly suitable for educational use. The main advantages of this 2 axis model over the previous reactance models are the superior damping characteristics and the improved voltage response. One of the major problems with the reactance model is that a change in load on a machine produces a step change in terminal voltage, which then affects the electrical power measurement.

(3) The design, construction and analysis of the load units. The original constant power loads were found to be unstable when operated with generator units of the reactance machine model type, and analysis showed this to be due to voltage instability. A new design was produced for a constant current load unit, which was found to perform satisfactorily. The analysis of the system was found to agree with the measured results, and this enabled a suitable choice of loop gains to be made.

(4) The development of a system for interconnecting all of these units with the network model, and the development of all the instrumentation for the measurement of network quantities, such as power flows, voltages and angles.

(5) The invention of a novel technique whereby a high network frequency may be used in a real-time model where the frequency is continuously

variable. The direct method of just using a high frequency voltage-controlled oscillator is not feasible, since a very high degree of stability is required and this is not attainable with inexpensive equipment. The idea of the single sideband system was then concieved, and a prototype was constructed, which performed well. The advantages of a high network frequency lie mainly in the realms of signal processing, and the use of such a system should enable transient stability studies to be performed.

(6) The use of a digital boiler simulation with an analog model of a steam turbine. This system has been shown to perform as designed, and further work on the development of simple boiler models would be useful. For any other digital on-line simulation work, the use of integrating operators is recommended, since they can give a great increase in solution speed over conventional numerical integration methods.

(7) The investigation of the use of pseudo-random binary sequences for the identification of power system characteristics. Using this method, it has been possible to determine the effective inertia and the damping in the system, and it is felt that this method might have potential for use in real systems, where random power injections may be made over a d.c. line.

It is felt that the above list is a summary of the writer's own contribution, but inevitably more work was carried out than is described in this thesis, since much of it proved to be abortive.

10.3 Recommendations.

The recommendations which are to be made fall into two main categories; first, there are suggestions for improvements and further work which would continue the present line of investigation. Secondly there is a suggestion for a new type of model which could be used for system, rather than plant, control studies.

10.3.1 Hardware Improvements.

Improvements in the accuracy of the whole model could easily be achieved by using more expensive components. In particular, the use of higher quality analog multipliers would effect a great improvement. These are used in the phase-sensitive detectors in the load units, and for the measurement of electrical power in the generator units, two functions which determine directly the accuracy of the whole model. It is recommended that multipliers with an accuracy of the order of 0.25% are used, although these cost about £40 each; two would be required in each load and generator unit.

The amount of circuit calibration could be reduced if high-precision resistors were used more widely. Their accuracy should be better than 1%, for if several circuits using such resistors are cascaded, the errors soon accumulate. The use of precision capacitors is not recommended, as they can be very expensive, and for the limited number which are required, it is simple to make up parallel combinations to obtain the desired value. All pre-set resistors should be either of the wire-wound or the cermet type, since the long-term stability of the carbon track type is very poor.

Although type 741 operational amplifiers have been used almost exclusively throughout the present model, there are many situations where other, more expensive amplifiers would be useful. In the simulation of long time constants a high impedance type, such as a FET input amplifier is necessary, and there are other areas where low-offset or low drift amplifiers would be useful, as this would reduce the number of "zero-adjust" pre-sets.

For the whole system, it has been shown that a more compact arrangement is possible, and with care, the whole model could be fitted in two 6' racks, instead of the five now occupied. This would involve constructing all the circuits on printed circuit boards, and arranging the metering and the controls to be remote from the actual electronics.

The most fundamentalchange recommended is that the per-unit system of the model should be changed. The case for using a higher frequency has been put, in Chapter 7, and it is suggested that the base voltage should also be changed. The recommended value is 5 V rms, which would be within the range of operational amplifiers, and would simplify the design of the power amplifiers. These could be replaced with directly-coupled transformerless amplifiers, which would remove the currently weakest link in the system, the present amplifiers.

Also, there are several disadvantages with the present computer, the PDP-15. It is not reliable, and being physically remote from the model it is not convenient for this type of work. A further limitation is the limited time for which it is available to the Simulator group. A small mini-computer dedicated to the project would enable much faster progress to be made.

10.3.2 Further Work on This Project.

There are many directions in which this work could usefully develop. Further work on the hardware would be beneficial, particularly in respect of prime-mover simulations. The need for a hydro turbine model has already been mentioned, and this is an important priority. Other kinds of plant which should be considered are gas-turbines and diesel engines, both of which are now finding a role for peak-lopping purposes.

Further work on boiler modelling, in particular for different kinds of boiler, would be useful, to produce simple models suitable for real-time use. The verification of these simple models against either complicated models or, preferably, real data is an essential part of the work.

In the system control field, there is no limit to the schemes which can be evaluated. The simulator allows different algorithms to be evaluated in a realistic context, and comparisons between alternative methods may then be made. In particular, the simulator is suitable for the testing of whole systems of programs, for such complex tasks as the restoration of a whole system to a normal operating state following a major disturbance.

10.3.3 A New Type of Total System Model.

In recent years, interest has centered on the study of total system response, rather than on individual plant performance. In this type of model[11-13], all voltage and reactive power effects are neglected, and only the power balance between generation and load is considered. A typical scheme is shown in Fig. 10.1. The generation is grouped into blocks, according to the plant mix, of thermal, hydro, gas turbine and perhaps pumped storage plant, and their outputs are summed to give the total generated power. A load model, containing the load trend and its random fluctuations, gives the power demand, and the difference between generation and load gives the accelerating power. This is integrated to give the system frequency, the integrator gain being determined by the system inertia.

This can be extended to interconnected system operation, by integrating the frequency error to give the angular difference. This is shown in Fig. 10.2. The tie-line flow is assumed to be a linear function of the angle across the line, which is valid for small changes. The total infeed in one area is then added to the generated power.

Models of this kind have given useful results in studies on generation loss, load shedding strategies and tie-line tripping, as they give the whole system response with only a fraction of the computational effort which is required for a full dynamic analysis.

The new idea is to build a model which simulates such a system representation, with all the calculations being performed digitally. Suitable methods would involve using integrating operators, in order to achieve the necessary speed of execution. Such a system would involve using micro-processors for the solution of the equations, with one such processor for each area of the system. These would be interconnected via a data bus, but each processor would operate autonomously, as the only information required about another area is its angle. Each iteration cycle would be initiated by an interrupt, which would be sent to each processor in the system.

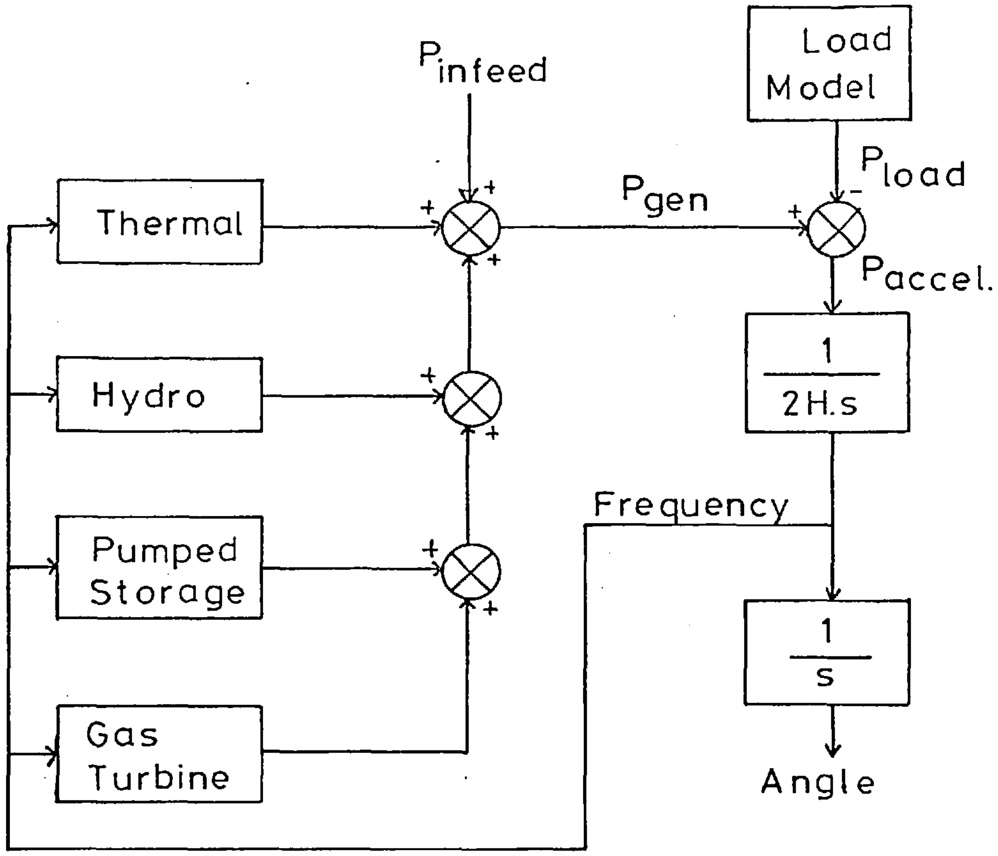

Fig. 10.1 Total System Model.

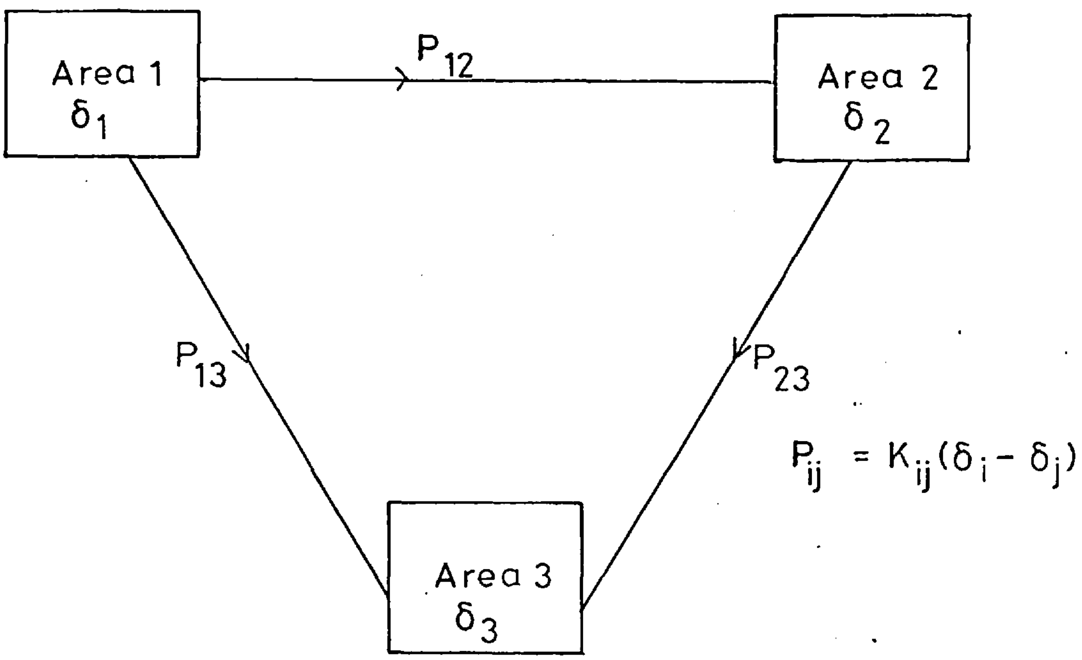

Fig. 10.2 Interconnected System Model.

Such a system would be inexpensive to build, although the initial programming of the plant euqations would be a lengthy process. However, the final system would have the advantages over analog equipment of drift-free and reproducible operation, whilst having the advantage of parallel operation.

The constraints imposed on the circuit design were mainly financial, and they demanded the use of inexpensive components. The main items to be affected are the operational amplifiers and the analog multipliers. These two areas will be considered first, and finally certain miscellaneous circuits will be explained.

Operational Amplifiers.

The ideal operational amplifier can be defined as having the following characteristics:

Infinite Input Impedance

Zero Output Impedance

Infinite Gain

Infinite Bandwith

Figs. A.1 to A.5 show some of the standard circuits which have been used, together with their transfer functions.

In any practical system, these circuits are subject to several limitations, depending on the characteristics of the operational amplifier which is employed. The main problem which arises in a simulation of the kind undertaken here is the representation of long time constants. These require a large RC product, and since the upper limit for capacitors lies in the range 1-10μF, high resistance values must be used. The limit for capacitors is determined by both their physical size and their price, since non-polarized types must be used, and they must possess good long-term stability.

The upper bound for resistance values is determined by the input characteristics of the amplifier, in particular the bias current taken by the input long-tail pair. This pair might be either bipolar or field-effect transistors, the former offering better temperature stability and lower drift, while the latter have the advantage of very small bias currents and higher input impedance.

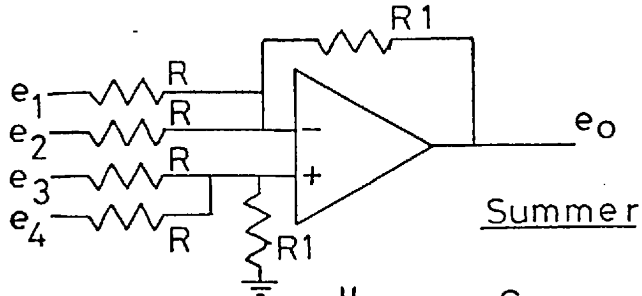

Summer

$$e_o = \frac{R1}{R}(e_3 + e_4 - e_2 - e_1)$$

A.1

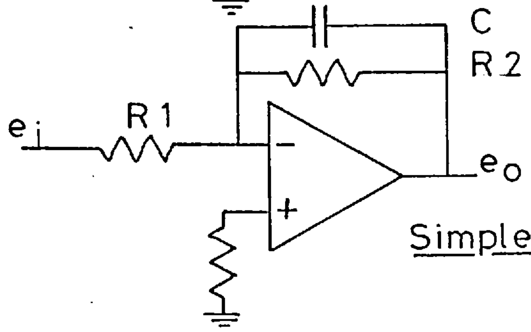

Simple Lag

$$\frac{e_o}{e_i} = \frac{R2}{R1}\left[\frac{1}{1 + sCR2}\right]$$

A. 2

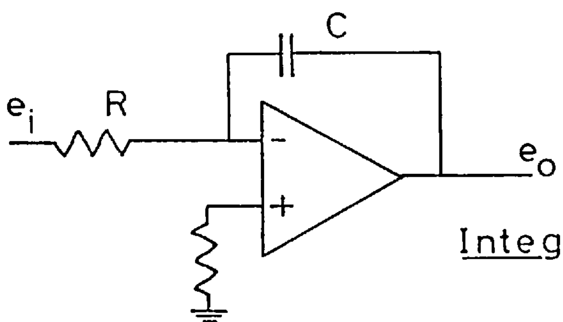

Integrator

$$\frac{e_o}{e_i} = \frac{1}{sRC}$$

A.3

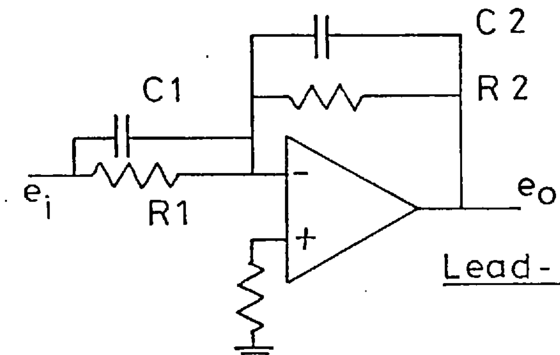

Lead-Lag

$$\frac{e_o}{e_i} = \frac{R2}{R1}\left[\frac{1 + sC1R1}{1 + sC2R2}\right]$$

A.4

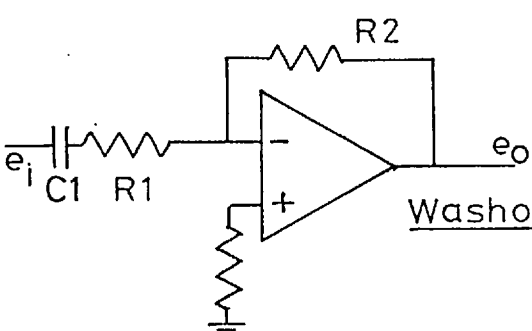

Washout

$$\frac{e_o}{e_i} = \frac{sC1R2}{1 + sC1R1}$$

A.5

Within the available financial range, one type of each such kind of amplifier was selected, the 741 op-amp, costing about 22 p, and a modified version of this amplifier, with a FET input stage, sold by Radiospares for about £2.50. These are both very inexpensive, but are quite suitable for use in the simulator. In any circuit which requires resistance values greater than about 200 kΩ, FET type amplifiers must be used. Although the use of higher quality amplifiers would improve the whole system, and reduce the number of adjustments, the extra expense would be considerable and the money would be better spent in other areas.

Analog Multipliers.

There are three main types of electronic multiplier in common use at the present time, these being:

The Transconductance Type

The Pulse Height/Width Modulator

The Hall Effect Type.

The Hall effect kind of multiplier is of no great use in electronic systems, since it is not only physically large, but is also very susceptible to temperature changes. This leaves the two other types, both of which are widely used. The pulse height/width modulator is capable of high accuracy, of the order of 0.1%, but is expensive, perhaps £50 for a 0.5% model. This leaves the variable transconductance type, which is shown in principle in Fig. A.6.

For the stage shown, it is possible to write

$$\Delta v = K . \Delta V . I_E$$

so that the voltage difference at the collectors is proportional to the product of the input voltage difference and the total emitter current. Such a property may be used in an analog multiplier, by having as one input the differential voltage, ΔV, and using the other voltage to control the current I_E.

The system must be designed to accommodate operation in all four quadrants, to allow input signals of both polarities. A practical multiplier has four main adjustments, each of which has a corresponding term in the expression for the output V_o.

$$V_o = K_x \left[(x-x_o).(y-y_o) \right] + V_{ox} + \text{higher terms}$$

where x, y are the respective inputs

K_x is the gain adjustment

x_o, y_o are the respective input offset adjustments

V_{ox} is the output offset adjustment

Two different devices were employed, one, The Motorola MC 1495, with an accuracy of 3%, and the other, the Analog Devices AD 533, with an accuracy of 1%. For the MC 1495 device, the output is a balanced signal, consisting of a large d.c. common-mode voltage, about 10 V, and a small signal voltage, about 0.5 V. The amplifier which follows the multiplier must have excellent common-mode rejection, and also the system requires highly stable power supplies, for otherwise variations in offset will occur.

The AD 533, however, contains its own supply regulators and output amplifier, and is much less sensitive to voltage variations. As a result, it is more convenient to use than the MC 1495, and is preferable despite its higher cost. For about £15 it is possible to buy complete multiplier chips which require no external adjustments, since these are all made in the factory during manufacture, by laser trimming. These would obviously be the best solution, if cost were no object.

Miscellaneous Circuits.

The first of these miscellaneous circuits is the limiter, shown in Fig. A.7. The circuit acts by the potential V_B becoming greater than v_{be} for the transistor, which turns on the transistor. The current through this transistor flows into the summing junction, and tends to reduce the output voltage, causing a limiting action. The potential V_B is determined by the output voltage V_o, a reference voltage V_R and the potential divider R_2 and R_3. The break-point of the limiter, V_x, is given by

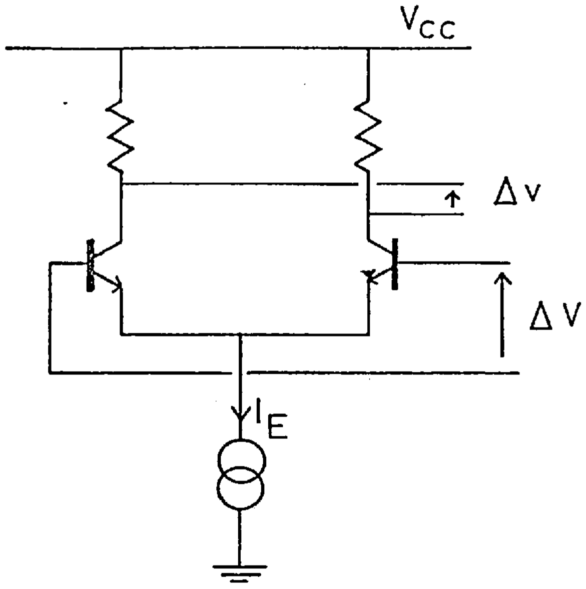

Fig. A.6 Multiplier Principle.

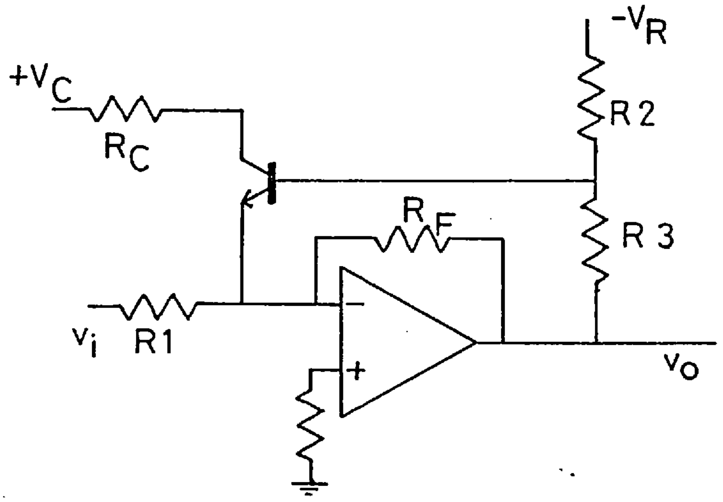

Fig. A.7 The Limiter.

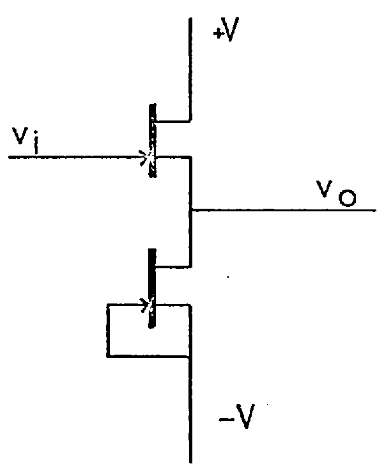

Fig. A.8 High -Z Buffer.

$$V_x = \frac{R_3}{R_2} V_R + \left[1 + \frac{R_3}{R_2} \right] v_{be}$$

and the slope of the limited portion by

$$\text{slope} = \frac{R_3}{\beta R_1}$$

In general, the slope can be made at least < 0.001, depending on the input resistor and the gain of the transistor. The diode is included to prevent reverse-breakdown of the base-emitter junction when the output voltage goes negative. By changing the transistor to a p-n-p type, reversing the diode and changing the polarity of V_R and V_C, a negative limiter can be produced.

In the instances where a very high input impedance is required, such as in "Hold" circuits, a dual FET is used, as shown in Fig. A.8. The upper device is connected as a source follower, while the lower device acts as a dynamic load. This gives a low offset between input and output, <10 mV, and the dual device offers good thermal tracking.

APPENDIX B LOAD UNIT ANALYSIS PARAMETERS

For an analysis of the behaviour of the load unit it is necessary to know how the magnitude of the terminal voltage varies with changes in the phase and quadrature components of the load current, when the unit is connected via a complex impedance, as shown in Fig. B.1.

The phasor diagram is shown in Fig. B.2, and it is apparent that

$$E^2 = (V + \Delta V)^2 + \delta V^2$$

$$E^2 = (V + RI_p + XI_q)^2 + (XI_p - RI_q)^2$$

By applying in turn small increments to I_p, I_q and E, the corresponding changes in V can be found, and the desired parameters obtained. These are:

$$\frac{\Delta V}{\Delta I_p} = - \frac{VR + I_p Z^2}{V + I_q X + I_p R} = K_{IPV}$$

$$\frac{\Delta V}{\Delta I_q} = - \frac{VX + I_q Z^2}{V + I_q X + I_p R} = K_{IQV}$$

$$\frac{\Delta V}{\Delta E} = \frac{1}{(1 + XI_q + RI_p)} = K_{EV}$$

The coefficients for the analysis of the system of Fig. 5.4(b) are given below; all the variables are defined in the text of Chapter 5.

Let

$$X1 = (1-K_A K_{EV})/T_E \qquad X2 = -(K_A K_{IPV})/T_E$$

$$X3 = 1/(R-K_{IPV}) \qquad X4 = X3.I.R.K_{EV}$$

And then

$$K_1 = (V.X1 + I.K_{IPV}.X3)/T_p$$

$$K_2 = (V.X4 + I.K_{IPV} + X4.K_{IPV}).T_p$$

$$K_3 = X2X3$$

$$K_4 = X1 + K_3$$

For the system of Fig. 5.15, the coefficients are given below:

Let

$$Y1 = (1 - e_{po}).K_{IPV} \qquad Y2 = (1 - e_{po}).K_{IQV}$$

$$Y3 = e_q.K_{IPV} \qquad Y4 = e_q. K_{IQV}$$

$$G = 1/R$$

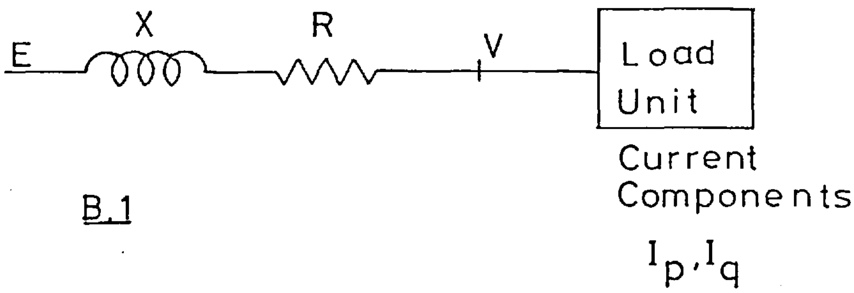

B.1

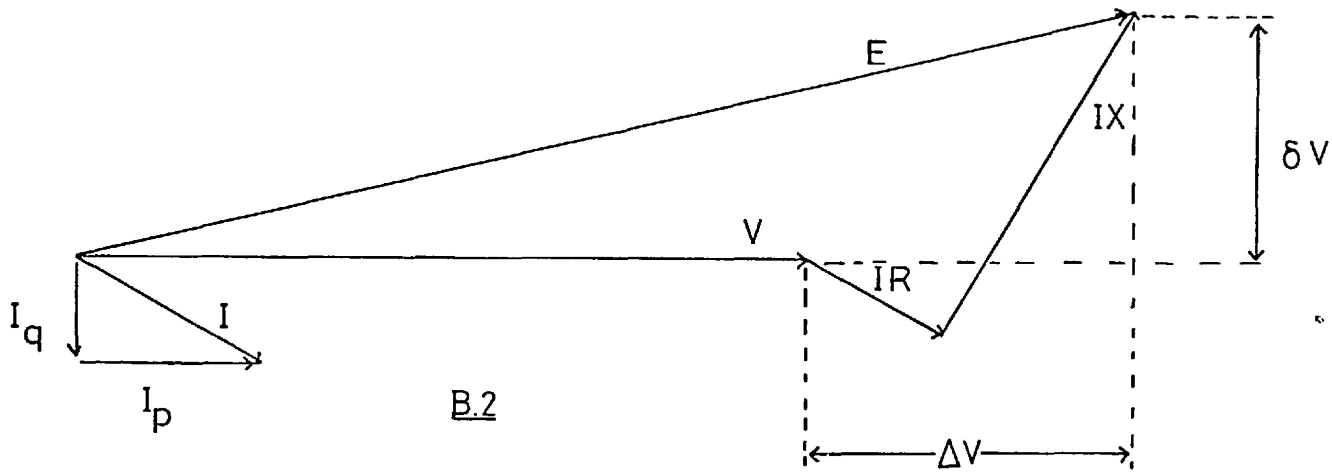

B.2

Load Unit Voltage Sensitivities.

And then

$$Z_A = G/\left(1 - GY4 - \frac{G^2.Y2Y3}{1 - GY1}\right)$$

$$Z_B = G^2Y3/((1 - GY4)(1 - GY1) - G^2Y2Y3)$$

$$Z_C = G^2Y2/((1 - GY1)(1 - GY4) - G^2Y2Y3)$$

$$Z_D = G/\left(1 - GY1 - \frac{G^2Y2Y3}{1 - GY4}\right)$$

APPENDIX C THE PSEUDO-RANDOM BINARY SEQUENCE GENERATOR

Such sequences are generated using a shift register, with feedback from its various outputs back into the inputs, via exclusive-OR gates, as shown in Fig. C.1. For a shift register of n stages, the sequence will repeat itself every 2^n-1 clock pulses. Such a sequence is called a maximal length sequence, and certain feedback connections have been established which will generate them. A table of such connections is given below:

Stages	Sequence Length	Feedback Connections
2	3	2,1
3	7	3,1
4	15	4,1
5	31	5,2
6	63	6,1
7	127	7,1
8	255	8,7,2,1

A generator was constructed on these principles, and is shown in block form in Fig. C.2. The clock frequency is determined by a division chain whose input is derived from a 1 MHz crystal oscillator. The first stage of the division chain in a 3 decade rate multiplier, controlled by three thumbwheel switches on the front panel. For an input of frequency f_o, the output can be adjusted to lie inthe range $0.001f_o$ to $0.999f_o$. Next there is a fixed division by 10^3, followed by a switchable division chain of three stages of $\div 10$. The internal clock may therefore be adjusted from 999 Hz to 0.001 Hz. There is also facility for using an external clock signal.

Before this signal is used to clock the shift register, there are 3 switchable $\div 2$ stages, to enable the generated sequence to run at a fraction (1, $\frac{1}{2}$, $\frac{1}{4}$, $\frac{1}{8}$) of the clock frequency, permitting synchronous sampling. The feedback connections around the shift register are also

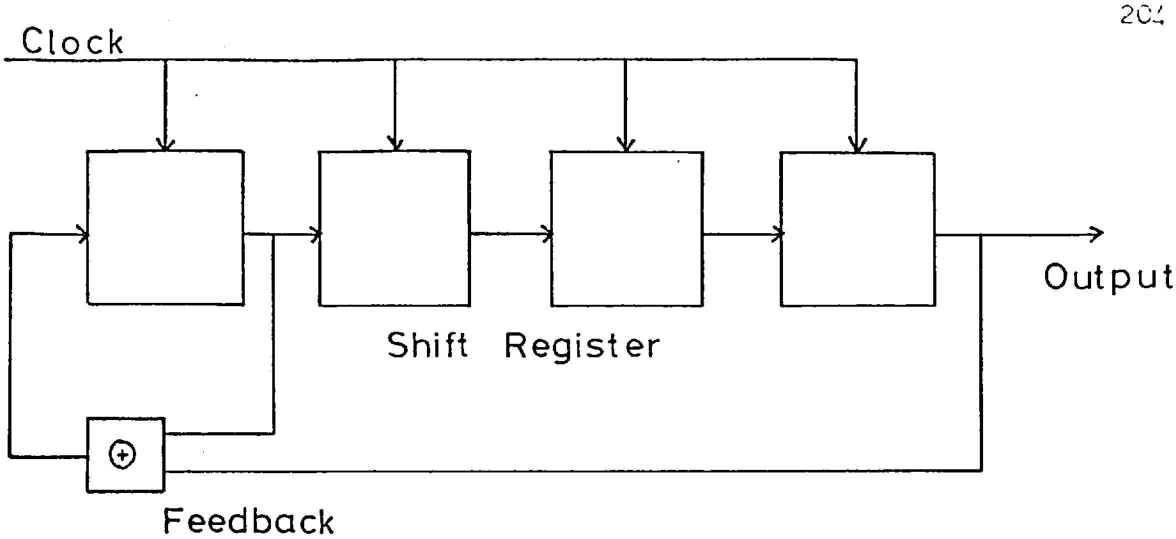

Fig. C.1 Principle of PRBS Generator.

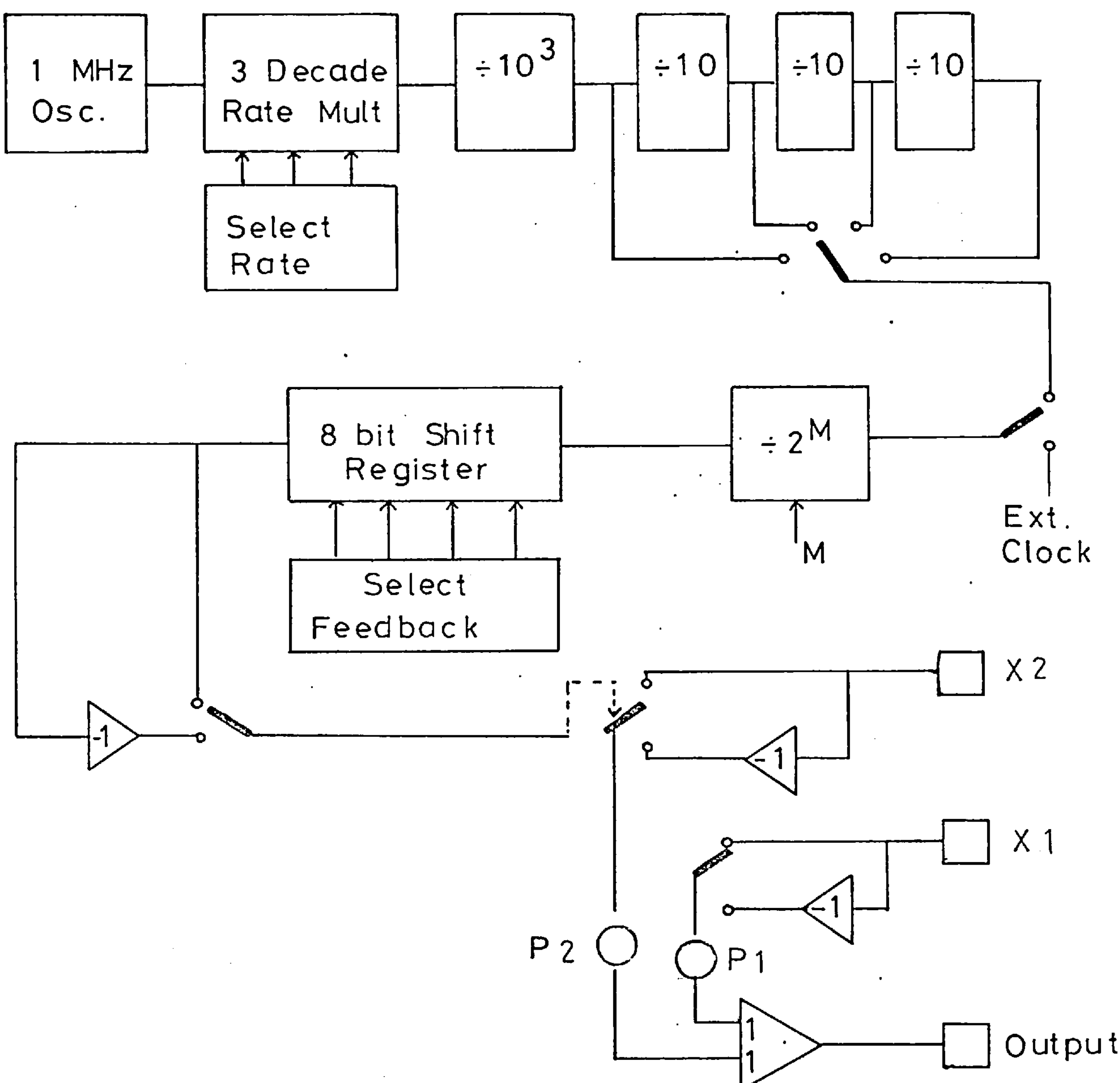

Fig. C. 2 PRBS Generator.

switchable, allowing 31, 63, 127 or 255 bit sequences to be generated.

The output sequence is a TTL compatible waveform, and an analog system has been attached to the output to provide control signals suitable for use with the model. This output consists of a fixed level, determined by input X_1 and potentiometer P_1, with an increment which is switched by the random sequence, of magnitude X_2P_2. Thus the output can be written as:

$$X_o = \pm X_1P_1 \pm \left[\pm (X_2P_2) \right]$$

switchable inversions — determined by sequence

An internal +10 V reference signal is also provided.

REFERENCES

1) D Liacco T. "Real Time Computer Control of Power Systems" Proc. IEEE 1974 vol. 62 No. 7.

2) Stagg G.W., Dopazo J.F., Klitin O.A. and VanSlyck L.S. "Techniques for the Real Time Monitoring of Power System Operations" IEEE Paper No. 69TP657-PWR presented at 1969 Summer Power Meeting.

3) Schweppe F.C. and Handschin E. "Static State Estimation in Electric Power Systems" Proc. IEEE 1974 Vol. 62 No. 7 pp 972-82

4) Benson A.R., Johannson D.E. and McNair H.D. "Centralized Load-Frequency Control for the U.S. Columbia River Power System" IEEE paper No. CP63-230

5) Limmer H.D. "Techniques and Applications of Security Calculations applied to Dispatching Computers" paper presented at 1969 PSCC

6) Dommel H.W. and Tinney W.F. "Optimal Power Flow Solution" IEEE 1968 PAS 87 pp 1866-76

7) Nabona N. and Freris L.L. "Optimization of Economic Dispatch Through Quadratic and Linear Programming" Proc. IEE 1973 Vol. 120 pp 574-80

8) "Power System Simulator - A Feasibility Study" Prepared by S. Miniesy and C.B. Giles - edited by M.J. Short. Elec. Eng. Dept. Imperial College 1976.

9) Concordia C. and Schultz R.P. "Appropriate Component Representation for the Simulation of Power System Dynamics" Paper presented at a Symposium on Adequacy and Philosophy of Modelling IEEE Winter Power Meeting 1975

10) Ghafurian A. "Application of Equivalents to Multi-Generator Transient Stability Studies" PhD Thesis 1975 University of London

11) DeMello F.P., Mills R.J. and B'Rells W.F. "Automatic Generation Control - Part I Process Modelling" IEEE 1973 PAS 92 pp 710-15

12) Taylor C.W. and Crasap R.L. "Real-Time Power System Simulation for Automatic Generation Control" IEEE 1976 PAS 95 pp 375-84

13) Ashmole P.H., Battlebury D.R. and Bowdler R.K. "Power System Model for Large Frequency Disturbances" Proc. IEE 1974 Vol. 121 pp 601-08

14) Bush V. and Hazen H.L. "Integraph Solution of Differential Equations" Franklin Institute Journal 1927 pp 575-615

15) Lyon W.V. and Edgerton J. "Transient Torque Angle Characteristics of Synchronous Machines" Trans. AIEE 1930 Vol. 49 p686

16) Boast W.B. and Rector J.D. "An Electric Analog Method for the Direct Determination of Power System Stability Swing Curves" Trans AIEE 1951 Vol. 70 Pt. 2 pp 1833-36

17) Kaneff S. "A High Frequency Simulator for the Analysis of Power Systems" Proc. IEE 1952 Vol. 100 Pt. 2 p 405

18) Adamson C., Barnes L. and Nellist B.D. "The Automatic Solution of Power System Swing Equations" Proc. IEE 1956 Vol. 104A pp 143-51

19) Adamson C. and El-Sarafi A.M.S. "Simulation of the Transient Performance of Synchronous Machines on an AC Network Analyser" Proc. IEE 1957 Vol. 104C pp 323-31

20) Miles J.G. "Analysis of Overall Stability of Multi-Machine Power Systems" Proc. IEE 1961 Vol. 109A pp 203-17

21) Aldred A.S "Electronic Analogue Computer Simulation of Multi-Machine Power System Networks" Proc. IEE 1962 Vol. 109A pp 195-202

22) Bain D.K.S. "Power System Model" Proc. IEE 1967 Vol. 114 pp 1131-38

23) "The AC/Hybrid Power System Simulator" Final Report of EEI Project RP-90-2 prepared by L. Michaels

24) "The Digital Differential Analyser" Ed. by T.R.H. Sizer Appendix A

25) Short M.J. "The Conjoint Use of a Network Analyser and Analogue Computer for Studies of the Automatic Governing and Regulating of Power Systems" PhD Thesis 1965 University of London

26) Sheldrake A.L. "The Design and Development of a Dynamic Power System Simulator" MSc Thesis 1969 University of London

27) Sheldrake A.L. "A Semiconductor Analogue for the Study of Dynamic Power Systems" PhD Thesis 1976 University of London

28) Bolton M.J.P., Sheldrake A.L. and Giles C.B. "Real-Time Hybrid Simulation of Electric Power Systems" Paper presented at 1974 DECUS Conference Zurich

29) Bolton M.J.P., Giles C.B., Ramakers H., Sheldrake A.L. and Short M.J. "Real-Time Hybrid Power System Simulator" PICA Conference 1975 Paper No. 75CH0962-1 PWR

30) Arriola-Valdes E.,Freris L.L., Giles C.B. and Short M.J. "Real-Time Hybrid Power System Simulator for ON-Line Control Studies" IEE Conference on The On-Line Operation and Optimization of Transmission and Distribution Systems

31) Adler R.B. and Mosher C.C. "Steady-State Voltage Power Characteristics for Power System Loads" IEE 1970 Paper No. CP706PWR

32) "The Effect of Voltage and Frequency on Power System Load" IEEE Committee Report CP6664 1966

33) Concordia C. "Representation of Loads" Paper presented at a Symposium on Adequacy and Philosophy of Modelling IEEE 1975 Winter Power Meeting

34) Berg G.J. and Kar A.K. "Model Representation of Power System Loads" 1971 PICA Conference

35) Bolton M.J.P. "The Simulation of Random Load Fluctuations for the Power System Model" Power System Report No. 96 Elec. Eng. Dept. Imperial College 1974

36) Tan S. "A Turboalternator Model for a Dynamic Power System Simulator" MSc Thesis 1974 University of London

37) Graeme J.G. and Tobey G.E. "Operational Amplifiers - Design and Applications" Mc Graw Hill 1971

38) Ehsan M. "Power System Modelling for Real-Time Load-Frequency Control Studies" PhD Thesis 1975 University of London

39) "A Precision Waveform Generator and Voltage-Controlled Oscillator" Intersil Applications Bulletin A012 1972

40) "Computer Representation of Excitation Systems" IEEE Committee Report Paper No. 31TP67-424 presented at 1967 Summer Power Meeting

41) "Excitation System Dynamic Characteristics" IEEE Committee Report Paper No. T72 590-8 presented at 1972 Summer Power Meeting

42) Kimbark E.W. "Power System Stability - Vol. III Synchronous Machines" Wiley 1956

43) Schlief F.R. "Excitation System Modelling" Paper presented at a Symposium on Adequacy and Philosophy of Modelling IEEE Winter Power Meeting 1975

44) Ramey D.G. and Skooglund J.W. "Detailed Hydrogovernor Representation for System Stability Studies" IEEE 1970 PAS 70 pp 106-12

45) Dennis N.G. "Water Turbine Governors" Proc. I.Mech.E. (B) 1952 Vol.1(B) pp379-401

46) Leum M. "The Development and Field Experience of a Transistor Electric Governor for Hydro Turbines" IEEE 1967 PAS 86 pp 443-53

47) Nechleba N. "Theory of Indirect Speed Control" Book.

48) "Dynamic Models for Steam and Hydro Turbines in Power System Studies" IEEE Committee Report Paper No. T73 089-0 presented at 1973 Winter Power Meeting

49) Young C.C. "Equipment and System Modelling for Large-Scale Stability Studies" Paper No. 71CP26-PWR-V-B presented at 1971 Pica Conference

50) Concordia C. and Kirchmeyer L.K. "Tie-Line Power and Frequency Control Performance - Part II" Trans. AIEE 1954 Vol. 73 Pt. III A pp 133-41

51) Shackshaft G. "General Purpose Turbo-Alternator Model" Proc. IEE 1963 Vol. 110 pp 703-13

52) Ramey D.G. and Byerley R.T. "Dynamic Simulation of Interconnected Systems" Paper presented at 1967 PICA Conference

53) Olive D.W. "New Techniques for the Calculation of Dynamic Stability" IEEE 1966 PAS 85 pp 767-77

54) Fitzgerald A.E. and Kingsley C. "Electric Machinery" McGraw Hill 1961

55) Boffi L.V. and Haas V.B. "Analogue Computer Representation of Alternators for Parallel Operation" Trans. AIEE 1957 Vol. 76 Pt. I pp 153-58

56) Soper J.A. and Fagg A.R. "Divided Winding Rotor Synchronous Generator" Proc. IEE 1969 Vol. 116 pp 113-26

57) Adkins B. "The General Theory of Electrical Machines"

58) Faragalla F.F. "A Synchronous Machine Analogue and its Application to Power System Dynamical Analysis" PhD Thesis 1954 University of London

59) Slemon G.R. "Equivalent Circuits for Transformers and Machines Including Non-Linear Effects" Proc. IEE Vol. 100 Pt. IV pp 129-43

60) Buhler H. "Model for the nvestigation of Alternator Regulation Characteristics" Bull. Oerlikon 1955 No. 308

61) Buhler H. "Theory and Design of an Improved Electronic Generator Model" Bull. Oerlikon 1958 No. 330

62) Butterworth S. "Electrical Characteristics of Overhead Lines" ERA 1954

63) "Component Application Data" Radiospares London 1971

64) Arriola-Valdes E. Personal Communication

65) Markus J. "Source-Book of Electronic Circuits" McGraw Hill

66) Stevenson W.D. "Elements of Power Systems Analysis" McGraw Hill

67) Black H.S. "Modulation Theory" Van Nostrand

68) Nezer Y. "Active Notch Filters" Wireless World 1975 Vol. 81 pp 307-10

69) Harris R.J. "The Design of Operational Amplifier Notch Filters" Proc. IEEE 1968 pp 1722-23

70) Johnson D. and Hilburn J. "Rapid Design of Active Filters" Wiley

71) Hund A. "Frequency Modulation" McGraw Hill

72) Mogridge L. "Basic Software for the Digital Computer Section of a Hybrid Power System Simulator" MSc Thesis 1975 University of London

73) Bolton M.J.P. Personal Communication

74) PDP-15 Systems Reference Manual

75) Bolton M.J.P. "The PDP-15 Digital Input/Output Unit" Power System Report No. 95 Elec. Eng. Dept. Imperial College 1974

76) Bolton M.J.P. "The Design for an Interface Between the Power System Model and the PDP-15 Computer" Power System Report No. 91 Elec. Eng. Dept. Imperial College 1972

77) DOS System Manual) Digital Equipment

78) RSX Real Time Executive Reference Manual) Corporation

79) McDonald J.P. "Representation of the Boiler-Turbine" Paper presented at a Symposium on Adequacy and Philosophy of Modelling IEEE Winter Power Meeting 1975

80) Dittel R.C. "Mathematical Models in Boiler Simulation Studies" MSc Thesis 1973 University of London

81) Domel H.W. and Sato N. "Fast Transient Stability Studies" IEEE 1972 PAS 91

82) Rosko J.S. "Digital Simulation of Physical Systems" Addison Wesley

83) Tustin A. "A Method of analysing the Behaviour of Linear Systems in Terms of Time Series" Journal IEE Vol. 94 Pt. II A

84) Fowler M.E. "A New Numerical Method for Simulation" Simulation 1965 Vol. 14 pp 324-330

85) Hurt J.M. "New Difference-Equation Technique for Solving Non-Linear Differential Equations" AFIPS Conf. Proc. 1964 No. 25 pp 169-79

86) Darrieus G. "Rational Regulation of Frequency and Distribution of Load Between Interconnected Power Systems" Bulletin de la Societé Francaise des Electriciens 1936 pp 501-12

87) Tou J.T. "Digital and Sampled Data Control Systems" McGraw Hill

88) Jury E.I. "Sampled Data Control Systems" Wiley

89) Eklund K. and Gustavsson I. "Identification of Drum Boiler Dynamics" Proc. 3rd IFAC Symposium on Identification and System Parameter Estimation 1973

90) Clarke D.W., Dyer D.A.J and Hastings-James R. "Identification and Control of a Pilot Scale Boiling Rig" ibid.

91) Briggs P.A.N., Godfrey K. and Hammond P.H. "Estimation of Process Dynamic Characteristics by Correlation Methods Using Pseudo-Random Signals" Proc. 1st IFAC Symposium on Identification in Automatic Control Systems 1967

92) Uznoglu V. "Analysis and design of Digital Systems" Gordon and Breach